School of Applied Chemistry

THE USE OF ADVANCED ANALYTICAL TECHNIQUES FOR STUDYING THE BIODEGRADATION OF AROMATIC HYDROCARBONS

Steven James Fisher

This thesis is presented as a part of the requirements for
the award of the Degree of Doctor of Philosophy
of the Curtin University of Technology

July 2002

Declaration

This thesis contains no material that has been accepted for the award of any other degree or diploma in any university.

To the best of my knowledge and belief this thesis contains no material previously published by any other person except where due acknowledgment has been made.

Signature:

Abstract

Two case studies are described where partially biodegraded petroleum residues were collected from the marine environment and analysed to investigate the changes in aromatic hydrocarbons with increasing biodegradation.

The first of these studies, involved following the weathering of sea-floor residues from drilling discharges from an offshore petroleum exploration and production platform situated off the coast of North Western Australia. During operations, formation cuttings with adhering oil-based drilling muds were discharged into the ocean *via* a chute into approximately 125m of water, forming a substantial mound at the base of the platform. A suite of seabed sediments was collected from 16 sampling sites at various distances from the platform immediately following the cessation of drilling operations. The distribution of hydrocarbons in the sediment directly under the cuttings chute was consistent with that found in drilling fluids formulated from a kerosene-like fluid. The samples from more remote sites exhibited the successive enhancement of an unresolved complex mixture relative to the *n*-alkanes, associated with the presence of residues from petroleum biodegradation processes. In a subsequent sampling some three years later, a 10 cm core was retrieved from the cuttings pile and divided into 1 cm depth intervals. Samples within 6 cm of the surface of the cuttings pile contained biodegraded residues of the drilling mud, where the extent of biodegradation increased with decreasing proximity to the surface, most likely indicative of aerobic biodegradation. Biodegradation was less evident in the underlying sediments, where anaerobic conditions prevailed. Analysis of the aromatic hydrocarbons in both sets of sediment extracts by using gas chromatography-mass spectrometry (GC-MS) revealed the successive depletion of alkylnaphthalenes, and due to the subtlety of changes in the extent of biodegradation, provided an excellent opportunity to examine the susceptibility of biodegradation towards the individual alkylnaphthalenes in the marine environment. Conventional GC-MS analysis of these mixtures is performed under chromatographic conditions where complete resolution of the mixture is not achieved and several isomers co-elute. The mass spectra of these co-eluting isomers

may be so similar that one is unable to differentiate between them, and their abundance may therefore not be determined. Since each isomer has a unique infrared spectrum, however, the abundance of each individual isomer was determined by comparing the infrared spectrum of the co-eluting compounds with the spectrum of each of the isomers. To this end, techniques were developed for the application of direct-deposition gas chromatography - Fourier transform infrared spectroscopy (GC-FTIR) to the analysis of the complex mixture of alkylnaphthalenes present in the petroleum. This technique was also extended to discriminate between individual alkylphenanthrene isomers, and to clarify the sorption behaviour of the dimethylphenanthrenes by mordenite molecular sieves. The identification of other compounds of geochemical significance in petroleum is also described. Analyses of the aromatic hydrocarbons in the contaminated sea-floor sediments using GC-FTIR enabled the unambiguous identification and quantification of each of the dimethylnaphthalene, trimethylnaphthalene and tetramethylnaphthalene isomers present in the samples, from which the relative extents of depletion of each with increasing extent of biodegradation were determined. It was apparent from the considerable differences in the observed susceptibility to biodegradation that a strong relationship exists between the compound structure and its susceptibility to biodegradation, with 1,6-disubstituted polymethylnaphthalenes being preferentially depleted relative to other isomers that lack this feature.

The second case study involved tracking the fate (weathering) of hydrocarbons from an accidental release of condensate from a buried pipeline into intertidal coastal (mangrove) sediments in North Western Australia. Sediment samples were collected on nine occasions over a three-year period. Chemical analysis of the saturated and aromatic hydrocarbon components of the petroleum extracts revealed that both hydrocarbon fractions exhibited an increasingly biodegraded profile with increased residence time in the sediments. In a similar manner to the first case study, detailed analysis of the aromatic hydrocarbons using GC-FTIR techniques was performed to determine the depletion of individual alkylnaphthalene isomers with increasing extent of biodegradation. It was apparent that a relationship similar to that observed for the sea-floor sediments exists between the alkylnaphthalene structure and its susceptibility to biodegradation. Changes in the distribution of methylphenanthrene

and dimethylphenanthrene isomer mixtures were also studied and the susceptibility to biodegradation amongst these determined in a similar manner. These relative susceptibilities to biodegradation of the aromatic hydrocarbons were then related to the established hierarchy of susceptibilities of the saturated hydrocarbons, in effect providing a second parallel system for the assessment of the extent of biodegradation.

Finally, a system of ratios calculated from the relative abundances of selected aromatic hydrocarbons was developed and used as indicators to differentiate between several crude oils that have been biodegraded to varying extents. These parameters also offer promise as indicators of multiple accumulation events in oil reservoirs where petroleum fluids biodegraded to differing extents are mixed.

Acknowledgments

I would like to thank my project supervisor Professor Robert Kagi for his advice, encouragement and support throughout the course of this work. My thanks also go to Professor Robert Alexander for his guidance and healthy scepticism, both of which helped in shaping the direction of the work described in this thesis.

I am indebted to the management of Woodside Energy Ltd and their Joint Venture Participants for their permission to present results from the investigation of sea-floor sediments and the intertidal coastal sediments from the North West Shelf. My sincere thanks also go to the management of Geotechnical Services Pty. Ltd., especially Dr. Birgitta Hartung-Kagi, for the sponsorship of my Australian Postgraduate Research Award – (Industry) Scholarship.

I would also like to thank the following people:

- Mr. Greg Oliver (Woodside Energy Ltd.) and Mr Adrian Chegwidden (Woodside Offshore Petroleum) for their assistance in planning and collection of sediment samples from the North West Shelf.
- Mr. Geoff Chidlow, for sharing his experience and knowledge of gas chromatography – mass spectrometry, and for maintenance of the instruments.
- Dr. Leroy Ellis for his collaboration with molecular sieving and pyrolysis experiments.
- Dr. Trevor Bastow for his collaboration on the identification of 9-methylretene and related compounds in crude oil.

Finally, I cannot thank my wife Anne enough for her patience and unwavering love and support throughout the several years it has taken to complete this work, and my daughters Amy, Nicole, Jodi and Zoe for giving life some perspective. Now you can have your husband and Dad back.

Table of Contents

CHAPTER 1

1 Overview of the thesis

1.1 Thesis summary

The body of work presented in this thesis has been compiled over approximately ten years. During this period, I have been employed both as an Environmental Chemist servicing the oil and gas industry, and later as a Research Scientist investigating the efficacy of strategies and techniques for the remediation of contaminated environments. This thesis has evolved primarily from environmental monitoring programs undertaken during this period, where petroleum was released into the marine environment.

The thesis is divided into four chapters where results and discussion are presented (Chapters 3 to 6). Each chapter is accompanied by an introduction pertinent to the ensuing discussion. In Chapter 3, the development of gas chromatography-Fourier transform infrared spectroscopy (GC-FTIR) as an analytical technique applicable to petroleum geochemistry is described. In particular, this technique was used to differentiate between co-eluting aromatic hydrocarbons. While the development of the technique was pivotal to work presented in the subsequent chapters, other examples where GC-FTIR has been successfully applied to solving analytical problems are also presented to give a more complete overview. These examples represent my contribution to collaborative studies leading to publications in conjunction with authors other than my supervisors (Alexander et al., 1995; Fisher et al., 1996; Ellis et al., 1999). Where appropriate, data contributed by these co-authors have been included in this thesis, and are acknowledged in the text.

Chapter 4 describes a case study into the biodegradation of hydrocarbons discharged onto the sea-floor during the drilling of offshore oil and gas wells. Immediately following the cessation of the drilling program, sediment samples were collected from the sea-floor on six occasions over a six-year period to determine the extent of

contamination of the seabed by drilling discharges and to investigate the biodegradation of components of the discharged hydrocarbon-based drilling fluid. Examination using gas chromatography-mass spectrometry (GC-MS) revealed that the hydrocarbons exhibited an increasingly biodegraded signature with increasing distance away from the discharge point, and with increasing proximity to the surface of the seabed. Analysis of the alkylnaphthalenes present in these biodegraded residues using GC-FTIR enabled the determination of the relative susceptibility to biodegradation for the individual dimethylnaphthalene, trimethylnaphthalene and tetramethylnaphthalene isomers. From this, a correlation between the susceptibility to biodegradation and the structure of the polymethylnaphthalenes was observed. A relationship was similarly observed for phenanthrene and the individual methylphenanthrene isomers. This work formed the basis for four publications, namely, Chegwidden et al. (1993), Fisher, Alexander and Kagi (1995; 1996) and Oliver and Fisher (1999). With the exception of the design of the initial sampling grid and the apparatus used for sample collection, both devised by Mr. A. Chegwidden (of Woodside Offshore Petroleum), and the results from biological and inorganic chemical analyses, provided by Mr. G. Oliver (of Woodside Energy Limited), this work is entirely my own.

Chapter 5 describes a case study into the biodegradation of petroleum accidentally discharged into a tropical coastal environment. Sediment samples were collected on nine occasions over a period of approximately three years, during which time the alteration of the hydrocarbons by weathering was studied. Analysis of the saturated and aromatic hydrocarbon components of the petroleum revealed that both hydrocarbon fractions exhibited an increasingly biodegraded profile with increased residence time in the sediments. In a similar approach to that described in Chapter 4, the order of susceptibility to biodegradation of each of the individual alkylnaphthalenes and alkylphenanthrenes with increasing biodegradation was determined. Furthermore, the hydrocarbons in the spilled petroleum encompassed a greater range molecular weight range of both saturated hydrocarbons and aromatic hydrocarbons than did the drilling fluid in Chapter 4. This allowed the extent of biodegradation to be assigned to each sample on the basis of the saturated hydrocarbon composition, to which the depletion of the alkylnaphthalenes and

alkylphenanthrenes by biodegradation under the conditions in the coastal sediments could be related. One publication resulted from this work (Fisher et al., 1998). Mr. G. Oliver managed the logistics of sample collection and pre-treatment.

Chapter 6 draws together many of the observations and concepts discussed earlier in the thesis. In Chapter 6, observations from the two case studies in the preceding chapters are compared. From similarities in the manner in which the aromatic hydrocarbon distributions were altered in these systems, molecular indicators were developed from which the extent of in-reservoir biodegradation of crude oils may be assessed. When considered in conjuction with the observations from the coastal environment, a coherent interpretation of the observations from the sea-floor sediments was also possible, revealing that each of the sea-floor sediment samples contained a mixture of petroleum biodegraded to varying extents. The utility of the aromatic hydrocarbons as indicators of multiple accumulation events in reservoirs was also investigated through the analysis of crude oils from a reservoir with multiple charges. Although two publications resulted from this work, namely Fisher et al. (1998) and Trolio et al. (1999), only results from the first of these are presented here. The contribution of Mr. G. Oliver to this publication is acknowledged above.

1.2 List of publications

1.2.1 Publications arising from this study

Alexander, R., Bastow, T.P., Fisher, S.J. and Kagi, R.I., 1995. Geosynthesis of organic compounds: II. Methylation of phenanthrene and alkylphenanthrenes. *Geochimica et Cosmochimica Acta*, **59**, 4259–4266.

Chegwidden, A., Fisher, S.J., Alexander, R. and Kagi, R.I., 1993. The fate of hydrocarbons associated with drilling from the North Rankin 'A' gas and condensate platform, Western Australia. *The APEA Journal,* **33**, 386-394.

Ellis, L., Fisher, S.J., Singh, R.K., Alexander, R., and Kagi, R.I., 1999. Identification of alkenylbenzenes in pyrolysates using GC-MS and GC-FTIR techniques: evidence for kerogen aromatic moieties with various binding sites. *Organic Geochemistry*, **30**, 651-665.

Fisher, S.J., Alexander, R. and Kagi, R.I., 1995. Hydrocarbons in sediments adjacent to an offshore gas production platform in North-Western Australia. In J.O. Grimalt and C. Dorronsoro (Eds.), Organic Geochemistry: Developments and Applications to Energy, Climate, Environment and Human History. A.I.G.O.A., San Sebastian, Spain, pp. 588-590.

Fisher, S.J., Alexander, R., Ellis, L. and Kagi, R.I., 1996. The analysis of dimethylphenanthrenes by direct deposition gas chromatography-Fourier transform infrared spectroscopy (GC-FTIR). *Polycyclic Aromatic Compounds*, **9**, 257-264.

Fisher, S.J., Alexander, R. and Kagi, R.I., 1996. Biodegradation of alkyl-naphthalenes in sediments adjacent to an offshore petroleum production platform. *Polycyclic Aromatic Compounds,* **11**, 35-42.

Fisher, S.J., Alexander, R., Kagi, R. I. and Oliver, G.A., 1998. Aromatic hydrocarbons as indicators of petroleum biodegradation and multiple accumulation events in North Western Australian Oil Reservoirs. In P.G. and R.R. Purcell (Eds.) *The Sedimentary Basins of Western Australia 2:* Proceedings of the Petroleum Exploration Society of Australia Symposium, Perth, WA, 1998, pp. 185-194.

Oliver, G.A. and Fisher, S.J., 1999. The persistence and effects of non-water based drilling fluids on Australia's North West Shelf: progress findings from three seabed surveys. *The APPEA Journal*, **39**, 648-662.

Trolio, R., Grice, K., Fisher, S.J., Alexander, R. and Kagi, R.I., 1999. Alkylbiphenyls and alkyldiphenylmethanes as indicators of petroleum biodegradation. *Organic Geochemistry*, **30**, 1241-1253.

1.2.2 Other publications relevant to this study

Alexander, R., Bastow, T.P., Fisher, S.J. and Kagi, R.I., 1993. Tetramethyl-naphthalenes in crude oils. *Polycyclic Aromatic Compounds*, **3**, 629-633.

Bastow, T.P., Alexander, R., Fisher, S.J., Singh, R.K. and Kagi, R.I., 2000. Geosynthesis of organic compounds. Part V - Methylation of alkylnaphthalenes. *Organic Geochemistry,* 31, 523-534.

Davis, G.B., Rayner, J.L., Fisher, S.J. and Patterson, B.M., 2000. Soil profile layering and seasonal effects on the fate and biodegradation of gasoline vapours in a sandy vadose zone. In C.D. Johnston (Ed.) *Contaminated Site Remediation: From Source Zones to Ecosystems.* Centre for Groundwater Studies, Perth, pp. 391-398.

Fisher, S.J., Alexander, R. and Kagi, R.I., 1993. The use of silicalite for removal of species which interfere in the trace analysis of polycyclic aromatic hydrocarbons in biota. *Polycyclic Aromatic Compounds*, **3**, 405-414.

Johnston, C.D., Fisher, S.J. and Rayner, J.L., 2001. Removal of petroleum from the vadose zone during multiphase extraction at a contaminated industrial site. In *Preprints of Papers, Third International Conference on Groundwater Quality, Groundwater Quality 2001*. Sheffield, United Kingdom, 18-21 June 2001, pp. 334-346.

Kagi, R.I., Fisher, S.J. and Alexander, R., 1988. Behaviour of petroleum in northern Australian waters. In P.G. and R.R. Purcell (Eds.), *Proceedings of the North West Shelf Symposium*. Petroleum Exploration Society of Australia, pp. 633-642

Papp, R. and Fisher, S.J., 1999. Drilling fluids and their environmental management: characterisation of base fluids and the introduction of quality control procedures. *The APEA Journal,* **39**, 628-639.

CHAPTER 2

2 Experimental

2.1 Materials and reagents

2.1.1 Solvents

Analytical grade *n*-pentane, *n*-hexane, diethylether and dichloromethane were purified by fractional distillation using procedures outlined by Perrin and Armarego (1988). These were checked for purity by evaporating 100 mL of each solvent to 100 μL followed by analysis of the residue by gas chromatography.

2.1.2 Reagents

Analytical grade reagents were used without further purification. Where these were not commercially available, laboratory grade reagents were purified using the procedures outlined by Perrin and Armarego (1988). Precipitated copper (Ajax, Technical Grade) was activated by washing with successive portions of hydrochloric acid (1 M), deionised water, ethanol and purified dichloromethane.

2.1.3 Liquid chromatography stationary phases

Alumina

Basic alumina (Ajax, Laboratory Grade) used for column liquid chromatography was extracted with purified dichloromethane for approximately 24 hours using a Soxhlet apparatus, dried, then activated by heating at 150°C for at least 24 hours prior to use. Thin layer chromatography plates were prepared by applying a 0.3 mm thick coating of neutral alumina (Merck) to 20 cm x 20 cm glass plates. The plates were pre-developed in *n*-hexane, and reactivated at 150°C for at least 12 hours prior to use.

Silica Gel

Kieselgel 60G (Merck) used for column liquid chromatography was similarly extracted using dichloromethane, then activated at 150°C for at least 24 hours prior to use.

Molecular Sieves

High-silica sodium mordenite and ZSM-5 molecular sieves (PQ Corporation) were heated under vacuum (0.1 Torr) at 150°C for at least 12 hours immediately prior to use in a Gallenkamp drying pistol.

2.2 Reference compounds

2.2.1 Alkylnaphthalenes

The dimethylnaphthalene isomers (DMNs) and trimethylnaphthalene isomers (TMNs) listed in Table 2.1, with the exception of 2,6-DMN and 1,8-DMN, were prepared by Dr. S.J. Rowland. The preparation and identification of these has been previously described (Alexander, Kagi and Sheppard, 1983; Rowland, Alexander and Kagi, 1984). An authentic sample of 2,6-DMN was obtained from Tokyo Kasei Organic Chemicals, Japan and 1,8-DMN was provided by Dr. M. Mocerino, synthesised from 1,8-naphthalic anhydride as described in Mitchell, Topsom and Vaughan (1962). The listed tetramethylnaphthalene isomers (TeMNs), were prepared by Dr. P.G. Forster. The preparation and identification of these has also been described previously (Forster, Alexander and Kagi, 1989).

2.2.2 Alkylphenanthenes

All of the methylphenanthrene isomers (MPs), dimethylphenanthrene isomers (DMPs) and ethylphenanthrene isomers (EPs) listed in Table 2.1 were obtained as reference compounds from Chiron Laboratories, Norway. The purity of each compound was determined by gas chromatography to be greater than 98%. 1,7,9-Trimethylphenanthrene and 1,9-dimethyl-7-isopropylphenanthrene (9-methylretene) were prepared from the appropriate alkylstilbenes by Dr. T.P. Bastow as described in Alexander et al. (1995).

2.2.3 Miscellaneous compounds

Polycyclic aromatic hydrocarbons

Naphthalene, phenanthrene, anthracene and chrysene were purchased from the National Institute of Standards and Technology (NIST), USA.

Table 2-1: All possible isomers of the DMNs, TMNs, TeMNs, MPs, EPs and DMPs. Compounds for which a reference compound was obtained are denoted (✓).

Alkylnaphthalenes						Alkylphenanthrenes			
1,2-DMN	✓	1,2,3-TMN	✓	1,2,3,4-TeMN	✓	1-MP	✓	1,2-DMP	✓
1,3-DMN	✓	1,2,4-TMN	✓	1,2,3,5-TeMN	✓	2-MP	✓	1,3-DMP	✓
1,4-DMN	✓	1,2,5-TMN	✓	1,2,3,6-TeMN	✓	3-MP	✓	1,4-DMP	x
1,5-DMN	✓	1,2,6-TMN	✓	1,2,3,7-TeMN	✓	4-MP	✓	1,5-DMP	✓
1,6-DMN	✓	1,2,7-TMN	✓	1,2,3,8-TeMN	x	9-MP	✓	1,6-DMP	✓
1,7-DMN	✓	1,2,8-TMN	✓	1,2,4,5-TeMN	✓			1,7-DMP	✓
1,8-DMN	✓	1,3,5-TMN	✓	1,2,4,6-TeMN	✓			1,8-DMP	✓
2,3-DMN	✓	1,3,6-TMN	✓	1,2,4,7-TeMN	✓	1-EP	✓	1,9-DMP	✓
2,6-DMN	✓	1,3,7-TMN	✓	1,2,4,8-TeMN	x	2-EP	✓	1,10-DMP	x
2,7-DMN	✓	1,3,8-TMN	✓	1,2,5,6-TeMN	✓	3-EP	✓	2,3-DMP	✓
		1,4,6-TMN	✓	1,2,5,7-TeMN	✓	4-EP	x	2,4-DMP	✓
		1,4,5-TMN	✓	1,2,5,8-TeMN	x	9-EP	✓	2,5-DMP	✓
		1,6,7-TMN	✓	1,2,6,7-TeMN	✓			2,6-DMP	✓
		2,3,6-TMN	✓	1,2,6,8-TeMN	x			2,7-DMP	✓
				1,2,7,8-TeMN	x			2,9-DMP	✓
				1,3,5,7-TeMN	✓			2,10-DMP	✓
				1,3,5,8-TeMN	x			3,4-DMP	x
				1,3,6,7-TeMN	✓			3,5-DMP	✓
				1,3,6,8-TeMN	✓			3,6-DMP	✓
				1,4,5,8-TeMN	✓			3,9-DMP	✓
				1,4,6,7-TeMN	✓			3,10-DMP	✓
				2,3,6,7-TeMN	✓			4,5-DMP	✓
								4,9-DMP	✓
								4,10-DMP	✓
								9,10-DMP	x

Alkylanthracenes

Authentic samples of 1-methylanthracene, 2-methylanthracene and 2-ethylanthracene were obtained from Tokyo Kasei Organic Chemicals, Japan.

Alkenylbenzenes and alykylbenzenes.

Dodec-11-enylbenzene, dodec-2-enylbenzene, *trans* dodec-1-enylbenzene and a mixture of *cis* and *trans* dodec-2-enylbenzene were prepared by Dr. L. Ellis as described in Ellis et al. (1999). Alkylbenzenes were also prepared by Dr. L. Ellis as described in Ellis, Kagi and Alexander (1992).

Chlorinated hydrocarbons

Analytical Grade 1-chlorooctane, 1-chlorodecane, 1-chlorotetradecane, 1-chloro-octadecane and 1,2-dichlorobenzene were obtained from BDH Chemicals.

2.3 Preparation of solutions of reference compounds

2.3.1 Calibration solutions for multicomponent GC-FTIR analysis

1,3,5-TMN and 1,4,6-TMN

Two separate solutions were prepared by dissolving authentic samples of 1,3,5-TMN (10 mg) and 1,4,6-TMN (10 mg) in 100 mL of *n*-hexane. Aliquots of each solution were mixed in various proportions to yield eight solutions containing both isomers: these were analysed using GC-MS with a BP20 column to determine the relative abundance of each compound in the mixture, shown in Table 2-2. The mixtures and the solutions containing single isomers were analysed using GC-FTIR.

1,2,4,6-TeMN, 1,2,4,7-TeMN and 1,4,6,7-TeMN

Three separate solutions containing an unknown concentration of one of the (co-eluting) 1,2,4,6-TeMN, 1,2,4,7-TeMN and 1,4,6,7-TeMN isomers were mixed with solutions containing 1 mg mL^{-1} of 1-MP, 2-MP and 9-MP respectively. Three solutions resulted, each comprising one TeMN and one MP as an internal standard.

Table 2-2: Composition of calibration standards of co-eluting TMNs determined volumetrically and using GC-MS analysis.

Mixture No.	Volume of aliquot		Relative abundance % (GC-MS)	
	1,3,5-TMN	1,4,6-TMN	1,3,5-TMN	1,4,6-TMN
1	5	95	7	93
2	15	85	17	83
3	25	75	26	74
4	50	50	51	49
5	55	45	55	45
6	70	30	70	30
7	80	20	80	20
8	95	5	93	7

These were each analysed using GC-MS and the relative areas of the two peaks from the total ion chromatogram expressed as a ratio (i.e. 1-MP/1,2,4,6-TeMN = 1.46; 2-MP/1,4,6,7-TeMN = 2.26; 3-MP/1,2,4,7-TeMN = 2.62). Aliquots of the solutions were mixed in various proportions to yield 13 solutions, each comprising the TeMN isomers and corresponding MP internal standards. Each of these mixtures was analysed using GC-MS, and the proportion of each of the co-eluting TeMNs calculated by multiplication of the established peak area ratio with the peak area of the appropriate MP internal standard. The calculated compositions of the 13 calibration standards are shown in Table 2-3.

Table 2-3: Composition of calibration standards of co-eluting TeMNs determined from GC-MS analysis.

Mixture	Relative Abundance (%)		
	1,2,4,6-TeMN	1,2,4,7-TeMN	1,4,6,7-TeMN
1	45	23	32
2	55	6	39
3	16	35	49
4	58	32	10
5	22	10	68
6	78	9	13
7	24	58	18
8	0	0	100
9	100	0	0
10	0	100	0
11	49	51	0
12	0	48	52
13	50	0	50

In each case, the sum of the calculated peak areas for the individual TeMNs was within 2% of the measured peak area of the co-eluting TeMNs. Each mixture was subsequently analysed using GC-FTIR

2-EP, 9-EP and 3,6-DMP

As for the TeMNs, separate solutions containing one of 2-EP, 9-EP and 3,6-DMP were mixed with solutions of the internal standards 2-MP, 9-MP and 1-MP respectively. Peak area ratios were established for each from GC-MS total ion chromatograms (2-MP/2-EP = 1.49; 9-MP/9-EP = 1.74 and 1-MP/3,6-DMP = 2.52). Aliquots of the solutions were mixed in various proportions to yield 6 solutions of varying composition of the DMP isomers and the corresponding MP internal standards. The composition of each of the mixtures, shown in Table 2-4, was determined using GC-MS analysis prior to analysis using GC-FTIR.

Table 2-4: Composition of calibration standards of co-eluting 2-EP, 9-EP and 3,6-DMP determined from GC-MS analysis.

Mixture	Relative abundance (%)		
	2-EP	9-EP	3,6-DMP
1	40	30	30
2	30	35	35
3	10	20	70
4	25	5	70
5	70	20	10
6	30	30	40

1,3-DMP, 2,10-DMP, 3,9-DMP and 3,10-DMP

As for the TeMNs, separate solutions containing one of 1,3-DMP, 2,10-DMP, 3,9-DMP and 3,10-DMP were mixed with solutions of the internal standards 3-MP, 2-MP, 9-MP and 1-MP respectively. Peak area ratios were established for each from GC-MS total ion chromatograms (3-MP/1,3-DMP = 1.95; 1-MP/3,10-DMP = 1.56; 9-MP/3,9-DMP = 2.41 and 2-MP/2,10-DMP = 0.99). Aliquots of the solutions were mixed in various proportions to yield 14 solutions of varying composition as shown in Table 2-5. Each solution was analysed using GC-FTIR.

Table 2-5: Composition of calibration standards of co-eluting DMPs determined from GC-MS analysis

Mixture No.	Relative abundance (%)			
	1,3-DMP	3,10-DMP	3,9-DMP	2,10-DMP
1	30	31	26	13
2	33	31	8	28
3	30	10	29	31
4	9	32	31	28
5	21	25	14	40
6	9	11	6	74
7	13	17	42	28
8	12	58	8	22
9	54	14	8	24
10	29	33	19	19
11	23	27	5	45
12	25	10	17	48
13	9	28	16	47
14	25	26	27	22

2.3.2 Internal and surrogate standards

A solution containing 1-chlorooctane, 1-chlorodecane, 1-chlorotetradecane, and 1-chlorooctadecane, used as surrogate standards in the extraction of hydrocarbons from marine sediments, was prepared by dissolving 102 mg, 110 mg, 106 mg and 101 mg of these compounds respectively in *n*-hexane (50 mL). 1,2-Dichlorobenzene (22 mg, BDH Chemicals), used as an internal standard for gas chromatographic analysis, was similarly dissolved in *n*-hexane (50 mL).

2.4 Geochemical techniques: sea-floor and coastal sediments

2.4.1 Sample preparation

The sediment samples were drained and then divided into halves. Dichloromethane (50 mL) was added to one half, which was stored at -10°C for future reference. A 50 μL aliquot of the surrogate standard solution containing 1-chlorooctane (10.2 μg), 1-chlorodecane (11.0 μg), 1-chlorotetradecane (10.6 μg) and 1-chlorooctadecane (10.1 μg), was added to the remaining sample. This sediment was allowed to dry in air for approximately one hour.

2.4.2 Extraction of soluble organic matter from sediments

The dried sediment (typically 100-200 g) was extracted with a mixture of dichloromethane (180 mL) and methanol (20 mL) under reflux in an ultrasonic bath for two hours. The extracted sediment was filtered off and allowed to dry at room temperature for approximately 24 hours, then at 105°C for a further 24 hours. The dried sediment was weighed to a constant weight.

The solvent extract was dried with anhydrous magnesium sulphate and filtered. The solvent was removed from the filtrate by fractional distillation *via* a Vigreux column to leave a residue of approximately 5 mL to which activated copper (approximately 0.1 g) was added to remove elemental sulphur. The mixture was agitated with the aid of ultrasonication, the copper was filtered off and the filtrate concentrated to approximately 500 μL using a Kuderna-Danish flask equipped with a micro Snyder column. The dichloromethane was carefully exchanged with *n*-pentane by evaporation using a gentle stream of nitrogen.

2.4.3 Fractionation of soluble organic matter by column liquid chromatography

Total petroleum hydrocarbon (TPH) fractions

Glass columns [20 cm x 1 cm internal diameter, (i.d.)] were packed with activated basic alumina (3 g) in *n*-pentane (15 mL). The concentrated sediment extract was applied to a column and a fraction containing the total petroleum hydrocarbons was eluted with a solvent mixture of dichloromethane (8 mL) and *n*-pentane (22 mL). The volume of solvent was reduced to approximately 500 μL by evaporation as described above and the residue was transferred to a pre-weighed glass sample vial. The neat TPH fraction was recovered by careful evaporation of the solvent in a stream of nitrogen and, where practical (i.e. > 1 mg), was weighed. The residue was dissolved in *n*-hexane (typically 500 μL per mg of TPH fraction) and a 10 μL aliquot of the internal standard solution was added, containing 1,2 dichlorobenzene (4.5 μg). The mixture was then analysed using capillary gas chromatography with flame ionisation detection (GC-FID).

Saturated and aromatic hydrocarbon fractions

An aliquot of the TPH fraction containing approximately 1 to 5 mg was further separated into saturated and aromatic hydrocarbon fractions by liquid chromatography. A Pasteur pipette was packed with silica gel (0.6 g) as a suspension in *n*-pentane (5 mL). The saturated hydrocarbons were eluted with *n*-pentane (4 mL) and the aromatic hydrocarbons with a solvent mixture of dichloromethane (0.5 mL) and *n*-pentane (3.5 mL). The fractions were concentrated by evaporation of the solvent and transferred to glass vials as described above prior to analysis by GC-FID, GC-MS and GC-FTIR.

2.4.4 Preparation of calibration standards for TPH quantification

A portion (32 mg) of the TPH fraction from one sample was dissolved in *n*-hexane (100 mL). Aliquots containing 32 μg, 64 μg, 192 μg, 320 μg, 640 μg, 960 μg and 1280 μg of the TPH fraction were removed from this solution and dissolved in *n*-hexane (500 μL). A 50 μL aliquot of the surrogate standard was added to each solution, and each was analysed using GC-FID.

2.4.5 Isolation of branched and cyclic alkanes

A Pasteur pipette was packed with ZSM-5 molecular sieves (1 g) as a suspension in *n*-pentane (5 mL). A sample of the saturated hydrocarbon fraction (approximately 2 mg) was applied to the top of the column and the system was allowed to stand for approximately 10 minutes. The branched and cyclic alkanes were eluted with *n*-pentane (approximately 5 mL) and concentrated by evaporation of the solvent to approximately 1mL using a Kuderna-Danish flask fitted with a micro Snyder column. The eluted fraction was analysed using GC-MS selected ion monitoring (SIM) techniques.

2.4.6 Isolation of the dinuclear and trinuclear aromatic hydrocarbon fractions

The aromatic hydrocarbon fraction from the column liquid chromatography separation was further fractionated using thin layer chromatography on a glass plate coated with 0.3 mm film of neutral alumina. Compounds were eluted with *n*-hexane and visualised using an ultra violet lamp (254 nm). Fractions containing dinuclear

aromatic hydrocarbons or trinuclear aromatic hydrocarbons were isolated by comparison with the retention behaviour of naphthalene and phenanthrene respectively, removing the appropriate section of stationary phase from the plate and extracting with dichloromethane. The solvent was evaporated as described above prior to analysis using GC-MS and GC-FTIR.

2.4.7 Isolation of TeMNs from the dinuclear aromatic hydrocarbon fraction

The dinuclear aromatic hydrocarbon fraction was further fractionated to obtain a TeMN fraction using thin layer chromatography on neutral alumina. The dimensions of the plate and stationary phase thickness were identical to that described above. Here, however, the alumina was deactivated prior to application of the dinuclear aromatic fraction by allowing the plate to absorb atmospheric moisture for approximately 30 minutes. Compounds were eluted with *n*-hexane and visualised using an ultra violet lamp (254 nm). A fraction enriched in TeMNs was isolated by comparison with the retention behaviour of several TeMNs contained in a mixture of reference compounds, and solvent extraction as described above.

2.5 Geochemical techniques: crude oils and ancient sediments

2.5.1 Sample preparation

Samples of sedimentary material from the Kelp-1, 2379 m and Geelvinck-1 boreholes were crushed in a N.V. Tema grinder to a particle size of approximately 150 μm.

2.5.2 Extraction of soluble organic matter from sediments

The soluble organic matter was extracted from the crushed sedimentary material from Kelp-1, 2379 m (approximately 20 g), desulphurised and concentrated in an identical manner to the sea-floor and coastal sediments, described previously (Section 2.4.2). The crushed Geelvinck-1 shale (5 g) was extracted three times using a mixture of dichloromethane (40 mL) and methanol (3 mL) with ultrasonic agitation for 2 hours each.

2.5.3 Geelvinck-1 shale pyrolysis

The solvent-extracted shale was placed in a Pyrex glass tube under vacuum (approximately 0.1 Torr) and inserted into a temperature-controlled furnace at 350° C. The tube was heated rapidly (50°C min^{-1}) to 550°C where the temperature was maintained for 15 min. The expelled volatile components were cryogenically trapped in a U-tube with liquid nitrogen, and later combined with dichloromethane washings of the pyrolysis residue and Pyrex tube. The solvent was evaporated to obtain the combined pyrolysate liquid. The polar material was removed from the pyrolysate using column chromatography on alumina to obtain a TPH fraction as described previously (Section 2.4.3). Subsequent to analysis using GC-MS, this fraction was further fractionated using thin layer chromatography on neutral alumina (Section 2.4.6) to remove polycyclic aromatic hydrocarbons. A fraction enriched in alkenes, alkanes and monoaromatic hydrocarbons was isolated by comparison with the retention behaviour of several alkylbenzenes and alkenylbenzenes contained in a mixture of reference compounds, and solvent extraction as described above. This fraction was concentrated and analysed using GC-FTIR.

2.5.4 Fractionation of crude oils and rock extracts

The crude oils and extract from Kelp-1, 2379 m were treated in an identical manner to the TPH fractions isolated from the sea-floor and coastal sediments to obtain aromatic and dinuclear and trinuclear aromatic hydrocarbon fractions. Lambert-1 crude oil was further fractionated using thin layer chromatography to obtain a fraction enriched in TeMNs (Section 2.4.7).

2.5.5 Fractionation of alkylphenanthrenes using mordenite molecular sieves

These techniques were applied to the trinuclear aromatic hydrocarbon fraction isolated from Lambert-1 crude oil (approximately 2 mg), and a mixture of authentic samples of 3,5-DMP and 2,6-DMP.

Flow-through separation

A Pasteur pipette was packed with mordenite molecular sieves (approximately 1 g) as a suspension in pentane (5 mL). The sample containing the alkylphenanthrenes was applied to the top of the column and the system was allowed to stand for

approximately 10 minutes. The column was washed with *n*-pentane (approximately 5 mL), and the eluted fraction collected and concentrated using a micro Kuderna-Danish apparatus as described above prior to analysis using GC-MS and GC-FTIR techniques. The sieves were removed from the column, covered with *n*-hexane (10 mL), then dissolved with a minimum volume (approximately 2 mL) of a 50% w/w solution of hydrofluoric acid. The aqueous solution was diluted with a 5% w/v solution of sodium chloride in water (50 mL), shaken and the *n*-hexane layer removed. The brine solution was extracted with successive portions of *n*-pentane (3 x 5 mL) and the extracts combined with the *n*-hexane layer. The organic extract was dried with anhydrous magnesium sulphate and the solution, containing hydrocarbons retained by the molecular sieves, was concentrated and also analysed using GC-MS and GC-FTIR.

Batch-wise (static) separation

The mordenite molecular sieve (approximately 1 g) was placed into a round-bottomed flask (10 mL) and covered with *n*-pentane (approximately 5 mL). A sample of the trinuclear aromatic hydrocarbon fraction (10 mg) was added, the flask was fitted with a reflux condenser, and the system agitated with the aid of ultrasonication for approximately 30 minutes. The sieves were filtered off using a vacuum filtration system, and rinsed with successive portions of *n*-pentane (3 x 1 mL). The filtrate and washings from the sieves, containing hydrocarbons not sorbed by the molecular sieves, were combined and concentrated. A solution containing the hydrocarbons retained by the sieves was obtained in a manner identical to that described for the flow-through method. Both fractions were analysed using GC-MS and GC-FTIR techniques.

2.5.6 Procedural blanks

Procedural blanks using the preparative procedures described in the preceding sections (2.4.1 to 2.4.7 and 2.5.1 to 2.5.5) were performed regularly during the course of the work described in this thesis. This process involved involved carrying out each procedure in the absence of a geochemical sample, and analysing the extract or fraction using GC-MS and GC-FTIR techniques as described in the following sections, to ensure that interference from analytical artefacts was eliminated.

2.6 Analytical methods and instrumentation

2.6.1 Gas chromatography with flame ionisation detection.

TPH fractions

Capillary gas chromatography was carried out using a Hewlett-Packard (HP) model 5880 gas chromatograph equipped with a vaporising injector, a 50 m x 0.22 mm i.d. fused silica column coated with a 0.25 μm film of 5% phenyl polysiloxane stationary phase (BP5, SGE, Australia), and a flame ionisation detector (FID). Hydrogen was used as the carrier gas at an initial linear flow velocity of 40 cm s^{-1}. Total petroleum hydrocarbon fractions were analysed using a temperature gradient of 4°C min^{-1} from 65°C to 280°C followed by holding the upper temperature isothermally for 20 minutes.

Analysis of pristane and phytane diastereomers

Analysis was performed using the instrument described above equipped with a 50 m x 0.22 mm i.d. fused silica column coated with a 0.25 μm film of 100% dimethyl-polysiloxane (BP1, SGE, Australia). Hydrogen was used as the carrier gas at an initial linear flow velocity of 40 cm s^{-1}. Saturated hydrocarbon fractions were analysed using a temperature gradient of 1°C min^{-1} from 65°C to 180°C and then 10°C min^{-1} to 280°C.

2.6.2 Gas chromatography - mass spectrometry

Hydrocarbon fractions other than branched and cyclic alkanes

GC-MS analysis was performed using a HP 5890 Series II gas chromatograph equipped with a HP 5971 Mass Selective Detector, a HP Model 7673A automatic cool on-column injection system with a programmable inlet pressure control and a 40 m x 0.18 mm i.d. fused silica open tubular column coated with a 0.4 μm film of 5% phenyl methylpolysiloxane (DB-5, J & W Scientific, USA). With the exception of the branched and cyclic alkane fraction, all fractions were analysed using identical operating conditions. The temperature of the oven was programmed from 70°C to 290°C at a rate of 3°C min^{-1}, then held isothermally for 10 minutes. Helium carrier gas was maintained at a constant linear velocity of 33 cm s^{-1} throughout the analysis.

Typical mass spectrometer conditions were: ionisation energy 70 eV; source temperature 200°C; electron multiplier voltage 2000 V; mass range 50 to 550 Daltons.

Branched and cyclic alkanes

The branched and cyclic alkane fraction was analysed using a similar instrument equipped with a 60 m x 0.18 mm i.d. fused silica open tubular column coated with a 0.4 µm film of 100 % methylpolysiloxane (DB-1, J & W Scientific, USA). The temperature of the oven was programmed from 50°C to 274°C at a rate of 8°C min^{-1}, then 1°C min^{-1} to 290°C where the temperature was held isothermally for 40 minutes. Helium carrier gas was maintained at a constant linear velocity of 33 cm s^{-1} throughout the analysis. The mass spectrometer was operated in the SIM mode where positive ions with a mass to charge ratio (m/z) of 123, 177, 191, 193 and 217 were monitored, each with a dwell time of 50 msec. Mass spectrometer conditions were otherwise identical to those described above.

Analysis using other stationary phases

A HP 5890 gas chromatograph equipped with a HP 5970 Mass Selective Detector and a HP Model 7673A automatic cool on-column injection system with manual inlet pressure control was equipped with columns other than DB-1 or DB-5. Typical mass spectrometer conditions were: ionisation energy 70 eV; source temperature 200°C; electron multiplier voltage 2000 V; mass range 45 to 450 Daltons.

With a 50 m x 0.22 mm i.d. fused silica open tubular column coated with a 0.25 µm film of polyethylene glycol stationary phase (BP20, SGE, Australia) installed, dinuclear aromatic hydrocarbon fractions were analysed by programming the temperature of the oven from 70°C to 240°C at a rate of 3°C min^{-1} where it was then held isothermally for 20 minutes. Helium carrier gas was maintained at a constant inlet pressure of 20 psi (138 kPa) throughout the analysis. Trinuclear aromatic hydrocarbons were analysed by programming the temperature of the oven from 70°C to 270°C at a rate of 15°C min^{-1} where it was then held isothermally for 40 minutes. Helium carrier gas was maintained at a constant inlet pressure of 40 psi (276 kPa) throughout the analysis.

With a 50 m x 0.22 mm i.d. fused silica open tubular column coated with a 0.25 μm film thickness of permethylated β-cyclodextrin (Cydex-B, SGE, Australia) installed, dinuclear aromatic hydrocarbon fractions were analysed by programming the temperature of the oven from 70°C to 240°C at a rate of 3°C min^{-1}, where it was then held isothermally for 10 minutes. Helium carrier gas was maintained at a constant inlet pressure of 25 psi (172.4 kPa) throughout the analysis.

2.6.3 Determination of gas chromatography retention indices

Retention indicies were determined on both a DB-5 and a BP20 capillary column for 1-methylanthracene, 2-methylanthracene, 2-ethylanthracene and the alkyl-naphthalenes and alkylphenanthrenes listed in Table 2-1 for which authentic samples were obtained.

DB-5 column

Several solutions of these reference standards in *n*-hexane were prepared (approximately 5 to 30 μg mL^{-1}), each containing a mixture of no more than three (non-coeluting) isomers from each of the DMNs, TMNs, TeMNs, MPs, EPs and DMPs. A solution containing the alkylanthracenes was also prepared. An aliquot of a separate solution containing naphthalene, phenanthrene and chrysene (each approximately 100 μg mL^{-1}) was added to each of the solutions of reference standards. The resulting solutions were analysed in triplicate using GC-MS under identical conditions to those described above for the analysis of fractions other than branched and cyclic alkanes.

BP20 column

Solutions containing only alkylnaphthalene, alkylphenanthrene or alkylanthracene reference standards were prepared. A solution containing naphthalene and phenanthrene was added to each of the alkylnaphthalene solutions prior to analysis of each as described above for dinuclear aromatic hydrocarbon fractions. Under these conditions, naphthalene and phenanthrene elute during the temperature gradient, allowing the retention indicies to be calculated according to the method described in Lee et al. (1979). Phenanthrene and chrysene were added to each of the alkylphenanthrene and alkylanthracene solutions and these were analysed as

described for trinuclear aromatic hydrocarbon fractions. In this way, phenanthrene and chrysene eluted from the column while it was held isothermally at 270°C, enabling the determination of retention indicies (Lee et al., 1979) of the alkylphenanthrenes and alkylanthracenes without exceeding the maximum temperature restriction of 270°C for this phase.

2.6.4 Direct deposition GC-FTIR

Infrared data were acquired by direct deposition GC-FTIR using a Bio-Rad Digilab Tracer® accessory interfaced with a HP 5890 gas chromatograph and a Bio-Rad Digilab Model FTS-60A Fourier transform infrared spectrometer. The gas chromatograph was equipped with an OCI-3 on-column injector (SGE, Australia) connected to a 60 m x 0.22 mm i.d. fused silica open tubular column coated with a 0.25 μm film of stationary phase (DB-5, J & W Scientific, USA). The temperature of the oven was programmed from 40°C to 290°C at a rate of 3°C min^{-1}, then held isothermally for 10 minutes. Hydrogen was the carrier gas at a linear flow velocity of 30 cm s^{-1} at the initial operating temperature.

The column effluent was passed through a fused silica transfer line (1 m x 0.15 mm i.d.) to the fused silica deposition tip (1 cm x 0.05 mm i.d.). The temperature of both of these heated transfer zones was maintained at 290°C. The eluants were cryogenically focussed onto a moving zinc selenide slide (60 mm x 30 mm x 2 mm) held at approximately -180°C. The resultant frozen deposits described a continuous square wave pattern of 1.2 mm amplitude and 0.2 mm period. The slide speed which controls the post-GC resolution of the compounds was maintained at a nominal setting of 2 enabling compounds separated by a minimum of two seconds to be resolved. The infrared beam was focussed by a cassagrainian microscope onto a fast response mercury/cadmium/telluride (MCT) detector.

The infrared spectrum was scanned between 650 cm^{-1} and 4000 cm^{-1} at a resolution of 8 cm^{-1} and a scan rate of 4 scans per scanset producing an absorbance spectrum every 0.8 seconds. Functional group chromatograms were collected in selected regions of the infrared spectrum, typically 700 cm^{-1} to 920 cm^{-1}, 1400 cm^{-1} to

1650 cm^{-1} and 2800 cm^{-1} to 3000 cm^{-1}. High resolution of selected components were obtained by re-examining the solid deposited material after the chromatographic analysis was completed. These spectra were obtained by the addition of the interferograms of 256 successive scans at a resolution of 2 cm^{-1}.

CHAPTER 3

3 The use of direct deposition gas chromatography–Fourier transform spectroscopy (GC-FTIR) for the analysis of individual components in complex mixtures of aromatic hydrocarbons.

3.1 Abstract

Aromatic hydrocarbons occur naturally as complex mixtures in crude oils and sedimentary rock extracts and in synthetic materials such as petroleum fractions, coal tar, shale oil, and commercial hydrocarbon fuels. Conventionally these mixtures are analysed in isolated aromatic fractions using gas chromatography-mass spectrometry (GC-MS) on a capillary column coated with a medium polarity stationary phase. Under these conditions, the mixture is usually not completely resolved with several isomers co-eluting. Furthermore, the mass spectra of these co-eluting isomers may be so similar that one is unable to differentiate between them, and their abundance may therefore not be determined. To address this issue, the application of direct deposition GC-FTIR spectroscopy to the analysis of co-eluting alkylnaphthalenes and alkylphenanthrenes commonly occurring in petroleum was investigated. In a typical Australian crude oil, all instances where co-eluting mixtures of dimethylnaphthalenes, trimethylnaphthalenes, tetramethylnaphthalenes and dimethylphenanthrenes occurred were identified using GC-FTIR techniques. Since each compound has a unique infrared spectrum, the relative abundance of each isomer in the mixture could be determined by comparing the spectrum of the peak from the combined co-eluting compounds with the spectrum of each of the isomers. Further, this technique was used to elucidate the sorption behaviour of ethylphenanthrenes and dimethylphenanthrenes into mordenite molecular sieves. Further examples of the use of these compound specific GC-FTIR techniques include the identification of compounds which do not necessarily co-elute. For example 1,9-dimethyl-7-isopropylphenanthrene was, for the first time, unambiguously identified in extracts obtained from a sedimentary rock, while two homologous series

of alkenylbenzenes were identified in pyrolysis products obtained from a shale, including the hitherto unknown *trans* alk-1-enylbenzenes.

3.2 Introduction

3.2.1 Resolution of co-eluting aromatic hydrocarbons

Alkylnaphthalenes and alkylphenanthrenes are ubiquitous in petroleum and occur as complex mixtures in crude oils, sedimentary rock extracts and many other materials (Worrall, 1996). Differences in the relative abundances of several isomers within these compound classes have been used to indicate the thermal maturity (Radke 1987; Budzinski et al., 1993a), the origin (Alexander et al., 1988; Radke, Rullkötter and Vriend, 1994; Budzinski et al.,1995a) and the extent of biodegradation of the petroleum (Volkman et al., 1984; Williams et al.; 1986; Rowland et al., 1986).

Conventionally, the mixtures of aromatic hydrocarbon isomers are analysed using GC-MS techniques using a column with a medium polarity stationary phase; however, chromatographic resolution of all isomers is not achieved under this regime and several of these compounds co-elute. Furthermore, as shown in Figure 3-1, the mass spectra of these co-eluting isomers may be so similar that one is unable to differentiate between them, and their abundance may therefore not be determined.

Although all of the dimethylnaphthalene (DMN) isomers and trimethylnaphthalene (TMN) isomers may be resolved by analysis on two columns of differing polarity stationary phases as shown in Table 3-1, resolution of all of the tetramethyl-naphthalene (TeMN) isomers under these conditions is not possible (Alexander et al., 1993; Forster, Alexander and Kagi, 1989). To achieve this separation, a third analysis using a shape selective stationary phase is required, which will be discussed further later.

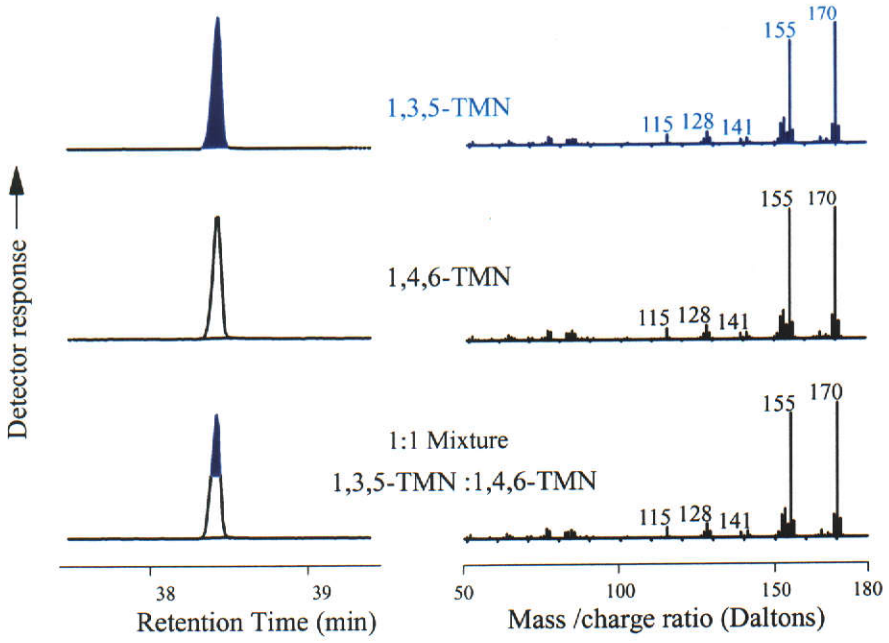

Figure 3-1: Mass spectra obtained from (a) 1,3,5-TMN, (b) 1,4,6-TMN and (c) a mixture of both TMN isomers

The extent of co-elution is even more pronounced for the alkylphenanthrenes. For example, of the 5 possible ethylphenanthrene (EP) isomers and 25 dimethylphenanthrene (DMP) isomers, only 15 may be completely resolved and therefore unambiguously identified using a non-polar stationary phase such as a 5% phenyl polymethylsiloxane column (Fisher et al., 1996; Ellis, Alexander and Kagi, 1994).

Co-elution thus poses a severe limitation to the analysis and subsequent interpretation of these compounds where they occur as mixtures (e.g. petroleum). Several different approaches have been taken to overcome this. A method has been described (Radke et al., 1984; Garrigues et al., 1987), where high-resolution spectrofluorimetry at low temperatures (Shpol'skii effect) is applied to enable the identification of all of the DMP isomers. Briefly, this procedure required preliminary fractionation of the aromatic hydrocarbons using several HPLC separations to obtain a fraction containing only one to three EP and /or DMP isomers. Subsequent analysis of this fraction enabled the identification of the isomers on the basis of differences in their Shpol'skii emission spectra.

Table 3-1: Retention indices of polymethylnaphthalenes on DB-5 (J&W Scientific) and BP20 (SGE) stationary phases. Co-eluting compounds (DB-5) are grouped by shading.

Compound	Retention Index	
Stationary phase→	DB-5	BP20
2,6-DMN	239.79	225.55
2,7-DMN	239.98	225.68
1,3-DMN	242.52	229.59
1,7-DMN	242.55	228.83
1,6-DMN	243.09	229.64
1,4-DMN	245.72	233.20
2,3-DMN	245.79	233.67
1,5-DMN	246.33	233.99
1,2-DMN	248.34	236.67
1,8-DMN	251.68	241.80
1,3,7-TMN	260.15	240.95
1,3,6-TMN	261.05	241.64
2,3,6-TMN	263.51	245.32
1,4,6-TMN	264.17	244.24
1,3,5-TMN	264.18	245.34
1,2,7-TMN	266.13	247.57
1,6,7-TMN	266.42	248.43
1,2,6-TMN	266.79	248.50
1,2,4-TMN	269.25	252.23
1,2,5-TMN	270.44	252.90
1,2,3-TMN	n.d.	257.35
1,3,5,7-TeMN	279.97	256.21
1,3,6,7-TeMN	283.44	260.22
1,2,4,7-TeMN	286.08	262.77
1,4,6,7-TeMN	286.09	262.37
1,2,4,6-TeMN	286.16	262.80
1,2,5,7-TeMN	286.63	263.64
1,3,6,8-TeMN	287.05	n.d.
2,3,6,7-TeMN	287.52	264.82
1,2,6,7-TeMN	289.18	266.69
1,2,3,7-TeMN	289.89	267.74
1,2,3,6-TeMN	290.72	268.65
1,2,5,6-TeMN	293.29	271.16
1,2,3,5-TeMN	293.42	271.85
1,2,4,5-TeMN	295.58	275.33
1,4,5,8-TeMN	297.25	277.38
1,2,3,4-TeMN	299.87	280.37

Most of the DMP isomers have been resolved using a capillary gas chromatography column with a smectic liquid crystalline phase (Budzinski et al., 1992). This technique is advantageous since the laborious fractionation procedure described above is not required, however the column does not separate 1,5-DMP from 2,10-DMP and therefore identification of all isomers is not possible. Although it is likely that both of these techniques would be applicable to resolution of the TeMNs, neither has been reported to be successful.

An alternative to the above methods is analysis using GC-FTIR spectroscopy. This technique exploits the uniqueness of the infrared spectrum of each aromatic hydrocarbon to differentiate between the isomers in a similar manner to Shpol'skii spectrofluorimetry. For example, Mayer and Duswalt (1973) observed distinct differences in infrared spectra obtained from individually synthesised TMNs. This selectivity of detection amongst the alkylnaphthalenes, combined with the high resolving power of capillary gas chromatography, has the potential to enable the on-line identification of individual components of complex aromatic hydrocarbon mixtures.

Early GC-FTIR instruments employed a heated, gold coated pipe interface (i.e. a lightpipe), through which the GC effluent passed. An infrared beam was directed down the pipe through the effluent and the infrared absorbance measured. In general, the application of lightpipe GC-FTIR to the analysis of aromatic hydrocarbons in petroleum has been limited by the abundance of the compounds. For example, Budzinski et al. (1993b) differentiated between the co-eluting DMN isomers and methylphenanthrene (MP) isomers, compounds that are relatively abundant in petroleum. Some trimethylphenanthrenes have also been identified using lightpipe GC-FTIR techniques (Radke et al., 1993). The analysis, however, was restricted to the more abundant isomers due to the lack of sensitivity and deterioration in the chromatographic resolution due to the dilution of the gas effluent characteristic of the lightpipe analyser. Similar investigations into complex mixtures of DMPs have not been reported, presumably due to these characteristic limitations of the lightpipe interface.

Direct deposition GC-FTIR has been developed as an alternative to this technique where these limitations are largely overcome (Bourne et al., 1990a; 1990b). Briefly, this technique involves the cryogenic trapping of the GC effluent on a moving infrared-transparent zinc selenide window through which an infrared beam is focussed, as shown in Figure 3-2. The GC effluent passes *via* a fine (50 μm) fused silica capillary into the evacuated chamber and is trapped on a moving, chilled (by liquid nitrogen) zinc selenide slide.

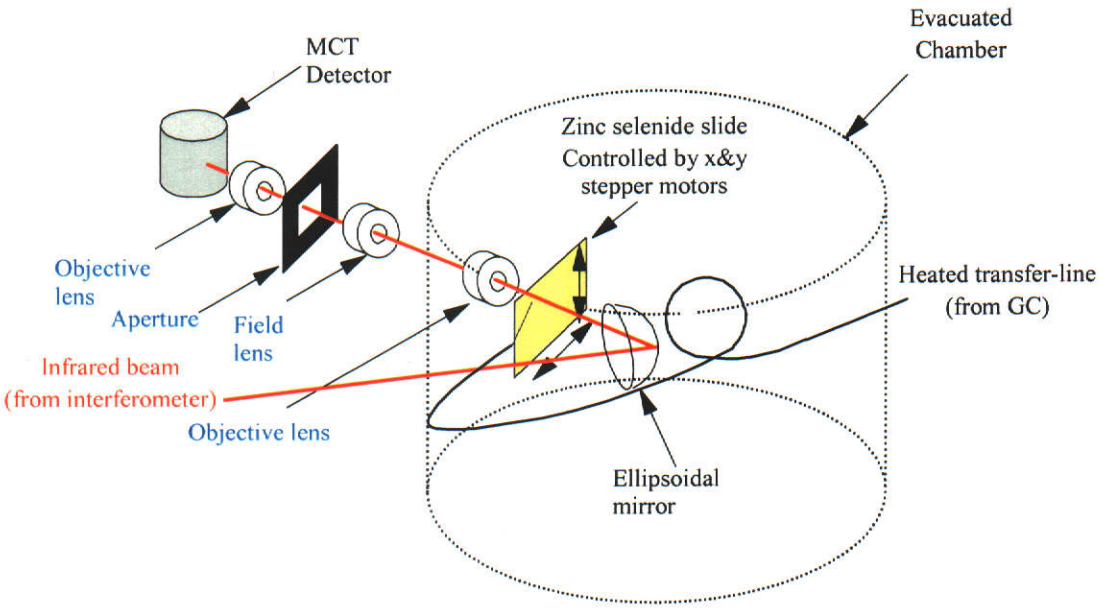

Figure 3-2: Schematic representation of the Tracer® direct deposition GC-FTIR interface.

As shown in Figure 3-3, the movement of the plate is described by a square wave, the amplitude and frequency of which are determined by the action of two stepper motors. Approximately one minute after deposition, the deposit is examined by an FTIR microscope, and provided there is sufficient material deposited to allow its location to be identified, the microscope can be returned subsequently to this location to accumulate many more spectra.

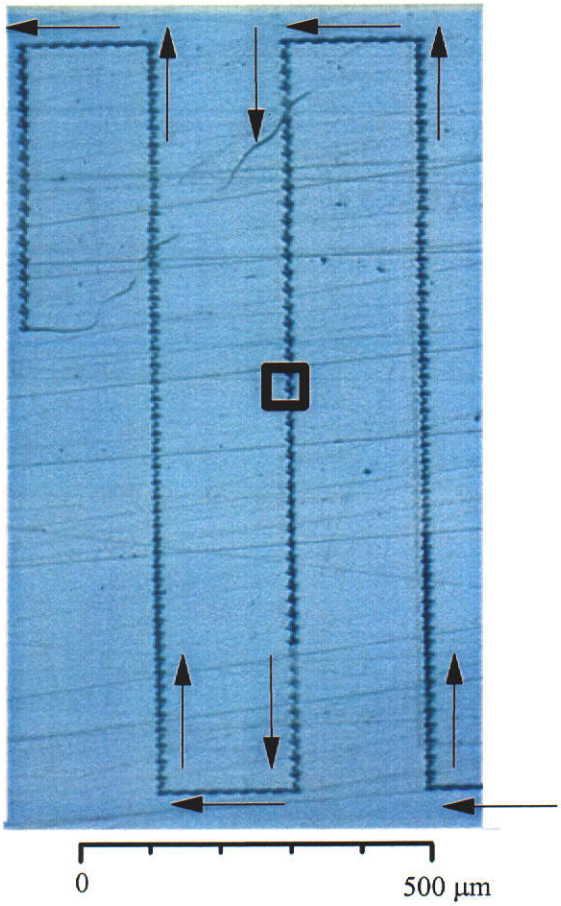

Figure 3-3: A photograph of the pattern described by the deposition tip across the zinc selenide slide (shown in blue) during direct deposition GC-FTIR analysis, where the amplitude of the square wave has been set to its maximum value of 120 µm. The arrows indicate the direction of the slide movement, while an aperture with a side length of 50 µm is represented by the black rectangle.

Although several applications of direct deposition GC-FTIR have been reported (Bourne et al., 1990a; 1990b; Visser and Vredenbregt, 1990; Smyrl et al., 1992), the analysis of complex mixtures of aromatic hydrocarbons is yet to be reported, and this is the subject of the present section of the thesis. The application of GC-FTIR as a complementary technique to GC-MS in such analyses is described in the following sections.

3.3 Method development and validation

3.3.1 Sensitivity

The sensitivity of analysis using direct GC-FTIR is dependant the following factors:

i. the number of infrared spectra acquired for each GC peak.
ii. the size and shape of the deposit on the zinc selenide slide.
iii. the accuracy of the alignment of the infrared beam to the deposited sample.
iv. the speed of movement of the zinc selenide slide.
v. the interference to the spectra by other compounds (i.e. background).

The first of these factors is largely dependent on the capability of the infrared spectrometer and associated data processing system, and is therefore determined specifically by the instrument. Each of the other factors are operational parameters of direct deposition GC-FTIR , and must therefore be optimised for each analysis.

According to Beer's law, for a single compound at a particular frequency, the intensity of absorbance (A) of infrared radiation is an exponential function of the concentration (c) of absorbing substance present and of the length of the path of the radiation (l) through the sample. Beer's law, where E represents the absorptivity of the substance may be expressed as follows:

$$A = Ecl$$

For direct deposition GC-FTIR, the path length is determined by the size and shape of the deposit on the zinc selenide slide. This is affected by interdependence of the alignment of the deposited column effluent with the infrared beam and the speed of the slide movement. The speed at which the zinc selenide slide is moved determines both the chromatographic resolution of the mixture analysed and the sensitivity of the analysis. With increasing slide speed, the distance separating compounds deposited onto the slide increases. However, this is accompanied by a broadening of the deposit on the slide resulting in a shorter path length of the infrared radiation through the deposit and decreased sensitivity. A compromise therefore must be reached between the sensitivity of the analysis and the degree to which the analytes

must be separated on the slide. With well-resolved chromatographic peaks, and for partially co-eluting peaks, a slow setting is used for the slide speed to provide dense deposits and better infrared sensitivity. For closely eluting resolved peaks, a higher setting is required, set by trial and error, so that operation of the analyser does not confound chromatographic separation.

The alignment of the deposited effluent with the infrared beam is dependent on the correct installation of the transfer line and deposition tip assembly. Although the procedure for positioning of the deposition tip in the Tracer® interface is documented by the manufacturer (Bio-Rad, Digilab Division), inspection of the fused silica transfer lines installed during this study revealed that the construction of each of these was not uniform. In particular, the length and shape of the fused silica deposition tip varied considerably. Microscopic inspection of the tip showed that the orientation of the orifice to the transfer line assembly varied, affecting the alignment of the deposition tip to the zinc selenide slide and therefore the shape and size of the column effluent deposited onto the slide. Some modifications to the installation procedure were therefore adopted. Following installation of the transfer line into the vacuum chamber, the shape of the deposition tip was modified by abrasion using emery paper until the end of the tip was parallel to the plane of the zinc selenide slide. The position of the modified tip was adjusted so that the centre of the orifice was positioned at approximately 10 μm from the slide surface (cf. 20 μm as specified by the manufacturer). Using this setting, diagnostic tests for the alignment of a deposit of ice with the infrared beam indicated that a typical size deposit occupied a circular area of the slide less than 100 μm in diameter after implementing these modifications. This deposit was significantly smaller than that obtained using an unmodified deposition tip where the deposit exceeded 100 μm in diameter.

The implications of increasing the amount per area (density) of the deposit were twofold: the infrared absorbance increased due to the longer path length through the centre of the deposit, and a smaller representative section of the infrared beam could be sampled after its passage through the deposit. The portion of the infrared beam sampled was determined by the size of the aperture in the microscope assembly. Reducing the size of the aperture effectively reduces the size of the section of the

deposit that is spectroscopically examined. For example, at a slide speed of 50 μm sec^{-1} and with a square aperture of side length of 100 μm, the infrared radiation detected is that which has passed through a section of column effluent deposited during 2 seconds of the chromatogram. The resolution between deposits using an aperture of 100 μm and slide speed of 50 μm sec^{-1} may be maintained using a 50 μm aperture and a slide speed of 25 μm sec^{-1}. In the present study, the latter combination of parameters, aperture size (50 μm), slide speed (25 μm sec^{-1}) were observed to give optimum performance when applied to the analysis of alkylnaphthalenes and alkylphenanthrenes in complex aromatic hydrocarbon mixtures. Comparison of the chromatograms shown in Figure 3-4 obtained from GC-MS and GC-FTIR analysis of the same petroleum aromatic hydrocarbon fraction on the same GC column reveals that the chromatographic resolution is comparable using these operating conditions, indicating that the chromatographic resolution is not adversely affected by the GC-FTIR analyser.

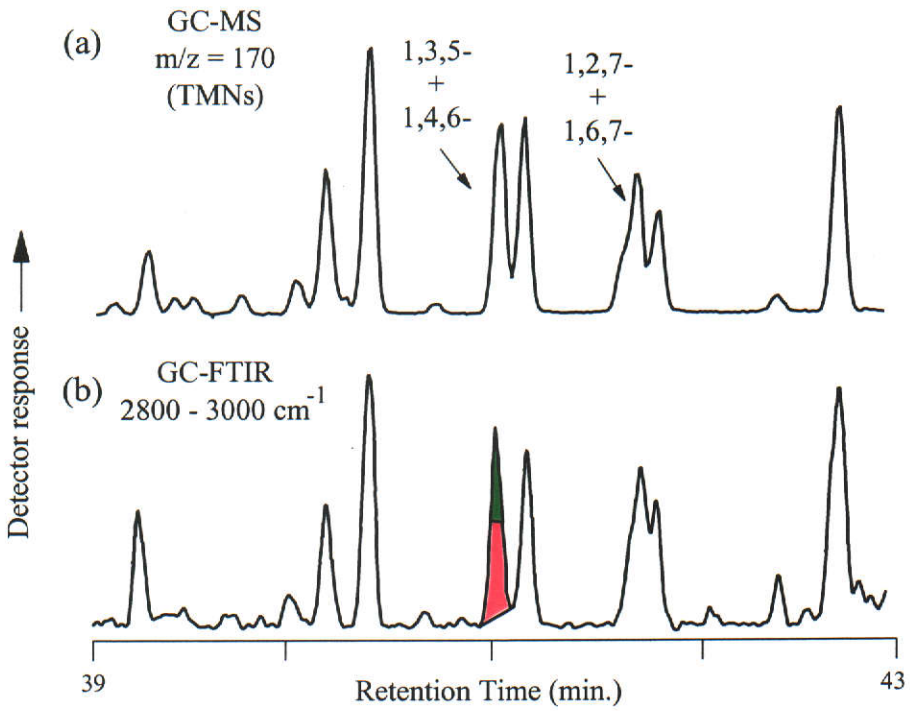

Figure 3-4: Partial (a) mass chromatogram (m/z 170) and (b) GC-FTIR functional group chromatogram (2800 cm^{-1}- 3000cm^{-1}) showing trimethylnaphthalenes in the aromatic hydrocarbon fraction isolated from a crude oil.

Maintenance of chromatographic resolution within the direct deposition interface is critical to the usefulness of the technique in analysis of complex hydrocarbon mixtures. In this study, the intention is to apply the GC-FTIR technique to complement information obtained beforehand using GC-MS analysis. It is therefore imperative that chromatograms obtained from the GC-FTIR bear an unmistakable resemblance to their GC-MS analogues. To achieve this, the differences in absorptivity of the compounds and the way in which chromatograms are constructed using the GC-FTIR must be considered.

Chromatograms are obtained from the Tracer® GC-FTIR in an analogous manner to selected ion monitoring in GC-MS analysis. Portions of the infrared spectrum to which the analytes respond must be chosen prior to gas chromatographic analysis of the mixture to provide selectivity between components of the mixture based on differences in infrared response. These portions are monitored during the analysis to produce functional group chromatograms and the responses added together to form a Gram-Schmidt chromatogram. Upon completion of the analysis, chromatograms other than those selected beforehand cannot be reconstructed from the infrared data. Unlike for selected ion analysis, however, infrared spectra are acquired over the entire working range of the MCT detector (650 cm^{-1} to 4000 cm^{-1}), so there is no enhancement in sensitivity.

The functional group chromatogram shown in Figure 3-4(b) resulted from monitoring the interval between 2800 cm^{-1} and 3000 cm^{-1} in the infrared spectrum to detect the stretching vibrations of the carbon to hydrogen (C-H) bonds in the methyl moieties of the TMNs (Roeges, 1994). This interval was chosen since all TMNs absorb infrared radiation in this frequency range in a similar manner, as illustrated by the similarity between the functional group chromatogram and the m/z 170 mass chromatogram shown in Figure 3-4(a). A contrasting example where functional group chromatograms are used to differentiate between compounds will be discussed in detail in a later section (3.7.3).

A particularly useful feature of the direct deposition GC-FTIR technique is the ability to acquire infrared spectra from deposits (with the slide held stationary) after the chromatographic analysis has finished. In this post-analysis mode, both the signal to noise ratio and the (spectral) resolution at which the infrared spectra are acquired may be improved by increasing the time that the infrared beam passes through a deposit on the slide. This is illustrated by the spectra of biphenyl shown in Figure 3-5, where the improvement in both signal and spectral resolution between the uppermost spectrum, obtained during analysis, and the other two spectra obtained from post-analysis acquisition is evident. The time taken to perform each of the post-analysis examinations is also shown in Figure 3-5. It is noteworthy that while these spectra are being accumulated, carrier gas is focussed onto the zinc selenide slide *via* the deposition tip, resulting in the deposition of impurities contained in the gas stream (e.g. water vapour) onto the slide. In this study, to minimise interference from such material, high-resolution spectra were obtained from post-analysis examination of the deposits by the addition of interferograms from 256 successive scans at a resolution of 2 cm^{-1}, an operation taking approximately 3 minutes.

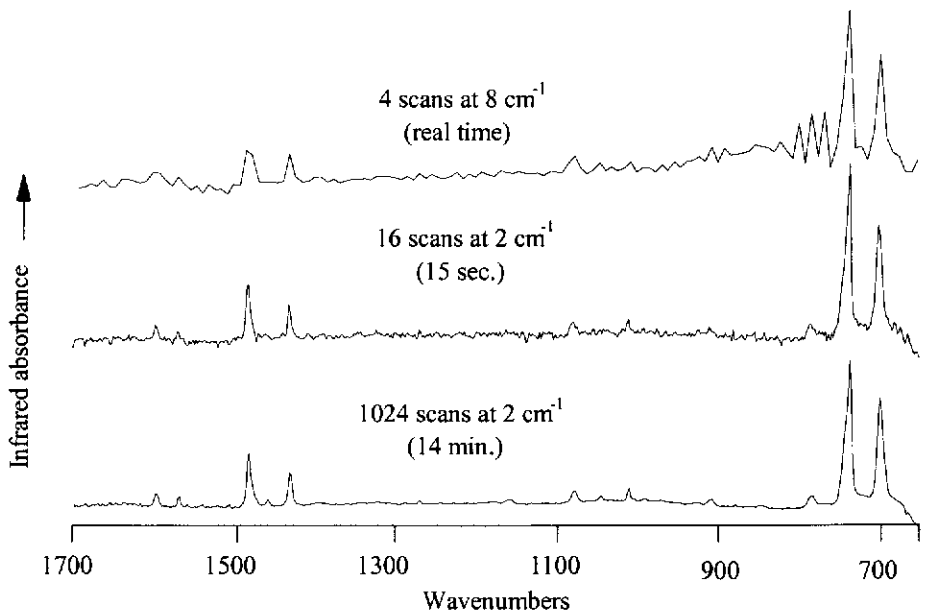

Figure 3-5: Partial infrared spectra of a 4 ng deposit of biphenyl obtained by GC-FTIR analysis using various operating parameters.

3.3.2 Linearity of the detector response

Using the optimised operating conditions described above, the response of the MCT infrared detector to aromatic hydrocarbons was investigated using 3,6-DMP as a model compound. Various amounts of this compound were analysed by injecting triplicate aliquots of solutions containing a mixture of varying concentrations of 3,6-DMP (1.6 ng μL^{-1} to 26 ng uL^{-1}) and a constant concentration of the internal standard biphenyl (18 ng μL^{-1}). This concentration range of 3,6-DMP approximates that of individual analytes typically analysed in capillary gas chromatography.

During the analysis, two functional group chromatograms were monitored. The first of these showed infrared absorbance between 720 $cm^{-1}$and 920 cm^{-1} responding to the out-of-plane bending of the C-H bonds of the aromatic nuclei (Roeges, 1994). A second showed infrared absorbance between1400 $cm^{-1}$and 1600 cm^{-1} responding to the stretching of the carbon to carbon (C-C) bonds of the aromatic nuclei (Roeges, 1994). For each analysis, the area of the peak corresponding to 3,6-DMP in each functional group chromatogram was normalised against that of the internal standard to eliminate errors from varying sample injection volumes. The results of these analyses are presented in Figure 3-6, where the abundance of 3,6-DMP is compared with the mean normalised MCT detector response. It is apparent from the values of the correlation coefficients for these relationships that the detector response remains linear for the range of abundances investigated here.

The linearity of the MCT detector response compares well with that observed for mass selective detection as shown in Figure 3-7. Here the peak areas from the total ion chromatograms obtained from GC-MS analysis of the above mentioned solutions of 3,6-DMP were normalised and plotted against the normalised peak areas from GC-FTIR functional group chromatograms. The difference in gradient observed between the two functional group chromatograms in both Figure 3-6 and Figure 3-7 shows that, relative to biphenyl, the infrared absorbance of 3,6-DMP is greater in the 720 cm^{-1}- 920 cm^{-1} region than in the 1400 cm^{-1}- 1600 cm^{-1} interval. Analysis of the 1.6 ng deposit of 3,6-DMP yielded a signal to noise ratio of approximately 5 for both chromatograms, therefore approximating the practical limit of sensitivity for 3,6-DMP using GC-FTIR functional group monitoring.

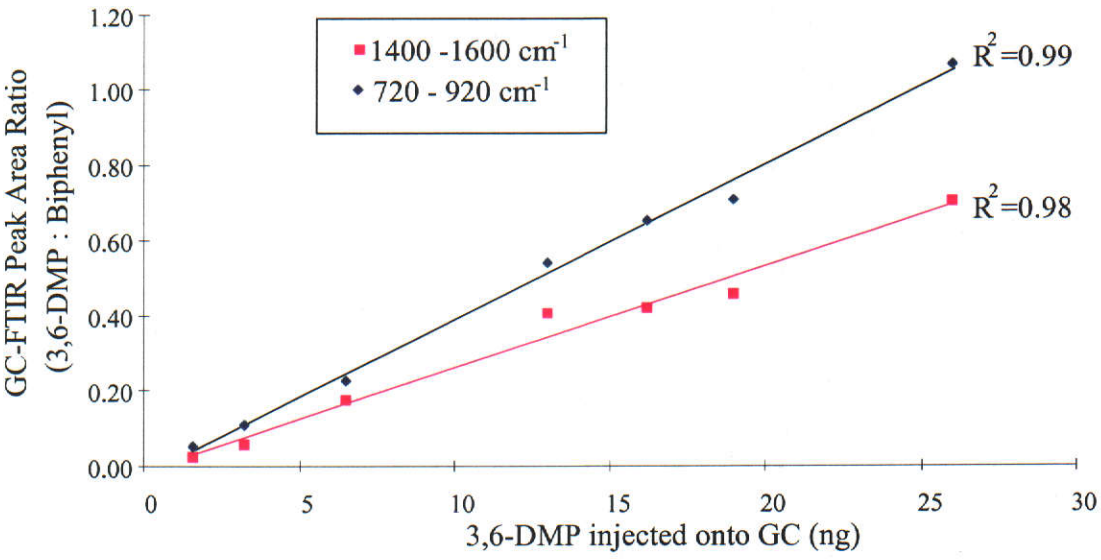

Figure 3-6: Graphs showing the correlation between GC-FTIR detector response and abundance of 3,6-dimethylphenanthrene calculated from the peak areas from two functional group chromatograms (720 cm^{-1}- 920 cm^{-1} and 1400 cm^{-1}- 1600 cm^{-1}). Each data point represents the mean value of triplicate GC-FTIR measurements.

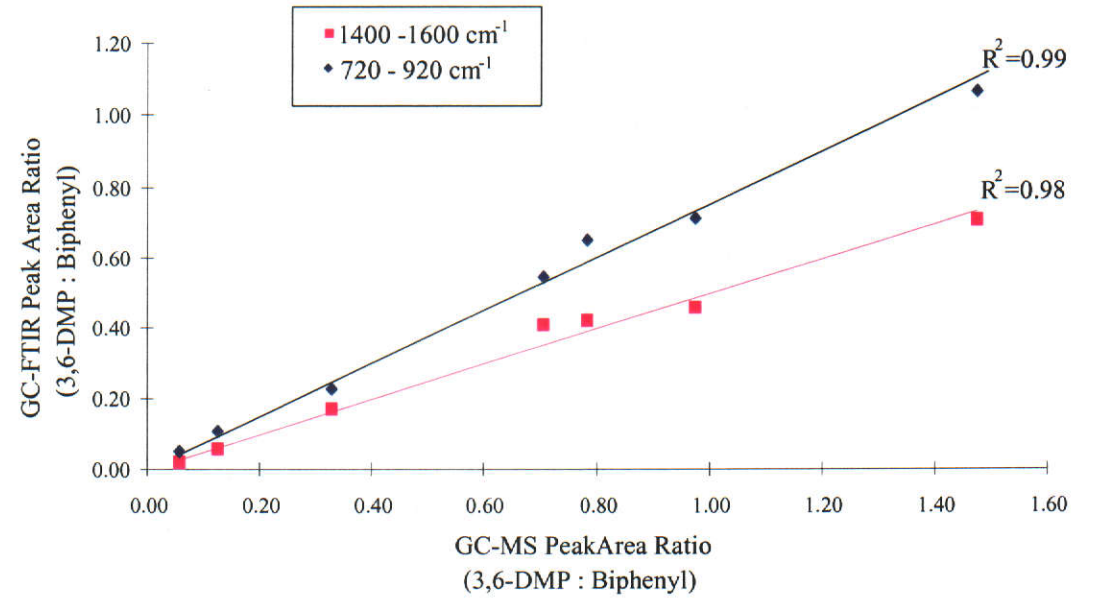

Figure 3-7: Graphs showing the correlation between GC-MS and GC-FTIR peak areas from the quantitative analysis of 3,6-dimethylphenanthrene using biphenyl as an internal standard. Each data point represents the mean value of triplicate GC-FTIR and GC-MS measurements.

3.3.3 Calculation of response factors

The infrared absorptivity is a characteristic of the substance analysed. To quantify individual compounds in mixtures using GC-FTIR, the detector response of each compound to the infrared absorbance must be established. As an alternative to the approach described above for 3,6-DMP, it is proposed here to use GC-FTIR as a complementary technique to GC-MS analysis. In this way, compounds are quantified and tentatively identified using GC-MS, then each component of the mixture is unambiguously identified using GC-FTIR by comparison of its infrared spectrum with that of an authentic sample. Using this approach, in conjunction with the calculated retention indices shown in Table 3-1, it is possible to identify where co-elution of compounds occurs. Only the abundance of each of the co-eluting compounds relative to each other therefore need be determined.

As an example of this approach, consider the comparison of the partial infrared spectra of a co-eluting mixture of equal abundances of 1,3,5-TMN and 1,4,6-TMN with the spectra of the individual components shown in Figure 3-8. Here, the signals due to out-of-plane C-H bending vibrations are presented, and as expected, the isomers have distinctly different infrared absorbance spectra. The most significant differences between the spectra are the occurrence of an absorbance peak at 826 cm^{-1} in the spectrum of 1,4,6-TMN and at 853 cm^{-1}, 796 cm^{-1} and 748 cm^{-1} in that of 1,3,5-TMN. Each of these peaks is absent from the spectrum of the other isomer, is clearly distinguishable in the infrared spectrum of the isomer mixture, and therefore may be used to distinguish between the two isomers in the mixture.

Consider the peaks at 853 cm^{-1} and 826 cm^{-1} in the spectrum of the mixture. Here the infrared absorbance at 826 cm^{-1}, arising from 1,4,6-TMN, is approximately 1.6 times as intense as at 853 cm^{-1} (from 1,3,5-TMN). From triplicate analyses of this mixture, the mean value for the ratio of the areas of these peaks was calculated to be 1.6, which represents the difference in response for the isomers when considering these absorbance bands.

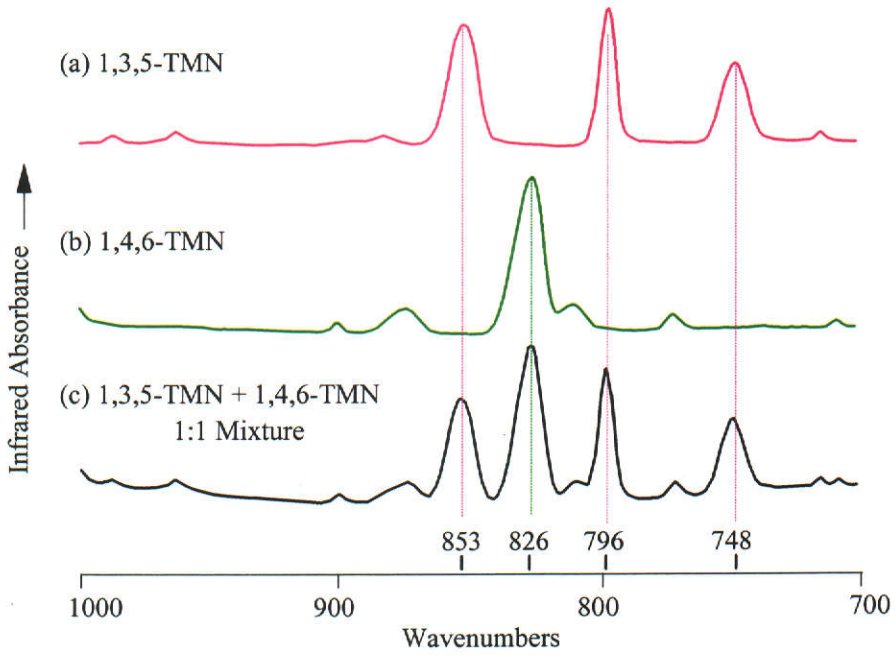

Figure 3-8: Partial infrared spectra of (a) 1,3,5-TMN, (b) 1,4,6-TMN and (c) a mixture of equal abundances of each of these co-eluting isomers. Spectra were obtained by analysis using direct deposition GC-FTIR.

To investigate whether this response factor is constant, several mixtures of varying abundances of 1,3,5-TMN and 1,4,6-TMN were prepared. The relative abundances of the isomers in each was confirmed by GC-MS analysis of the mixtures using a BP20 column with operating parameters under which the isomers are completely resolved (refer to Table 3-1). The mixtures were also analysed using GC-FTIR and the areas of these selected characteristic infrared absorbance peaks were obtained. The relationship between the relative abundance of the isomers to the ratio of these peak areas is shown in Figure 3-9. The curve shown here was fitted to the data by applying several successive iterations of the Levenberg-Marquardt algorithm to minimise the sum of the squares of the deviations (χ^2) of a theoretical (rectangular) hyperbola from the experimental points as described by Press et al. (1992). The resulting hyperbola may be described by the equation:

$$y = \frac{x}{-0.55x + 0.58}$$

where y represents the ratio of infrared absorbance peaks while the relative abundance of 1,4,6-TMN in the mixture is represented by x. Substitution of a value

of 0.5 for the relative abundance of 1,4,6-TMN into the above equation yields a value of 1.6 for the ratio of absorbance peaks.

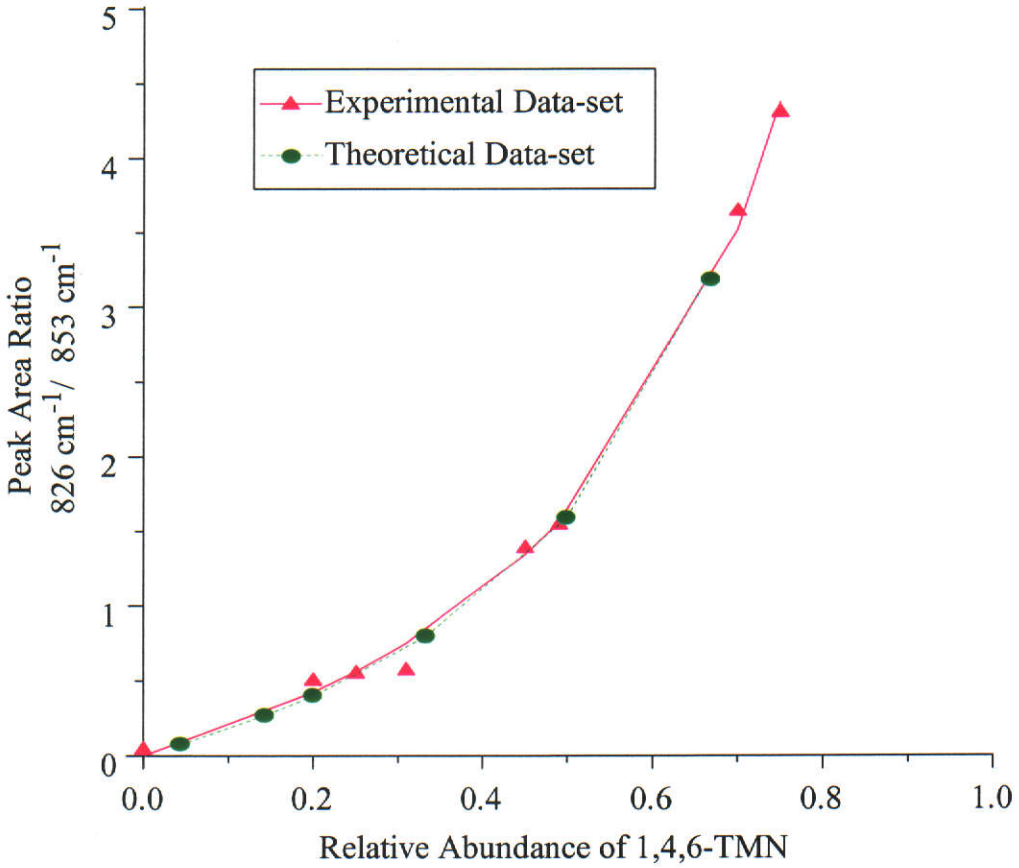

Figure 3-9: The relationship between the relative abundances of the co-eluting compounds 1,4,6-TMN and 1,3,5-TMN and the ratios of the peak areas of characteristic infrared absorbance of each compound. Each data point represents the mean value of triplicate GC-FTIR measurements.

Also shown in Figure 3-9, is a hyperbola fitted to a theoretical data-set, where the difference in response between the absorbance peaks at 826 cm^{-1} and 853 cm^{-1} has been constrained to 1.6 for each of six different relative abundances of the two isomers. The curve fitting was performed in an identical manner to that applied to the experimental data. It is apparent that both hyperbolae fit the experimental data points closely, an observation confirmed by the low value (0.01) of χ^2 for the experimental data points. The close alignment of the theoretical curve and that derived experimentally indicates that the observed difference in response by a factor

of 1.6 between the two absorbance peaks measured in one mixture containing 50 % of each isomer is constant for the range of concentrations investigated here. This calibration curve may therefore be used to determine the composition of a mixture of unknown proportions of the isomers.

An alternative approach to the determination of the response factors for the two TMN isomers was also investigated, where the infrared spectrum obtained from an authentic sample of each isomer was examined over the frequency range of 650 cm^{-1} to 4000 cm^{-1}, as shown in Figure 3-10. The C-H stretching vibrations from the methyl moiety of the molecule absorb infrared radiation in the frequency range of approximately 2850 cm^{-1} to 3000 cm^{-1}. The intensity of these absorbance peaks is dependent upon the number of methyl fragments contained in the molecule, but is independent of the position the methyl substituents occupy on the aromatic nucleus. Therefore, isomers of any poly-methylated naphthalene respond similarly in this region of the infrared spectrum and the intensity of these absorbance bands may be considered as a constant against which other absorbance intensities may be normalised.

To test this approach, the sum of the areas of the absorbance peaks resulting from the C-H bond stretching vibrations in the methyl substituents of 1,3,5-TMN and 1,4,6-TMN was determined. For each spectrum, the peak areas of the characteristic absorbances assigned to the out-of-plane bending vibrations of the C-H bond were divided by this sum. The resulting normalised spectra were then compared, revealing that the absorbance at 826 cm^{-1} in the spectrum of 1,4,6-TMN was 1.6 times as intense as that at 853 cm^{-1} in the spectrum of 1,3,5-TMN, an identical value to that obtained from the (hyperbolic) calibration curve described above. This observation has important implications, since the intensity of the absorbance for each isomer at these frequencies does not appear to be perturbed by the presence of the other. Spectral perturbation, where interactions that occur between the components of a mixture cause a deviation from Beer's Law, has been investigated previously (e.g. Gillette, Lando and Koenig, 1983; Culler et al., 1984). This interference occurs in regions of the infrared spectra where absorbance peaks are common to two or more of the components. The resultant spectrum of the mixture in this region

represents overlapping absorbance peaks from each component where the intensity of the peaks in the mixture does not equal the sum of the intensities of the individual components. Specific examples of analysis of multi-component mixtures of alkylnaphthalenes and alkylphenanthrenes where this confounding spectral perturbation is apparent are discussed in detail later.

The interference to the infrared spectra by frozen water vapour (ice), appearing as a broad negative band between approximately 3100 cm^{-1} and 3500 cm^{-1}, is also shown in Figure 3-10. Using the Tracer interface®, the infrared spectrum of a cryo-trapped compound is enhanced by the subtraction of a spectrum obtained from a background region of the slide, usually from a background portion of the chromatogram (i.e. where peaks are absent from the chromatogram). The interference by ice thus occurs as a negative signal, when the intensity of the infrared absorbance due to the (hydrogen bonded) O-H stretching vibrations is greater through the background region than through the deposited compound from which it has been subtracted.

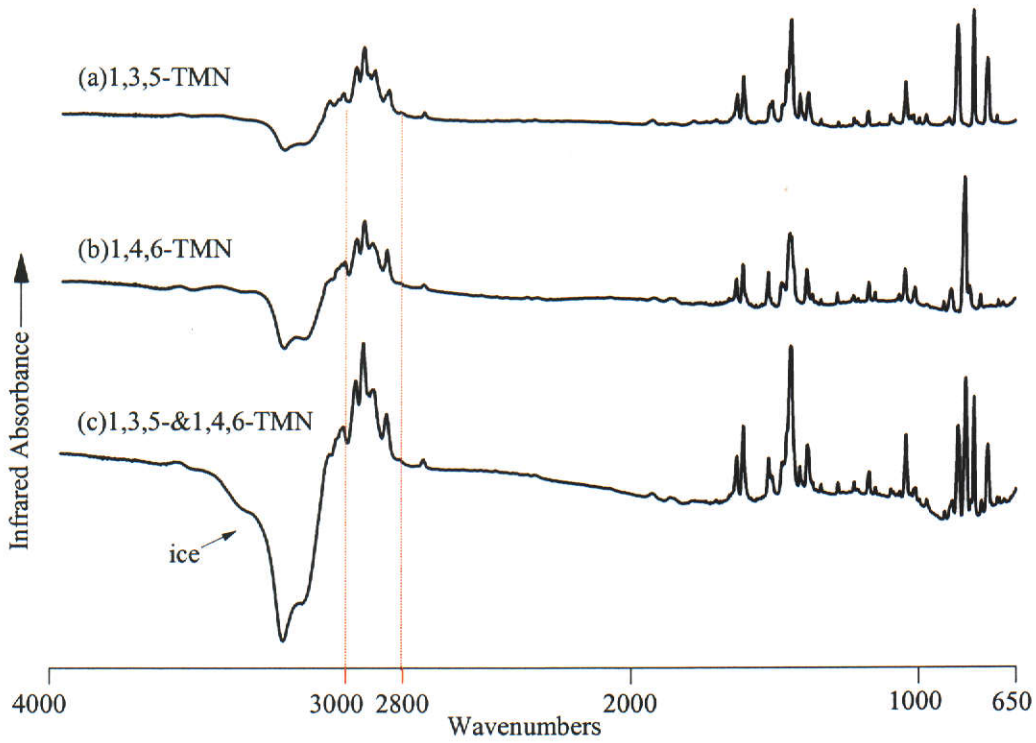

Figure 3-10: Infrared spectra of (a) 1,3,5-TMN, (b) 1,4,6-TMN and (c) a mixture of equal abundances of each of these co-eluting isomers. Spectra were obtained by analysis using direct deposition GC-FTIR.

In Figure 3-10, although the ice background interference is apparently more prominent in the spectrum of the isomer mixture than for either of the two single isomers, it is proportionate to the intensity of the C-H stretching vibrations from the methyl moiety of the TMNs between 2850 cm^{-1} to 3000 cm^{-1}. For the TMNs and other aromatic hydrocarbons, the interference by ice does not impinge on the interpretation of the infrared spectrum, and is therefore not discussed in further detail here.

3.4 Determination of co-eluting polymethylnaphthalenes in petroleum

3.4.1 Determination of retention indices of alkylnaphthalenes

These indicies, shown in Table 3-1, were calculated according to the method adopted by Lee et al. (1979) using the following equation.

$$I(x) = 100 \cdot \left[\frac{tr(x) - tr(z)}{tr(z+1) - tr(z)} \right] + 100 \cdot z$$

Here, $I(x)$ represents the retention index and $tr(x)$ is the retention time of the compound of interest. The compounds benzene, naphthalene, phenanthrene, chrysene and picene are assigned as standard aromatic hydrocarbons. Here z is the number of aromatic rings present in the standard aromatic hydrocarbon eluting prior to the compound of interest (in this case naphthalene), $tr(z)$ is the retention time of this standard aromatic hydrocarbon and $tr(z+1)$ is the retention time of the standard aromatic eluting after the compound of interest (i.e. phenanthrene).

It is apparent from Table 3-1 that the retention behaviour of polymethylnaphthalenes varies with the stationary phase of the GC column to the extent that elution order is altered substantially. The following discussion refers to separation achieved using a capillary column coated with 5% phenyl methylpolysiloxane stationary phase (DB-5, J&W Scientific), using the chromatographic conditions as described in Chapter 2.

Mass chromatograms showing the DMNs (m/z 156) and TMNs (m/z 170) obtained from analysis of the dinuclear aromatic hydrocarbon fraction isolated from Lambert-1 crude oil are shown in Figure 3-11. The polymethylnaphthalenes have been identified by comparison with the retention indices of reference compounds given in Table 3-1. The co-eluting mixtures are marked clearly, and in the following section, the application of direct deposition GC-FTIR to the analysis of individual compounds in these mixtures in this crude oil is discussed.

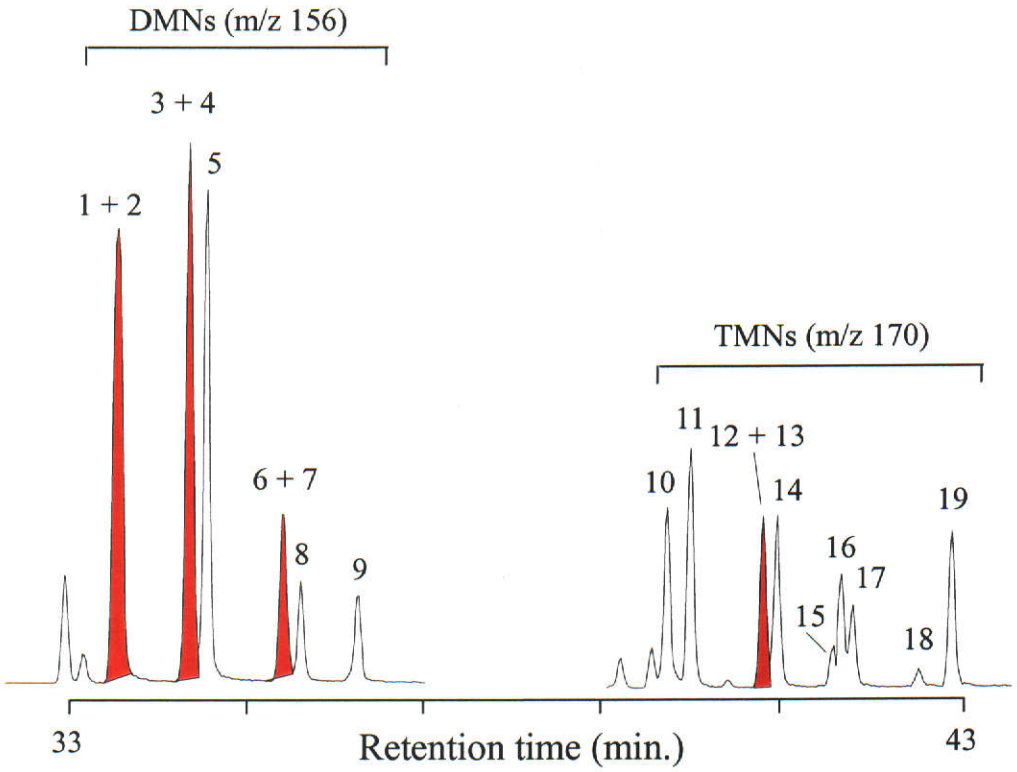

Figure 3-11: Partial mass chromatograms showing the presence of dimethylnaphthalenes (DMNs, m/z 156) and trimethylnaphthalenes, (TMNs, m/z 170) and tetramethylnaphthalenes (TeMNs, m/z 184) in Lambert-1 crude oil. Peaks due to co-eluting isomers are shaded red. Peak identifications are as follows: (1) 2,6-DMN; (2) 2,7-DMN, (3) 1,3-DMN; (4) 1,7-DMN; (5) 1,6-DMN; (6) 1,4-DMN; (7) 2,3-DMN; (8) 1,5-DMN; (9) 1,2-DMN; (10) 1,3,7-TMN; (11) 1,3,6-TMN; (12) 1,3,5-TMN; (13) 1,4,6-TMN; (14) 2,3,6-TMN, (15) 1,2,7-TMN; (16) 1,6,7-TMN; (17) 1,2,6-TMN; (18) 1,2,4-TMN and (19) 1,2,5-TMN.

3.4.2 Dimethylnaphthalenes (DMNs)

There are 10 possible DMN isomers, nine of which commonly occur in petroleum. The exception is 1,8-DMN, which is rarely identified in petroleum (Alexander et al., 1985). Its absence is most likely due to its high instability as a consequence of the *peri* interaction between the methyl substituents on carbons 1 and 8.

Inspection of the chromatogram shown in Figure 3-11 reveals that three co-eluting pairs of DMN isomers may occur in the crude oil, namely: 2,6-DMN and 2,7-DMN; 1,7-DMN and 1,3-DMN; and 1,4-DMN and 2,3-DMN. The contribution by each isomer to the peak due to each of these isomer pairs was determined using direct deposition GC-FTIR, where in each case the infrared spectrum obtained from the mixture was compared with spectra from authentic samples of the component isomers.

Partial infrared spectra of 2,6-DMN and 2,7-DMN are shown in Figure 3-12. The spectra of these reference compounds have been normalised using the C-H stretching bands at 2850-3000 cm^{-1}. It is apparent from comparison of these spectra that the isomers have distinctly different infrared absorbance spectra in the out-of-plane bending region, the most significant differences being the occurrence of an absorbance peak at approximately 816 cm^{-1} for the 2,6-DMN and at 836 cm^{-1} for the 2,7-DMN. Each of these peaks is absent from the spectrum of the other isomer and may therefore be used to distinguish between the two. The ratio of these peak areas in the spectrum from the co-eluting isomers in the crude oil, corrected for differences in intensity of infrared absorbance, indicates that Lambert-1 crude oil contains an equal proportion of both 2,6-DMN and 2,7-DMN.

Similarly, the normalised infrared spectra of 1,3-DMN and 1,7-DMN and those of 2,3-DMN and 1,4-DMN are shown in Figure 3-13. Inspection of these spectra reveals that each exhibits at least one out-of-plane bending absorbance peak that enables one co-eluting isomer to be distinguished from the other. The frequency at which the more intense of these diagnostic infrared absorbances occurs is detailed in Table 3-2. In each case, these peaks are clearly visible in the spectrum obtained from

the component in the crude oil, confirming the presence of both isomers in Lambert-1 crude oil. From the areas of these peaks, the contribution of 1,4-DMN (25 %) to the co-eluting mixture with 2,3-DMN (75 %) and 1,3-DMN (40 %) to the co-eluting mixture with 1,7-DMN (60 %) was determined.

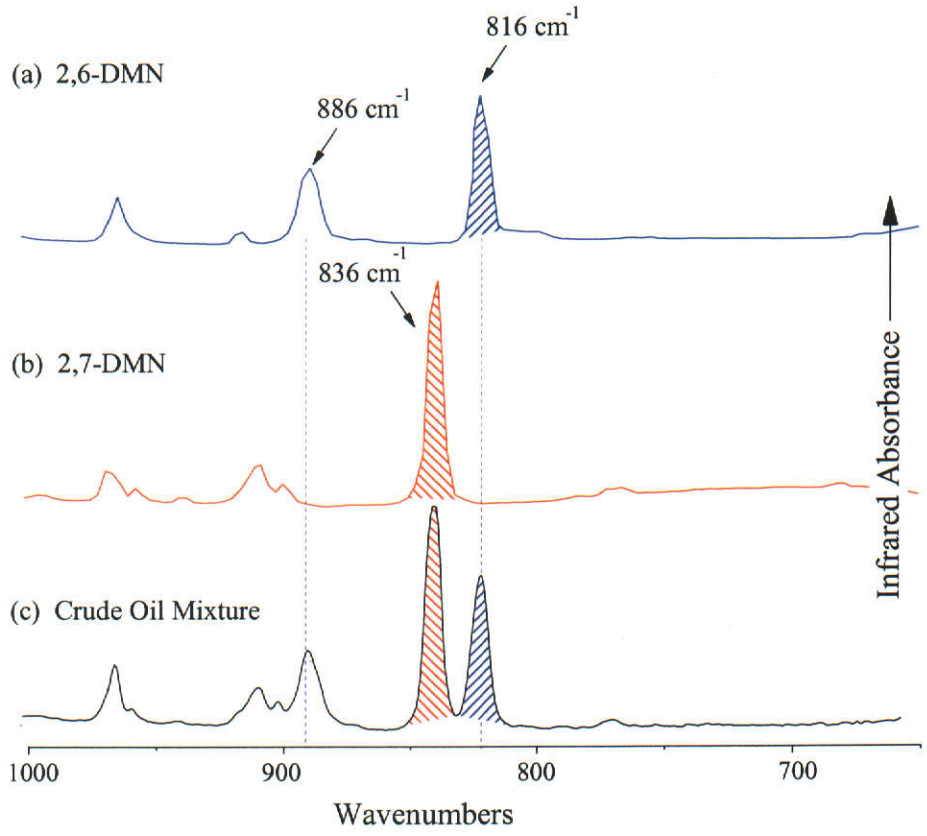

Figure 3-12: Partial infrared spectra of authentic samples of (a) 2,6-DMN and (b) 2,7-DMN and (c) the mixture of these compounds occurring in Lambert-1 crude oil. Spectra were obtained using GC-FTIR at a resolution of 2 cm^{-1}.

Table 3-2: Summary of the characteristic infrared absorbance frequencies corresponding to C-H out-of-plane bending vibrations of co-eluting dimethylnaphthalene isomers.

Isomer	Frequency of Characteristic Absorbance Peak(s)
2,6-DMN	816 cm^{-1}, 886 cm^{-1}
2,7-DMN	836 cm^{-1}
1,3-DMN	773 cm^{-1}, 849 cm^{-1}
1,7-DMN	824 cm^{-1}
1,4-DMN	760 cm^{-1}, 825 cm^{-1}
2,3-DMN	745 cm^{-1}, 875 cm^{-1}

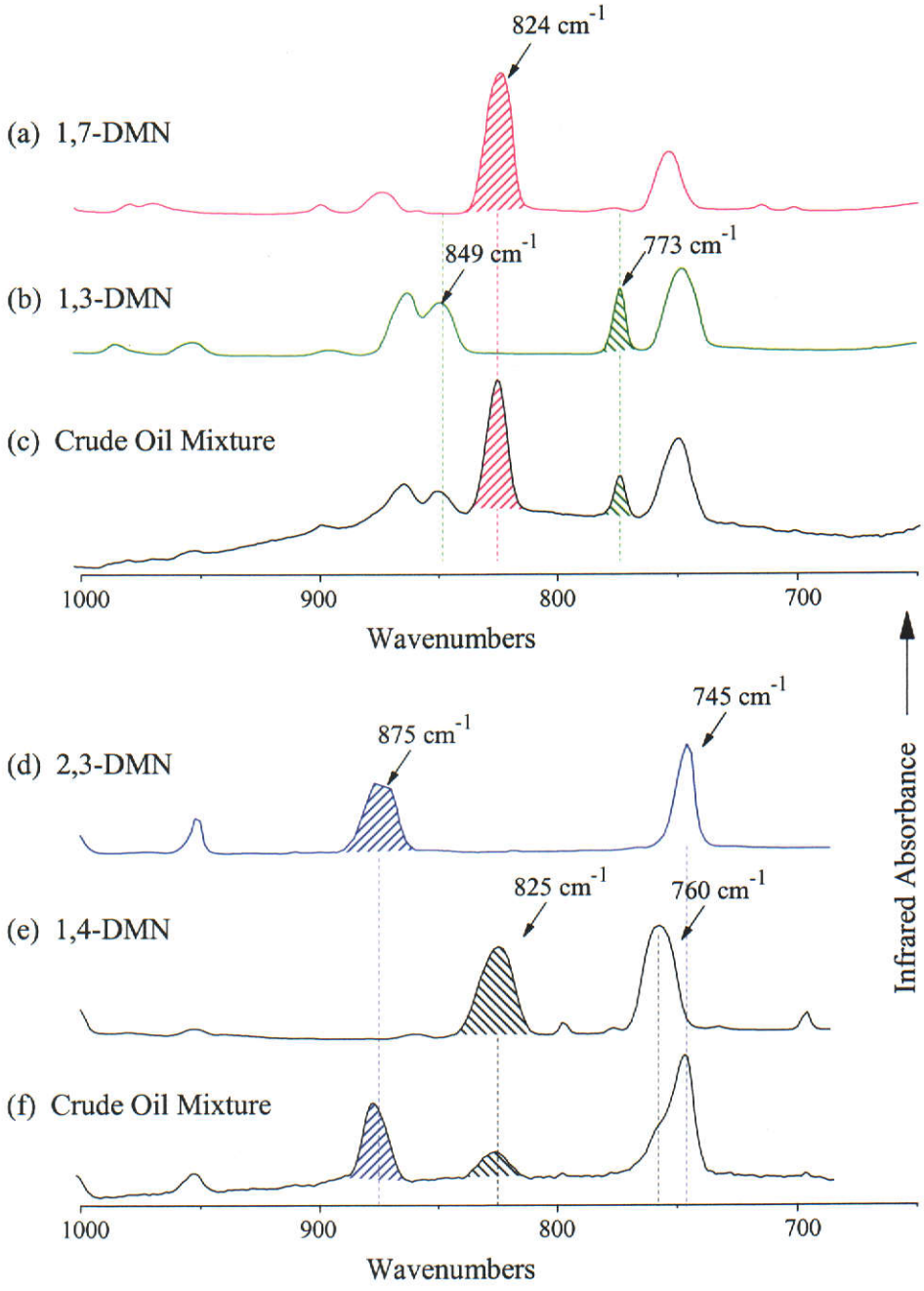

Figure 3-13: Partial infrared spectra of authentic samples of (a) 1,7-DMN, (b) 1,3-DMN and (c) the mixture of these compounds occurring in Lambert-1 crude oil. Partial spectra are also shown for authentic samples of (d) 2,3-DMN, (e) 1,4-DMN and the mixture of these compounds occurring in Lambert-1 crude oil. Spectra were obtained using GC-FTIR at a resolution of 2 cm^{-1}.

3.4.3 Trimethylnaphthalenes (TMNs)

There are 14 possible TMN isomers. Again, isomers exhibiting *peri* methyl substitution of the naphthalene nucleus (1,2,8-TMN, 1,3,8-TMN and 1,4,5-TMN) rarely occur in petroleum (Alexander et al., 1985). Interestingly, the very sterically hindered 1,2,3-TMN is occasionally observed (e.g., Bastow et al., 2000) and the remaining 10 isomers are common constituents of petroleum (e.g. Radke, Garrigues and Willsch, 1990; Radke, Rullkötter and Vriend, 1994).

Most of the TMN isomers that commonly occur in petroleum are sufficiently well resolved using the standard GC operating conditions to allow their determination using GC-MS. The analysis of the co-eluting 1,3,5-TMN and 1,4,6-TMN has been discussed in detail in a previous section (Section 3.3.3). From the infrared spectrum of this isomer mixture in Lambert-1 crude oil, shown in Figure 3-14, we may conclude that the crude oil contains equal proportions of both isomers.

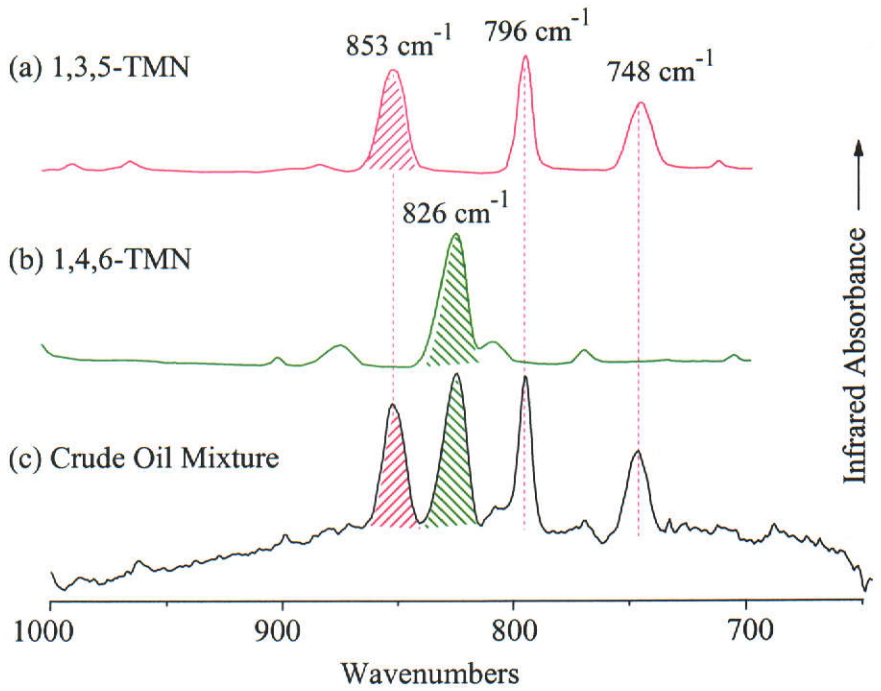

Figure 3-14: Partial infrared spectra of authentic samples of (a) 1,3,5-TMN and (b) 1,4,6-TMN, and (c) the mixture of these compounds occurring in Lambert-1 crude oil. Spectra were obtained using GC-FTIR at a resolution of 2 cm^{-1}.

Close inspection of the chromatogram of the TMNs in Lambert-1 crude oil, shown in Figure 3-11, reveals that 1,2,7-TMN, 1,6,7-TMN and 1,2,6-TMN (peaks 15, 16 and 17) are not completely separated from each other. Although the resolution between these is sufficient to quantify these isomers, a slight deterioration in the efficiency of the chromatographic separation may result in varying extents of severity of co-elution between these three compounds as shown in Figure 3-4.

Partial infrared spectra of authentic samples of each of these isomers, normalised to the C-H stretching peaks, are shown in Figure 3-15. From these it is evident that 1,2,7-TMN (832 cm^{-1}), 1,2,6-TMN (814 cm^{-1}) and 1,6,7-TMN (753 cm^{-1} and 785 cm^{-1}) have distinctive absorbance peaks by which their infrared spectra may be differentiated. Analysis of partially separated mixtures of these isomers using GC-FTIR requires that the infrared spectrum be obtained from a larger section of the deposited material than in the mixtures considered thus far.

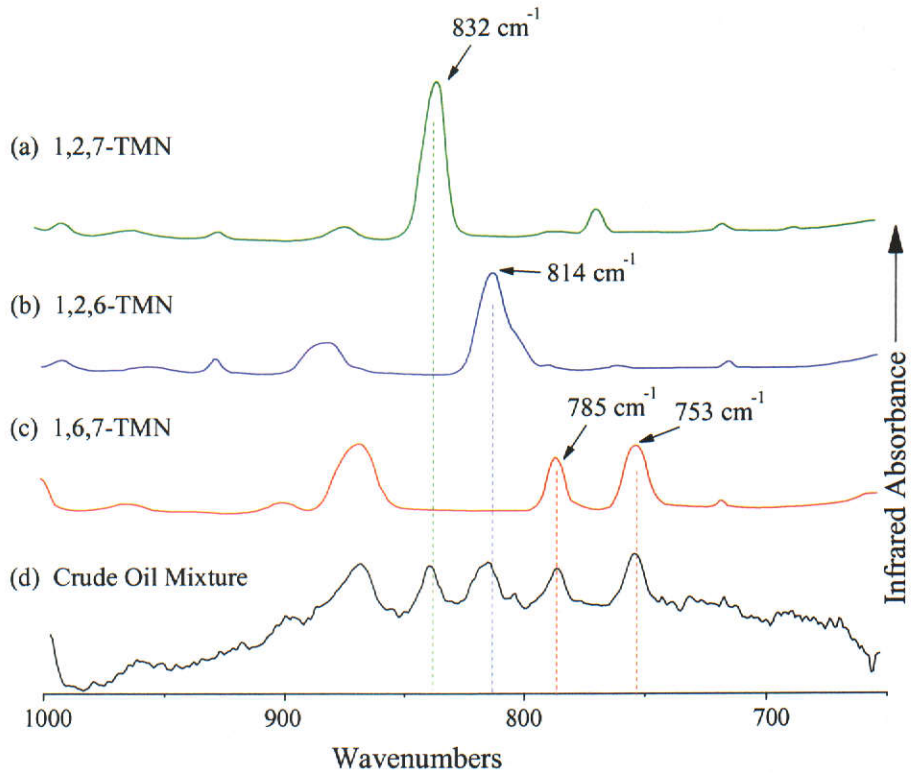

Figure 3-15: Partial infrared spectra of authentic samples of (a) 1,2,7-TMN and (b) 1,2,6-TMN, (c) 1,6,7-TMN and (d) the mixture of these compounds occurring in Lambert-1 crude oil. Spectra were obtained using GC-FTIR at a resolution of 2 cm^{-1}.

The infrared spectrum of the mixture in Lambert-1 crude oil, also shown in Figure 3-15, was therefore obtained by averaging the spectrum across the whole of the co-eluting mixture deposited on the slide. As a consequence, the sensitivity of the technique is reduced due to the reduced path-length through the material close to the edges of the deposit. Despite the reduced sensitivity, these TMNs are of sufficient abundance in the crude oil to be quantified using GC-FTIR. The contributions by 1,2,7-TMN (15%), 1,6,7-TMN (60%) and 1,2,6-TMN (25%) to the mixture of isomers determined in this way, were confirmed from GC-MS analysis using a DB-5 column (Figure 3-11) and a separate analysis on the more polar BP20 column.

3.4.4 Tetramethylnaphthalenes (TeMNs)

There are 22 possible TeMN isomers, nine of which contain *peri* methyl substituents namely 1,2,3,8-TeMN, 1,2,4,5-TeMN, 1,2,4,8-TeMN, 1,2,5,8-TeMN, 1,2,6,8-TeMN, 1,2,7,8-TeMN, 1,3,5,8-TeMN, 1,3,6,8-TeMN and 1,4,5,8-TeMN. Together with the sterically hindered 1,2,3,4-TeMN, these compounds are rarely observed in petroleum (Forster, Alexander and Kagi, 1989) and have not been considered further here. The remaining 12 isomers are common constituents of petroleum (Alexander et al., 1993). Five of these compounds are not resolved using the standard GC conditions and are therefore candidates for analysis using GC-FTIR. These occur in two mixtures of co-eluting isomers namely 1,2,5,6-TeMN and 1,2,3,5-TeMN, and 1,2,4,6-TeMN, 1,2,4,7-TeMN and 1,4,6,7-TeMN.

Inspection of the total ion and m/z 184 mass chromatograms, shown in Figure 3-16, reveals that some of the TeMNs also co-elute with other compounds in the dinuclear aromatic hydrocarbon fraction obtained from the crude oil. On the basis of their mass spectra, these compounds most likely comprise a mixture of C_4- and C_5-naphthalenes and alkylbiphenyls, alkylfluorenes and alkyldiphenylmethanes (Trolio et al., 1999) which do not exhibit a strong m/z 184 ion. These compounds interfere with the GC-FTIR analysis of the TeMNs, since there is no region in the infrared spectrum that is unique to TeMNs and it is therefore not possible to construct a functional group chromatogram from the acquired infrared spectra that responds only to the TeMNs in the presence of other co-eluting hydrocarbons.

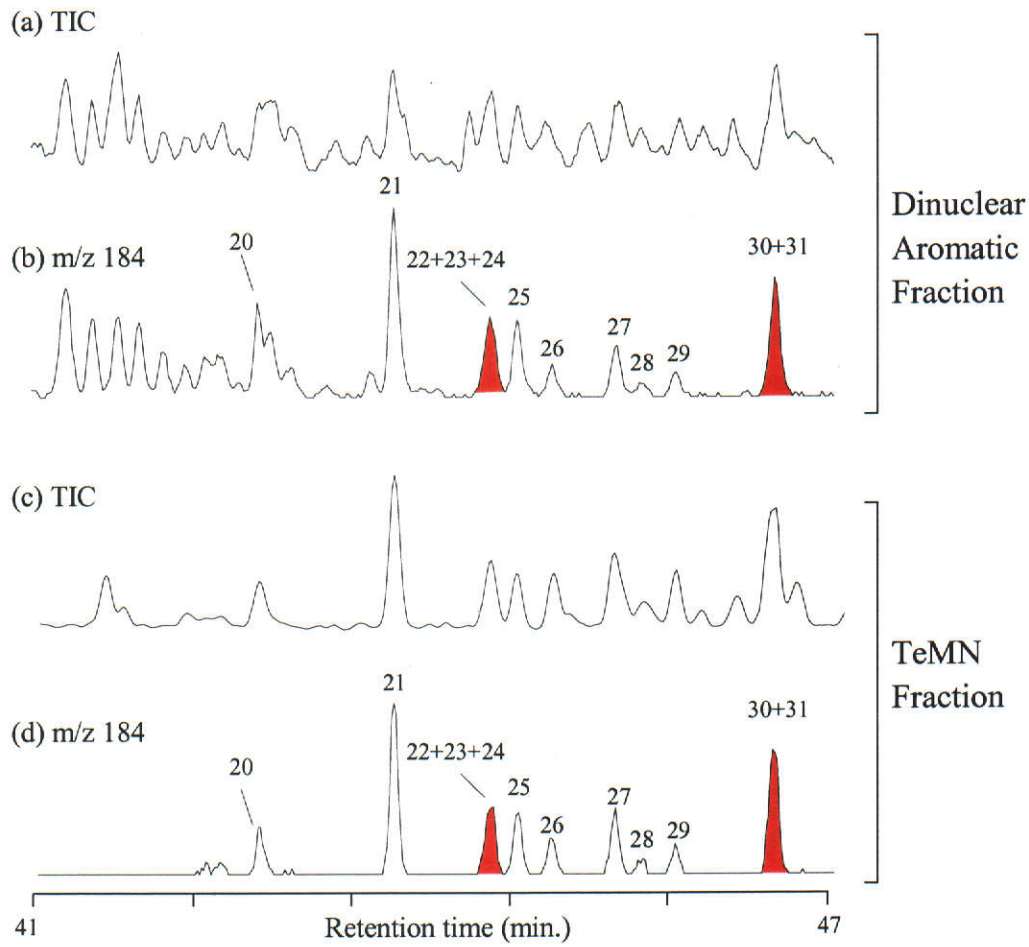

Figure 3-16: Partial gas chromatograms showing the TeMNs in aromatic fractions obtained from Lambert-1 crude oil. The total ion chromatogram and m/z 184 mass chromatograms from analysis of the dinuclear aromatic fraction are shown in (a) and (b) respectively. Chromatograms obtained from a fraction enriched in TeMNs are shown in (c) and (d).

This illustrates a major disadvantage of GC-FTIR in comparison with GC-MS in the analysis of complex mixtures of hydrocarbons, as well as emphasising how the two techniques complement each other. While differences in the infrared spectra of compounds may be used to differentiate between isomers of hydrocarbons, infrared spectroscopy is less useful in differentiating between different types of hydrocarbon assemblages. Mass selective detection exhibits the converse of this. Further, unlike GC-MS analysis where selected ion monitoring may be used to filter the charged species prior to their reaching the detector, the entire column effluent is stored and detected during direct deposition GC-FTIR analysis.

To facilitate analysis of TeMNs using GC-FTIR, a fraction enriched in TeMNs was obtained from the crude oil by subjecting the dinuclear aromatic hydrocarbon fraction to further thin layer chromatography using deactivated neutral alumina as the stationary phase. The TeMNs were thereby isolated from the interfering co-eluting compounds, illustrated by the similarity between the total ion chromatogram and the m/z 184 mass chromatogram from this fraction, shown in Figure 3-16. The co-eluting isomer mixtures in this fraction were analysed using GC-FTIR.

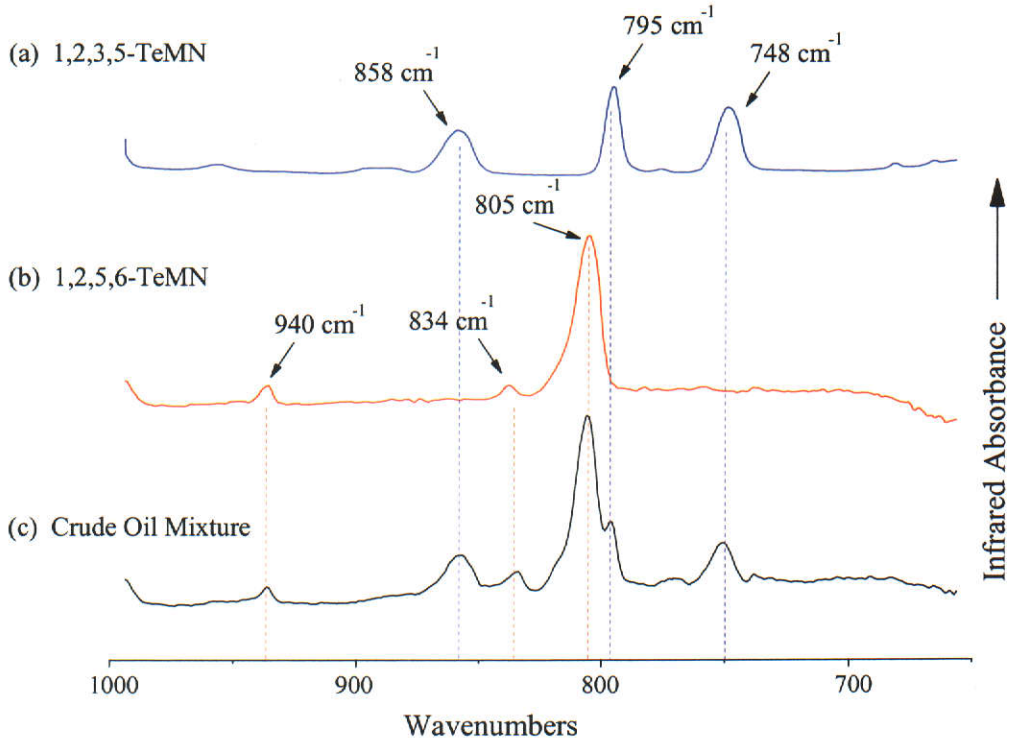

Figure 3-17: Partial FTIR spectra of authentic samples of (a) 1,2,3,5-TeMN and (b) 1,2,5,6-TeMN and (c) the mixture of these compounds occurring in Lambert-1 crude oil. Spectra were obtained using GC-FTIR at a resolution of 2 cm^{-1}.

1,2,5,6-TeMN and 1,2,3,5-TeMN

Partial infrared spectra of 1,2,5,6-TeMN and 1,2,3,5-TeMN, normalised using the C-H stretching vibration are shown in Figure 3-17, compared with the spectrum of the corresponding compounds contained in the TeMN fraction isolated from the crude oil. It is clear that differences in the infrared spectra may be used to distinguish between, and quantify the contribution of these compounds to the crude

oil mixture. The total area of absorbance peaks at 805 cm^{-1}, 834 cm^{-1} and 940 cm^{-1}, characteristic of 1,2,5,6-TeMN, compared with the total of those at 748 cm^{-1}, 795 cm^{-1} and 858 cm^{-1} for 1,2,3,5-TeMN, when corrected for differences in response, reveals that Lambert-1 crude oil contains a mixture of these isomers in the proportion 60% (1,2,5,6-TeMN) to 40% (1,2,3,5-TeMN).

1,2,4,6-TeMN, 1,2,4,7-TeMN and 1,4,6,7-TeMN

Determination of these isomers when they occur as a mixture poses a more difficult analytical challenge. The retention indices for these compounds, shown in Table 3-1, indicate that all three isomers display identical retention behaviour using a DB-5 capillary GC column. From inspection of the partial infrared spectra of these compounds, shown in Figure 3-18, it is evident that each isomer has a unique infrared spectrum. The differences in these spectra, however, are more subtle than those shown in the preceding studies of co-eluting polymethylnaphthalenes. Comparison with the spectrum obtained from the isomer mixture present in the crude oil reveals that only 1,4,6,7-TeMN exhibits an absorbance peak that does not suffer interference from peaks in the spectrum of at least one of the other co-eluting isomers. This peak occurs at 1494 cm^{-1}, corresponding to one of the stretching frequencies of the C-C bonds in the naphthalene nucleus. Therefore, using a similar simplistic approach to that described for the above-mentioned co-eluting polymethylnaphthalenes, only 1,4,6,7-TeMN may be determined on the basis of its infrared spectrum.

A more thorough investigation of the infrared spectra was necessary to determine each of the isomers. In this case, where several absorbance peaks overlap, spectral perturbation causes a deviation in Beer's Law. Determination of the components is therefore not as simple as solving simultaneous equations based on relative peak areas or heights obtained from spectra of the individual components. Instead, multi-component quantitative analysis, discussed in detail by several workers (Sternberg, Stillo and Schwendeman, 1960; Barnett and Bartoli, 1960; Brown et al., 1982; Maris, Brown and Lavery, 1983; Brown, 1984), using a P-matrix approach was adopted.

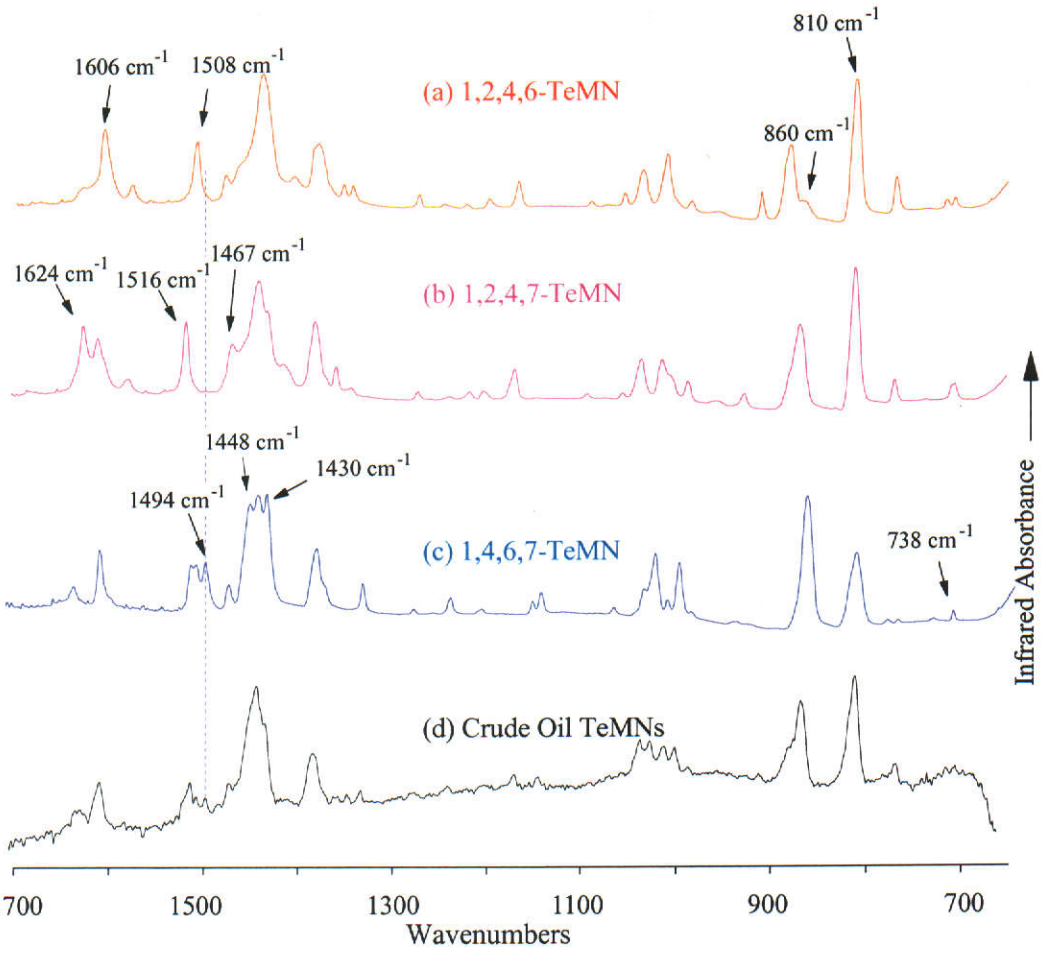

Figure 3-18: Partial FTIR spectra of authentic samples of (a) 1,2,4,6-TeMN and (b) 1,2,4,7-TeMN, (c) 1,4,6,7-TeMN and (d) the mixture of these compounds occurring in Lambert-1 crude oil. Spectra were obtained using GC-FTIR at a resolution of 2 cm^{-1}.

Briefly, this approach is based on a modified version of Beer's Law, namely:

$$C = PA$$

where C is the matrix of concentrations, P is the matrix relating absorbance to concentration and A is the matrix of absorbances.

In practice, a set of calibration standards (C) of varying known compositions of mixtures of the co-eluting TeMN components is analysed. From the infrared absorbance spectra (A) of these standard mixtures, the P matrix is calculated. The composition of an unknown mixture can therefore be calculated from the measured absorbance spectrum. The entire infrared spectrum, localised frequency ranges or

single frequencies may comprise the P-matrix data and these may be varied to obtain the best quality calibration. The quality of the calibration may be determined by applying the calibration matrix to the spectra used to determine the matrix and comparing the calculated composition with the known composition of the mixture. The experimental error may be determined by applying the matrix to the spectrum obtained from a mixture of known composition not used in the calibration

Determination of the TeMN calibration matrix involved the following sequential operations:

i. The high resolution (2 cm^{-1}) infrared spectra of 13 mixtures of the co-eluting isomers were acquired using GC-FTIR techniques. The compositions of these calibration mixtures are shown in Table 3-3. The spectra obtained from 12 of these were used to determine the calibration matrix, and that of the remaining mixture used to determine the experimental error.

ii. Frequencies which reflect a good linear response of absorbance to increasing concentration for each of the isomers were identified from these spectra by applying a standard least squares fit using the *Specfit* program from the commercially available software package *Quant32 (Bio-Rad Laboratories Inc.)*. At least three frequencies, summarised in Table 3-4, were selected for each isomer.

iii. Using the absorbance values extracted from the calibration set spectra at these frequencies, P-matrix analysis was performed using the *mult* program, also from the *Quant32* package. The parameters of this operation were set so that the sum of the per cent compositions were forced to equal 100 %.

The results of the calibration are summarised in Table 3-3. Here the relative isomer abundances of each of the 13 mixtures determined by GC-MS analysis is compared against those obtained from the GC-FTIR calibration. For each of the first 12 mixtures, the isomer abundance is calculated using the spectra of the other 11 mixtures as a calibration matrix. The remaining mixture of the reference compounds (Mixture 13) was prepared independently, and is not included in the GC-FTIR calibration matrix. In this case, the calibration matrix comprises all of the other 12 calibration mixtures. Inspection of the results shows that the deviation of the

calculated composition from the known relative abundance for each component in the mixtures used to perform the P-matrix analysis is less than 5%. The experimental error, estimated from mixture 13 was also approximately 5%.

Table 3-3: A summary of the results from a P-matrix analysis applied to the determination of the composition of a mixture of three tetramethylnaphthalene isomers. Calculated (Calc.) values refer to those obtained using GC-FTIR techniques while actual values were determined using GC-MS analysis.

Mixture No.	Relative Isomer Abundance (%)					
	1,2,4,6-TeMN		1,2,4,7-TeMN		1,4,6,7-TeMN	
	Calc.	Actual	Calc.	Actual	Calc.	Actual
1	46	45	24	23	30	32
2	52	55	5	6	43	39
3	16	16	36	35	48	49
4	22	22	10	10	68	68
5	76	78	8	9	16	13
6	24	24	58	58	18	18
7	4	0	1	0	95	100
8	101	100	2	0	-3	0
9	0	0	100	100	0	0
10	49	49	51	51	0	0
11	-2	0	48	48	54	52
12	48	50	0	0	52	50
13	55	58	34	32	11	10
Crude Oil	35	38	35	34	30	28

The spectrum obtained from the mixture of co-eluting 1,2,4,6-TeMN, 1,2,4,7-TeMN and 1,4,6,7-TeMN in the isolate from Lambert-1 crude oil was similarly analysed using the P-matrix calibration set. The relative abundance of each of these isomers is also given in Table 3-4. The composition of the mixture calculated in this way is in close agreement with those obtained from two separate GC-MS analyses using two different GC stationary phases: the relatively polar polyethylene glycol (BP-20 column) and the shape selective permethylated-β-cyclodextrin (Cydex-B column) described by Keim, Kohnes and Meltzow (1991) and Alexander et al. (1992). As expected from the retention indicies shown in Table 3-1, analysis using the BP20 column separated 1,4,6,7-TeMN from the co-eluting 1,2,4,6-TeMN and 1,2,4,7-TeMN. The Cydex-B column allowed the separation of 1,2,4,6-TeMN from the

other two isomers (Bastow, 1998). The relative abundances of each of the three isomers in the crude oil isolate could therefore be deduced from the two analyses, and these are shown as the actual abundances in Table 3-3.

Table 3-4: Selected frequencies for the P-matrix multi-component analysis of co-eluting tetramethylnaphthalene isomers (Refer to Figure 3-18).

Frequency (cm^{-1})	Isomer
738	1,4,6,7-TeMN
810	1,2,4,6-TeMN
860	1,2,4,6-TeMN
1430	1,4,6,7-TeMN
1448	1,4,6,7-TeMN
1467	1,2,4,7-TeMN
1494	1,4,6,7-TeMN
1508	1,2,4,6-TeMN
1516	1,2,4,7-TeMN
1606	1,2,4,6-TeMN
1624	1,2,4,7-TeMN

3.5 Determination of co-eluting alkylphenanthrenes using GC-FTIR

Alkylphenanthrenes occur as complex mixtures in crude oils and sedimentary source rock extracts. Conventional GC-MS analyses using apolar or medium polarity columns, yield only partial separation of the complex mixture of MPs, DMPs and ethylphenanthrenes (EPs). The retention behaviour of these has been well documented (Radke et al., 1984; Radke, Willsch and Welte, 1984; Garrigues et al., 1987) and is summarised in Table 3-5.

As for the alkylnaphthalenes, retention indicies were calculated for 24 isomers of DMPs and EPs (C_2-phenanthrenes, C_2-Ps) with the DB-5 stationary phase used in the present study, also shown in Table 3-5. These included all of the isomers for which co-elution has been previously reported (Radke et al., 1984; Radke, Willsch and Welte,1984; Garrigues et al., 1987), with the exception of 1,4-DMP and 3,4-DMP, both of which co-elute with 1,5-DMP on a similar phase (Garrigues et al., 1987). These three isomers each contain a 4- (equivalent to 5-) methyl substituent, are of low thermodynamic stability (Budzinski et al., 1993a), and therefore do not

commonly occur in crude oils and extracts from mature sedimentary rocks (e.g. Budzinski et al., 1995a).

The trinuclear aromatic hydrocarbon fraction isolated from Lambert-1 crude oil was analysed using GC-MS and direct deposition GC-FTIR (DB-5). The portion of the m/z 206 mass chromatogram in which the mixture of C_2-Ps elute is shown in Figure 3-19(a). The isomers possibly contained in the crude oil were tentatively identified by comparison with the retention indicies shown in Table 3-5. From this chromatogram, it is apparent that five of the peaks may represent co-eluting mixtures of C_2-Ps. The absence of the peak at the retention time for the 1,5-DMP indicates that the co-eluting mixture with 3,4-DMP and1,4-DMP does not occur in Lambert-1 crude oil and these compounds will not be discussed further.

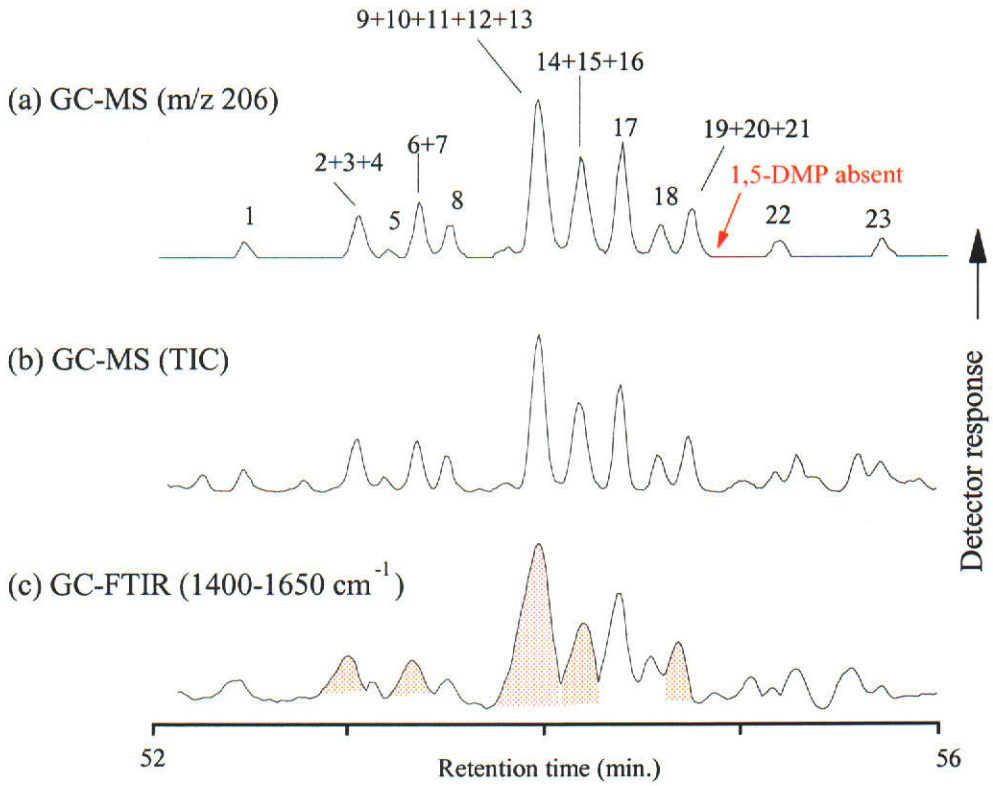

Figure 3-19: Partial (a) mass chromatogram (m/z206), (b) total ion chromatogram and (c) GC-FTIR functional group chromatogram (1400 cm^{-1}- 1650cm^{-1}) showing C_2-Ps in the trinuclear aromatic hydrocarbon fraction isolated from Lambert-1 crude oil. Peak identifications: (1) 3-EP; (2) 3,6-DMP; (3) 9-EP; (4) 2-EP; (5) 1-EP; (6) 3,5-DMP; (7) 2,6-DMP; (8) 2,7-DMP; (9) 3,9-DMP; (10) 3,10-DMP; (11) 2,10-DMP; (12) 1,3-DMP; (13) 2,4-DMP; (14) 1,6-DMP; (15) 2,9-DMP; (16) 2,5-DMP; (17) 1,7-DMP; (18) 2,3-DMP; (19) 1,9-DMP; (20) 4,9-DMP; (21) 4,10-DMP; (22) 1,8-DMP; (23) 1,2-DMP.

Table 3-5: Retention indices of phenanthrene, anthracene, and some of their alkylated homologues on DB-5 (J&W Scientific) and BP20 (SGE) stationary phases. Indices for MPs and the C_2-Ps are compared with values obtained on similar phases by (a) Garrigues et al. (1987), (b) Radke et al. (1984) and (c) Radke, Willsch and Welte (1984). Co-eluting compounds (DB-5) are grouped by shading.

Compound	Retention index on various gas chromatography stationary phases					
Stationary phase→	DB-5	BP20	CP-Sil 8CB[a]	SE-54[b]	Ultra 2[c]	Silar 10C[a]
Phenanthrene	300.00	300.00	300.00	300.00	300.00	300.00
Anthracene	301.70					
3-MP	319.02					
2-MP	320.01					
2-MA	321.29					
9-MP	323.16					
4-MP	323.25					
1-MA	323.38					
1-MP	324.01					
4,5-DMP	327.59	303.31	327.16			332.36
9-MA	329.17					
4-EP			331.59			
3-EP	333.66	307.44	332.60			317.02
9-EP	336.28	309.18	335.40		336.18	318.65
3,6-DMP	336.66	309.36	335.40	336.43	336.18	321.04
2-EP	336.33	308.99	335.44			318.22
1-EP	337.00		336.05			318.77
3,5-DMP	337.41	309.18	336.45	337.12		318.80
2-EA	337.88					
2,6-DMP	337.92	310.10	337.04		337.01	320.80
2,7-DMP	338.56	310.36	337.70	338.37	337.67	320.89
2,10-DMP	340.80	311.63	339.80		340.16	323.53
3,10-DMP	340.79	311.69	339.90	340.41	340.16	323.30
1,3-DMP	340.78	312.00	340.00	340.6	340.16	323.93
2,4-DMP	340.88	311.90	340.13			
3,9-DMP	340.91	311.73	340.20			323.32
1,6-DMP	341.50	312.14	340.80	341.40	340.96	324.42
2,5-DMP	341.65	312.04	340.84			322.84
2,9-DMP	341.84	312.37	340.60	341.53	340.96	323.02
1,7-DMP	342.62	312.82	341.80	342.33	341.91	324.53
2,3-DMP	343.50	313.47	342.90		342.71	327.01
4,9-DMP	344.15	313.66	343.20	343.85		324.79
1,9-DMP	344.24	314.06	343.40	343.95	343.52	327.21
4,10-DMP	344.34	313.78	343.40			324.86
1,4-DMP			344.00			
1,5-DMP	344.82	314.00	344.30	344.55		325.56
3,4-DMP			344.40			
1,8-DMP	346.29	315.00	345.20	346.05	345.53	328.30
1,2-DMP	348.84	316.91	347.90		347.98	332.65
9,10-DMP			348.52			
1,10-DMP			349.97			

Comparison of the total ion chromatogram, shown in Figure 3-19(b), with the 1400 cm^{-1}- 1650 cm^{-1} functional group chromatogram from GC-FTIR analysis [Figure 3-19(c)] reveals that although the chromatographic resolution is diminished by the GC-FTIR analyser, peaks corresponding to the C_2-Ps are apparent in the functional group chromatogram. Infrared spectra obtained from the five peaks due to co-eluting mixtures of isomers were examined to determine the contribution by each isomer to the mixture.

3.5.1 1,6-DMP, 2,9-DMP and 2,5-DMP

Figure 3-20 shows the partial infrared spectrum of authentic samples of each these three DMPs, compared with the spectrum obtained from the deposited material with the same retention time in the GC-FTIR chromatogram of the crude oil. As for the polymethylnaphthalenes, the spectra of the reference compounds have been normalised against the 2850 cm^{-1}- 3000 cm^{-1} absorbance peaks to correct for differences in the intensities of infrared absorbances. It is apparent that each of these DMPs has a characteristic spectrum. With respect to the other co-eluting isomers, 2,5-DMP has unique infrared absorbance peaks at 714 cm^{-1} and 826 cm^{-1} which arise from the out-of-plane bending vibrations from the C-H bonds in the unsubstituted aromatic ring positions. Similarly, 1,6-DMP has unique bands at 807 cm^{-1} and 835 cm^{-1} and 2,9-DMP at 722 cm^{-1} and 898 cm^{-1}. In addition, 2,9-DMP has a characteristic absorbance peak at 1492 cm^{-1}, attributable to differences in the stretching vibrations of the C-C bonds of the aromatic nucleus.

From inspection of the spectrum of the co-eluting DMPs present in the crude oil, the absence of those absorbance peaks unique to 2,5-DMP indicates its absence from the crude oil, consistent with the absence of the other thermodynamically unstable isomers (Budzinski et al., 1993a). Conversely, the occurrence of the other two isomers is confirmed by the presence and relative intensities of their characteristic absorbance peaks. The concentrations of the 2,9-DMP and 1,6-DMP were calculated to be approximately equal in the crude oil.

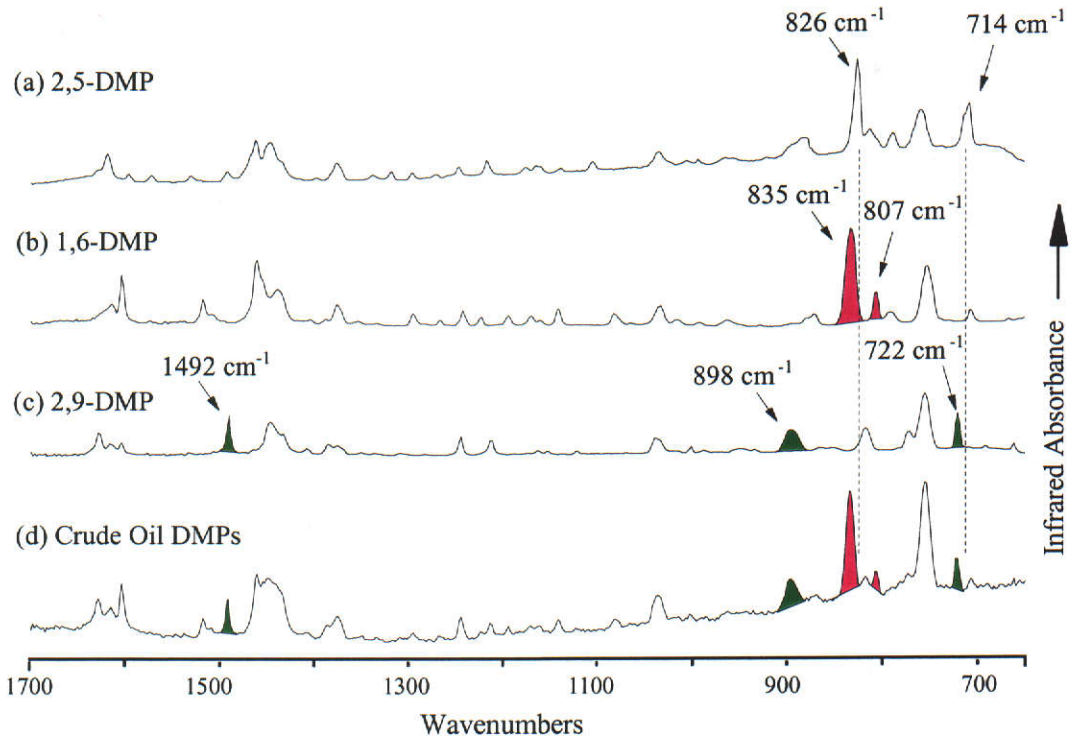

Figure 3-20: Partial infrared spectra of authentic samples of (a) 2,5-DMP, (b) 1,6-DMP and (c) 2,9-DMP reference compounds. The partial spectrum of the compounds in Lambert-1 crude oil with the same retention time as these co-eluting isomers is shown in (d). All spectra were obtained using GC-FTIR analysis at a resolution of 2 cm^{-1}.

3.5.2 2,6-DMP and 3,5-DMP

The co-eluting 2,6-DMP and 3,5-DMPs were similarly analysed and their infrared spectra are compared with that obtained from the crude oil in Figure 3-21. The spectra of the authentic samples of the DMPs are similar, however infrared absorbance peaks at 1610 cm^{-1}, 1250 cm^{-1} and 780 cm^{-1} indicate the presence of 2,6-DMP in the crude oil. The absorbance peak maximising at 760 cm^{-1} may be used to determine the proportion of 3,5-DMP in the isomer mixture. It is apparent from these observations that this component of Lambert-1 crude consists entirely of 2,6-DMP.

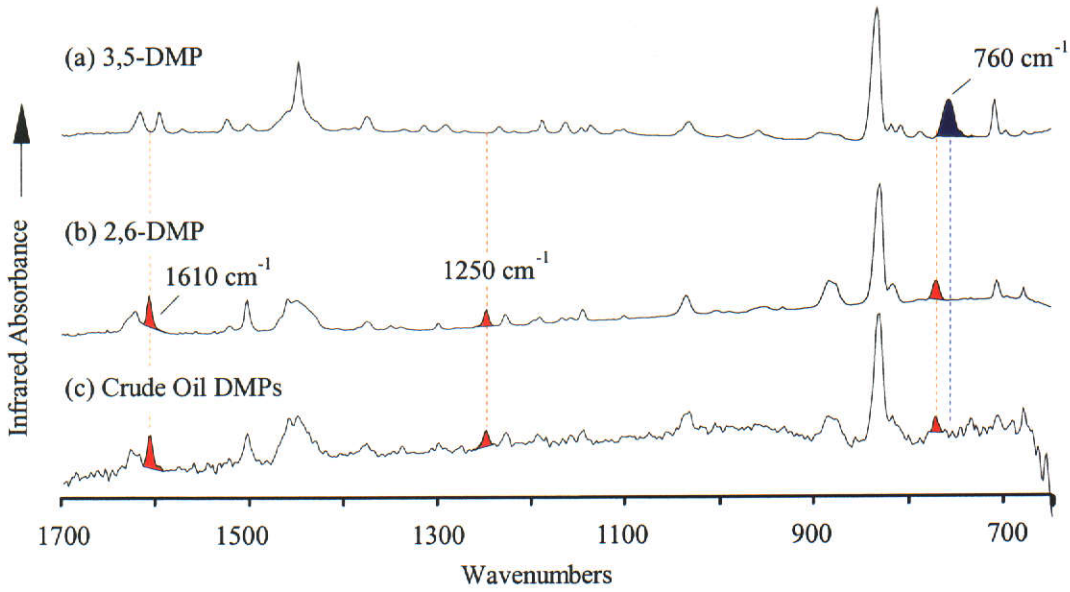

Figure 3-21: Partial FTIR spectra of (a) 3,5-DMP and (b) 2,6-DMP reference compounds. The partial spectrum of the compounds in Lambert-1 crude oil with the same retention time as these co-eluting isomers is shown in (c). All spectra were obtained using direct deposition GC-FTIR.

3.5.3 1,9-DMP, 4,9-DMP and 4,10-DMP

Figure 3-22 shows partial infrared spectra of 1,9-DMP, 4,9-DMP and 4,10-DMP reference compounds compared with the spectrum obtained from the crude oil component with the same retention time. The spectra of the three reference compounds are similar since each isomer has a 9-methyl (equivalent to 10) substituent. However, 1,9-DMP may be differentiated from both of the other isomers by the occurrence of an absorbance peak at 690 cm^{-1} which is absent from the other spectra. As one would expect from the close structural similarity, the spectra of 4,9-DMP and 4,10-DMP are nearly identical. Close inspection, however, reveals that an intense peak at 733 cm^{-1} and relatively weakly absorbing signals at 1490 cm^{-1} and 1120 cm^{-1} are unique to the spectrum of 4,10-DMP. Similarly, 4,9-DMP is characterised by peaks at 675 cm^{-1}, 725 cm^{-1} and 1200 cm^{-1}. It is apparent from the spectrum obtained from the Lambert crude oil component that 1,9- DMP is the only isomer of these three detected in this sample. Considering the similarity in the frequencies of the more intense absorbance peaks of these three isomers, however, it would be difficult to determine the proportion of each isomer in mixtures were they to co-occur.

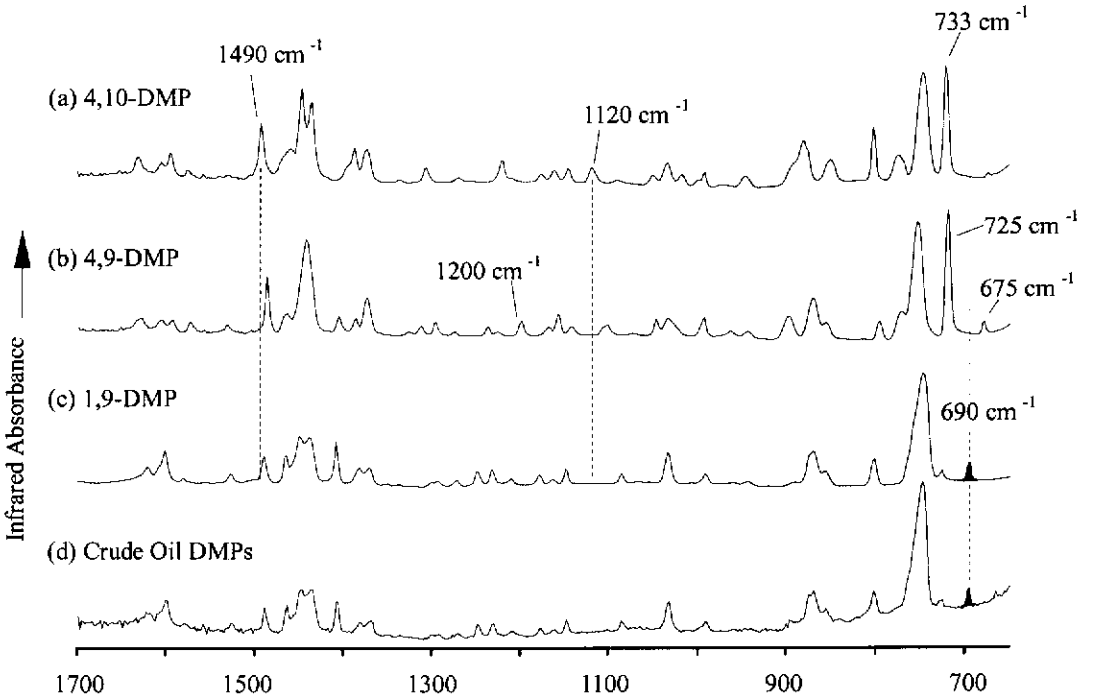

Figure 3-22: Partial FTIR spectra of (a) 4,10-DMP, (b) 4,9-DMP and (c) 1,9-DMP reference compounds. The partial spectrum of the compounds in Lambert-1 crude oil with the same retention time as these co-eluting isomers is shown in (d). All spectra were obtained using GC-FTIR analysis at a resolution of 2 cm^{-1}.

3.5.4 1,3-DMP, 3,10-DMP, 3,9-DMP, 2,10-DMP and 2,4-DMP

Determination of the co-eluting isomers 1,3-DMP, 3,10-DMP, 3,9-DMP, 2,10-DMP and 2,4-DMP poses a more complex problem than the previous examples. One would predict from the thermodynamic stabilities of the isomers (Budzinski et al., 1993a) that 2,4-DMP is likely to be absent from the mixture, while the four other components should be present. The absence of 2,4-DMP in this mixture was confirmed by the absence of absorbance peaks at 710 cm^{-1} and 795 cm^{-1} in the combined spectrum shown in Figure 3-23. These frequencies are unique to 2,4-DMP with respect to the other four DMPs in the mixture. Inspection of the infrared spectra of these remaining four isomers, and that of Lambert-1 crude oil revealed that although each isomer is shown to have a characteristic infrared spectrum, the contribution by each to the mixture in the crude oil is difficult to apportion due to the overlap of absorbance peaks. The simplification of this spectrum by sequentially subtracting the contribution of each of the reference spectra was therefore investigated.

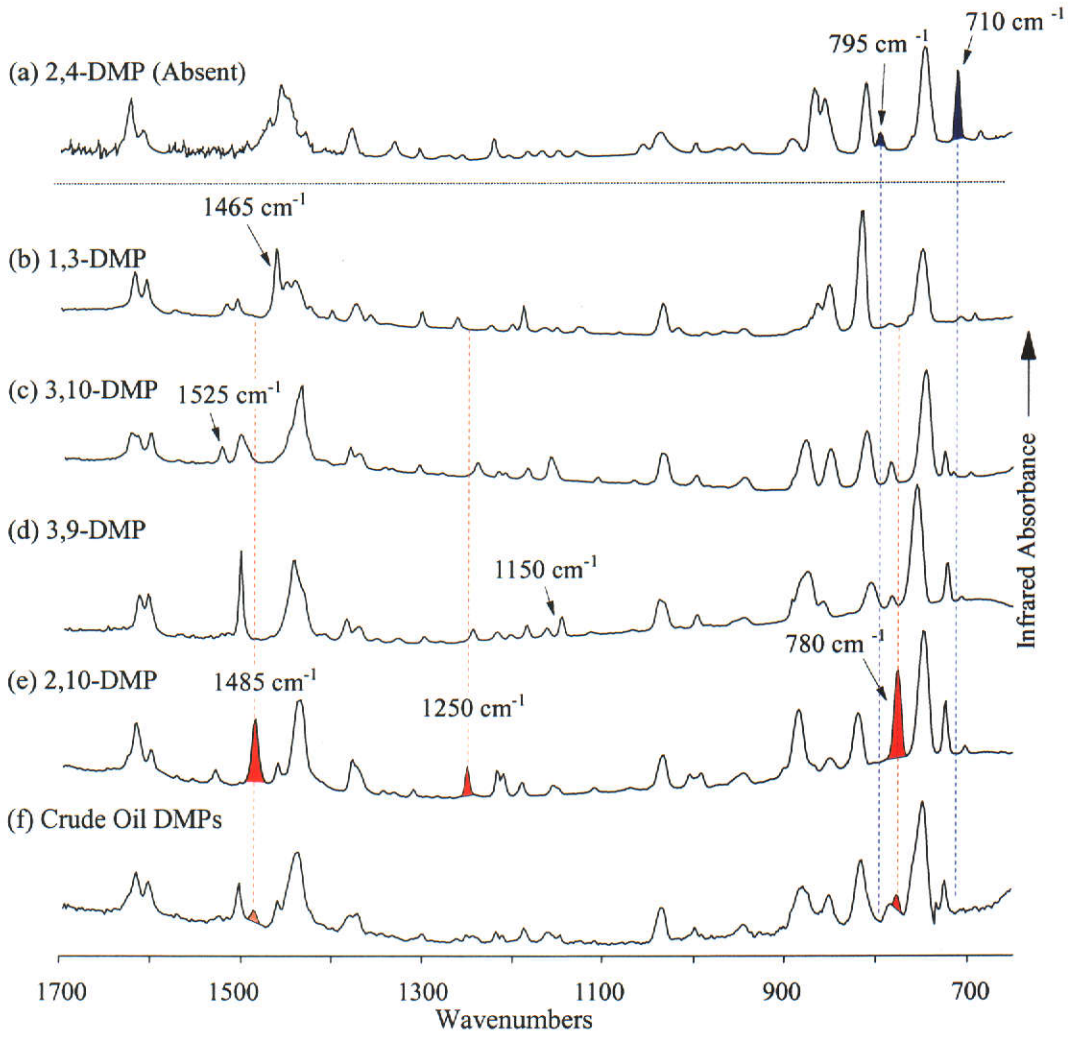

Figure 3-23: Partial FTIR spectra of (a) 2,4-DMP, (b) 1,3-DMP, (b) 3,10-DMP, (c) 3,9-DMP and (d) 2,10-DMP. The partial spectrum of the compounds in Lambert-1 crude oil with the same retention time as these co-eluting isomers is shown in (e). All spectra were obtained using direct deposition GC-FTIR.

Of the four co-eluting isomers, only 2,10-DMP exhibits characteristic peaks in its infrared spectrum (at 1485 cm^{-1}, 1250 cm^{-1} and 780 cm^{-1}) that may be identified in the spectrum of the mixture. The spectrum of 1,3-DMP does not contain a unique absorbance peak, however the peak at approx 1465 cm^{-1} co-occurs only in the spectrum of 2,10- DMP. Therefore, we can calculate the relative abundance of 1,3-DMP by subtracting the contribution of 2,10-DMP to this peak. After subtraction of the spectra of 1,3-DMP and 2,10-DMP from the total spectrum in the proportions calculated above, the residual spectrum represents the contributions of 3,10-DMP and 3,9-DMP. These two compounds may now be determined from this

simplified spectrum using differences in their spectra at approximately 850 cm^{-1} and 1525 cm^{-1} (3,10-DMP) and 1150 cm^{-1} (3,9-DMP).

From this approach, there is evidence for contribution from each of the isomers (1,3-DMP; 3,9-DMP; 2,10-DMP and 3,10-DMP) in approximate concentrations of 25%, 20%, 25% and 30% respectively; however, the resulting spectrum of the mixture, after subtraction of the contributing spectra of the four isomers, displays broad absorbance bands and does not resemble that of a background region of the chromatogram.

To confirm the somewhat questionable results obtained by the successive subtraction of the contribution of each isomer to the mixture (with associated errors), the P-matrix approach described earlier (see Section 3.4.4) for the co-eluting 1,2,4,6-TeMN, 1,2,4,7-TeMN and 1,4,6,7-TeMN was applied to this co-eluting mixture of DMPs. Briefly, the high resolution (2 cm^{-1}) infrared spectra of 13 mixtures of varying known compositions of the reference compounds were acquired to obtain a calibration matrix, while another independently prepared mixture was analysed to assess the experimental error. The concentration of each isomer in each of the mixtures in the matrix was confirmed using GC-MS analysis; however, since the DMPs co-elute using the chromatographic conditions applied here, MP isomers were used as internal standards against which the peak area of the co-eluting DMPs were compared.

The result of the calibration is summarised in Table 3-6. In spite of the potential error associated with the determination of the actual abundance of each calibration mixture, there is generally good agreement between the calculated and actual abundances. Quantification of the isomers using the two methods, i.e. successive subtraction and the P-matrix calibration, agreed to within less than the experimental error defined by the results from mixture 14, suggesting the estimates are reasonably robust. Although not demonstrated here, it is likely that the proportions of other co-eluting DMPs, where each has a similar infrared spectra (e.g. 1,9-DMP, 4,9-DMP and 4,10-DMP), might also be determined using these methods.

Table 3-6: Summary of the P-matrix analysis applied to the determination of the composition of a mixture of four dimethylphenanthrene isomers. Calculated values refer to those obtained using GC-FTIR techniques while actual values were determined using GC-MS analysis.

Mix	Relative Isomer Abundance (per cent)							
No.	1,3-DMP		3,10-DMP		3,9-DMP		2,10-DMP	
	Calc.	Actual	Calc.	Actual	Calc.	Actual	Calc.	Actual
1	29	30	31	31	25	26	15	13
2	34	33	32	31	8	8	26	28
3	30	30	6	10	31	29	33	31
4	10	9	31	32	32	31	27	28
5	22	21	28	25	12	14	38	40
6	8	9	11	11	5	6	76	74
7	14	13	18	17	41	42	27	28
8	11	12	59	58	9	8	21	22
9	55	54	13	14	8	8	24	24
10	27	29	35	33	18	19	20	19
11	24	23	25	27	6	5	45	45
12	26	25	10	10	18	17	46	48
13	8	9	28	28	15	16	49	47
14	25	25	26	26	24	27	25	22
Oil	25	n.d.	28	n.d.	24	n.d.	23	n.d.

3.5.5 3,6-DMP, 2-EP and 9-EP

The co-eluting C_2-Ps, 3,6-DMP, 2-EP and 9-EP may also be determined using differences in their infrared spectra as shown in Figure 3-24. Here the infrared spectrum of authentic samples of each of these compounds and the crude oil component is displayed between two intervals, namely 2800 cm^{-1} to 3200 cm^{-1} and 650 cm^{-1} to 1700 cm^{-1}. It is apparent from these spectra that the two EPs may be distinguished from the 3,6-DMP by the high intensity of the absorbance peak at 2950 cm^{-1}, arising from the asymmetric stretching vibration of the C-H bonds of the methylene moiety in the ethyl substituent (Roeges, 1994). Close inspection of the spectra in the 650 cm^{-1} to 1700 cm^{-1} interval also reveals that 3,6-DMP has unique peaks at 840 cm^{-1} and 1520 cm^{-1}. Similarly, 2-EP has unique absorbances at 805 cm^{-1} and 710 cm^{-1}, and 9-EP at 725 cm^{-1}. The crude oil component therefore comprises mainly 3,6-DMP (840 cm^{-1} and 1520 cm^{-1}) although there is some contribution from the ethylphenanthrenes (2950 cm^{-1}). Peaks at 805 cm^{-1} (2-EP) and the broad peak at 740 cm^{-1}–750 cm^{-1}, due to the combined (unresolved) absorbances

from both 2-EP (750 cm^{-1}) and 9-EP (745 cm^{-1}), indicate that both EPs are present in the mixture.

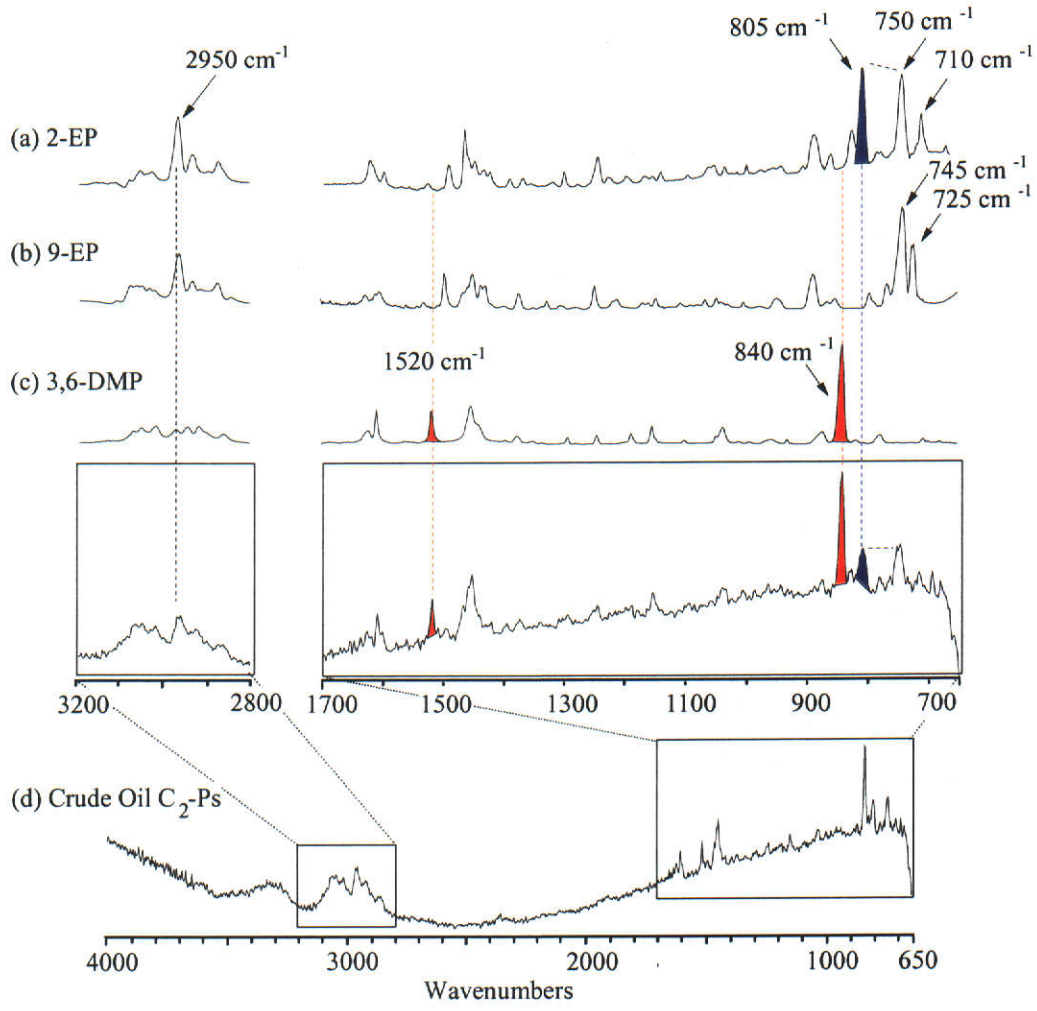

Figure 3-24: FTIR spectra of (a) 2-EP, (b) 9-EP and (c) 3,6-DMP reference compounds. The spectrum of the compounds in Lambert-1 crude oil with the same retention time as these co-eluting isomers is shown in (d). All spectra were obtained using direct deposition GC-FTIR.

While the spectra of 9-EP and 2-EP may be normalised using the 2850 cm^{-1} to 3000 cm^{-1} infrared absorbance peaks for comparison against one another, differences in absorbance intensity of the methylene C-H stretching vibrations (9-EP, 2-EP) as opposed to the methyl C-H stretching (3,6-DMP) prevents comparison with 3,6-DMP in this way. The calibration P-matrix approach was therefore applied to quantify the contribution by each of these compounds to the co-eluting mixture in the crude oil, results of which are summarised in Table 3-7.

Table 3-7: Summary of the P-matrix analysis applied to the determination of the composition of a mixture of 2-EP, 9-EP and 3,6-DMP. Calculated values refer to those obtained using GC-FTIR techniques while actual values were determined using GC-MS analysis.

Mix	Relative Isomer Abundance (per cent)					
	2-EP		9-EP		3,6-DMP	
	Calc.	Actual	Calc.	Actual	Calc.	Actual
1	39	40	31	30	30	30
2	29	30	34	35	37	35
3	8	10	19	20	73	70
4	24	25	3	5	73	70
5	68	70	19	20	13	10
6	29	30	32	30	39	40
Oil	13	n.d.	17	n.d.	70	n.d.

3.6 The application of GC-FTIR to investigate the fractionation of C_2-phenanthrenes using mordenite molecular sieves

3.6.1 GC-MS analysis of mordenite sieve fractions

The use of mordenite molecular sieves to fractionate aromatic hydrocarbons has been previously investigated (Ellis, Kagi and Alexander, 1992; Ellis, Alexander and Kagi, 1994). Using this technique, alkylphenanthrenes that have a substituent at carbon number 9 of the phenanthrene nucleus are selectively excluded from the sieve pores due to their relatively large molecular dimensions. These are thereby physically separated from some of the otherwise substituted C_2-Ps that are included into the sieve pores. The sorption by these sieves of the other C_2-Ps, however, has not been unequivocally established due to the severe interference to the GC-MS analysis caused by co-elution of these compounds.

Here, the trinuclear aromatic hydrocarbon fraction from Lambert-1 crude oil was passed through an open tubular column packed with mordenite molecular sieves in a manner analogous to conventional liquid chromatographic techniques. Two fractions from the flow-through separation were recovered and analysed using GC-MS: the retained (included) fraction, containing compounds completely sorbed by the sieves was isolated by dissolving the sieves in hydrofluoric acid, and the eluted (excluded) fraction, containing compounds not sorbed by the sieves.

Figure 3-25 shows m/z 206 mass chromatograms of the C_2-Ps present in each of these fractions compared with that obtained from the crude oil prior to treatment with the molecular sieves (separation and analysis performed by L. Ellis). The compounds contributing to the co-eluting mixtures in the crude oil prior to sieving were identified according to the results from the GC-FTIR analysis discussed above. It is evident from these chromatograms that eight of the C_2-Ps contained in the crude oil are completely included into the sieve pores. These are summarised in Table 3-8. Of the C_2-Ps excluded from the sieves, only 1,9-DMP does not co-elute with other compounds in the crude oil and can therefore be established immediately as completely excluded from the mordenite sieve pores. Of the remaining nine co-eluting C_2-Ps, peaks corresponding to these compounds occur in varying abundances in the chromatograms of both fractions, and their sorption behaviour on the basis of GC-MS analysis cannot therefore be determined. The retained and eluted fractions from the molecular sieve separation were subsequently examined using GC-FTIR to determine the sorption behaviour of these compounds.

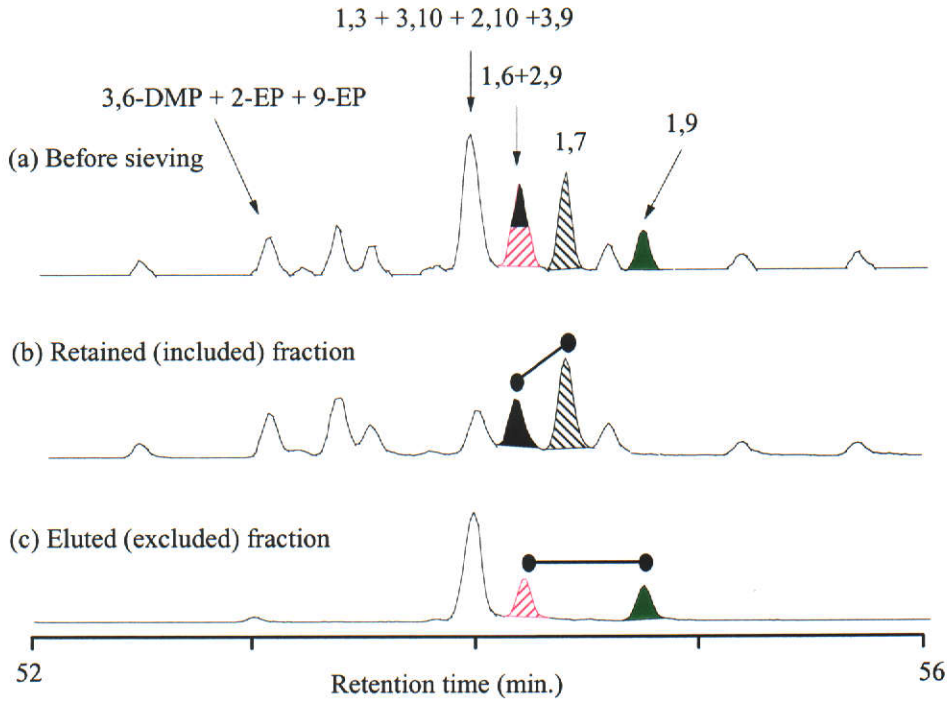

Figure 3-25: Partial mass chromatogram (m/z 206) showing the C_2-Ps (a) contained in the trinuclear aromatic hydrocarbon fraction isolated from Lambert-1 crude oil, (b) included into the pores of mordenite molecular sieves and (c) excluded from the mordenite molecular sieve. Numerals represent the substitution patterns of the DMPs. (Data provided by L. Ellis).

Table 3-8: The sorption by mordenite molecular sieves of C_2-phenanthrenes occurring in Lambert-1 crude oil (determined using GC-MS analysis).

Sorption Behaviour Established by GC-MS		
Included	Excluded	Undetermined
3-EP	1,9-DMP	3,6-DMP
1-EP		2-EP
2,6-DMP		9-EP
2,7-DMP		1,3-DMP
1,7-DMP		2,10-DMP
2,3-DMP		3,9-DMP
1,8-DMP		3,10-DMP
1,2-DMP		1,6-DMP
		2,9-DMP

3.6.2 GC-FTIR analysis of sieve fractions to establish sorption behaviour of the C_2-phenanthrenes

1,3-DMP; 3,9-DMP; 2,10-DMP and 3,10- DMP

Consider the mass chromatograms obtained prior to sieving and that of the included fraction shown in Figure 3-25. From comparing the abundance (peak area) of 1,7-DMP with that of the total of the compounds in this mixture, it is apparent that approximately 25 per cent of the mixture is included into the sieve pores. Similar comparison with the abundance of 1,9-DMP before sieving and in the eluted fraction reveals that the remaining 75 % of the mixture is excluded. Since 1,3-DMP is the only isomer in this mixture that does not have a methyl substituent in the 9 or 10 positions, and considering that prior to sieving the proportion of 1,3-DMP in the mixture was 25 % (see Table 3-6), one would expect that the included fraction of these four isomers would contain only 1,3-DMP. Examination of the spectrum obtained from the retained fraction, shown in Figure 3-26 confirms the sole presence of 1,3-DMP. Multi-component analysis of the spectrum obtained from the eluted fraction, also shown in Figure 3-26, revealed that the contribution of 1,3-DMP to the excluded mixture was below the limits of detection of the analysis (less than 2%). Furthermore, the 2,10-DMP, 3,10-DMP and 3,9-DMP were present in approximately equal abundance, in agreement with the determination of the mixture prior to sieving as shown earlier in Table 3-6.

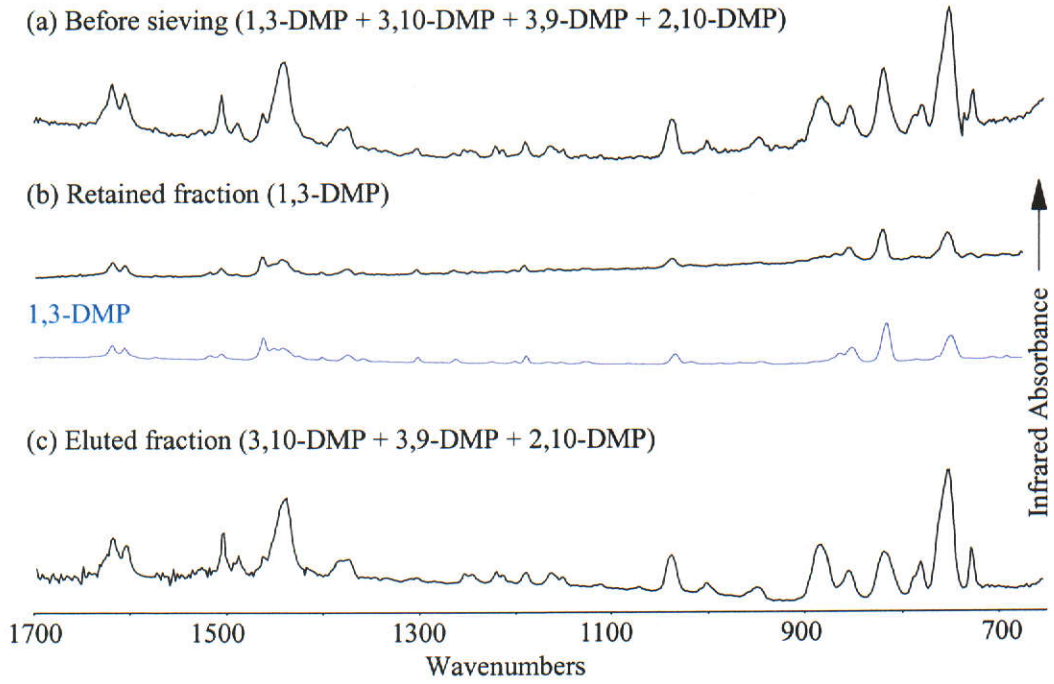

Figure 3-26: Partial FTIR spectra of (a) the co-eluting mixture of 1,3-DMP, 3,10-DMP, 3,9-DMP and 2,10-DMP in Lambert-1 crude oil, (b) the portion of this mixture retained by mordenite sieves and (c) the fraction eluted from mordenite sieves. The spectrum obtained from an authentic sample of 1,3-DMP is also shown.

3,6-DMP, 2-EP and 9-EP

Partial infrared spectra from the peak due to 3,6-DMP, 2-EP and 9-EP obtained from the retained and eluted fractions are shown in Figure 3-27. Inspection of these reveals that the retained fraction comprises a mixture of 3,6-DMP and 2-EP, and that 9-EP is absent from this fraction. These observations were confirmed by multi-component analysis of the spectra using the calibration matrix described earlier (Table 3-7). Conversely, the eluted fraction of this mixture contains only 9-EP.

1,6-DMP and 2,9-DMP

Partial infrared spectra of both the included and excluded components of this mixture are shown in Figure 3-28, revealing that the retained fraction contained exclusively 1,6-DMP and the eluted fraction contained only 2,9-DMP.

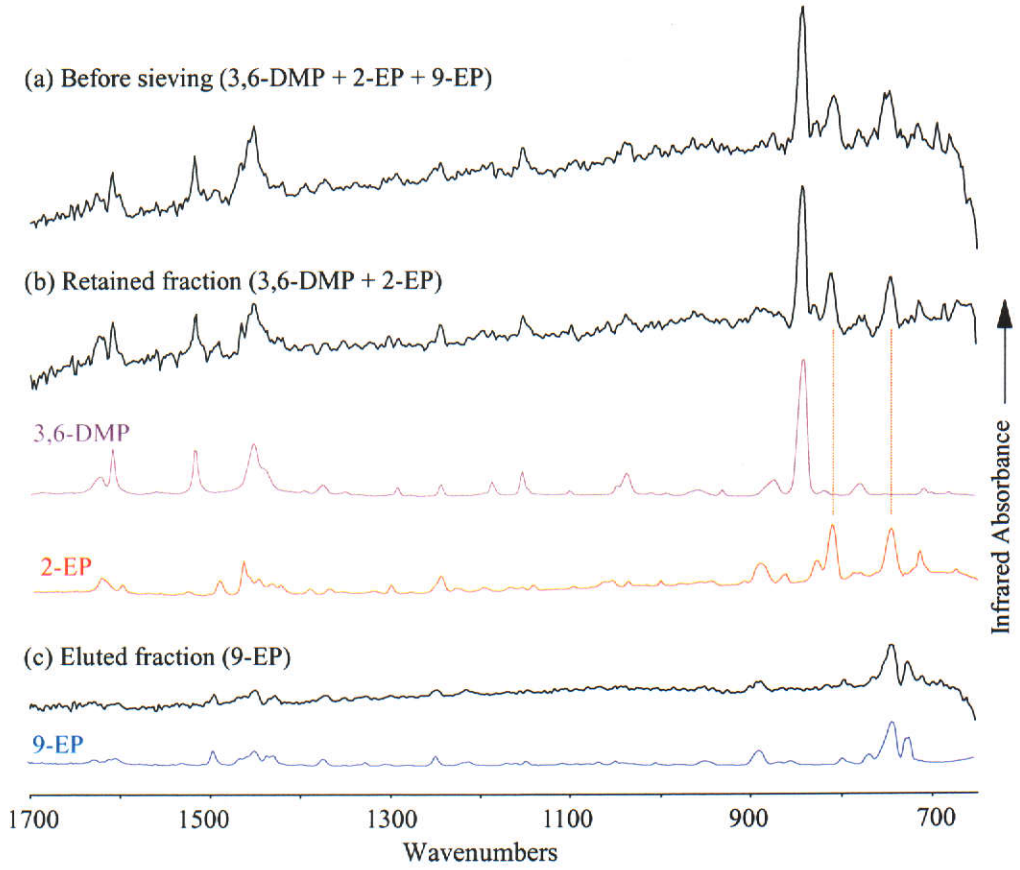

Figure 3-27: Partial FTIR spectra of (a) the co-eluting mixture of 2-EP, 9-EP and 3,6-DMP in Lambert-1 crude oil, (b) the portion of this mixture retained by mordenite sieves and (c) the fraction eluted from mordenite sieves. Spectra obtained from authentic samples of each of these compounds are also shown.

It is apparent from these analyses that the C_2-Ps present in the crude oil were either completely excluded from or completely included into the molecular sieve. The sorption behaviour of each these C_2-Ps are summarised in Table 3-9. Only those EPs and DMPs containing a substituent in the 9 position (or the equivalent 10 position) were excluded from the sieve pores, while all of the remaining isomers and homologues were completely included. These observations, although generally consistent with those made by earlier workers (Ellis, Alexander and Kagi, 1994), greatly simplify the interpretation of the sorption behaviour of these alkylphenanthrenes since "partial sorption" did not occur for any of these compounds.

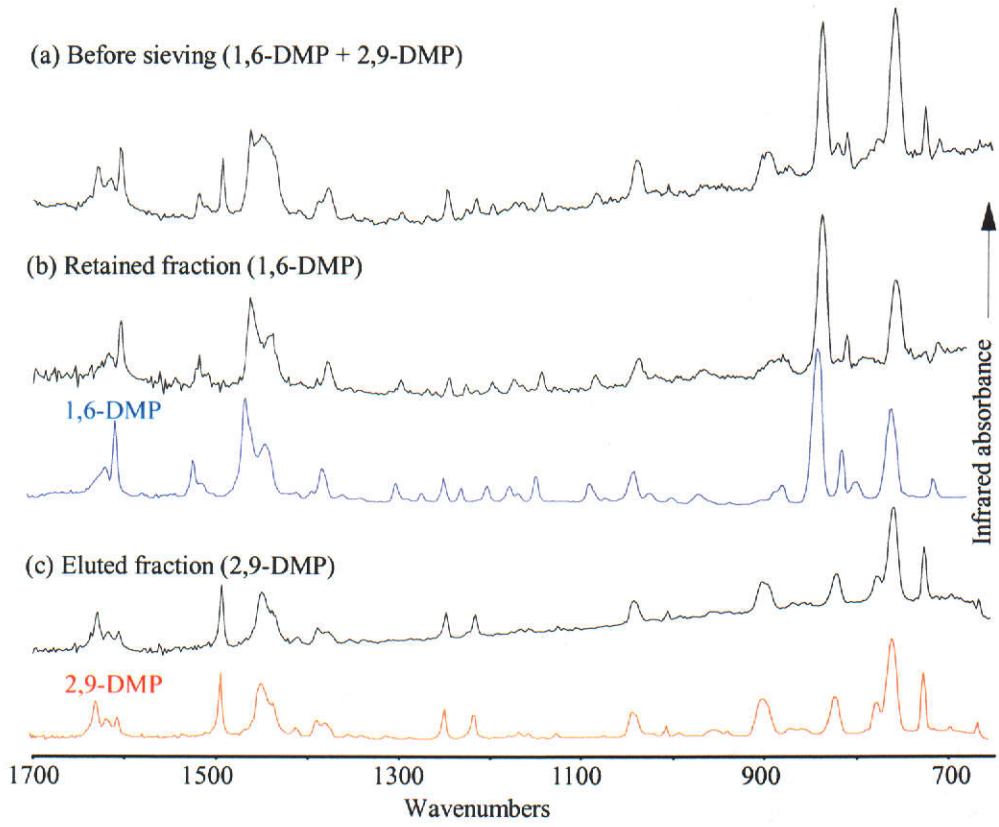

Figure 3-28: Partial FTIR spectra of (a) the co-eluting mixture of 1,6-DMP and 2,9-DMP in Lambert-1 crude oil, (b) the portion of this mixture retained by mordenite sieves and (c) the fraction eluted from mordenite sieves. Spectra obtained from authentic samples of 1,6-DMP and 2,9-DMP are also shown.

Table 3-9: The sorption by mordenite molecular sieves of C_2-phenanthrenes occurring in Lambert-1 crude oil determined using GC-MS and GC-FTIR analyses.

Sorption Behaviour	
Included	Excluded
3-EP	9-EP
3,6-DMP	2,10-DMP
2-EP	3,9-DMP
1-EP	3,10-DMP
2,6-DMP	2,9-DMP
2,7-DMP	1,9-DMP
1,3-DMP	
1,6-DMP	
1,7-DMP	
2,3-DMP	
1,8-DMP	
1,2-DMP	

3.6.3 Investigation of the effects of moisture content on the sorption of C_2-phenanthrenes

In sorption experiments using individual reference compounds, Ellis, Alexander and Kagi (1994) observed that 1,3-DMP, 2,5-DMP and 3,5-DMP occurred in both the retained and eluted fractions. The weak sorption of these compounds by the molecular sieve lead to the conclusion that the molecular dimensions of these compounds did not exclusively control the sorption behaviour. Here, one of these experiments was repeated with an authentic sample of 3,5-DMP, which contrary to the study by Ellis, Alexander and Kagi (1994), was completely excluded from the mordenite sieve. The differences in sorption behaviour of the alkylphenanthrenes between the two studies might be explained by differences in the moisture content of the molecular sieves. Where the sieve pores contained water molecules, the alkylphenanthrenes are more weakly sorbed than in cases where the sieves are completely anhydrous.

This hypothesis was tested by treating a mixture of 2,6-DMP and 3,5-DMP with mordenite molecular sieves of differing moisture contents: 2,6-DMP was chosen as a model for compounds included into the mordenite pores and 3,5-DMP for those compounds excluded. Duplicate aliquots of a solution containing 2,6-DMP (60 μg) and 3,5-DMP (40μg) were prepared. One of the aliquots was separated into retained and eluted fractions as described earlier using mordenite sieves that had been dried at 100°C under vacuum immediately prior to use. Another separation was carried out on the other aliquot after the moisture content of the sieves had been allowed to equilibrate with the atmosphere for 48 hours. Results of these experiments are summarised in Figure 3-29.

GC-MS analysis (BP20 column) of the fractions obtained from the separation using anhydrous sieves revealed that 2,6-DMP and 3,5-DMP were completely included and completely excluded respectively. The sieves deactivated with atmospheric moisture also yielded a retained fraction that contained only 2,6-DMP, however the eluted fraction comprised both isomers where the abundance of the 2,6-DMP had decreased by approximately 60% relative to 3,5-DMP. This fraction was subsequently treated

with the deactivated sieves for a second time, again yielding an eluted fraction containing both isomers but further depleted in 2,6-DMP by approximately 60%. The retained fraction again contained only 2,6-DMP. It is evident from these experiments that the 3,5-DMP was always excluded regardless of the moisture content of the mordenite sieve pores. The sorption of 2,6-DMP, however, was dependent on the moisture content of the sieve, with moist sieves sorbing it more weakly.

To further investigate the effect of moisture on the size exclusion characteristics of mordenite, the triaromatic fraction isolated from the crude oil was also fractionated using sieves deactivated by exposure to atmospheric moisture. Contrary to the observations from the initial experiment carried out under anhydrous conditions, here 1,3-DMP and 3,6-DMP were completely excluded and 2,6-DMP was weakly sorbed by the moist mordenite. A probable explanation for this behaviour is that not withstanding the hydrophobicity of the mordenite pore structure, with exposure to moisture, water molecules occupy the pores, and although hydrocarbons with sufficiently small molecular dimensions to enter the pores are preferentially absorbed thereby displacing the water, the energy requirement to do so exceeds that of this system.

This conclusion was confirmed by treating the trinuclear aromatic hydrocarbon isolate in a batch-wise procedure with the humidified molecular sieves in refluxing hexane with the aid of ultrasonication. Analysis of the excluded fraction using GC-FTIR yielded identical results to the flow-through fractionation using anhydrous mordenite sieves. Based on this evidence it seems that each of the C_2-Ps is either completely sorbed or completely excluded from mordenite molecular sieves under anhydrous conditions. There should therefore be no advantage in efficiency of separation afforded by performing the fractionation in a flow-through rather than in a batch-wise manner. Thus, when the fractionation of the trinuclear aromatic hydrocarbon isolate was carried out in a batch-wise manner using anhydrous mordenite the results were identical to those obtained using the column procedure.

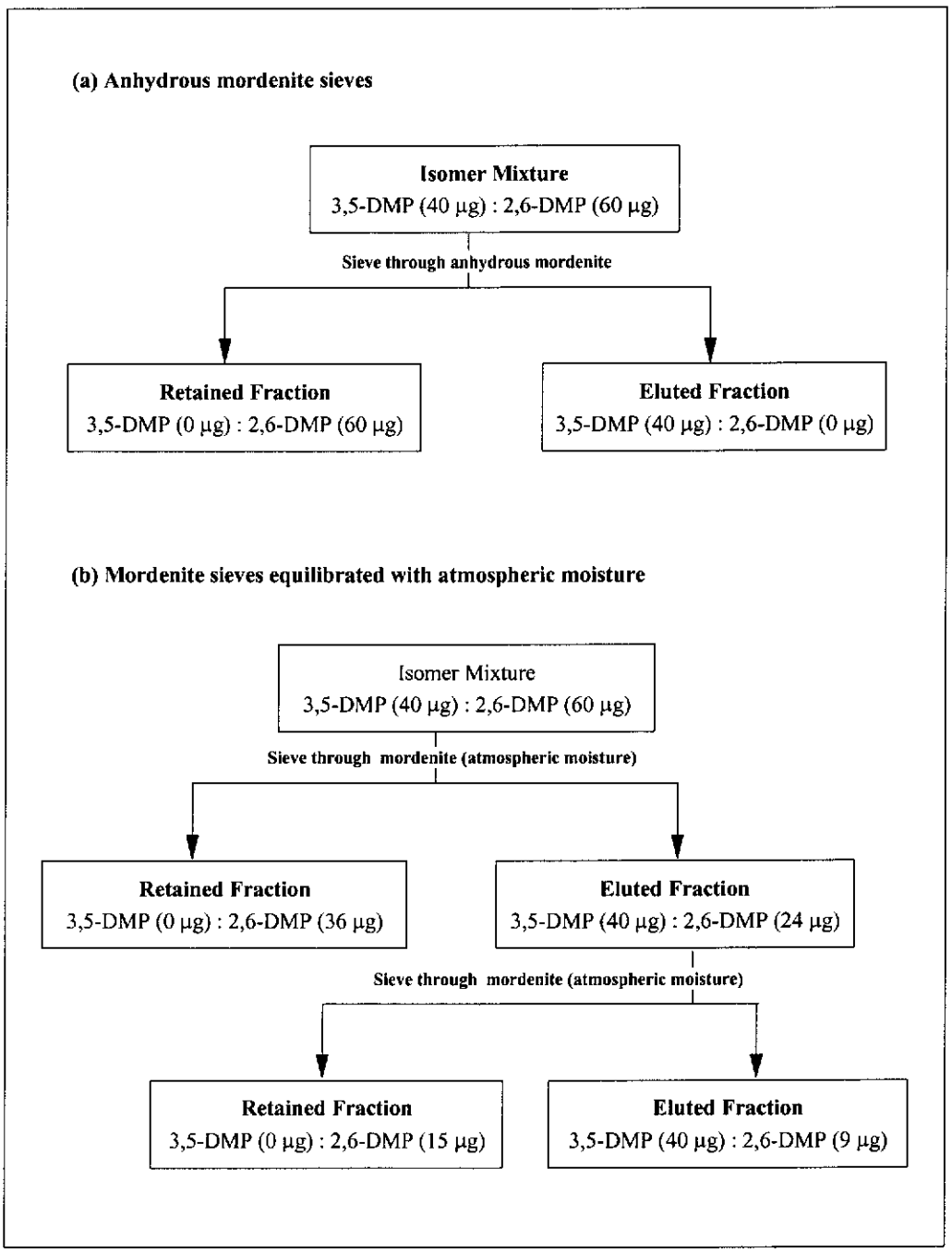

Figure 3-29: Flow charts showing the fractionation of a mixture of 2,6-DMP and 3,5-DMP using mordenite molecular sieves with different moisture contents.

3.7 Identification of miscellaneous aromatic hydrocarbons in petroleum

In addition to determining the composition of co-eluting mixtures of isomers, the application of GC-FTIR to the unambiguous identification of several aromatic hydrocarbons was investigated.

3.7.1 Alkylanthracenes

Occasionally, unusual distributions of alkylphenanthrenes are observed in extracts from sedimentary rocks (e.g. Garrigues et al., 1984) and crude oils (e.g. Li et al., 1998). These distributions are signified by the co-occurrence of anthracene and several other compounds, some of which interfere with the analysis of the MPs and DMPs. Figure 3-30 shows mass chromatograms of such distributions observed in an extract from sedimentary material (Kelp-1, 2389 m). From inspection of the mass chromatogram, which shows responses for the methylphenanthrenes (MPs, m/z 192), two peaks that are usually not observed are apparent. The first of these (marked with an asterisk) elutes between 2-MP and 9-MP and the second co-elutes with 9-MP.

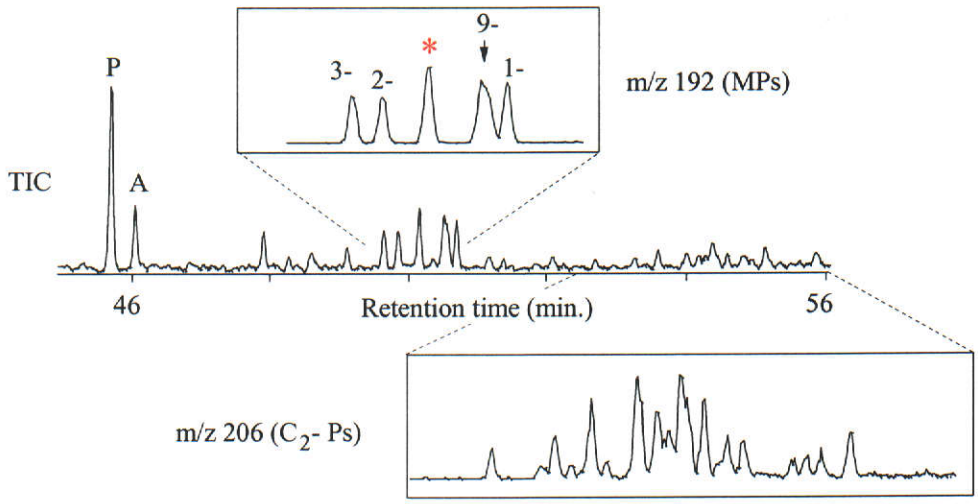

Figure 3-30: Partial GC-MS chromatograms obtained from an aromatic hydrocarbon fraction isolated from sedimentary material from Kelp-1 (2389 m). Phenanthrene (P) and anthracene (A) were identified from their mass spectra and retention time. Unusual mixtures of methylphenanthrenes (MPs) and dimethylphenathrene and ethylphenanthrene (C_2-Ps) are shown in the inset mass chromatograms.

Compounds with similar retention behaviour have previously been assigned as 2-methylanthracene (2-MA) and 1-methylanthracene (1-MA) respectively on the basis of their retention time and mass spectra (George, 1992; Smith, George and Batts, 1995; Li et al., 1998) and their (Shpol'skii) fluorescence emission spectra (Garrigues et al., 1984.) The extract was analysed using direct deposition GC-FTIR and the infrared spectra of the compounds corresponding to the two above-mentioned peaks were acquired. Figure 3-31 shows the infrared spectrum of the first eluting peak compared with a similarly acquired spectrum of 2-MA reference compound. The striking similarity of these spectra in conjunction with the similarity in retention behaviour enables the unambiguous identification of the compound in the sedimentary rock extract as 2-MA alone.

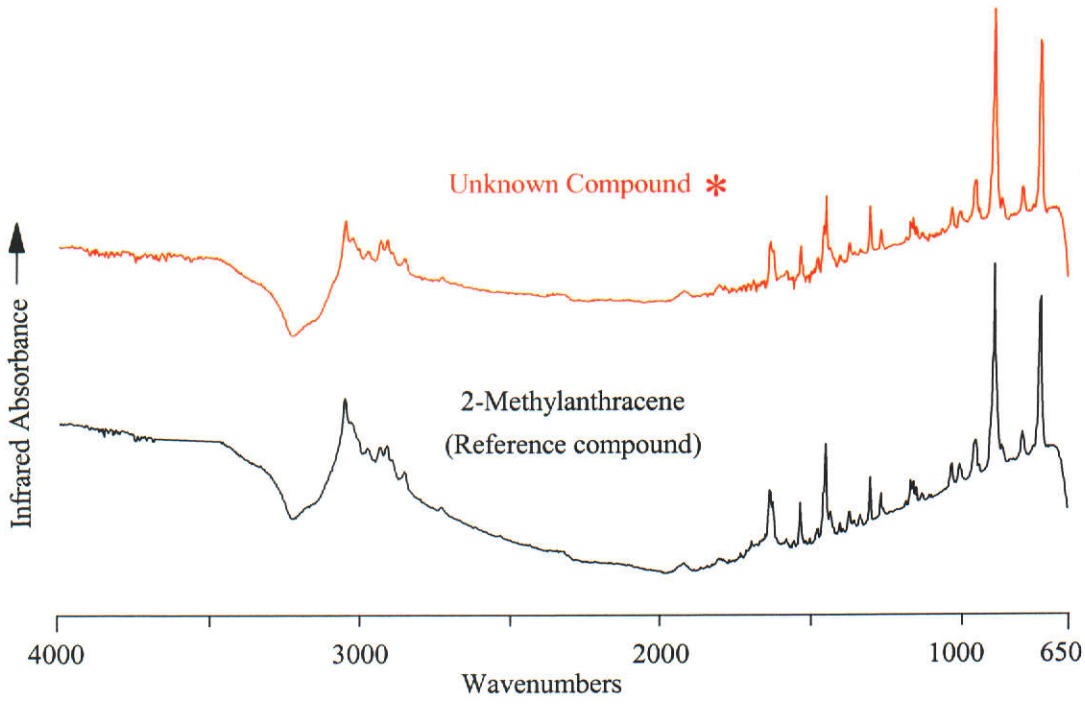

Figure 3-31: Comparison of FTIR spectra of an unknown compound occurring in sedimentary material from Kelp-1 (2389 m) and an authentic sample of 2-methylanthracene. Both spectra were obtained using GC-FTIR techniques.

The partial infrared spectrum of the peak with a similar retention time to 9-MP is shown in Figure 3-32. Here the spectra of the reference compounds 9-MP, 1-MA and 4-MP are also shown. It is apparent from these spectra that the peak does not simply represent a mixture of 9-MP and 1-MA, but comprises all three compounds including 4-MP, which is interesting because it should be less thermally stable than the other MP isomers.

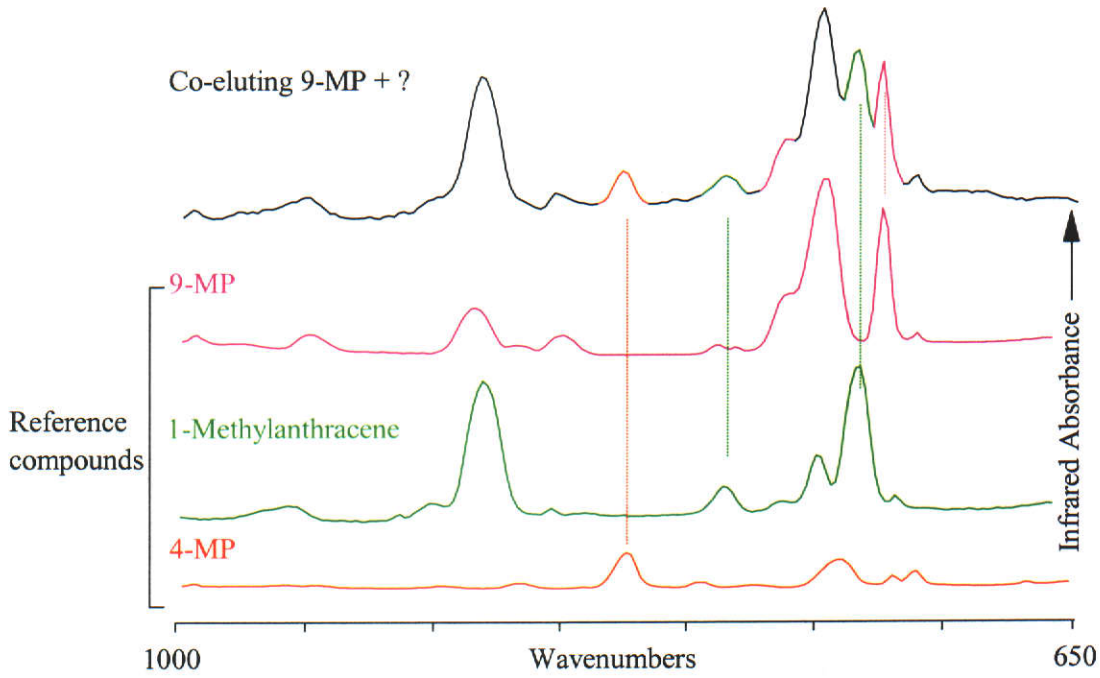

Figure 3-32: Comparison of partial FTIR spectra of 9-MP and co-eluting unknown compound(s) occurring in sedimentary material from Kelp-1 (2389 m), and authentic samples of 9-MP, 4-MP and 1-methylanthracene. All spectra were obtained using GC-FTIR techniques.

The mass chromatogram (m/z 206) showing the distribution of C_2-Ps contained in the extract from Kelp-1 is compared with that of Lambert-1 crude oil in Figure 3-33. It is apparent from these chromatograms that the sedimentary rock extract contains several components that either partially or completely co-elute with the C_2-Ps. Since two of the MA isomers and all five of the MP isomers have been identified in this extract, it is probable that these compounds comprise the C_2-anthracenes as well as the less thermally stable (and hence less commonly observed) C_2-Ps.

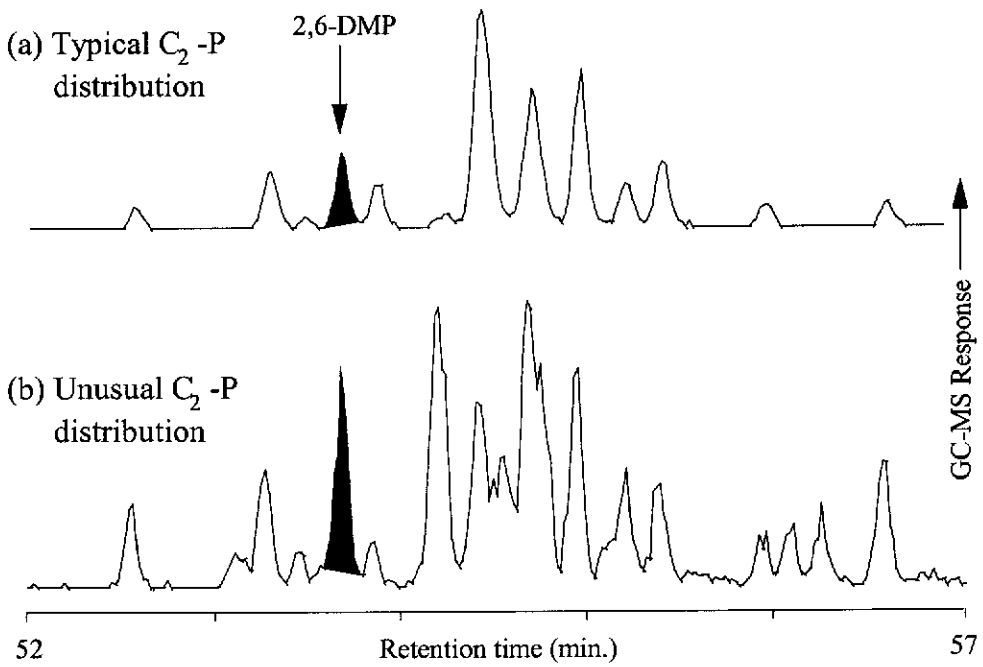

Figure 3-33: Mass chromatograms (m/z 206) showing the comparison of a typical distribution of C_2-phenanthrenes found in Lambert-1 crude oil and the unusual distribution of these and co-eluting unknown compounds occurring in Kelp-1 (2389m) sedimentary material.

Analysis of the peak with a retention time identical to 2,6-DMP yielded the infrared spectrum shown in Figure 3-34, where the partial spectra of 2,6-DMP, 3,5-DMP and 2-ethylanthracene are also shown. Comparison of the spectra reveals that the peak in the gas chromatogram from the rock extract is due to a mixture of all three compounds (also refer to retention indices shown in Table 3-5). Although the contribution of 2-ethylanthracene to the combined spectrum is obvious from its unique absorbance peak at 730 cm^{-1}, it is difficult to apportion the contribution of each of the two DMP isomers in this complex mixture. An approach similar to that described earlier to elucidate the co-eluting 1,3-DMP, 3,10-DMP, 2,10-DMP, and 3,9-DMP might reveal the proportion of each of these compounds in this mixture.

These examples where the alkylanthracenes and uncommonly observed alkylphenanthrenes interfere with the analysis of the alkylphenanthrenes, emphasise the utility of direct deposition GC-FTIR to unambiguously identify components of aromatic fractions from petroleum samples. As well, the perils of identifying alkyl aromatic hydrocarbons only on the basis of retention time and GC-MS are evident.

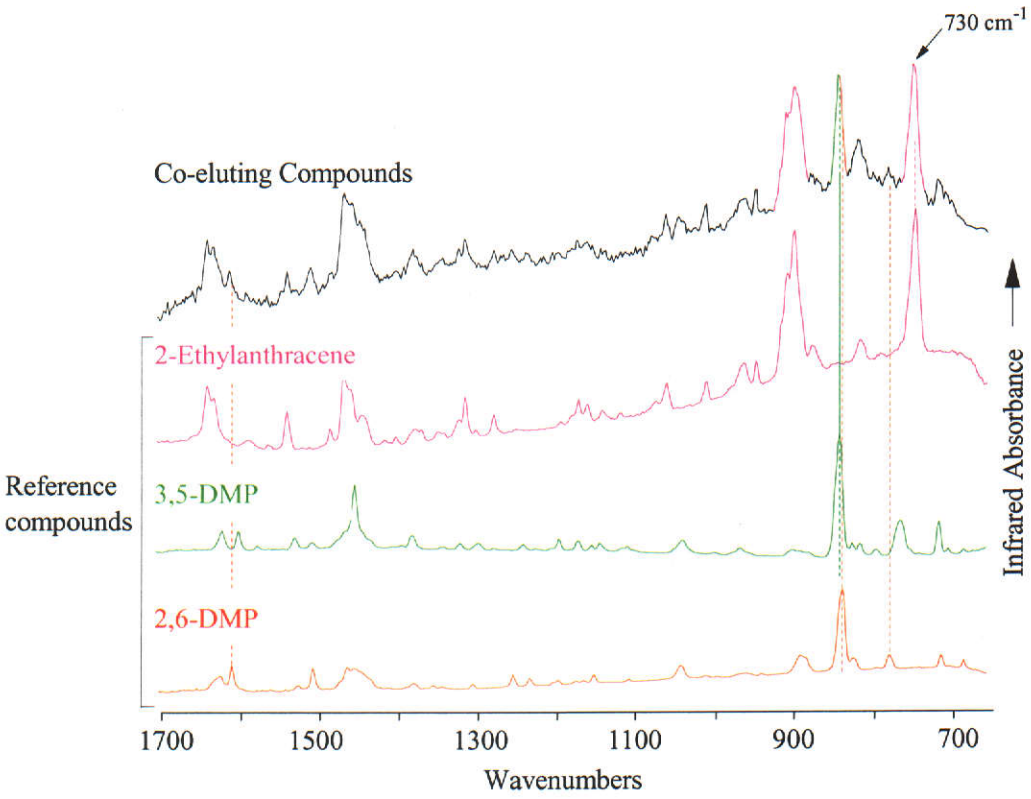

Figure 3-34: Comparison of partial FTIR spectra of co-eluting unknown compounds occurring in sedimentary material from Kelp-1 (2389 m), and authentic samples of 2-ethylanthracene, 3,5-DMP and 2,6-DMP. All spectra were obtained using GC-FTIR techniques.

3.7.2 Identification of 9-methyl(alkyl)phenanthrenes in crude oil

Thus far, the illustrations have described only the application of GC-FTIR to confirm the presence of a compound of known retention time in a complex mixture. In instances where co-elution is known to occur, the contribution of each to the mixture has been determined. The uniqueness of the infrared spectrum of a compound may also be used to confirm the identity of a compound for which the retention time is unknown, in a complex mixture such as a crude oil.

The trinuclear aromatic hydrocarbon fraction, isolated from Moorari-4 crude oil using thin layer chromatography, was further fractionated using mordenite molecular sieves with the flow-thorough technique described earlier (Section 3.6). The eluted fraction was analysed using GC-MS and GC-FTIR techniques and the resultant chromatograms are shown in Figure 3-35. (Isolation and GC-MS analysis of the fractions was performed by T.P. Bastow.)

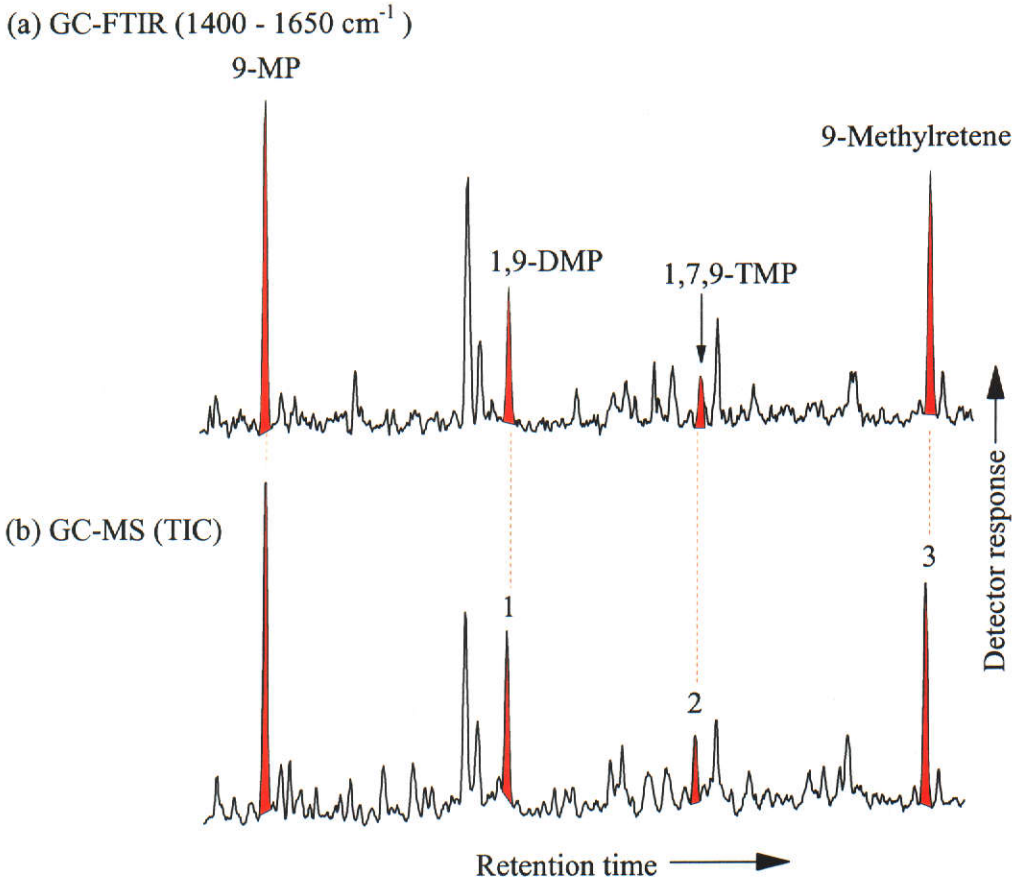

Figure 3-35: Partial (a) GC-FTIR functional group (1400 - 1650 cm^{-1}) chromatogram and (b) corresponding GC-MS total ion chromatogram (TIC) showing alkylphenanthrenes in Moorari-4 crude oil that were excluded from mordenite molecular sieves. (GC-MS data provided by T.P. Bastow).

The striking similarity in the two chromatograms enabled the infrared spectra obtained from the GC-FTIR analysis to be assigned to the corresponding compounds giving rise to the GC-MS chromatogram. In essence, using this approach, both the infrared spectrum and mass spectrum of each of the components of the mixture was obtained.

As discussed previously (Section 3.6), one would expect the eluted fraction to contain MPs and DMPs with a methyl substituent in the 9- position on the aromatic nucleus. Analysis of the FTIR spectra confirmed that 9-MP and 1,9-DMP, each of which may occur in co-eluting mixtures, was the sole compound contributing to the detector response. 1,7,9-Trimethylphenanthrene (1,7,9-TMP) was initially tentatively identified in the mixture by comparison with published retention data

(Radke et al., 1993) and subsequently with the retention time of an authentic sample (prepared by T.P. Bastow). The mass spectrum of the component assigned as 1,7,9-TMP (i.e. Component 2, Figure 3-35) also had a mass spectrum consistent with that of the reference compound, but indistinguishable from the other 55 possible isomers, in particular 1,6,9-TMP, 2,3,5-TMP and 2,3,7-TMP, all of which share very similar retention behaviour with 1,7,9-TMP (Radke et al., 1993). Although only two of these isomers (1,6,9-TMP and 1,7,9-TMP) contain a 9-methyl substituent, the fractionation of TMPs using mordenite molecular sieves has not previously been investigated and identification on this basis is therefore tentative. The most compelling evidence confirming the identity of this component was provided by the almost identical FTIR spectrum obtained from the authentic sample of 1,7,9-TMP as shown in Figure 3-36.

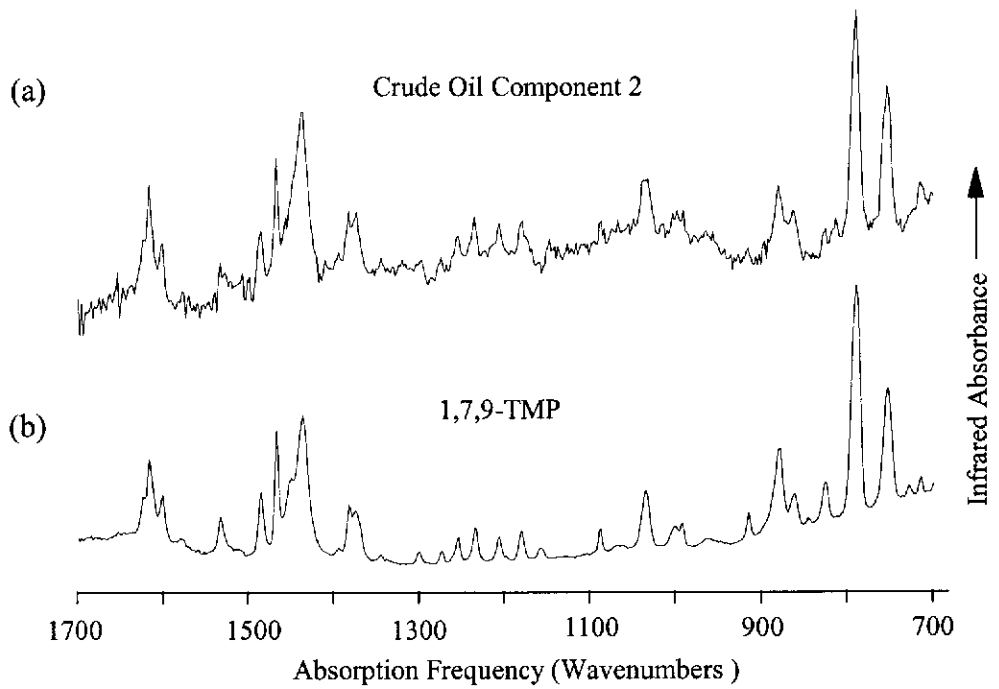

Figure 3-36: Partial FTIR spectra of (a) Moorari-4 crude oil Component 2 and (b) an authentic sample of 1,7,9-TMP, obtained by GC-FTIR analysis.

A similar approach was taken to identify 1,7-dimethyl-9-isopropyl-phenanthrene (9-methylretene) in the fraction from Moorari-4 crude oil, although for this compound there was no published retention data or mass spectrum. The mass spectrum

obtained from Component 3 (refer to Figure 3-35) in the crude oil fraction mixture, compared with that from an authentic sample of 9-methylretene is shown in Figure 3-37 (provided by T.P. Bastow).

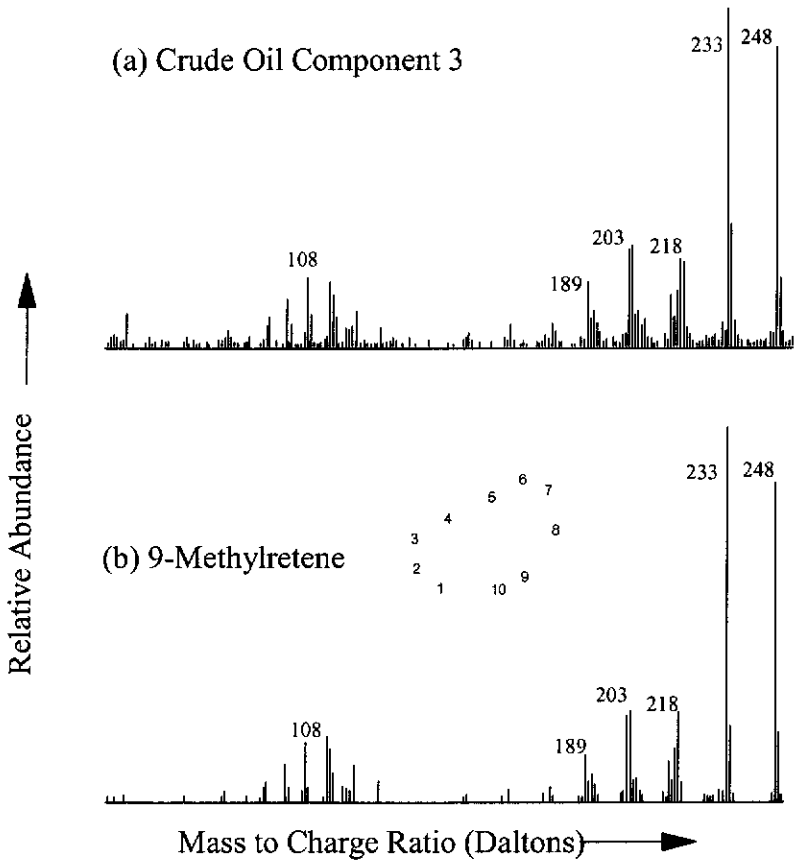

Figure 3-37: Mass spectra of (a) Component 3 from Moorari-4 crude oil and (b) an authentic sample of 1,9-dimethyl-7-isopropylphenanthrene (9-methylretene). [Data provided by T.P. Bastow].

A strong similarity also exists between the infrared spectra of 9-methylretene and the crude oil Component 3 shown in Figure 3-38, and again provides compelling evidence that the assignment of 9-methylretene to the component in the crude oil is valid. The unambiguous identification of 9-MP, 1,9-DMP, 1,7,9-TMP and 9-methylretene in petroleum described here, was pivotal to the investigation of sedimentary methylation processes (Alexander et al., 1995), where substituted phenanthrenes such as retene were shown to be preferentially methylated at the 9-position when heated with a methyl donor and a clay catalyst.

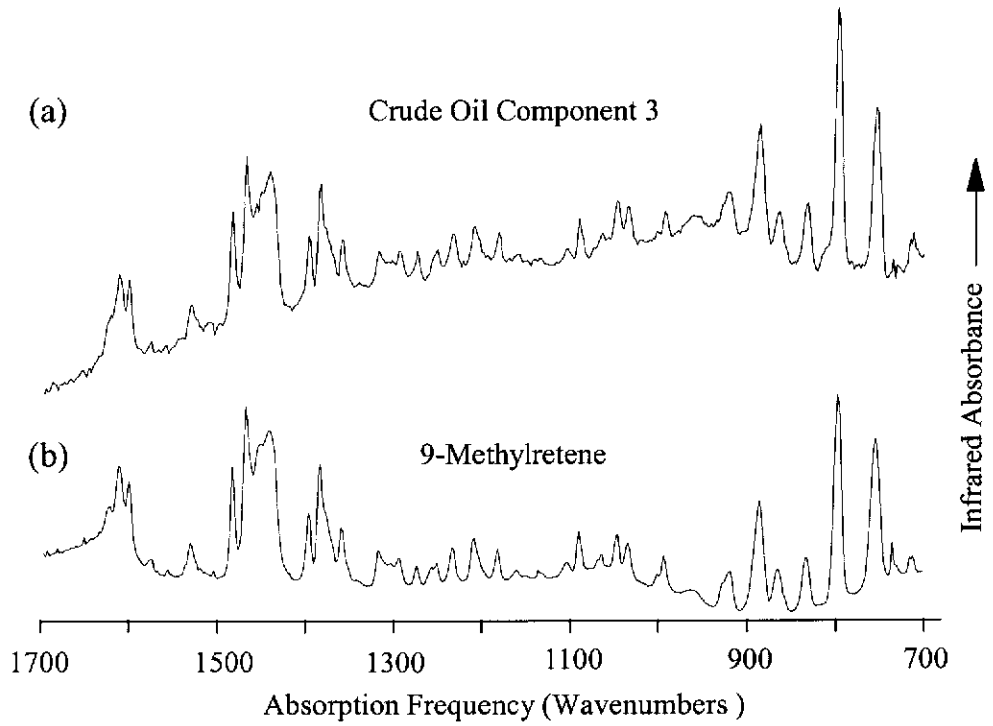

Figure 3-38: Partial FTIR spectra of (a) Component 3 of Moorari-4 crude oil and (b) an authentic sample of 9-methylretene obtained from GC-FTIR measurements. (The sample of 9-methylretene was prepared by T.P. Bastow.)

3.7.3 Alkenylbenzenes

The identification of components of the products of pyrolysis of a shale *via* the application of these compound specific GC-FTIR techniques is also investigated. Thermal degradation of kerogen followed by identification of the products is a commonly used approach to obtain information about the structure of kerogens (Larter and Horsfield, 1993). The hydrocarbon components of Type I and II kerogen pyrolysates typically include alkane/alkene pairs, substituted benzenes, naphthalenes and phenanthrenes. Functionalised compounds such as phenols may also become predominant in Type III kerogens. Careful pyrolytic breakdown of kerogen biopolymers has been shown to release unique hydrocarbon moieties, which are essentially representative of the gross parent structure of the kerogen. For this approach to be effective the pyrolysis procedure must limit secondary reactions of the labile products so that their molecular structures are a true reflection of the structural units of the kerogen. In addition to preserving the gross structure in the

pyrolysis products, preservation of the position of unsaturation enables the position of attachment to kerogen to be determined.

Many of the characteristic hydrocarbons generated from pyrolysis provide unique insights into the macro-molecular structure of the parent kerogen. In particular, homologous series of alkylcyclohexane and alkylbenzene hydrocarbons formed from the pyrolysis of these materials has been well documented (Allan, Bjorøy and Douglas, 1980; Largeau et al.; 1986; Derenne et al., 1990; Gelin et al., 1994). The occurrence of these compounds in pyrolysates is proposed to result from cyclisation and aromatisation reactions of incorporated linear functionalised precursors such as fatty acids and fatty alcohols (Allan, Bjorøy and Douglas, 1980; Largeau, et al., 1986; Dubreil et al., 1989; Derrene et al., 1990; Douglas, et al., 1991).

Cleavage and degradation reactions of these kerogen moieties due to cleavage of carbon-carbon, carbon-sulphur, ester and ether linkages in these bound materials ultimately leads to the formation of unsaturations at or around the point of cleavage (Derenne et al., 1990). Terminally unsaturated alkyl chains such as those commonly observed in homologous series of alkenes and alkylcyclohexanes are often the results of such reactions (Largeau et al., 1986; Gelin et al., 1994).

Here, the molecular structures of some hitherto unknown alkenyl monoaromatic compounds in the pyrolysate produced from a shale are reported. The position of attachment of these aromatic moieties to kerogen is inferred from the locations of the double bonds, determined using the complementary techniques of GC-MS and GC-FTIR. (L. Ellis provided the shale pyrolysate and the results from its GC-MS analysis).

Geelvinck-1, an oil shale from the Perth basin, Australia was subjected to a rapid temperature programmed off-line pyrolysis under conditions (0.1 Torr vacuum) that allowed the pyrolysate to be rapidly removed from the reaction site and collected in a cold trap. The pyrolysis products were therefore considered to represent fragments cracked from the kerogen with a minimum of secondary reaction and should therefore provide insights into the structure of the kerogens. The isolate from the

shale pyrolysis was subjected to preparative liquid chromatography on neutral alumina to remove polar compounds. The less polar hydrocarbon fraction was analysed using GC-MS, the total ion chromatogram of which is shown in Figure 3-39. This chromatogram shows a complex mixture of hydrocarbons, with the most prominent peaks representing alkylbenzene / alkenylbenzene and alkane / alkene pairs.

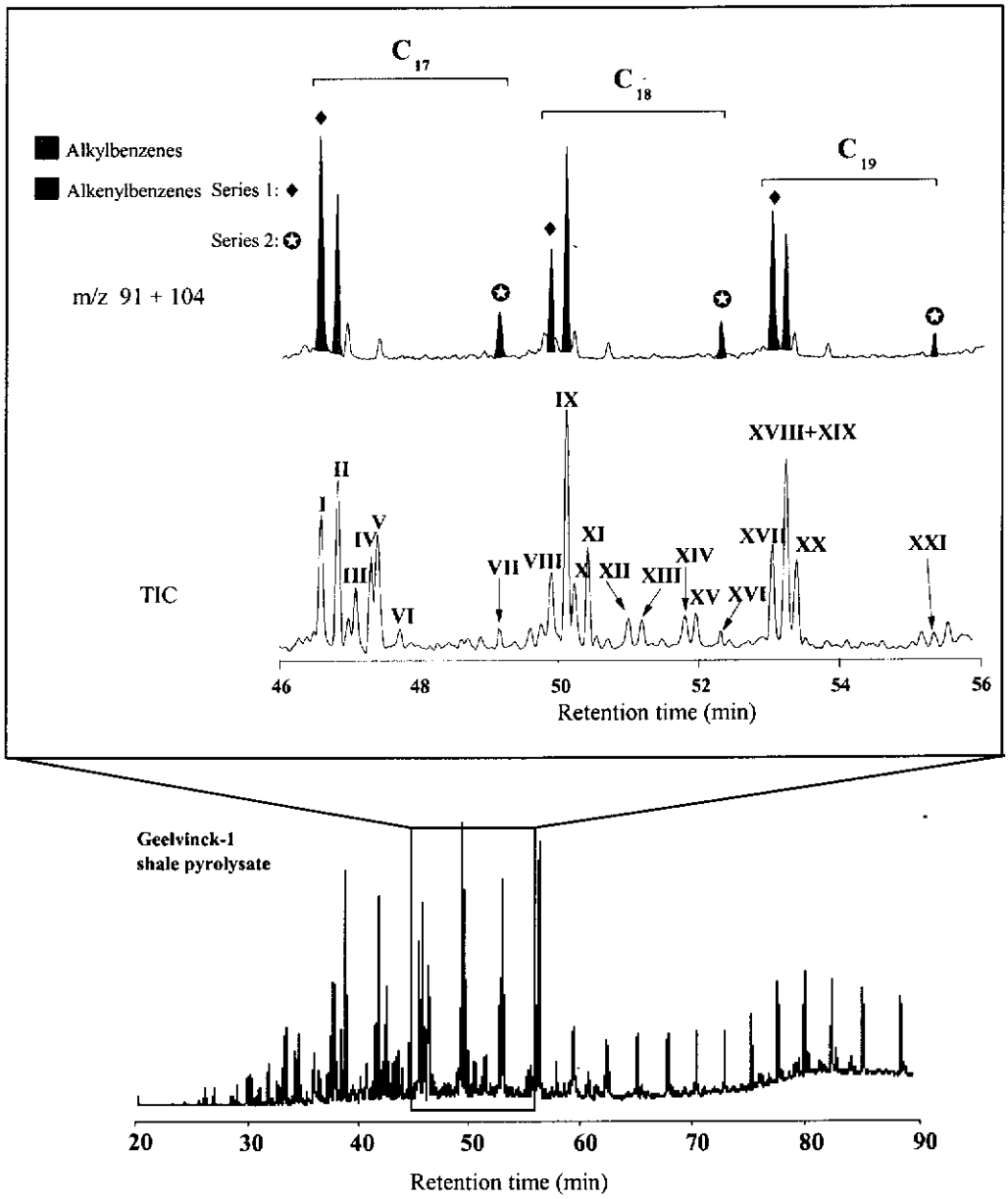

Figure 3-39: Total ion chromatogram (TIC) of the hydrocarbon fraction isolated from the Geelvinck-1 shale pyrolysate. The inset shows the TIC and summed m/z 91+104 mass chromatogram showing the C_{17} to C_{19} alkenylbenzene components, where the numbers refer to the total carbon number of each species (data provided by L. Ellis).

These were tentatively identified based on the evidence provided by their mass spectra and comparison of GC retention time with synthesised reference compounds as described in detail in Ellis et al. (1999). The portion of the chromatogram representing the C_{17}, C_{18} and C_{19} analogues of these compounds is shown in detail in the inset to Figure 3-39, along with the summed mass chromatograms (m/z 91+104) showing the responses of the alkylbenzene and alkenylbenzene components of the pyrolysate. As described in detail elsewhere (Ellis et al., 1999), examination of the latter chromatogram and the mass spectra of the component compounds revealed the presence of two distinct series of alkenylbenzene compounds. Members of the first series (Series 1-♦) are similar in abundance to, and elute just prior to, the corresponding alkylbenzene of the same carbon number, while the second series (Series 2-✪) is observed at longer retention times and lower abundance.

Identification of alkenylbenzenes in Series 1

Further evidence for the identification of the alkenylbenzenes comprising Series 1 was obtained by analysis of the shale pyrolysate using GC-FTIR techniques. Prior to analysis, the pyrolysate was subjected to further treatment using thin layer chromatography to remove the polycyclic aromatic hydrocarbons and their alkylated homologues from the hydrocarbon mixture. Two GC-FTIR functional group chromatograms of this fraction are shown in Figure 3-40(a) and (b). The first of these displays response to a frequency range of 2950 cm^{-1} to 3000 cm^{-1}, selective for compounds with asymmetric and symmetric C–H stretching vibrations associated specifically with methyl substituents. The second chromatogram, 2800 cm^{-1} to 3000 cm^{-1}, shows responses to compounds with (non-aromatic) C–H stretching vibrations i.e. including methyl, methylene and methyne functional groups (Nakanishi and Solomon, 1977; Roeges, 1994). In the case of alkylbenzenes and alkenylbenzenes, a compound that is represented by a peak in the 2800 cm^{-1} to 3000 cm^{-1} chromatogram but not in the 2950 cm^{-1} to 3000 cm^{-1} chromatogram must contain an alkyl chain that is terminated by an unsaturation on both ends. Where a peak appears in both chromatograms, the alkyl chain must contain a methyl group, i.e. it must be either saturated on at least one end or have a branch in the chain which is terminated by the methyl group.

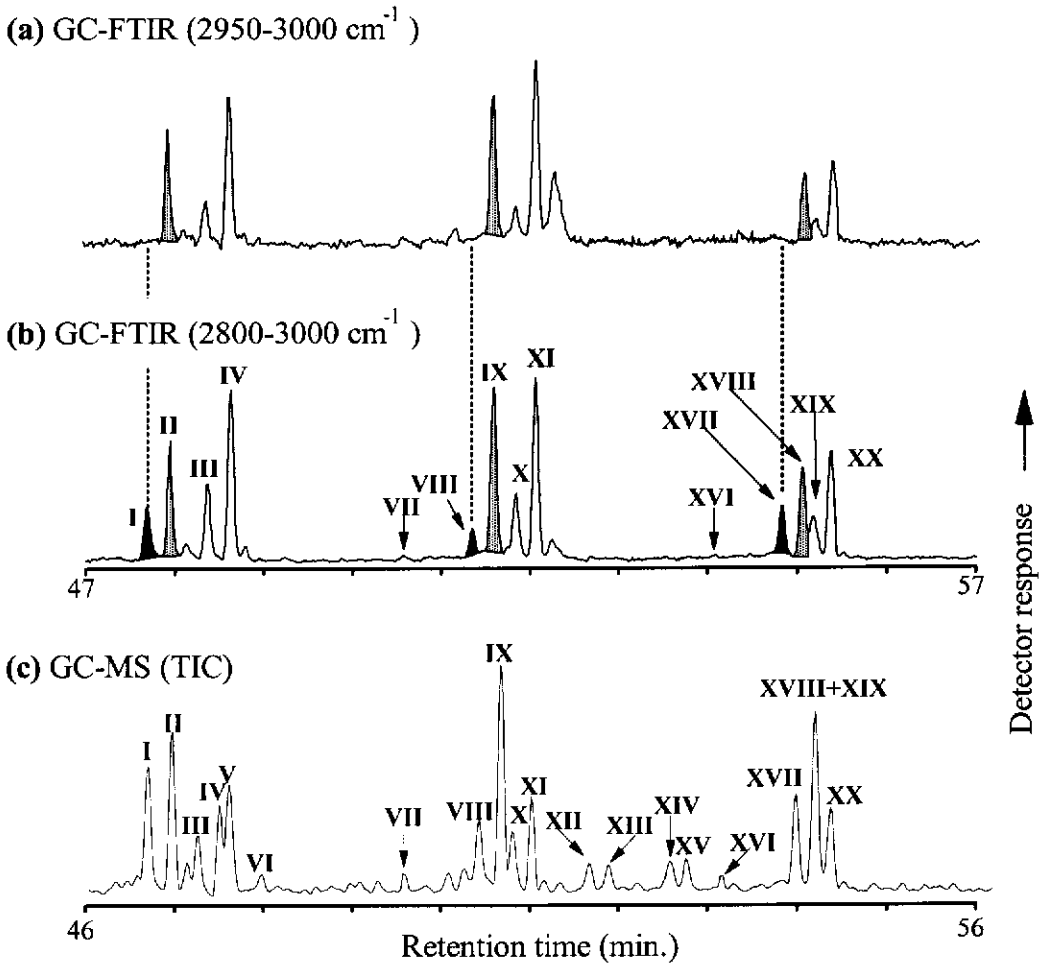

Figure 3-40: Gas chromatograms from analysis of the pyrolysate from Geelvinck-1 shale. Functional group chromatograms, where the selected infrared intervals of (a) 2950 cm^{-1}-3000 cm^{-1} and (b) 2800-3000 cm^{-1} were monitored were obtained by GC-FTIR analysis of a fraction of the pyrolysate from which the PAHs had been removed. The partial TIC shown in (a) was obtained by GC-MS analysis of the hydrocarbons isolated from the pyrolysate prior to removal of PAHs.

It is apparent that there is a strong resemblance between the 2950 cm^{-1} to 3000 cm^{-1} functional group chromatogram and the TIC from GC-MS analysis of the pyrolysate shown in Figure 3-40(c), without which collation of the infrared and GC-MS data would be problematic. Separate homologous series of alkanes, alkenes and alkylbenzenes identified by GC-MS are represented by peaks in both infrared chromatograms since all have at least one methyl substituent terminating an alkyl chain. In the case of alkene and alkylbenzene compounds, the alkyl chain is terminated by a methyl group at one end, while each member of the alkane series contains two methyl groups and are similarly represented. In the case of the alkenylbenzenes, however, it is apparent that the three compounds (I, VIII and XVII),

comprising Series 1 in the C_{17} to C_{19} carbon range do not contain a methyl group as indicated by the lack of detector response in the characteristic 2950 cm^{-1} to 3000 cm^{-1} range.

The infrared spectrum of each of these compounds, obtained from the GC-FTIR analysis of the pyrolysate, is typified by that of the C_{17} member of the series (i.e. Compound I) shown in Figure 3-41(b). Interpretation of this spectrum is facilitated by comparison with that obtained from Compound II, shown in Figure 3-41(a). As one would expect for two such similar compounds, these spectra have many common absorption bands, which are summarised in Table 3-10. Significant differences are also apparent, the most useful of which is the absence of absorption bands at 2960 cm^{-1} and 2870 cm^{-1} in the spectrum of the terminal alkenylbenzene which correspond to the frequency of the asymmetric and symmetric C–H stretching vibrations of methyl substituents respectively. This is highlighted in the inset, and justifies the rationale for monitoring the selected intervals in the infrared spectrum during GC-FTIR analysis.

Another significant and potentially useful difference between the spectra is the unique presence of absorption bands at 910 cm^{-1}, 990 cm^{-1} and 1645 cm^{-1} in the spectrum of the terminal alkenylbenzene. These wavelengths are diagnostic for terminal vinylic alkenes, specific to compounds containing terminal unsaturations, regardless of whether additional methyl substituents are also attached. Although not attempted here, monitoring these characteristic absorbance bands to produce a functional group chromatogram could also provide a very selective positive indicator of the presence of the series of terminal alkenylbenzenes. This approach is also potentially useful in distinguishing between this and other homologous series in pyrolysates such as alkenyltoluenes, where the presence of a methyl substituent on the aromatic nucleus would preclude the use of the 2950 cm^{-1} to 3000 cm^{-1} methyl C–H stretching vibration frequency range monitored here.

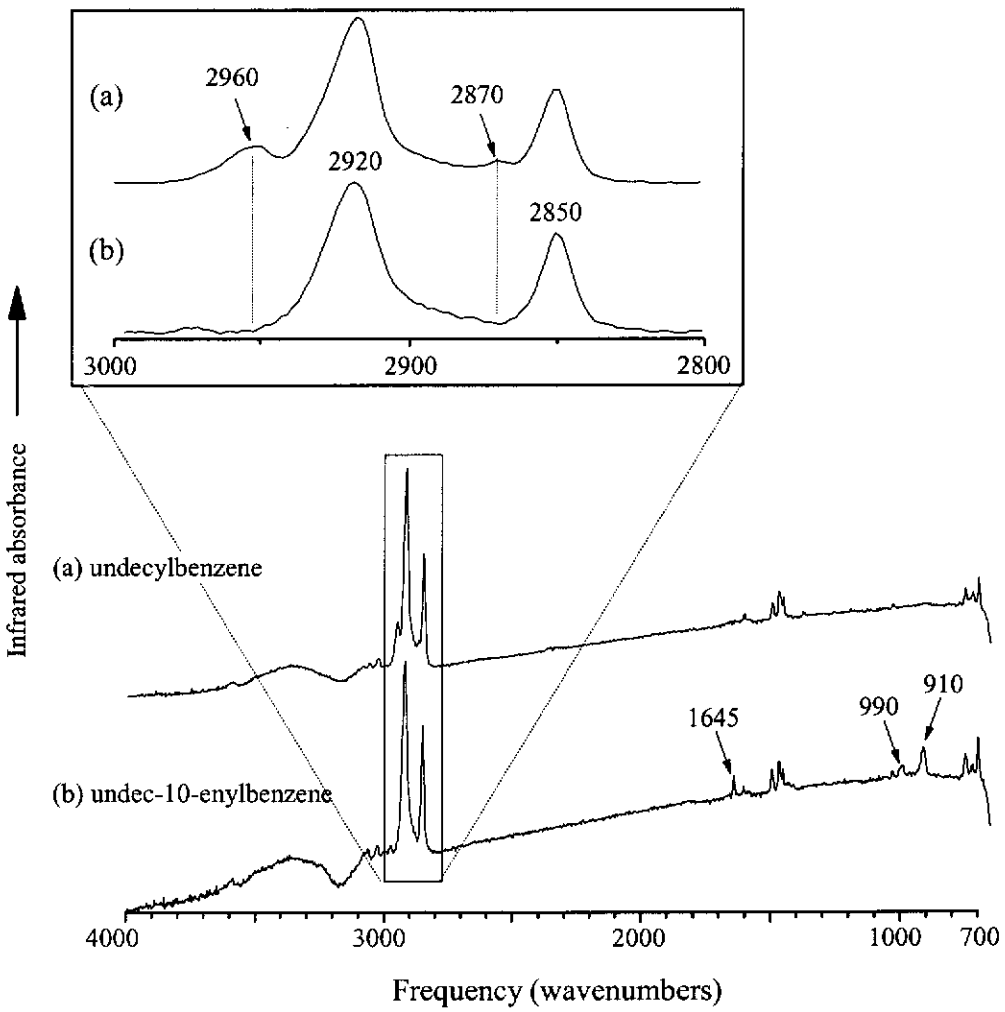

Figure 3-41: FTIR spectra of (a) undecylbenzene and (b) undec-10-enylbenzene identified in the pyrolysate from Geelvinck-1 shale using GC-FTIR techniques. The inset shows the expanded region of both spectra where absorption bands due to asymmetric and symmetric stretching of the carbon to hydrogen bond occurs. The frequencies of selected absorption bands are expressed in wavenumbers (cm^{-1}).

It is apparent from the assignment of the absorbance bands in Table 3-10, that the infrared spectra shown in Figure 3-41(a) and (b) are consistent with that of an alkylbenzene and a terminal alkenylbenzene respectively. Further, in conjunction with the interpretation of the GC-MS spectra and the retention behaviour of authentic reference samples described in Ellis et al. (1999), these can be unequivocally identified as undecylbenzene and undec-10-enylbenzene respectively. Similarly, compounds VIII, IX, XVII and XVIII, may be identified as dodec-11-enylbenzene, dodecylbenzene, tridec-12-enylbenzene and tridecylbenzene.

Table 3-10: Summary of infrared absorption bands of alkylbenzenes and alkenylbenzenes (Frolov and Smirnov, 1994; Roeges, 1994; Nakanishi and Solomon, 1977).

Functional Group	Absorption Band(cm^{-1})	Vibrational modes
R–CH_3	2960, 2870	asymmetric, symmetric –CH_3 stretch
R–CH_2–R'	2920, 2850	asymmetric, symmetric –CH_2 stretch
Ar–HC=CH–R	1650	conjugated double bond stretch
R–HC=CH_2	1645	terminal vinyl double bond stretch
benzene nucleus	1597, 1492, 1446	aromatic –HC=CH– stretch.
benzene nucleus	1576	aromatic –HC=CH– stretch conjugated with double bond
R–CH_2–R'	1468	–CH_2– scissoring
R–C=CH_2	990, 910	terminal vinyl C–H out of plane bending
R–HC=CH–R'	965	C–H out of plane bending (in-phase *trans* –HC=CH– wag)
benzene nucleus	650 - 900	aromatic C–H out of plane bending

Identification of alkenylbenzenes in Series 2

The other series of alkenylbenzenes (Series 2) could not be identified by direct analysis using GC-FTIR due to the very low response to these compounds (VII and XVI) in the functional group chromatogram shown in Figure 3-40(b), emphasising the reduced sensitivity of this technique relative to GC-MS. Although this series of compounds was tentatively identified by interpretation of their mass spectra as containing a double bond conjugated with the benzene nucleus (Ellis et al., 1999), the configuration of the geometry about the double bond could not be determined using these techniques.

To address this, an authentic sample of dodec-1-enylbenzene was synthesised (by L. Ellis). GC-MS analysis of the product revealed a single peak in the summed m/z 91+104 mass chromatograms, tentatively assigned as *trans* dodec-1-enylbenzene.

Dodec-2-enylbenzene was also synthesised (by L. Ellis), yielding a mixture, which, upon analysis using GC-MS, revealed two peaks presumably corresponding to the *cis* and *trans* isomers (Ellis et al., 1999). Each of these products was analysed using GC-FTIR and the infrared spectra obtained, excerpts of which are shown in Figure 3-42.

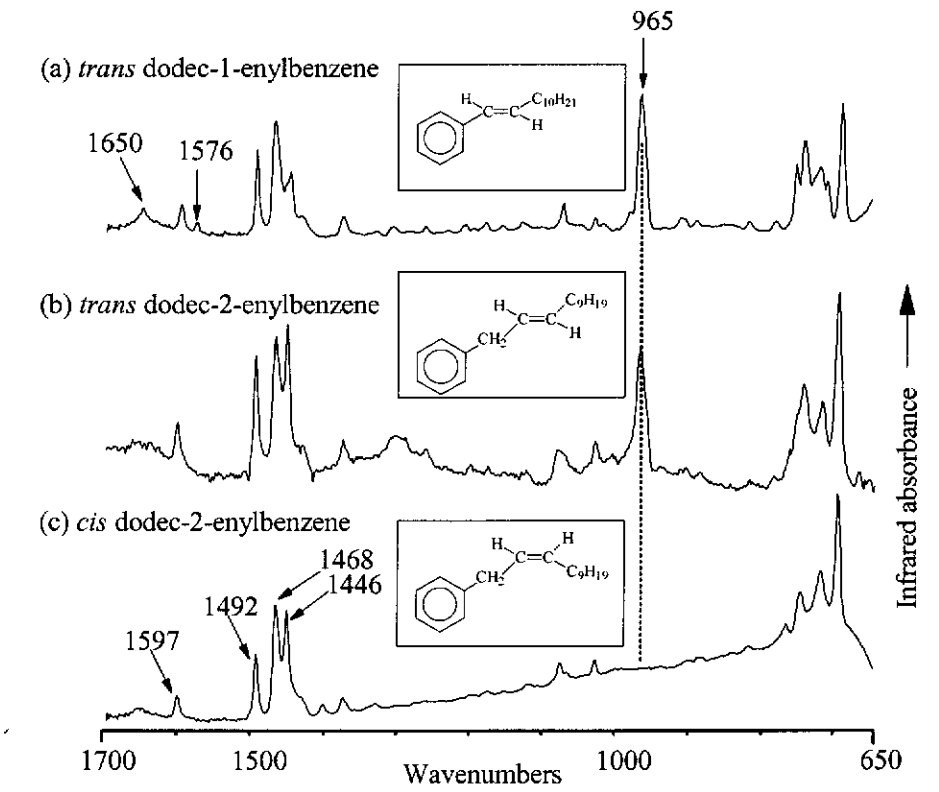

Figure 3-42: Partial FTIR spectra of synthesised reference compounds (a) *trans* dodec-1-enylbenzene, (b) *trans* dodec-2-enylbenzene and (c) *cis* dodec-2-enylbenzene obtained by GC-FTIR analysis. The frequencies of selected absorption bands are expressed in wavenumbers (cm^{-1}).

The absorbance bands in the infrared spectrum of each the three synthesised compounds are also summarised in Table 3-10. The most striking feature of these spectra is the occurrence of the absorbance band at 965 cm^{-1}, characteristic of both isomers tentatively assigned as having the *trans* configuration about the double bond and attributed to the out of plane bending vibration of the C–H bonds on either side of the double bond. The frequency of this vibration is consistent with that attributed to compounds containing *trans* di-substituted double bonds (Frolov and Smirnov, 1994; Roeges, 1994; Nakanishi and Solomon, 1977) and is evidently useful in distinguishing between the *cis* and *trans* isomers. Unfortunately, vibrations

characteristic of the *cis* configuration occurring between 680 cm^{-1} and 710 cm^{-1} are probably masked in the spectrum of *cis* dodec-2-enylbenzene by the out-of-plane bending vibrations of the C–H bonds in the benzene nucleus.

The spectrum assigned to *trans* dodec-1-enylbenzene also displays unique, albeit weak, infrared absorbances at 1650 cm^{-1} and 1576 cm^{-1}. These are diagnostic for conjugated phenyl-alkene systems (Roeges, 1994), and also show potential for discriminating between conjugated alkenyl aromatic hydrocarbons from non-conjugated alkenyl aromatic species.

It is apparent from the GC-FTIR analysis of these alkenylbenzenes that, in fact, the synthesised sample of dodec-1-enylbenzene possesses the *trans* configuration about the double bond. Co-injection of this compound with the pyrolysate reveals that the authentic sample of *trans* dodec-1-enylbenzene co-elutes with compound XVI. Although this compound was not identified directly by analysis of the pyrolysate using GC-FTIR techniques, strong evidence has been mounted supporting the assignment.

The identity of all of the compounds examined in the pyrolysate produced from the shale is summarised in Table 3-11. Although all of these could be tentatively identified using GC-MS techniques alone, unambiguous identification of compounds I, II, III, VII, VIII, X, XVI, XVII, XIX and XXI was not possible without corroboration *via* the (GC-FTIR) infrared spectra. The geochemical implications of the identification of these compounds amongst the pyrolysis products of the shale are discussed in detail by Ellis et al. (1999), but briefly the presence of alkylbenzenes in shale pyrolysates is strong evidence for their presence as natural components of crude oils and not just artefacts from sample contamination by alkylbenzenes from petrochemical synthesis.

Table 3-11: Major compounds identified in pyrolysate from Geelvinck-1 shale. Numerals refer to peak labels in Figures 3-39 and 3-40.

Peak No.	Compound	Peak No.	Compound
I	undec-10-enylbenzene	XII	3-methylphenanthrene
II	undecylbenzene	XIII	2-methylphenanthrene
III	octadec-1-ene	XIV	9-methylphenanthrene
IV	*n*-octadecane	XV	1-methylphenanthrene
V	phenanthrene	XVI	dodec-1-enylbenzene
VI	anthracene	XVII	tridec-12-enylbenzene
VII	undec-1-enylbenzene	XVIII	tridecylbenzene
VIII	dodec-11-enylbenzene	XIX	eicos-1-ene
IX	dodecylbenzene	XX	*n*-eicosane
X	nonadec-1-ene	XXI	tridec-1-enylbenzene
XI	*n*-nonadecane		

3.8 Conclusions

The technique of direct deposition GC-FTIR has been shown to be applicable to the analysis of complex mixtures of polymethylnaphthalenes and alkylphenanthrenes in aromatic hydrocarbon fractions isolated from crude oil and sedimentary rocks. It is possible to quantitatively determine co-eluting compounds based on the differences in their infrared spectra, however interpretation of the resultant spectrum may be difficult in multi-component mixtures where differences in the spectra are not pronounced. Although in most instances presented here, no sample preparation in addition to that required for GC-MS analysis was required, determination of the TeMN was confounded by co-elution with compounds other than co-eluting isomers and further sample fractionation was required.

The GC-FTIR technique has also been shown to enable the unambiguous identification of previously unknown compounds in complex mixtures when corroborated by evidence from GC-MS analysis. The selectivity of the technique was also illustrated by the monitoring of GC-FTIR functional group chromatograms, in an analogous manner to GC-MS selected ion monitoring, of the terminal alkenylbenzene isomers to discriminate between saturated and mono-unsaturated alkenylbenzenes in pyrolysates.

CHAPTER 4

4 Biodegradation of petroleum hydrocarbons associated with development drilling from the North Rankin Alpha gas and condensate platform, Western Australia.

4.1 Abstract

A case study is described where 23 development wells were drilled from a platform situated 134 km off the coast of North-Western Australia. Low toxicity oil-based drilling mud (LTOBM), formulated from a kerosene-like hydrocarbon fluid was used to assist with the drilling, with the resultant formation cuttings being discharged into the ocean *via* a chute into approximately 125 m of water. Immediately following the cessation of the drilling program, sediment samples were collected from the sea-floor at 16 sites positioned at various distances from the platform along two transects, one in the direction of the prevailing current and the other perpendicular to this, primarily to determine the extent of contamination of the seabed by drilling discharges. As a part of this study, the hydrocarbon concentration of these sediments was determined. As distance from the platform increased, the hydrocarbon concentration decreased rapidly from 75000 mg kg^{-1} directly under the chute to 37 mg kg^{-1} at a site 800 m away in the direction of the prevailing current, and even more rapidly along the perpendicular transect
(1.3 mg kg^{-1} at 800 m). Examination using gas chromatography-mass spectrometry (GC-MS) revealed that the hydrocarbons also exhibited an increasingly biodegraded signature. Analysis of the alkylnaphthalenes present in these biodegraded residues using direct deposition gas chromatography-Fourier transform infrared spectroscopy (GC-FTIR) enabled the determination of the relative susceptibility to biodegradation for the individual dimethylnaphthalene, trimethylnaphthalene and tetramethyl-naphthalene isomers. From this, a correlation between the susceptibility to biodegradation and the structure of the polymethylnaphthalenes was observed. Subsequent sediment sampling and chemical analysis yielded similar information for phenanthrene and the individual methylphenanthrene isomers.

4.2 Introduction

The process of drilling petroleum exploration and production wells requires the use of drilling muds (or fluids). The primary functions of these muds include cooling and lubrication of the drill bit, counteraction of formation pressure, stabilisation of the well bore, and transportation of the drill cuttings to the surface. Historically, drilling muds have been broadly classified as either water-based mud (WBM) or oil based mud (OBM), depending on the character of the continuous phase from which they are formulated. In spite of their higher cost and perceived greater environmental impact, OBMs are often used in preference to WBMs in cases where directional drilling is required (e.g. Terrens, Gwyther and Keough, 1998).

Due mainly to concern over the environmental impact of discharged mud, the base fluids from which OBMs are composed have changed significantly (Papp and Fisher, 1999; Xiao and Piatti, 1995; Degouy et al., 1993; Friedheim and Pantermuehl, 1993). In summary, first generation OBMs used crude oils, which were replaced successively by diesel, highly refined petroleum fractions and, more recently, synthetic mixtures of organic compounds such as paraffins, olefins and esters. These later generation muds are therefore often described as non-water based muds (NWBMs) to distinguish them from those based on crude oils and diesel.

During a program of drilling exploration and production wells, discharges from offshore petroleum platforms can include cuttings, entrained drilling additives and formation hydrocarbons produced from the well. At the end of an extensive drilling program, the cuttings form a substantial mound at the base of the platform (e.g. Tibbetts and Large, 1986). From studies of such discharges in the North Sea, where there has been extensive use of oil-based drilling muds, considerable controversy has been generated regarding the extent of these mounds and their environmental impact on the seabed. Englehardt, Ray and Gillam (1989) observed that studies performed over the previous 10 years had shown that an environmental impact on the seabed could be detected in areas where oil contaminated cuttings had been discharged. There was, however, no consensus about the extent of this impact, whether it is of a long-term or short-term nature, and the dependence of the impact on local conditions.

A study from the British sector of the North Sea (Davies et al., 1989) has shown that where there has been extensive use of OBMs, hydrocarbon concentrations 250 m from the platform may be up to 1000 times background. Concentrations decrease rapidly with distance and background levels are usually reached 2000 m to 3000 m from the platforms, however traces of petroleum-derived hydrocarbons have been detected at distances as far as 10000 m from platforms.

In another study performed around the Norwegian Ekofisk oil field (Reiersen et al., 1989), it was concluded that the biological effects from the discharge of oil contaminated cuttings extended out as far as 3000 m from the platform. In contrast, the British scientists (Davies et al., 1989) only noted a decline in species abundance and diversity of the seabed biological community as far as 500 m from the platforms at the sites they studied. More recently, studies have been performed in the vicinity of offshore platforms in the Gulf of Mexico (Roscigno and Kennicutt, 1995; Kennicutt et al., 1996) where a multi-disciplinary approach incorporating oceanography, sedimentology, chemistry, toxicology and biology was taken to assess the effects of chronic contamination on marine ecosystems.

These studies provided the model for the present study of the sea-floor, undertaken adjacent to an oil and gas producing platform off the coast of north western Australia. Briefly, following an extensive drilling program utilising oil-based drilling muds, sea-floor sediment samples were collected and the hydrocarbon concentrations measured. Preliminary analysis of the hydrocarbons extracted from sediments at various sampling sites revealed varying extents of weathering. Although the degradation of the petroleum hydrocarbons from discharged OBMs on the sea-floor has been observed in many of the above studies, detailed investigation has been limited to gross changes in the composition of the OBM. For example Tibbetts and Large (1986) and Davies et al. (1989) observed an increase in the unresolved complex mixture (UCM) relative to *n*-alkanes with increasing distance from the platform.

The investigation of the biodegradation of the aromatic hydrocarbons present in OBMs, particularly the mixture of alkylnaphthalenes and alkylphenanthrenes, has

been neglected in most studies. For example, although the aromatic hydrocarbon content of the sediments has been reported (Davies et al., 1984; Reiersen et al., 1989; Brooks et al., 1990), the effect of biodegradation on the aromatic hydrocarbons was not studied in detail. Notable exceptions include investigations by Grahl-Nielsen et al. (1989), who recognised the susceptibility of alkylnaphthalenes relative to alkyldibenzothiophenes, and Massie, Ward and Davies (1985) who studied the mineralisation of aromatic hydrocarbons using radioactive labelled (^{14}C) naphthalene and (^{14}C) benzo(a)pyrene surrogates. In the latter investigation, the progress of biodegradation was monitored *in-vitro* in microcosm experiments using sediments sampled from various sea-floor sites as the inoculum.

The behaviour of individual alkylnaphthalene and alkylphenanthrene isomers upon biodegradation of petroleum has been the subject of few earlier studies (Solanas, et al., 1984; Volkman et al., 1984; Williams et al., 1986; Rowland et al., 1986; Kennicutt, 1988; Hostettler and Kvenvolden, 1994; Budzinski et al., 1995b, 1998; Colombo, Cabello and Arambarri, 1996; Nadalig et al., 1996; Gilcewicz et al., 1997; Ahmed, Smith and George, 1999). In this chapter, the detailed analysis of the LTOBM residues extracted from the sea-floor sediments is described using the complementary techniques of GC-MS and direct deposition GC-FTIR. In this way, the hydrocarbons, particularly the dimethylnaphthalene (DMN), trimethylnaphthalene (TMN) and tetramethylnaphthalene (TeMN) isomers will be thoroughly characterised, and the degree of alteration of these compounds by weathering processes will be investigated.

4.3 History of operations at the North Rankin Alpha platform

The North West Shelf Gas Project, operated by Woodside Energy Ltd, supplies natural gas to domestic markets and liquefied natural gas to overseas markets. Condensate, oil and liquefied petroleum gas are also produced. Gas and condensate are produced from two offshore production platforms: North Rankin Alpha (North Rankin 'A', NRA) and Goodwyn Alpha (Goodwyn 'A', GWA). Oil and gas are produced from three separate fields: Wanaea, Cossack and Lambert, which are tied back by sub-sea development to the Floating Production Storage and Offloading

(FPSO) facility *Cossack Pioneer*. Gas and condensate are delivered *via* a trunkline to an onshore treatment plant near the port of Dampier on the north western Australian coast. Oil is exported directly to shuttle tankers from the FPSO. The location of these North West Shelf (NWS) facilities are displayed in Figure 4-1.

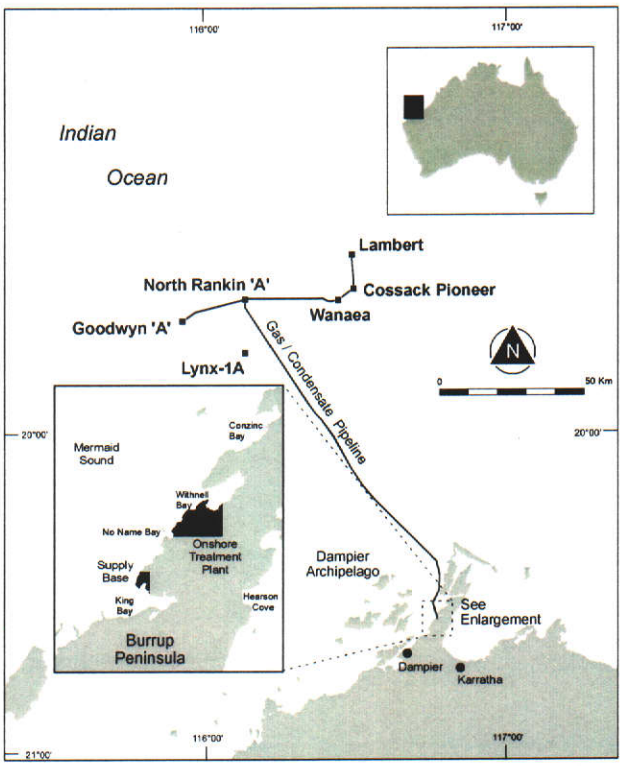

Figure 4-1: Map showing the location of some NWS exploration and production facilities.

To date, 42 production wells have been drilled on the NWS for the project.
The North Rankin gas field was discovered in 1971, 134 km north west of Dampier in 125 m of water. Presently, NRA is the largest capacity gas platform in the world, capable of producing gas at a rate of 47 Mm^3 per day. In addition, there is significant condensate production from the platform, the total of which was estimated to be 1.56 Mt for the year 1992.

4.3.1 Drilling operations at NRA

The first North Rankin development well was spudded from NRA in August 1983. Until completion of the first phase of drilling in 1991, 23 wells were drilled from the platform, comprising 18 production wells and five gas re-injection wells. Due to technical constraints, many of the wells have required the use of NWBMs in the mid-

and/or bottom-sections of the holes. The first 12 wells were drilled using WBM with the remaining 11 long-reach wells using variable amounts of WBM and what was then known as a low toxicity oil-based mud (LTOBM). For example, in 1991, the drilling program included the (then) world's longest hole from an offshore gas-oil platform with a horizontal reach of 5009 m and a target depth of 2836 m below seabed drilled almost exclusively using LTOBM. The LTOBM was formulated from a base mineral oil similar in composition to a typical kerosene fraction obtained from crude oil. The relatively high concentration of potentially toxic aromatic hydrocarbons in the LTOBM has since lead to its reclassification (Papp and Fisher, 1999) as an oil based mud (OBM).

Total surface losses of the LTOBM during drilling operations was calculated to be 1297 tonnes, some of which was discharged to the sea-floor entrained in the drilling cuttings. On NRA, drill cuttings and other drilling wastes were directed to the sea *via* a cuttings chute of 0.5 m diameter. The cuttings and wastes initially fell about 90 m from the drilling deck to the bottom of the chute, and then a further 80 m to the sea-floor through the water column. As a result, a mound of cuttings approximately 2 m in height at its highest point with a base area of several hundred square metres was formed on the sea-floor close to the platform.

4.3.2 Purpose of the sea-floor surveys at NRA

A program of investigations was established by the operator in consultation with the local regulatory authority, the West Australian Department of Minerals and Energy. This program entailed the collection of samples of surficial sediment from the sea floor in a series of surveys. The aim of these surveys was to determine the effect of drilling operations at NRA on the seabed by examining trace metal and hydrocarbon contamination, physical changes to sediment characteristics, and biological effects.

The first survey took place in August 1991, and involved the collection of a suite of sea-floor sediment samples at various distances from the NRA platform to assess the extent of the plume of discharged material on the sea-floor. Since then, opportunistic sampling of the sea-floor was performed at a site 800 m from the platform in December 1992, October 1993 and August 1997 to provide further information on

the persistence and weathering of hydrocarbons from the drilling operations. In October 1994, samples were retrieved from the cuttings pile to assess the change in hydrocarbon concentrations and the extent of weathering with increasing depth below the surface of the cuttings pile.

4.3.3 Study site environmental characteristics

The NWS is influenced by tropical storms (cyclones) between the months of November and April. On average the area receives 10.7 days of cyclone activity per annum. Wind speeds within these storms can reach in excess of 60 ms^{-1} (216 kmh^{-1}), with maximum wave heights likely to exceed 10 m (Steedman Science and Engineering, 1993). The passage of such cyclones can have significant influence on the redistribution of sea floor sediments and cuttings piles on the NWS. The sea-floor sediments consist of silty sands derived primarily from calcium carbonate. Sediment depths were previously determined by shallow seismic reflection profiling to be greater than 5 m in the vicinity of NRA. Near-bottom seawater temperatures at NRA range from 24°C in summer to 22°C in winter. Near-bottom current speed and direction, measured in 1991 (Steedman Science and Engineering, 1993) are summarised in Figure 4-2.

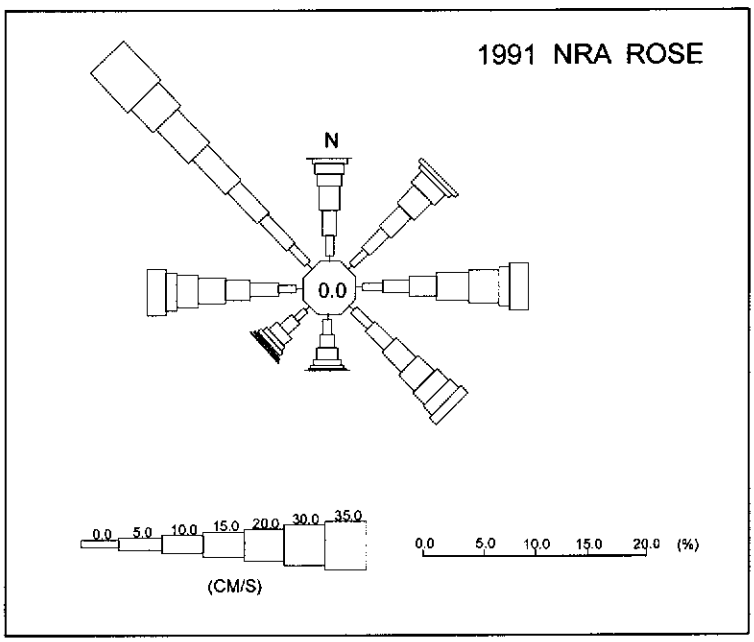

Figure 4-2: Current rose showing the direction, speed and prevalence of near sea-floor currents measured at the NRA Offshore Oil and Gas production platform in 1991.

In this diagram, increasing width of the rose ray indicates increasing current speed, while the length of the ray denotes prevalence. From this, it is apparent that the predominant current direction oscillates between the NW and SE direction under the influence of tides

4.4 Sampling strategy and technique

4.4.1 Sampling transects

The direction of the sampling transects were selected based upon the measured current speed and direction near the sea-floor. Two sampling transects were positioned according to the prevailing current direction, duration and strngth. The intention was to investigate the effect of the prevailing currents on the distribution of cuttings over the sea-floor. The longer sampling transect (10 km) was aligned parallel to the predominant north-west to south-east current direction from the cuttings chute. A shorter transect (1.2km) was positioned perpendicular to the first along a south-west to north-east axis as shown in Figure 4-3.

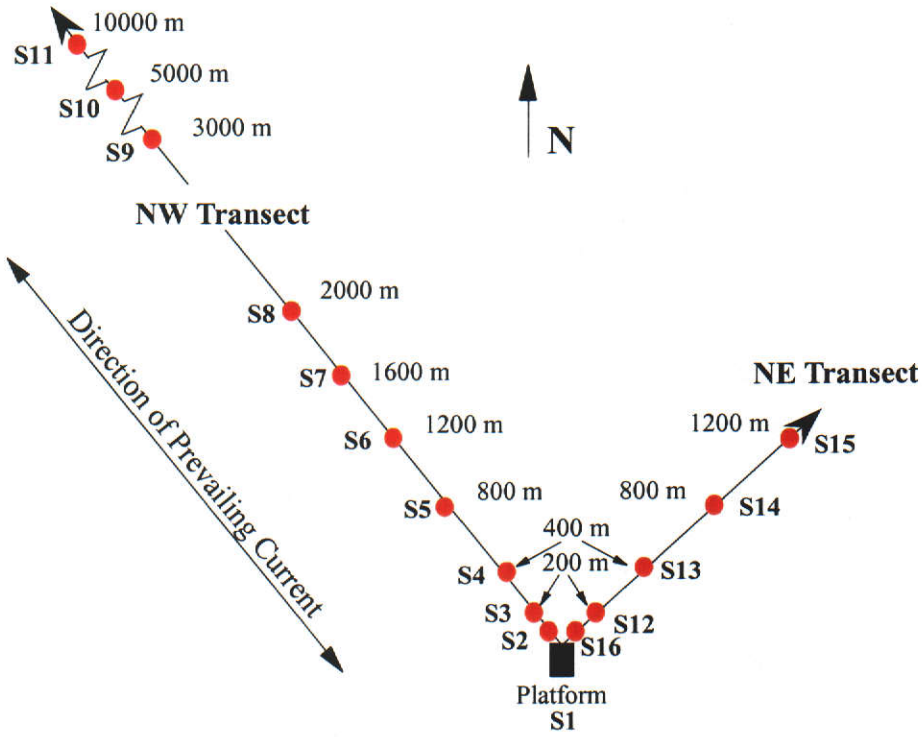

Figure 4-3: Sediment sampling locations on the sea-floor adjacent to the NRA production platform.

The distances along the transects from the cuttings chute to the various sampling sites were primarily selected based on previous similar surveys of the sea floor near to production platforms in the North Sea (Reiersen et al., 1989). Sufficient sample sites were included to incorporate the areas affected by drilling wastes suggested by these studies, with samples collected at 10000m along the NW Transect assumed to represent background samples representative of the sea-floor. For this survey, samples were also collected to study the effect of drilling discharges on benthic fauna; therefore information from previous surveys investigating these biological effects was also considered (Davies et al., 1989) when selecting the sample sites.

4.4.2 Sample collection methodology

Conventionally, a mechanical device is deployed from the ocean surface to collect sea-floor sediment samples. The grabs are collected either by remote activation from the surface *via* connecting cables, or by pressure activation upon contact with the sea floor. Using such techniques, it is difficult to ensure that the grab sample of sediment is representative of the sea-floor from which it was sampled due to loss of the sediment either during or after sample collection. For example, the surface sediment may scatter due to the pressure wave created by a spring loaded grab or due to the impact of the falling, remotely activated grab. In either case, the grab may land askew or fine material may be lost if the grab jaws remain slightly ajar during retrieval of the sampler. In addition it is difficult to access the location on the sea-floor from which the sample was collected. In the relatively deep (125 m) waters and currents prevalent around NRA, these problems are exacerbated.

The sampling system used in this study was specifically designed to overcome these problems. A schematic is shown in Figure 4-4. It consists of a remotely operated vehicle (ROV), deployed from a ship, fitted with a manipulator arm. The positioning of the ROV was controlled *via* acoustic coupling to a differential global positioning system (DGPS) aboard the dynamically positioned vessel. This sampling method enabled an accurate location of the sampling site to be established, usually to within approximately 10 metres of its actual position on the sea floor, vital to the precision of subsequent sampling visits to the region.

A stainless steel grab sampler was fitted to the ROV manipulator arm. The open grab covered a surface area of approximately 0.1 m^2 with a nominal depth of cut of 10 cm, dependent on the pressure applied by the manipulator arm. Two ports located on the top of the grab allowed sub-samples, including full depth profile cores, to be removed from the intact sample prior to opening the grab jaws. A screw mechanism, activated by the manipulator arm, was used to close the grab jaws to minimise disturbance of the surface sediments. Bearing surfaces requiring lubrication were quarantined from the surfaces likely to encounter the sediment sample. Photographs of the sampling device while deployed on the sea-floor have been published elsewhere (Chegwidden et al., 1993).

The ROV was also equipped with a video camera to monitor the deployment of the grab on the sea-floor and provided a permanent record of the sampling manipulations. It was also used to confirm the recovery of a sample of uniform volume cut into the sea-floor and that fine-grained sediment was not lost during retrieval of the grab. Furthermore, use of the video camera, in conjunction with the DGPS, ensured close proximity (i.e. less than 1m) between replicate samples, and that these were similar in physical appearance. Grab samples that did not meet these criteria could be discarded onto the sea floor without recovery to the surface.

At each location, six grab samples were obtained from approximately 1 m^2 of the sea-floor: three for physical and chemical analysis and three for biological analysis. Each grab was carefully opened onto a clean polyethylene board. Inspection of the sediment revealed that the material removed from below approximately 5 cm from the surface of the grab sample was darker in colour than the overlying sediment. A strong odour of hydrogen sulphide emanated from this dark-coloured material, indicating that these underlying sediments were retrieved from an anaerobic (sulphate reducing) environment.

The contents of the grab were homogenised, including the dark coloured sediments, and a representative sample (approximately 500 g) was removed for hydrocarbon analysis. Samples were placed in pre-cleaned 500 mL glass jars and were stored immediately after collection in a freezer maintained at approximately -25°C to

minimise loss of organic compounds due to volatilisation and microbial biodegradation. Samples remained frozen until they were processed in the laboratory prior to analysis.

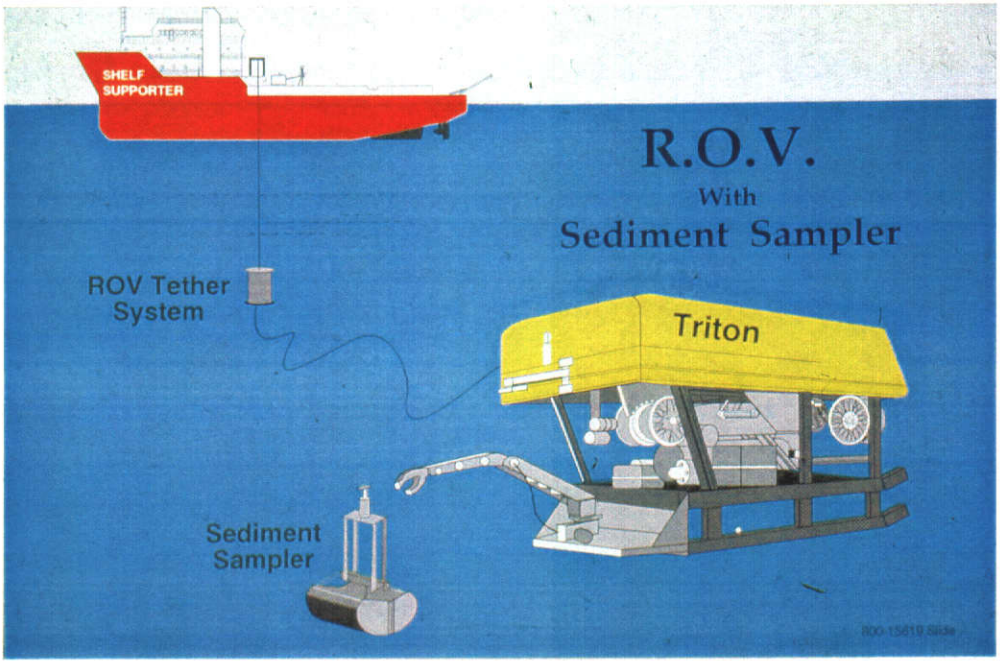

Figure 4-4: Schematic representation of the equipment used for collecting sea-floor sediment samples.

4.5 Petroleum hydrocarbons isolated from the sea-floor sediments

4.5.1 General hydrocarbon composition

Upon thawing, surrogate standards were added to the sediment sample, which was then allowed to partially dry at room temperature. Here, four chloroalkanes were chosen as surrogates for the petroleum hydrocarbons, namely 1-chlorooctane, 1-chlorodecane, 1-chlorotetradecane and 1-chlrorooctadecane. Hydrocarbons were extracted from the dried sediment samples by ultrasonically assisted solvent extraction using a mixture of dichloromethane and methanol as described in detail earlier (Chapter Two). An internal standard (1,2-dichlorobenzene) was also added to the hydrocarbon isolate immediately prior to analysis using GC-FID.

The gas chromatograms obtained from the hydrocarbon fractions isolated from sediments collected from three sites along the NW transect are shown in Figure 4-5. These chromatograms have been selected to illustrate the variation in composition of the hydrocarbons between sites. The hydrocarbons isolated from directly under the cuttings chute in the cuttings pile [Fig. 4-5(a)] are largely confined to a narrow molecular weight range approximately between that of n-C_{12} and n-C_{18}. This is consistent with the composition of the kerosene-like oil (Worrall, 1996) used to formulate drilling mud during the production and development program, indicating that this is the likely source of the hydrocarbons in the sea-floor sediment.

The hydrocarbons isolated from each of the 16 sites, including those sampled from directly under the cuttings chute, also contained an unresolved complex mixture (UCM) of hydrocarbons, appearing as a characteristic hump in the gas chromatogram. In sediments collected from the five sites within 800 m from the cuttings chute in the direction of the prevailing current, the contribution of the UCM to the overall distribution of hydrocarbons increased with increasing distance from the cuttings chute. This is illustrated by comparing the gas chromatogram obtained from the total petroleum hydrocarbon fraction isolated from sediments 800 m from the cuttings chute, shown in Fig 4-5(b), with that obtained from the hydrocarbons contained in the cuttings pile directly below the cuttings chute.

Also apparent from comparison of these chromatograms is the change in the composition of the resolved hydrocarbons, in particular the depletion of the n-alkanes relative to the isoprenoid pristane. Similar alterations in the composition of the hydrocarbons was observed in sediments collected from the sites located 100 m and 200 m away from the cuttings chute in the NE direction. These observations, consistent with alteration of the hydrocarbons by microbial biodegradation processes (Blumer, Ehrhardt and Jones, 1973; Gough, Rhead and Rowland, 1992) will be discussed in further detail later.

The composition of hydrocarbons isolated from more remote locations are typified by those found in sediments collected from the 2000 m (NW) site. The chromatogram obtained from these, shown in Figure 4-5(c) is dominated by peaks

arising from the surrogate standards added to the sediment prior to extraction, and the internal standard, added to the hydrocarbon isolate just prior to GC analysis. The predominance of these compounds, used to quantify hydrocarbons in the samples, indicates the lower concentration of hydrocarbons in this sediment sample, relative to the other two sites. Closer inspection of the chromatogram also reveals the presence of the hump arising from the UCM.

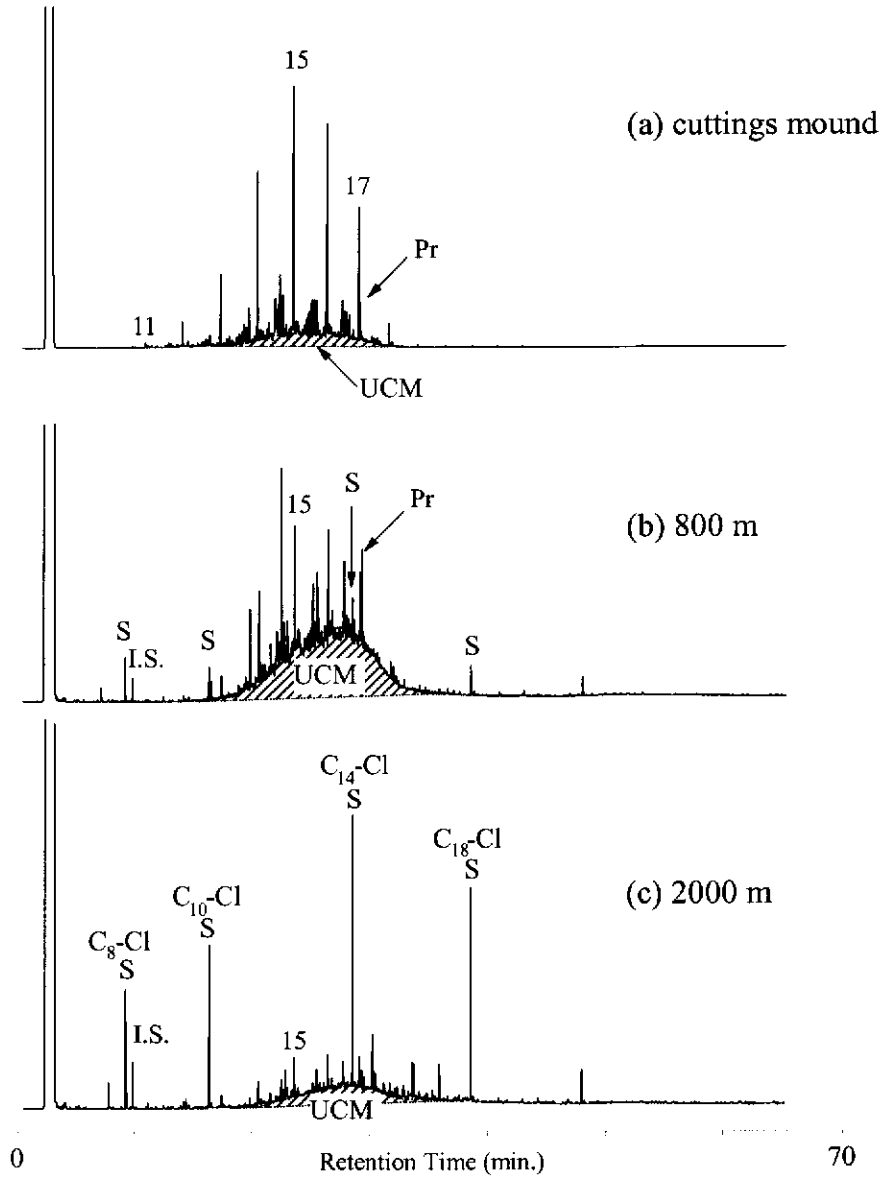

Figure 4-5: Gas chromatograms from GC-FID analysis of the total petroleum hydrocarbon fraction isolated from sea-floor sediments. These were collected (a) directly under the cuttings chute, and at distances of (b) 800 m and (c) 2000 m in the direction of the prevailing current. Peaks for the internal standard and the four chloroalkane surrogate standards are labelled I.S. and S respectively. Peaks labelled 11, 15, 17 and Pr correspond to *n*-C_{11}, *n*-C_{15}, *n*-C_{17}, and pristane respectively.

4.5.2 Quantification of total petroleum hydrocarbons

The values measured for hydrocarbon concentrations from the 16 locations are shown in Table 4-1 and Figure 4-6. At each site, the concentrations are mean values from the individual analysis of the three triplicate samples. In each case the individual values agreed to within 10 per cent, and the gas chromatograms were similar, indicating that the samples are representative of the sediment hydrocarbons present at each sampling site.

Table 4-1: Concentrations (mg kg^{-1}, dry weight) of total petroleum hydrocarbons extracted from sediments collected from the sea-floor adjacent to the NRA gas and condensate platform. Concentrations are the average value of triplicate samples and have been corrected for losses during treatment in the laboratory using the value of the per cent recovery, also shown where determined.

Distance from the cuttings chute(m)	TPH Concentration (mg kg^{-1}, dry weight)	Average Recovery (%) of surrogates
(Northwest Transect)		
0	75000	n.d.
100	7700	n.d.
200	1500	n.d.
400	280	n.d.
800	37	80
1200	19	85
1600	2.4	80
2000	1.8	80
3000	**11**	75
5000	0.090	80
10000	<0.010	85
(Northeast Transect)		
100	2100	n.d.
200	24	80
400	5.7	75
800	1.3	75
1200	2.5	85

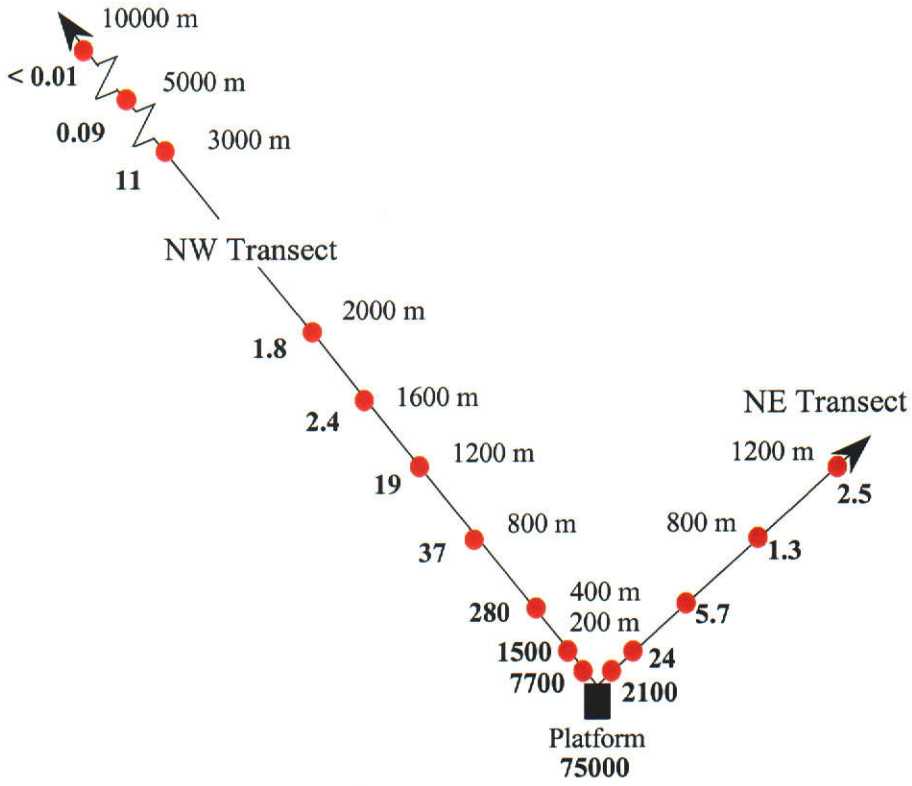

Figure 4-6: Sediment sampling locations on the sea-floor adjacent to the NRA platform. Total hydrocarbon concentrations (mg kg^{-1}, dry weight) are shown in bold text.

It is apparent from Table 4-1 and Figure 4-6 that the hydrocarbon concentrations decrease very rapidly along both transects with distance from the platform, with an apparently anomalously high value at 3000 m along the northwest transect. The reason for this slightly elevated value (11 mg kg^{-1}) is not clear, but it might be due to irregularity in the seabed at this site affecting the accumulation of material discharged from the platform.

In samples where the weight of the neat hydrocarbon isolate exceeded 1 mg, the hydrocarbon concentrations were determined gravimetrically by expressing the weight of the isolate as a proportion of the dry weight of the sediment from which it was extracted. Where there was insufficient hydrocarbon isolate to accurately weigh (i.e. less than 1 mg) the hydrocarbon concentration was determined from the gas chromatogram by comparison of the total peak area of the hydrocarbons with that of the surrogates.

To address concern that the occurrence of the UCM in the chromatograms would confound the quantification of the hydrocarbons, a stock solution of known concentration of hydrocarbons isolated from the sediment collected from 200 m along the NW transect was prepared. This solution was considered to be representative of the composition of the petroleum hydrocarbons in the sediment extracts from the other sites. A serial dilution of this solution was performed and an identical amount of the surrogate and internal standard solutions was added to each of the portions of the diluted isolate as was added to each of the sediment samples. Each solution was analysed using GC-FID and the total peak area from the gas chromatograms was normalised against the area of the peak arising from the known concentration of the surrogate standards added. The normalised total peak area was plotted against the concentration of the hydrocarbons and the equation of the line of regression was determined as shown in Figure 4-7. The hydrocarbons isolated from the sediments were analysed and the normalised peak area calculated in an identical manner to that described above. For each isolate, the concentration of the hydrocarbons was calculated from the equation of the line of regression determined from the calibration graph.

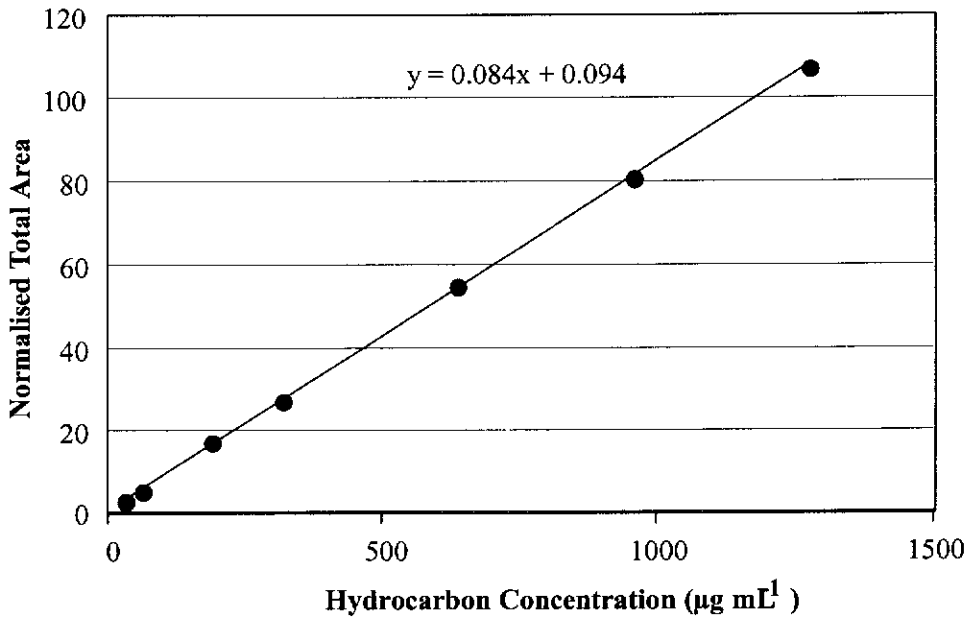

Figure 4-7: Calibration graph for the quantification of petroleum hydrocarbons in sediments collected from the sea-floor adjacent to the NRA platform.

The efficiency of extraction of hydrocarbons from the sediments was estimated from the recovery of the surrogate standards from the sediments. For each hydrocarbon isolate, the abundance (peak area) of each of the surrogate compounds was normalised (N_{SAMPLE}) against that of the internal standard. The normalised abundance ($N_{STANDARD}$) of each chloroalkane was similarly determined for a solution containing aliquots of the surrogate standard mixture and the internal standard solution identical to that added for the determination of hydrocarbons in the sea-floor sediments. These normalised abundances ($N_{STANDARD}$) are the maximum values attainable for the surrogates recovered from the sediments; that is, they represent 100 % recovery. The recovery of each of the surrogate compounds was therefore calculated as a percentage of this value using the following equation.

$$\%\text{Recovery} = \frac{N_{SAMPLE}}{N_{STANDARD}} \times (100)$$

Given that the surrogate standards were added in similar concentrations, it is apparent from Figure 4-5(c) that the recovery of the most volatile of these, 1-chlorooctane, was less than that of the other three for this sediment sample. Calculation of the recoveries reveals that these were in fact 65%, 85%, 90% and 90% respectively. Similar recoveries (65%, 90%, 90% and 90%) were also observed in the hydrocarbon isolate from sediments collected at the 800 m NW site.

The lower recovery of 1-chlorooctane is most likely due to evaporative losses during the initial drying of the sediment sample and the several subsequent operations in the analytical technique involving evaporation of solvents. The abundance of hydrocarbons more volatile than 1-chlorodecane may therefore have been significantly altered in these samples during the analytical procedure. Where possible, the concentrations shown in Table 4-1 have been corrected for losses upon treatment in the laboratory by multiplying the calculated concentration by the inverse of the per cent recovery of the surrogate compounds. The average recovery of the four surrogates, averaged over the triplicate analyses of sediments from each site, is also shown in Table 4-1.

Concentrations have not been corrected for samples where the recovery could not be determined, i.e. where results were determined gravimetrically. For example, inspection of Figure 4-5(a) reveals that, due to the high abundance of drilling mud hydrocarbons, neither peaks arising from the surrogates nor the internal standard are observable in the chromatogram obtained from sediments collected from directly under the cuttings chute. Similarly, recoveries could not be assessed for the three other sites within 400 m from the cuttings chute along the NW transect and the site 100 m NE from the cuttings chute.

4.5.3 Effect on the sea-floor of discharged drilling muds

To determine the effect of drilling discharges on the sea floor, the hydrocarbon concentrations presented here were interpreted in conjunction with the concentration of selected heavy metals, the sediment grain size distribution and biological species richness and abundance obtained from this sample set, none of which are presented here. The results of this investigation are discussed in detail elsewhere (Oliver and Fisher, 1999), but the conclusions may be summarised as follows.

Petroleum hydrocarbons

The high concentration of petroleum hydrocarbons in sea-floor samples recovered from directly under the cuttings chute (75000 mg kg^{-1} or 7.5% w/w) is comparable to the maximum allowable concentration of oil on cuttings (10% w/w) discharged from NRA, indicating that the material sampled consisted almost entirely of discharged cuttings rather than sea-floor sediment. The decreasing hydrocarbon concentrations with distance from NRA indicate that the transition between affected and unaffected sediments occurs between one kilometre to several kilometres in the direction of the prevailing current (NW). Along the NE transect, hydrocarbon concentrations decreased rapidly beyond approximately 200 m.

Trace metals

The concentrations of the trace metals zinc, iron, lead, cadmium, chromium, vanadium, nickel and copper decreased rapidly with increasing distance from the platform, with levels returning to background along the NW transect between

1600 m and 3000 m, and between 200 m and 400 m in the NE direction from the platform. This delineates a transition zone similar to that indicated by the hydrocarbon concentrations.

Sediment particle size

The greater dispersal in the NW direction with the prevailing current was also evident from examination of the sediment grain size distribution. Along the NW transect, the median particle size fraction of sediments collected from the site 10 km from the cuttings chute was 125 μm to 250 μm. This median particle size was observed for all of the sites located at distances greater than and including 2000 m from the cuttings chute. Sediments collected closer than this to the cuttings chute displayed a lower median particle size fraction of 63 μm to 125 μm, indicating the increased presence of drilling additives such as bentonite clay in the sediments. Along the NE transect, however, the median particle size fraction of 125 μm to 250 μm was attained much closer to the platform at 200 m.

Species richness and abundance

From a total of 45 grab samples collected at NRA, a total of 454 animals were counted, representing 93 taxa. The majority of the animals were polychaetes and crustaceans, with molluscs and echinoderms making up the bulk of the remaining animals. Post-drilling species richness and abundance of the NRA fauna samples were relatively low, averaging 12.6 (range 0 – 200) and 28.7 (range 0-87) per grab respectively. Sixty-five percent of the taxa from NRA were represented by two or less individuals and less than 8 % of the taxa were represented by 10 or more individuals. The most abundant species present was the polychaete worm *Nebalia* sp.1, represented by 138 individuals. Within 100m of the NRA cuttings discharge point, where the sediment hydrocarbon concentrations reanged from 2100 mg kg^{-1} (100m NE)to 7700 mg kg^{-1} (100m NW), 111 individuals were collected. Species richness, however, was depressed near the cuttings pile. *Nebalia* sp.1 was the only species represented 100 m from the cuttings discharge point along the NW Transect and no species were collected from the cuttings pile itself where hydrocarbon concentrations were measured at 75000 mg kg^{-1}.

Excluding *Nebalia* sp.1, decreases in species richness and abundance correlated with increasing hydrocarbon concentration along the NW transect. Acute effects were clearly evident within the cuttings pile and at the 100 m and 200 m sites. Richness and abundance then increased rapidly along the NW Transect at 400 m, and then appeared to increase only gradually with increasing distance from the platform. At a distance of 10 km from the discharge point, 20 species were identified, only a few more than at 3000 m and 5000 m. Given the natural variability in richness, it may be that background levels were attained at 3000 m. Consequently, based on qualitative analysis of richness and abundance, a transition zone between 400 m and 3000 m along the NW transect was tentatively established. In the NE direction, no trend was easily discernible, although richness and abundance increased rapidly at 200m from the platform.

4.5.4 Gross changes in hydrocarbon composition on the sea-floor with increasing distance from the platform

Sediments from seven of the sixteen sampling sites were chosen for further scrutiny to investigate the change in hydrocarbon composition with increasing distance from the cuttings discharge point. In addition to the discharge point (0 m), these included the four sites closest to the platform along the NW transect (100 m, 200 m, 400 m and 800 m) and the two sites closest to the platform along the NE transect (100 m and 200 m). For each of these, the solvent extracts from each set of triplicate samples were combined to obtain a greater mass of soluble organic material from sediments from each site. Each of the combined extracts was separated into saturated hydrocarbon and aromatic hydrocarbon fractions using liquid chromatography on silica gel. Each of these was subsequently analysed using GC-MS. The total ion chromatograms of these fractions are shown in Figure 4-8.

Considering the chromatograms of both hydrocarbon fractions isolated from the sample collected from directly under the cuttings chute (0 m), it is apparent that the distributions of saturated and aromatic hydrocarbons are largely confined to a narrow molecular weight range of *n*-C_{12} to *n*-C_{18} and C_2-naphthalenes to C_4-naphthalenes respectively.

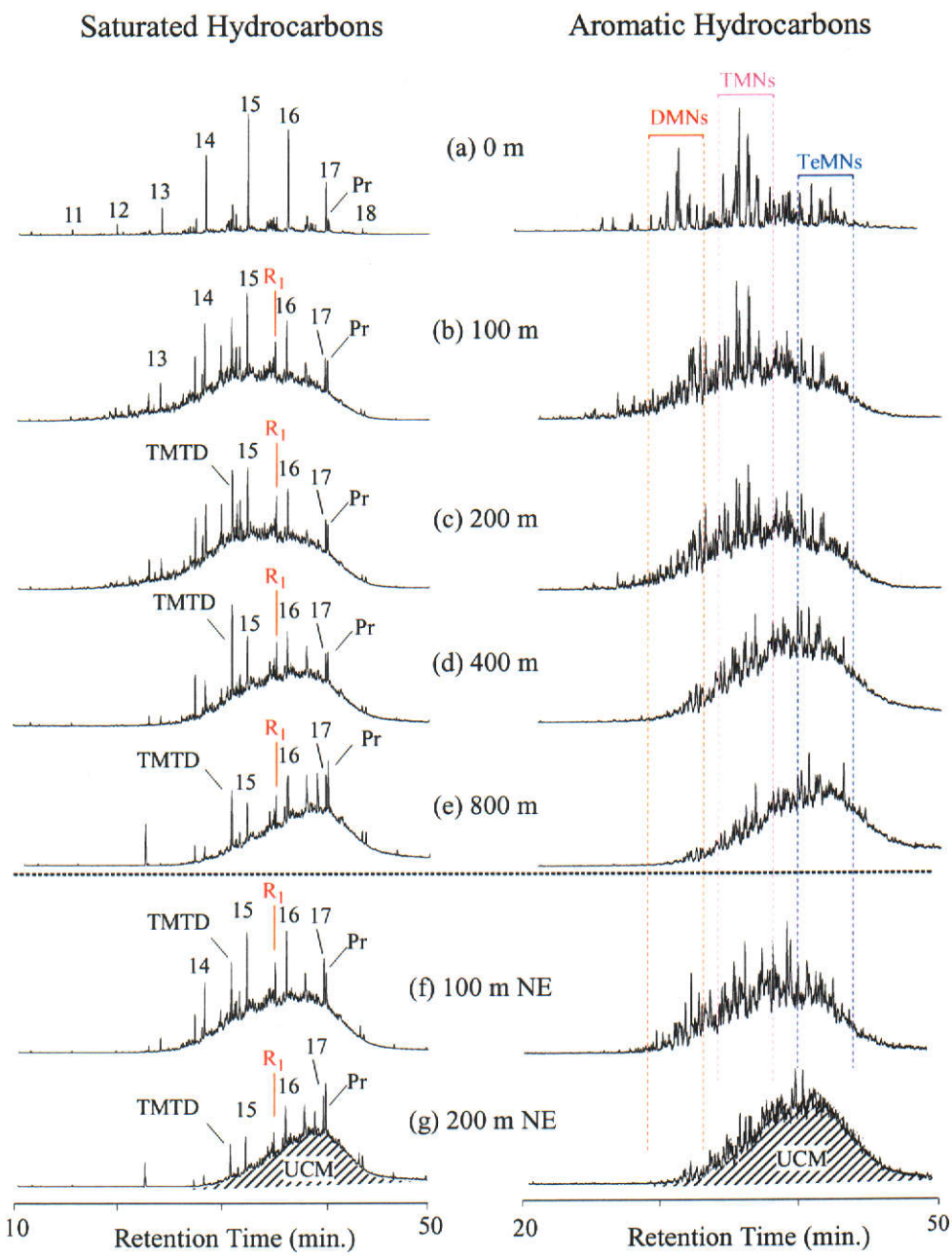

Figure 4-8: Total ion chromatograms of the saturated and aromatic hydrocarbon fractions isolated from sea-floor sediments. These were collected from (a) directly under the cuttings chute, and at distances of (b) 100 m, (c) 200 m, (d) 400 m and (e) 800 m away from the NRA cuttings chute in the direction (NW) of the prevailing current. Chromatograms from (f) 100 m and (g) 200 m away from the cuttings along the NE transect are also shown. The identity of the labelled peaks are as follows: 11 through 18 = *n*-C_{11} to *n*-C_{18}; Pr = pristane; TMTD = 2,6,10-trimethyltridecane; R_1 = the rearranged analogue of 8β(H)-drimane (Alexander et al., 1984); DMNs = dimethylnaphthalenes; TMNs = trimethylnaphthalenes; TeMNs = tetramethyl-naphthalenes.

This is consistent with the composition of the kerosene-like oils (Worrall, 1996) used to formulate drilling muds during the final phase of the production and development program (Papp and Fisher, 1999), indicating that these are the likely source of the hydrocarbons in the sea-floor sediment.

4.6 The effect of biodegradation on saturated hydrocarbon abundances

4.6.1 Gross changes in composition

The change in the composition of the saturated hydrocarbons in sediments at the seven locations closest to the cuttings discharge chute is illustrated in Figure 4-8. Comparing the chromatograms obtained from directly under the platform and the two locations closest to the platform along the NW transect, it is evident that the resolved peaks are increasingly attenuated relative to the UCM with increasing distance away from the platform, indicating the progression of biodegradation (Connan, 1984; Grimalt et al., 1991; Gough, Rhead and Rowland, 1992). These observations may be quantified by comparing the abundances (peak areas) of the resolved hydrocarbons and the UCM shown in Table 4-2. Here the ratio of the relative abundance of resolved compounds to the UCM reaches a minimum value at 200 m NW of the platform. This value maintains an approximately constant value for the two more distant locations on that transect.

Between locations S3 (200 m) and S4 (400 m), there is a perceptible loss of lower molecular weight components of the UCM. This loss is even more apparent when comparing the chromatograms from the 400 m and 800 m (S5) locations in Figure 4-8. Similar observations may be made for the two sampling sites along the NE transect, however the depletion of hydrocarbons between S16 (100 m) and S12 (200 m) is greater than that observed in the NW transect sediments. Table 4-2 reveals that although the saturated hydrocarbon composition is broadly similar at the two locations closest to the cuttings discharge point on each transect (i.e. 100 m), the hydrocarbons from 200 m NE exhibit values more comparable to those at the 800 m location on the NW transect.

The increasingly biodegraded hydrocarbon signature with increasing distance from the platform is most likely explained by the increased accessibility of the hydrocarbon residues to alteration by biodegrading organisms as well as dissolution in water at locations more remote from the platform. These will be discussed in detail later (see Section 4-10), however, these observations allow more detailed exploration of molecular susceptibility to microbial attack.

Table 4-2: Relative abundances of the total of resolved saturated alkane peaks (resolved), the unresolved complex mixture (UCM), *n*-tetradecane (*n*-C_{14}), *n*-pentadecane (*n*-C_{15}), *n*-heptadecane (*n*-C_{17}), trimethyltridecane (TMTD), pristane (Pr) and 8β(H)-homodrimane (C_{16}-D). With the exception of C_{16}-D, determined from the m/z 123 mass chromatogram, peak areas were obtained from the total ion chromatogram of saturated hydrocarbons extracted from sea-floor sediments adjacent to the NRA platform.

Site	Distance from Cuttings Chute	Peak Area Ratio					
		Resolved / UCM	*n*-C_{14} / *n*-C_{17}	*n*-C_{15} / TMTD	*n*-C_{17} / Pr	*n*-C_{16} / C_{16}-D	Pr / C_{16}-D
S1	0 m	1.2	1.4	4.6	3.0	280	50
	NW Transect						
S2	100 m	0.21	1.7	1.1	0.87	12	6.9
S3	200 m	0.14	1.5	0.80	0.85	8.1	5.5
S4	400 m	0.16	1.4	0.60	0.64	7.3	5.3
S5	800 m	0.16	0.39	0.57	0.45	12.1	15
	NE Transect						
S16	100 m	0.17	1.2	1.1	1.0	12.7	7.1
S12	200 m	0.16	0.25	0.98	0.53	12.4	19

4.6.2 Changes in the abundance of resolved hydrocarbons

Amongst the residual resolved peaks in the chromatograms from each of the five locations along the NW transect, the *n*-alkanes are depleted relative to the acyclic isoprenoids 2,6,10-trimethytridecane (TMTD) and pristane. This is illustrated by the peak areas of these isoprenoids relative to that of the most closely eluting *n*-alkane, presented in Table 4-2. The most rapid change in abundance of the *n*-alkanes occurs within 100 m of the platform along both transects; beyond 100 m their abundances relative to the isoprenoids decrease more gradually with distance.

As shown in Figure 4-8, the depletion of the *n*-alkanes in the sediments remote from the platform also reveals the presence of the C_{16}-bicyclic alkane 8β(H)-homodrimane (C_{16}-D). The presence of this compound and other bicyclic alkanes, namely 8β(H)-drimane (C_{15}-D), and the two rearranged analogues of C_{15}-D (R_1 and R_2), was confirmed in all seven samples using selected ion monitoring (SIM) as described by Alexander et al. (1984), from which the m/z 123 mass chromatograms are shown in Figure 4-9.

The resistance of these compounds to biodegradation relative to the *n*-alkanes and the acyclic isoprenoids has been reported by Volkman et al. (1984). On this basis, C_{16}-D was selected as a biodegradation-resistant internal marker against which the abundance of the *n*-alkanes and the isoprenoids were compared. These results are also shown in Table 4-2. It is evident that both *n*-C_{16} and pristane, the model compounds for the *n*-alkanes and isoprenoids respectively, are depleted relative to C_{16}-D with increasing distance from the cuttings chute at all locations, with the exception of S5 (800 m NW) and S12 (200 m NW). At both of these sites, there is an anomalously high normalised abundance of both *n*-C_{16}, and particularly pristane. Comparing these abundances at S5 with the other samples shown in Table 4-2, the value for *n*-C_{16} (*n*-C_{16}/ C_{16}-D = 12) is identical to that at S2, while pristane at S5 (Pr/C_{16}-D = 15) exceeds that measured at S2 (6.9). The S12 sample also shows a similar elevated relative abundance of pristane (19).

One explanation for the unexpectedly high abundance of pristane in these samples is that there has been an input of pristane from a separate source. The characteristic limited molecular weight range of the hydrocarbons extracted from the sediments indicates that contamination by other petroleum, for example formation fluids from the drilling cuttings is very unlikely. Non-petrogenic sources of pristane may also be discounted since very high resolution gas chromatographic analysis of both samples revealed a distribution of diastereomers characteristic of petroleum-derived pristane, as described by Gassmann (1981). From this, one is lead to conclude that the pristane is native to the LTOBM and that its enhanced abundance in the sediments eventuated from biodegraded residues, from which the *n*-alkanes have been relatively

depleted. Further evidence for mixing of hydrocarbons of varying extents of biodegradation will be discussed in detail later.

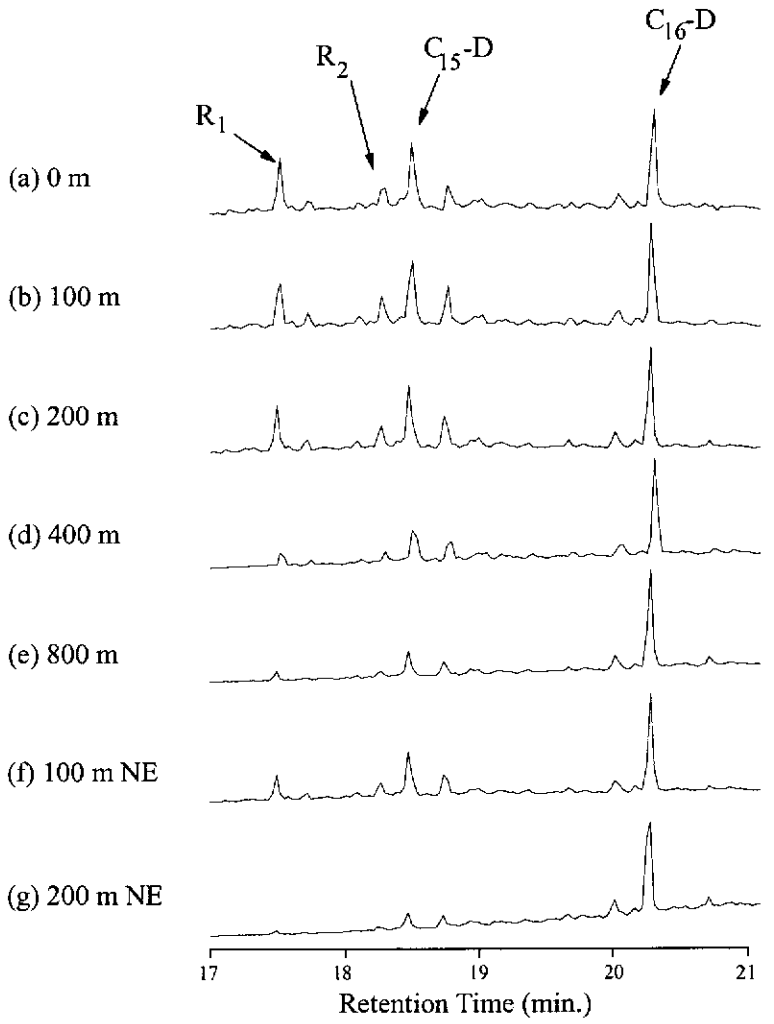

Figure 4-9: Selected ion chromatograms (m/z 123) from GC-MS analysis of the saturated hydrocarbon fractions isolated from sea-floor sediments. These were collected from (a) directly under the cuttings chute, and at distances of (b) 100 m, (c) 200 m, (d) 400 m and (e) 800 m away from the NRA cuttings chute in the direction (NW) of the prevailing current. Chromatograms from (f) 100 m and (g) 200 m away from the cuttings along the NE transect (perpendicular to the prevailing current) are also shown. The identity of the labelled peaks are as follows: C_{15}-D = 8β(H)-drimane; C_{16}-D = 8β(H)-homodrimane; R_1 and R_2 = the two rearranged analogues of C_{15}-D (Alexander et al., 1984).

Alteration amongst the bicyclic alkanes

It is evident from inspection of the mass chromatograms shown in Figure 4-9 and the relative abundance of each of the bicyclic alkanes, indicated by the peak area ratios shown in Table 4-3, that the rearranged drimanes R_1 and R_2 are depleted relative to the C_{15}-drimane, which in turn is more readily depleted than the C_{16}-homodrimane. In contrast to the *n*-alkanes, the depletion of the C_{15}- bicyclic alkanes is most marked in sediments at locations beyond 200 m NW and 100 m NE. There is also some discrimination in the extent of depletion amongst the two rearranged C_{15}-drimanes at these more remote locations. Inferring biodegradation susceptibilities from these changes in distribution of the rearranged drimanes should be made with some caution, however, since the extent to which the isomers are depleted from the mixture correlates with their volatility, as indicated by their elution order on the non-polar GC column.

Table 4-3: Relative abundances of 8β(H)-drimane (C_{15}-D) and its two rearranged analogues (R_1 and R_2), and 8β(H)-homodrimane (C_{16}-D) in sea-floor sediments adjacent to the NRA platform. Peak areas, obtained from SIM m/z 123 mass chromatograms are not corrected for differences in detector response.

Site	Distance from Cuttings Chute	Peak area ratio					
		$\frac{R_1}{C_{15}\text{-D}}$	$\frac{R_2}{C_{15}\text{-D}}$	$\frac{R_1+R_2}{C_{15}\text{-D}}$	$\frac{R_1}{R_2}$	$\frac{C_{15}\text{-D}}{C_{16}\text{-D}}$	$\frac{R_1+R_2}{C_{16}\text{-D}}$
S1	0 m	0.70	0.36	1.1	1.9	0.69	0.73
	NW Transect						
S2	100 m	0.68	0.40	1.1	1.7	0.73	0.79
S3	200 m	0.69	0.36	1.1	1.9	0.68	0.71
S4	400 m	0.32	0.24	0.56	1.3	0.43	0.24
S5	800 m	0.30	0.28	0.59	1.1	0.27	0.16
	NE Transect						
S16	100 m	0.47	0.31	0.78	1.5	0.54	0.42
S12	200 m	0.23	0.33	0.56	0.71	0.17	0.09

With the exception of samples S5 (800 m NW) and S12 (200 m NE), the ratio of abundances of *n*-C_{14} and *n*-C_{17} shown in Table 4-2 is relatively constant, indicating that components of the mixture less volatile than *n*-C_{14} have not been preferentially removed by evaporation. In addition to this, the chromatogram shown in Figure 4-10, reveals that in spite of the observed loss of more volatile components of the UCM at S5 (800 m NW), it is clear that a significant portion of the residual hydrocarbon mixture is more volatile than the C_{15}-rearranged drimanes (R_1 and R_2). It is also evident that the loss of volatile components from the hydrocarbon mixture at this location is not accompanied by the loss of the surrogate standard 1-chloro-decane, relative to the less volatile 1-chlorotetradecane or 1-chlorooctadecane. It is therefore unlikely that the hydrocarbon mixture has been altered during manipulation in the laboratory. The abundance of R_2 relative to C_{15}-D is less likely to be affected by possible evaporative losses, considering the similarity in their GC retention times. This ratio, presented in Table 4-3 is therefore perhaps a more suitable indicator of the *in-situ* alteration of the bicyclic alkanes on the sea-floor.

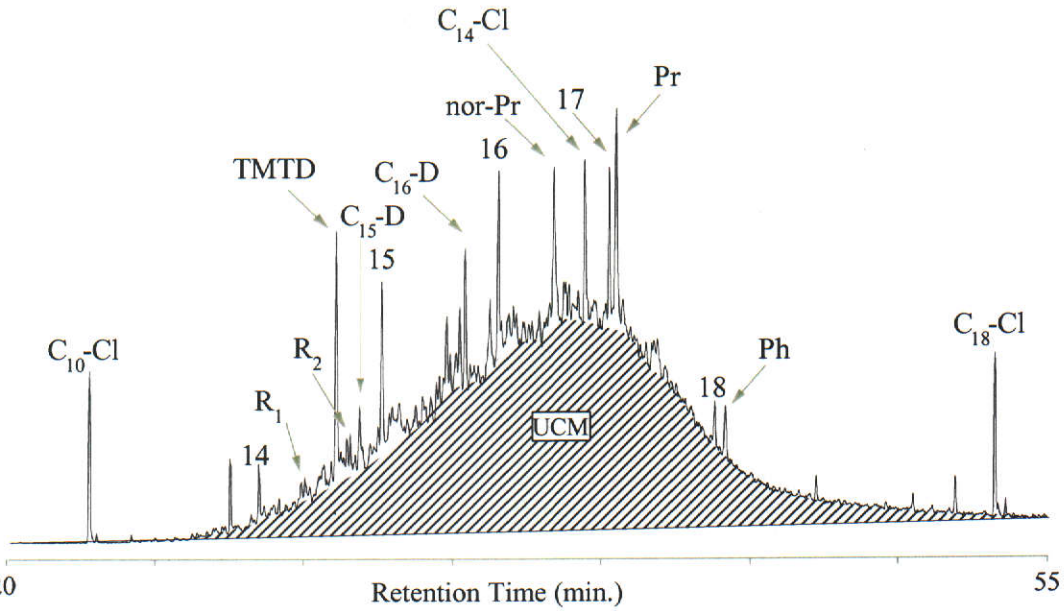

Figure 4-10: Total ion chromatogram of the saturated hydrocarbon fraction isolated from sea-floor sediments 800 m from the NRA cuttings chute in the direction (NW) of the prevailing current. The identity of the labelled peaks are as follows: C_{10}-Cl, C_{14}-Cl, C_{18}-Cl = surrogate standards 1-chlorodecane, 1-chlorotetradecane and 1-chlorooctadecane; 14 through 18 = *n*-C_{14} to *n*-C_{18}; TMTD = 2,6,10-trimethyltridecane; C_{15}-D = C_{15} drimane; C_{16}-D = C_{16} drimane; R_1 and R_2 = rearranged C_{15}-D; nor-Pr = nor-pristane; Pr = pristane; Ph = phytane.

Summary

In general, the saturated hydrocarbons display an increasingly biodegraded signature with increasing distance from the cuttings chute. The alteration of the saturated hydrocarbons is most pronounced between the sample collected from directly under the cuttings chute S1 (0 m), and the samples closest to this on each transect, namely, S2 (100 m NW) and S16 (100 m NE). Changes between these and the remaining samples are more subtle. The unusually high abundance of pristane at S5 (800 m NW) and S12 (200 m NE) are perhaps indicative of multiple accumulations of LTOBM of varying extents of biodegradation.

4.7 The effect of biodegradation on aromatic hydrocarbon abundances

4.7.1 Gross changes in composition

In Figure 4-8, the total ion chromatograms for the aromatic fractions are shown alongside those of the saturated hydrocarbon fractions from the seven sampling sites. As observed with the saturated hydrocarbons, with increasing distance from the platform, the aromatic hydrocarbon chromatograms show an increasingly biodegraded signature. This is revealed by comparing the signal for the UCM relative to the resolved alkylnaphthalenes.

To further explore the relative susceptibilities to biodegradation of the aromatic hydrocarbons, for each chromatogram the relative abundances of the dimethylnaphthalenes (DMNs), trimethylnaphthalenes (TMNs) and tetramethylnaphthalenes (TeMNs) were calculated from the sum of the peak areas corresponding to each of the isomers, corrected for differences in the mass selective detector response. From these, shown in Figure 4-11, it is apparent that in broad terms, the rates of depletion of the alkylnapthhalenes were in the order DMNs > TMNs >TeMNs. This is consistent with observations made for in-reservoir biodegraded crude oils (Rowland et al., 1986; Volkman et al., 1984). It also appears from inspection of Figure 4-11 that although the DMNs are depleted more rapidly than the TMNs, the depletion occurs concurrently.

This behaviour is especially evident when considering the results from the four locations closest to the platform along the NW transect, where, relative to the TeMNs, the removal of DMNs and TMNs occurs monotonically rather than in a stepwise manner associated with a sequential removal. This is also perceptible along the NE transect sediments, despite there being only two sampling locations.

The relative abundances of alkylnaphthalenes in sediments collected from location S5 (800 m NW), however, do not neatly fit into the sequence described by the other samples. Instead, the extent of biodegradation as described by these compounds is similar to, if not less than that observed in sediments at location S4 (400 m NW). This anomalous behaviour will be discussed further in detail later.

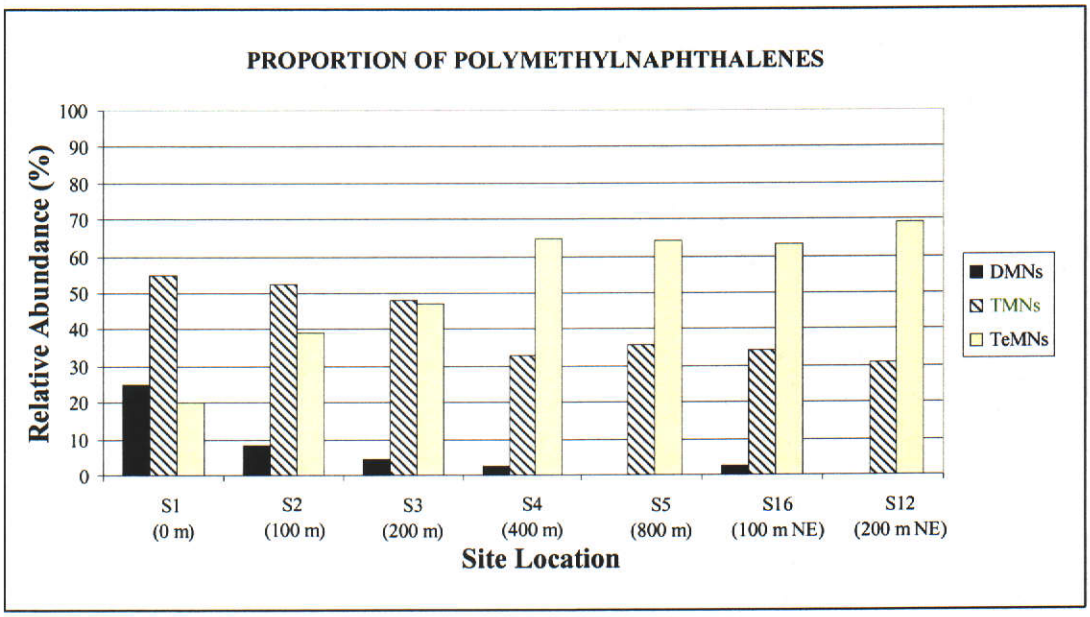

Figure 4-11: Relative abundances of dimethylnaphthalenes (DMNs), trimethylnaphthalenes (TMNs) and tetramethylnaphthalenes (TeMNs) in aromatic hydrocarbon fractions isolated from sea-floor sediments adjacent to NRA.

4.8 Studies using GC-FTIR and GC-MS to identify individual polymethylnaphthalenes

4.8.1 Dimethylnaphthalenes

Mass chromatograms (m/z 156) revealing the DMNs contained in the aromatic hydrocarbon fraction obtained from three sediment extracts are shown in Figure 4-12. The mixture of the polymethylnaphthalene isomers contained in sediments collected from directly under the cuttings discharge chute is similar to that one would obtain from a typical mature crude oil (cf. Figure 3-11). It is apparent that the relative abundances of the DMN isomers changes with increasing distance from the cuttings chute, clearly illustrated by the depletion in abundance of 1,6-DMN relative to the other isomers. The co-elution of some isomers however, confounds more detailed interpretation of the analysis, since the differences in the mass spectra of these isomers are not sufficient to allow them to be distinguished.

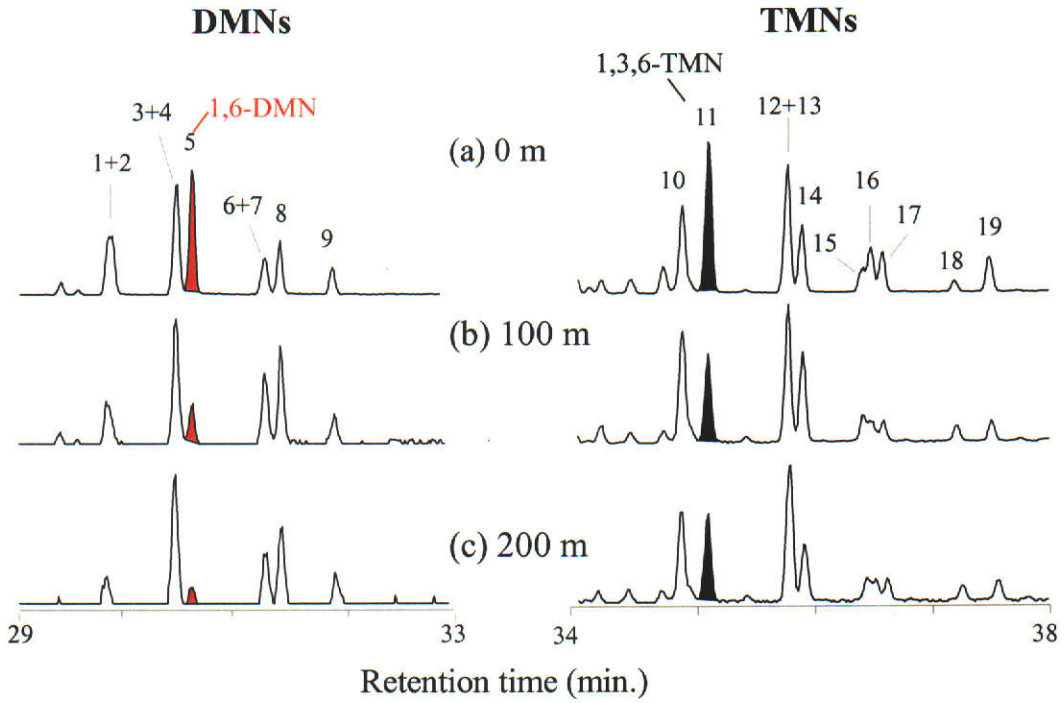

Figure 4-12: Mass chromatograms showing the DMNs (m/z 156) and TMNs (m/z 170) present in sediments collected from (a) directly under the cuttings chute, and at distances of (b) 100 m and (c) 200 m away from the cuttings chute in the direction of the prevailing current. Peak identifications: (1) 2,6-DMN; (2) 2,7-DMN; (3) 1,7-DMN; (4) 1,3-DMN;(5) 1,6-DMN; (6) 1,4-DMN; (7) 2,3-DMN; (8) 1,5-DMN; (9) 1,2-DMN;(10) 1,3,7-TMN; (11) 1,3,6-TMN; (12) 1,4,6-TMN; (13) 1,3,5-TMN; (14) 2,3,6-TMN; (15) 1,2,7-TMN; (16) 1,6,7-TMN; (17) 1,2,6-TMN; (18) 1,2,4-TMN; (19) 1,2,5-TMN.

To enable the quantification of the co-eluting DMNs, the alkylnaphthalene fractions were also analysed using direct deposition GC-FTIR, as described in Chapter 3. Since each polymethylnaphthalene has a unique infrared spectrum, the relative abundance of each of the co-eluting isomers could be determined on the basis of differences in their infrared spectra. This is illustrated in Figure 4-13, where the partial GC-FTIR spectra obtained from authentic samples of 2,3-DMN and 1,4-DMN are compared with that of the mixture of co-eluting isomers contained in the sediment collected from directly below the cuttings chute. The spectra of the reference compounds have been normalised to correct for differences in the intensities of infrared absorbance. This approach showed that 60% of the peak in the sediment extract was due to 1,4-DMN, while the contribution of 2,3-DMN was 40%.

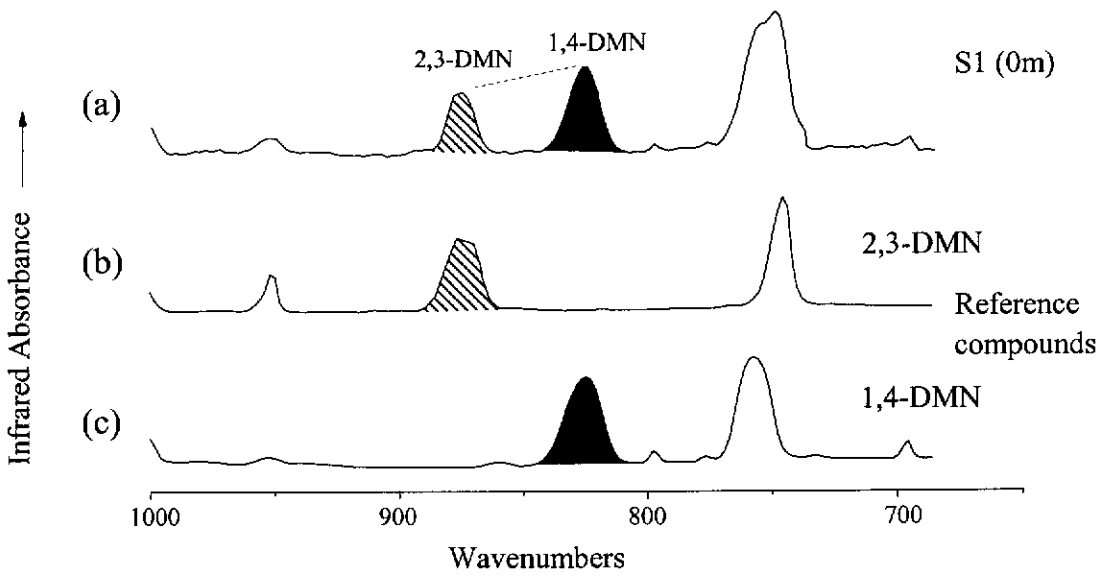

Figure 4-13: Partial FTIR spectra of co-eluting DMN (a) present in sediments collected from directly under the cuttings chute and the reference compounds (b) 2,3-DMN, and (c) 1,4-DMN obtained by direct deposition GC-FTIR.

The other pairs of co-eluting isomers, namely 2,6-DMN / 2,7-DMN and 1,3-DMN / 1,7-DMN were similarly resolved on the basis of differences in their infrared spectra.

4.8.2 Trimethylnaphthalenes

Mass chromatograms showing the TMNs contained in the aromatic fractions of three sediment extracts are presented in Figure 4-12. As with the DMNs, the composition

of this mixture of compounds also changes with increasing distance from the cuttings chute, with 1,3,6-TMN apparently being the most rapidly depleted isomer. Co-elution of the 1,3,5-TMN and 1,4,6-TMN isomers precludes the determination of all of the TMN isomers using GC-MS analysis alone. Analysis using direct deposition GC-FTIR, however, confirms that the 1,4,6-TMN is the more depleted isomer as the extent of biodegradation proceeds, as is shown in Figure 4-14.

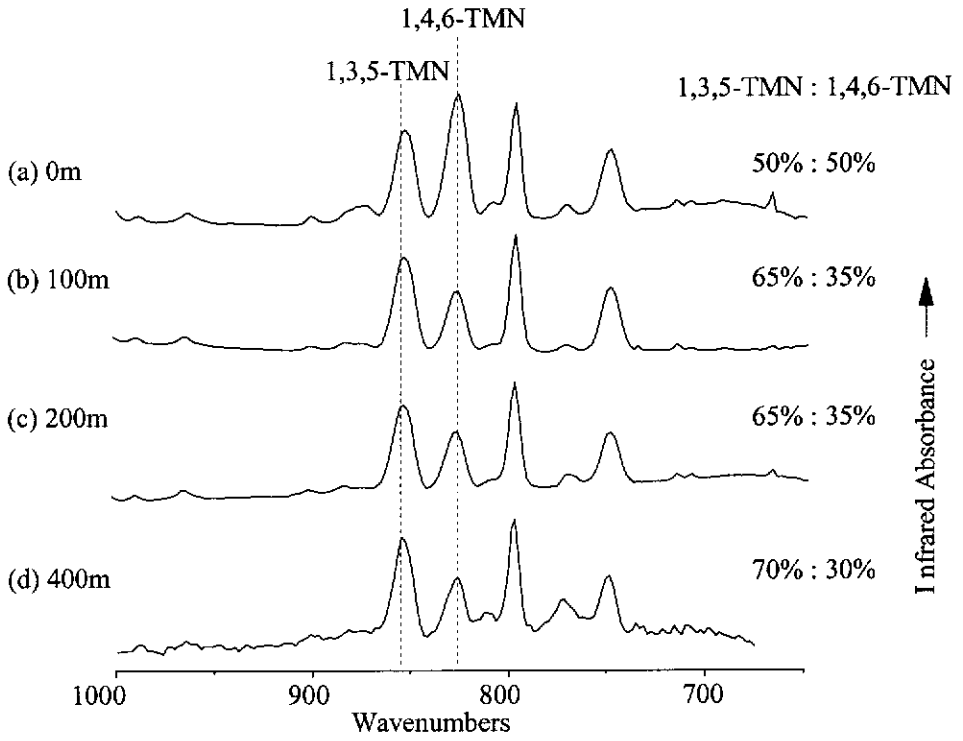

Figure 4-14: Partial FTIR spectra of 1,3,5-TMN and 1,4,6-TMN in sea-floor sediments collected from (a) directly under the cuttings chute, and at distances of (b) 100 m (c) 200 m and (d) 400 m away from the cuttings chute in the direction of the prevailing current.

4.8.3 Tetramethylnaphthalenes

The relative abundance of each of the TeMN isomers present in the sediments was also determined using the complementary techniques of GC-MS and GC-FTIR. From inspection of the mass chromatograms shown in Figure 4-15, it appears that 1,3,6,7-TeMN is the isomer most susceptible to microbial attack. Conversely, 1,3,5,7-TeMN is the least susceptible. Both observations were confirmed using GC-FTIR analysis. Since these two isomers differ only slightly in molecular shape, the disparity in their rates of depletion shows that the rate of microbial attack on the individual polymethylnaphthalenes is very susceptible to slight differences in

structure. Further, considering the earlier observation that the TeMNs are more resistant to biodegradation than are the TMNs and DMNs, it follows that 1,3,5,7-TeMN is the most resistant to biodegradation of the polymethylnaphthalenes identified in these samples. This compound is therefore useful as a conserved benchmark against which the change in abundance of each of the alkylnaphthalenes may be compared.

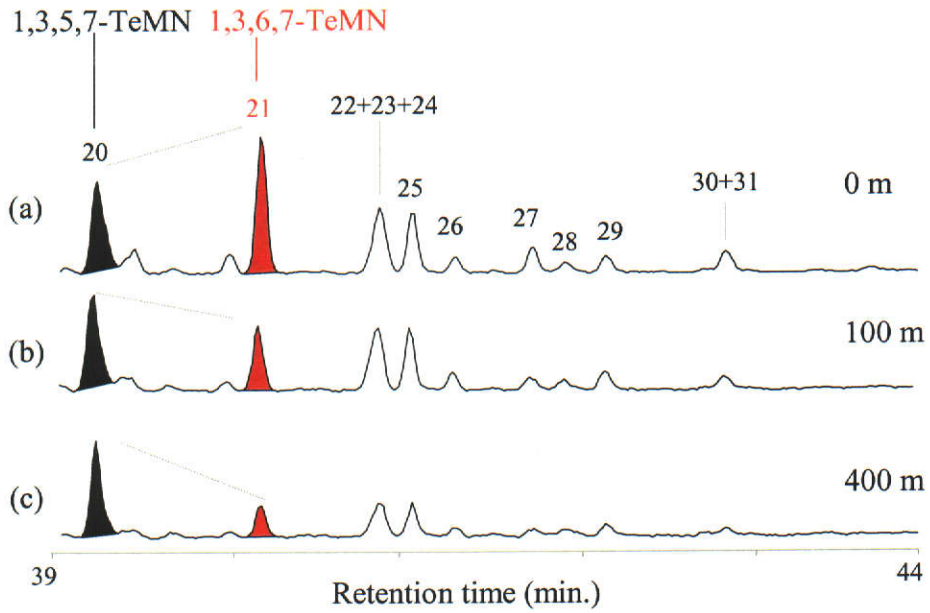

Figure 4-15: Mass chromatograms (m/z 184) showing the TeMNs present in sediments collected from (a) directly under the cuttings chute, and at distances of (b) 100 m away from and (c) 400 m away from the cuttings chute in the direction of the prevailing current.. Peaks correspond to the TeMN isomers as follows: (20) 1,3,5,7-; (21) 1,3,6,7-; (22) 1,2,4,6-; (23) 1,2,4,7-; (24) 1,4,6,7-; (25) 1,2,5,7-; (26) 2,3,6,7-; (27) 1,2,6,7-; (28) 1,2,3,7-; (29) 1,2,3,6-;(30) 1,2,3,5-; (31) 1,2,5,6-.

4.9 Relative susceptibilities of individual polymethylnaphthalene isomers to biodegradation

The peak areas corresponding to each of the DMNs, TMNs and TeMNs were measured from the appropriate mass chromatograms. At each location, the peak area for each compound was divided by the peak area corresponding to 1,3,5,7-TeMN to yield a normalised, unit-less abundance for each compound. The area of peaks arising from co-eluting isomers was apportioned to each isomer based on the results of GC-FTIR analysis. Results for the DMNs are shown in Figure 4-16, where the normalised abundance at each location is expressed as a proportion of that measured

in sediments directly under the cuttings discharge chute. Using this approach, differences in the initial abundance (i.e. in sediments from location S1) between isomers are negated and therefore do not bias the comparison of the extent of depletion. From inspection of these, it is possible to establish a ranking amongst the polymethylnaphthalene isomers of their susceptibility to biodegradation.

4.9.1 Dimethylnaphthalenes

It was not possible to obtain meaningful data using GC-FTIR techniques from locations S4, S5, S16 and S12 due to the low concentration of the DMNs in these sediments. Abundances of all isomers are therefore only reported for the remaining three locations closest to the platform, as shown in Figure 4-16.

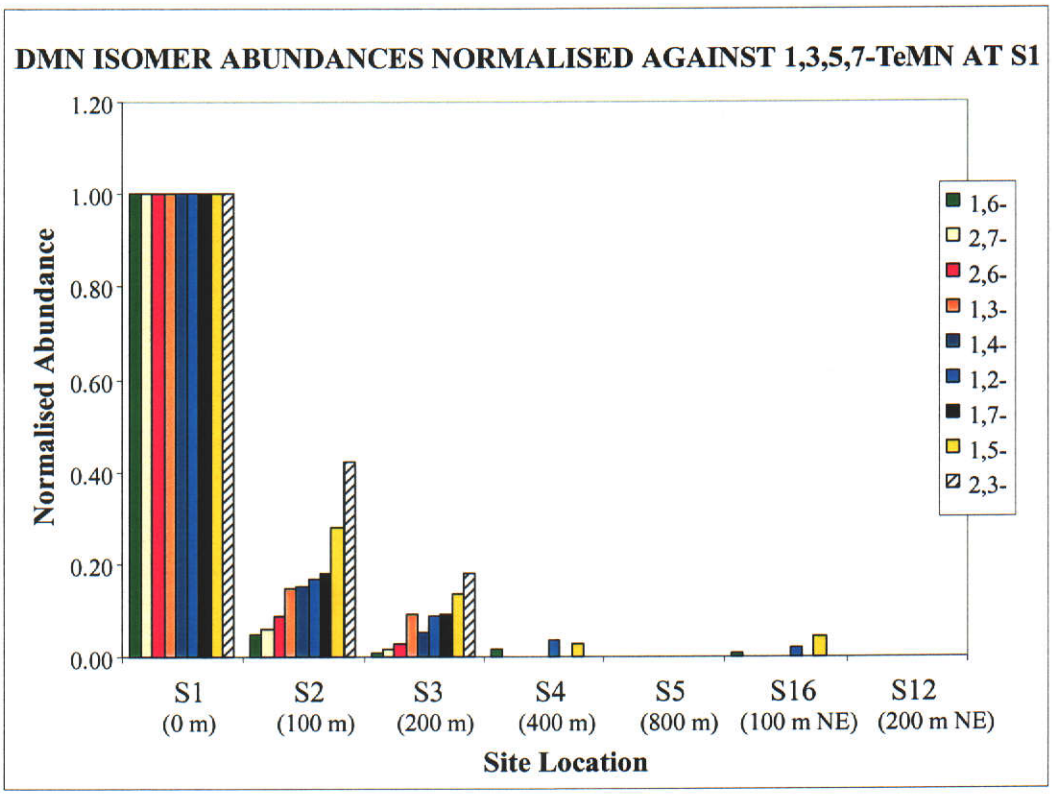

Figure 4-16: A bar chart showing changes in the relative abundances of individual DMN isomers present in sediments collected from the sea-floor adjacent to NRA. Abundances are normalised against that of 1,3,5,7-TeMN and are expressed as a proportion of those measured at site S1, directly under the discharge chute.

Considering the change in abundances between locations S1 and S2, it is apparent that 1,6-DMN is depleted by approximately 90%: the most of all isomers. Conversely, 2,3-DMN is the least depleted isomer, showing a decrease in abundance of approximately 55%. The depletion of the remaining seven DMN isomers is intermediate between these. In general, the observed order of extent of depletion is maintained between locations S2 and S3, that is: 1,6-DMN (most depleted) ~ 2,7-DMN > 2,6-DMN >> 1,3-DMN ~ 1,4-DMN ~ 1,2-DMN ~ 1,7-DMN >> 1,5-DMN > 2,3-DMN (least depleted).

4.9.2 Trimethylnaphthalenes

As expected from the total TMN abundances shown in Fig 4-11, the changes in abundances of the individual TMNs were more gradual than observed for the DMNs. The TMNs were present in sufficiently high abundance in the sediments from the five locations along the NW transect to allow normalised abundances to be determined for all TMN isomers present. At S16 and S12, however, the abundances of the co-eluting 1,4,6-TMN and 1,3,5-TMN were too low for them to be assigned using GC-FTIR. The most striking features of the results, shown in Figure 4-17, are the apparent susceptibility of 1,3,6-TMN and the resistance of 1,2,4-TMN to depletion with increasing distance from the platform. Other more subtle changes in the composition of the isomer mixture are also observed, indicating that although all of the isomers are depleted relative to 1,3,5,7-TeMN with increasing distance from the platform, their removal occurs at different rates.

Comparison of sites S1 and S2 reveals greater depletion of 1,3,6-TMN, 1,6,7-TMN, 1,2,6-TMN, 1,2,5-TMN and 1,4,6-TMN, relative to the other isomers in the mixture. Between S2 and S3, the abundance of these isomers remains approximately constant while particularly 2,3,6-TMN and 1,3,7-TMN and to a lesser extent 1,2,7-TMN are more rapidly depleted. The extent of depletion of 1,2,7-TMN relative to other isomers is accentuated between locations S3 and S4, and similarly for 1,3,5-TMN comparing S4 and S5.

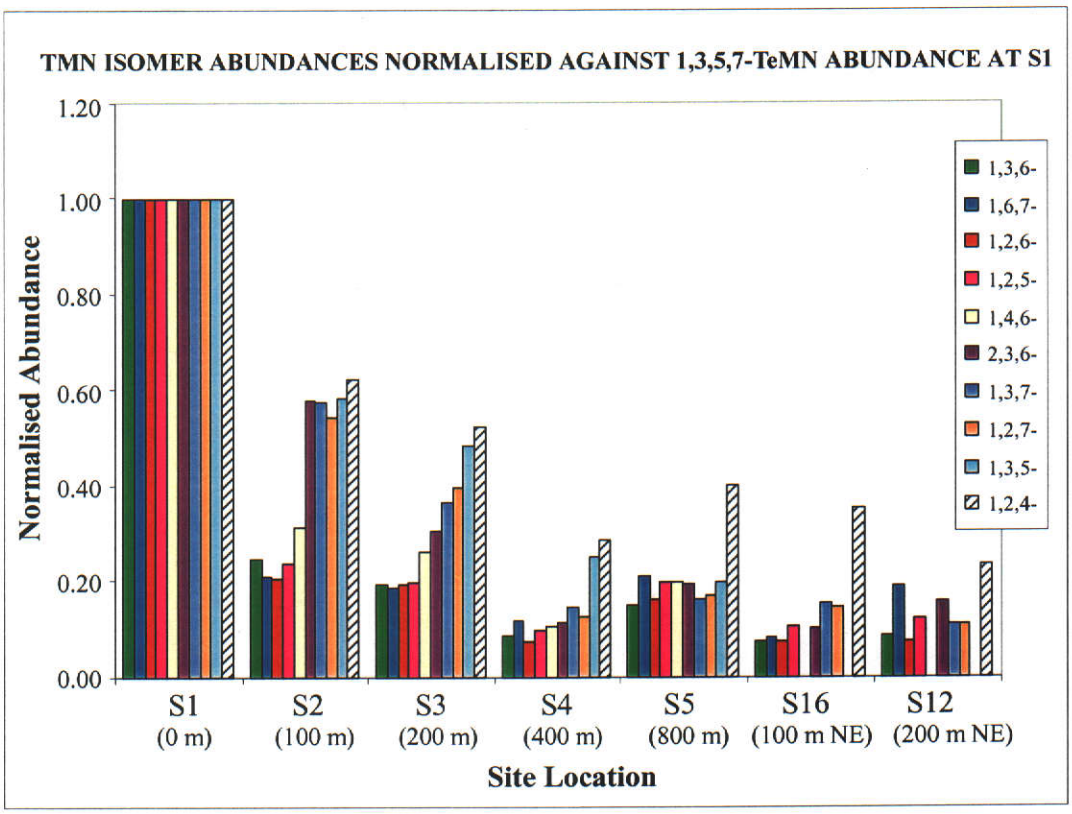

Figure 4-17: A bar chart showing changes in the relative abundance of individual TMN isomers present in sediments collected from the sea-floor adjacent to NRA. Abundances are normalised against that of 1,3,5,7-TeMN and are expressed as a proportion of those measured at site S1, directly under the discharge chute.

Comparison of the composition of the TMN mixtures in sea-floor sediments at the cuttings discharge point (S1) and at a distance of 800 m (S5) reveals they are only differentiated by the relative depletion of 1,3,6-TMN and the increased prominence of 1,2,4-TMN. This is confirmed by comparing the chromatograms obtained from sediments at both of these locations as shown in Figure 4-18. The distribution of TMNs at S5 is consistent with a mixture of relatively undegraded TMNs, similar to those in S1, mixed with more degraded residues containing an increased abundance of the resistant 1,2,4-TMN isomer. This is also consistent with the anomalously high abundance of pristane observed in this sample as discussed earlier.

In summary, the observed order of extent of depletion of the TMNs is: 1,3,6-TMN (most depleted) ~ 1,6,7-TMN ~ 1,2,6-TMN ~ 1,2,5-TMN > 1,4,6-TMN > 2,3,6-TMN > 1,2,7-TMN ~ 1,3,7-TMN > 1,3,5-TMN > 1,2,4-TMN (least depleted).

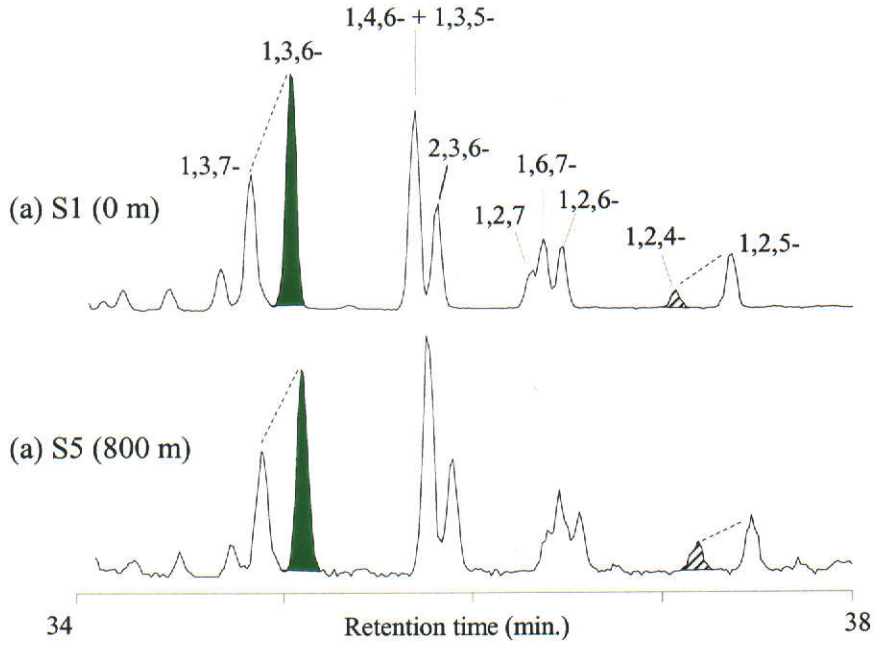

Figure 4-18: Mass chromatograms (m/z 170) showing the TMNs present in sediments collected from (a) directly under and (b) 800 m away from the cuttings chute in the direction of the prevailing current. Peaks are identified by the positions of the methyl substituents on the naphthalene nucleus.

4.9.3 Tetramethylnaphthalenes

The change in abundance of the individual TeMNs between the seven sea-floor locations is shown in Figure 4-19. In general, the depletion of these compounds is much less advanced than for the TMNs, with most of the isomers persisting at relative abundances of greater than 50% in the sediments exhibiting the most biodegraded hydrocarbon signature.

Although the relative persistence of the TeMNs limits the interpretation of these results, several features are noteworthy, the most striking of which is the susceptibility of 1,3,6,7-TeMN, 1,2,5,6-TeMN and 1,2,6,7-TeMN to depletion. Conversely 1,2,3,7-TeMN, 2,3,6,7-TeMN and 1,3,5,7-TeMN are the most resistant of the isomers, with the remaining six isomers exhibiting a susceptibility intermediate these two groupings.

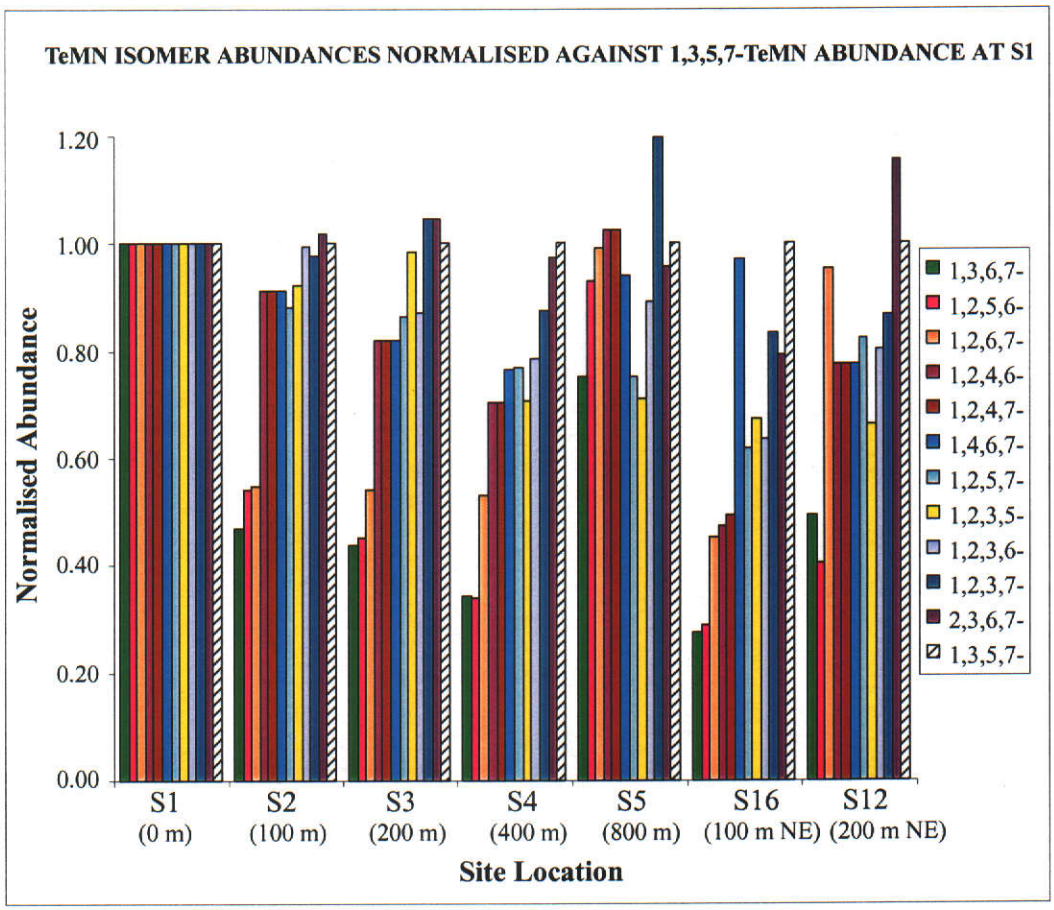

Figure 4-19: A bar chart showing changes in the relative abundances of individual TeMN isomers present in sediments collected from the sea-floor adjacent to NRA. Abundances are normalised against that of 1,3,5,7-TeMN and are expressed as a proportion of those measured at site S1, directly under the discharge chute.

From closer inspection of the results from locations S5 and S12, it appears that the abundance of 1,2,3,7-TeMN and 2,3,6,7-TeMN increases relative to 1,3,5,7-TeMN. At first glance, this might suggest that 1,3,5,7-TeMN is an inferior choice as a conservative marker for biodegradation in preference to either 2,3,6,7-TeMN or 1,2,3,7-TeMN. Inspection of the chromatograms shown in Figure 4-16, however, reveals that the abundance of both of these alternatives is much lower and the associated error in measuring the peak area is greater than for 1,3,5,7-TeMN. For sediments from location S12 in particular, the abundances of many of the TeMN isomers are close to the detection limit, and it is to this that the unexpected increases in relative abundance are attributed.

The unusual results for 1,2,3,7-TeMN at location S5 might also be due to the low abundance of this compound. Less easily dismissed, however, is the poor fit at this

location to the trend of isomer depletion observed at the four locations closer to the platform. Based on this trend, one would expect the location of S5 (800 m NW) to be intermediate between S1 and S2 (100 m NW). The most likely explanation for this observation is that the hydrocarbons at this location comprise a mixture of residues of the drilling fluid biodegraded to different extents. Here the biodegradation signature in the TeMNs is masked somewhat by the presence of a relatively unaltered distribution of TeMNs from less degraded fluid.

Evidence supporting this explanation may be found by reconsidering the TMNs at this location, where upon close scrutiny of Figure 4-11, it appears that there is a perceptibly larger than expected total TMN abundance. Furthermore, the close resemblance between the relative abundance of isomers at S1 and S5 shown in Figures 4-17 and 4-18 indicates that the effect on the biodegradation signature in the TMNs may also have been diminished by mixing with a proportion of less degraded material.

In summary, based on isomer abundances measured at the four locations closest to the platform (i.e. S1 to S4), the observed order of extent of depletion of the TeMNs is: 1,3,6,7-TeMN (most depleted) > 1,2,5,6,-TeMN > 1,2,6,7-TeMN >> 1,2,4,6-TeMN ~ 1,2,4,7-TMN ~ 1,4,6,7-TeMN ~ 1,2,5,7-TeMN ~ 1,2,3,5-TeMN ~ 1,2,3,6-TeMN > 1,2,3,7-TeMN ~ 2,3,6,7-TeMN ~ 1,3,5,7-TeMN (least depleted).

4.9.4 Summary of polymethylnaphthalene depletion

The order of susceptibility to biodegradation, established for this sample set, is summarised below, where the numbers refer to the position of methyl substituents on the naphthalene nucleus. It should be noted that although not apparent from their nomenclature, 1,2,5-TMN, 1,2,5,7-TeMN, 1,2,4,7-TeMN and 1,2,3,5-TeMN contain methyl substituents on carbon atoms 1 and 6 of the naphthalene nucleus. From these relationships, it is evident that polymethylnaphthalenes with a 1,6-dimethyl substitution pattern (shown in bold) are more susceptible to biodegradation than other isomers that lack this feature.

Most susceptible Least susceptible

DMNs

1,6 ~ 2,7 > 2,6 >> 1,3 ~ 1,4 ~ 1,2 ~ 1,7 >>**1,5** >> 2,3

TMNs

1,3,6 ~ **1,6,7** ~ **1,2,6** ~ **1,2,5** > **1,4,6** > 2,3,6 > 1,2,7 ~ 1,3,7 > 1,3,5 > 1,2,4

TeMNs

1,3,6,7 > **1,2,5,6** > **1,2,6,7** >> **1,2,4,6** ~ **1,2,4,7** ~ **1,4,6,7** ~ **1,2,5,7** ~ **1,2,3,5** ~ **1,2,3,6** > 1,2,3,7 ~2,3,6,7 ~ 1,3,5,7

4.10 Subsequent sampling of the sea-floor

After the initial survey in 1991, sediment samples were collected on several occasions to follow the weathering of the drilling fluid hydrocarbons on the sea-floor. A particular objective of these studies was to clarify the correlation between the extent of biodegradation and distance from the platform. Financial and logistical constraints limited the extent and frequency of the sampling events to two sites at irregular intervals. One was located within the inferred transition zone or fringe between contaminated and uncontaminated sediments (800 m NW from the cuttings chute) and the other within the cuttings pile directly under the cuttings chute.

4.10.1 Sediments from the transition zone

Sediment was recovered from the sea-floor within close proximity of the 800 m NW site (i.e. within 10 m) on three occasions: in 1992, 1993 and 1997. On each occasion, the samples were removed from a single grab sample. The TPH concentrations obtained from these are compared with those from the 1991 survey in Table 4-4.

Table 4-4: TPH concentrations measured in sediments collected from the sea-floor 800 m NW from the NRA platform collected on four separate occasions.

Sampling date	TPH Concentration ($mg\ kg^{-1}$, dry weight)
August 1991	37
December 1992	15
October 1993	9.0
August 1997	<0.010

From these results, it is apparent that during the first two years, concentrations decreased with an approximate half-life of one year. The attenuation of hydrocarbons was more rapid during the four-year period between October 1993 and August 1997, when the concentration did not exceed the limit of detection (0.010 mg kg^{-1}). Furthermore, analysis of sediment cores obtained from the samples collected in 1992 and 1993 revealed that the hydrocarbons were confined to the uppermost 5 cm of the sediment sample.

Studies of the oceanography of the NWS (Steedman Science and Engineering, 1993) indicate that the passage of cyclones and the action of long period internal waves greatly influences sediment and cuttings pile redistribution on the NWS. As discussed earlier, above-background trace metal concentrations and depressed median sediment grain size between 1600 m and 3000 m NW from the platform and 200 to 400 m NE, provides evidence that redistribution of the NRA cuttings pile may have occurred. Furthermore, the cuttings pile from drilling operations at the nearby Lynx-1A exploration well (see Figure 4-1) was completely dispersed in a 12 month period (Oliver and Fisher, 1999).

The observed decrease in hydrocarbon concentration with time may therefore be due in part to dilution by uncontaminated sea-floor sediment and redistribution of the contaminated cuttings on the sea-floor. Samples collected in 1991, 1992 and 1993, however, also displayed an increasingly weathered signature in the chromatogram obtained from the TPH fraction, indicating that microbial biodegradation was also probably implicated.

4.10.2 Sediment from within the cuttings pile

Two grab-samples were collected from the cuttings pile in October 1994. An acrylic tube was used to remove a 10 cm core from the first sample (Grab#1). This core was subsequently divided into 1 cm intervals prior to extraction and analysis. The other grab sample (Grab#2) was homogenised as in the 1991 study, and the hydrocarbon concentrations determined in the usual manner.

Total petroleum hydrocarbon concentrations from all sub-samples removed from the two grabs are shown in Table 4-5. It is apparent from the concentrations determined for the depth intervals from Grab#1 that sediments greater than 6 cm below the surface of the cuttings pile contain significantly higher concentrations of hydrocarbons than the overlying 6 cm of sediment. Furthermore, the lowest concentrations reside in the uppermost 4 cm of the core.

The average hydrocarbon concentration of the 10 cm sediment core, calculated from the sediment dry weight and concentration of each interval, is also shown in Table 4-5. This calculated value compares closely with that measured in the homogenised sediment sampled from Grab#2, indicating that the homogenised sample accurately represents the hydrocarbon content of the grab sample. Interestingly, the concentrations in both the sediment core and homogenate are lower than those measured in (homogenised) sediments collected from the same site in the initial 1991 survey.

Table 4-5: Concentrations (mg kg^{-1}, dry weight) of total petroleum hydrocarbons extracted from the NRA sea-floor cuttings pile. Sediments were collected in 1994 from various depths directly under the cuttings chute at the NRA offshore platform. The relative abundances of the total of the resolved peaks and the UCM from the total ion chromatograms obtained from these (refer to Fig. 4-20) are also shown.

Depth Below Cuttings Pile Surface (interval in cm)	TPH Concentration (mg kg^{-1}, dry weight)	Resolved / UCM	Biodegradation
0-1	3500	0.11	Most Biodegraded
1-2	6500	0.09	
2-3	5700	0.08	
3-4	8500	0.17	
4-5	24000	0.25	Intermediate
5-6	41000	0.36	
6-7	110000	0.69	Least Biodegraded
7-8	170000	0.71	
8-9	120000	0.69	
9-10	100000	0.68	
Average Grab #1 (0-10 cm)	55000	n.a.	Mixed
Homogenised Grab #2 (0-10 cm)	51000	0.68	
S1 (0-10 cm) [1991]	75000	0.85	

Total ion chromatograms obtained from each of the core depth intervals and the homogenised grab sample are shown in Figure 4-20, revealing that the hydrocarbons in the upper 5 cm of sediment contain a more biodegraded signature than those in the deeper sediments. The extent of biodegradation is quantified by the ratio of total resolved peaks to the UCM, shown in Table 4-5. From this, one is lead to conclude that aerobic biodegradation is the principal mechanism by which the hydrocarbons are removed from the upper section of the cuttings pile, and this may account for the decrease in concentration at depths 0 to 10 cm below the sea-floor surface at this site (S1, 0m) between 1991 and 1994. This is in broad agreement with the observations of Petersen, Kruse and Jensen (1991), who carried out laboratory microcosm experiments using sea-floor sediment cores contaminated with a LTOBM. In these experiments, microbial degradation was identified as having a vastly more profound effect on removal of the hydrocarbons from the sediment than dissolution in water. Biodegradation of the LTOBM was, however, restricted to the uppermost 1 cm portion of the sediment core. At greater depths in the sediment core, no diminution of the TPH concentration occurred as the redox potential of the system decreased sharply.

Here, it is evident that the composite sample collected from the cuttings pile contained a mixture of the same petroleum fluid biodegraded to different extents, where the relatively unbiodegraded hydrocarbons dominate the mixture. Conversely, in the transition zone samples collected from the 800 m NW location, all of the hydrocarbons were contained within 5 cm of the sea-floor surface where biodegradation is likely to proceed more rapidly due to greater access to electron acceptors such as oxygen or sulphate. All grab samples collected from the cuttings pile are therefore likely to contain relatively well-preserved hydrocarbons associated with deeper sediments. As distance from the cuttings chute increases, the depth of the cuttings layer decreases, thereby exposing a greater proportion of hydrocarbons to near-surface sediment conditions amenable to more rapid biodegradation. The sediments collected in the grab therefore contain an increasing proportion of weathered to preserved hydrocarbons, resulting in the increasingly weathered hydrocarbon signature with increasing distance from the cuttings chute as observed during the initial survey in 1991.

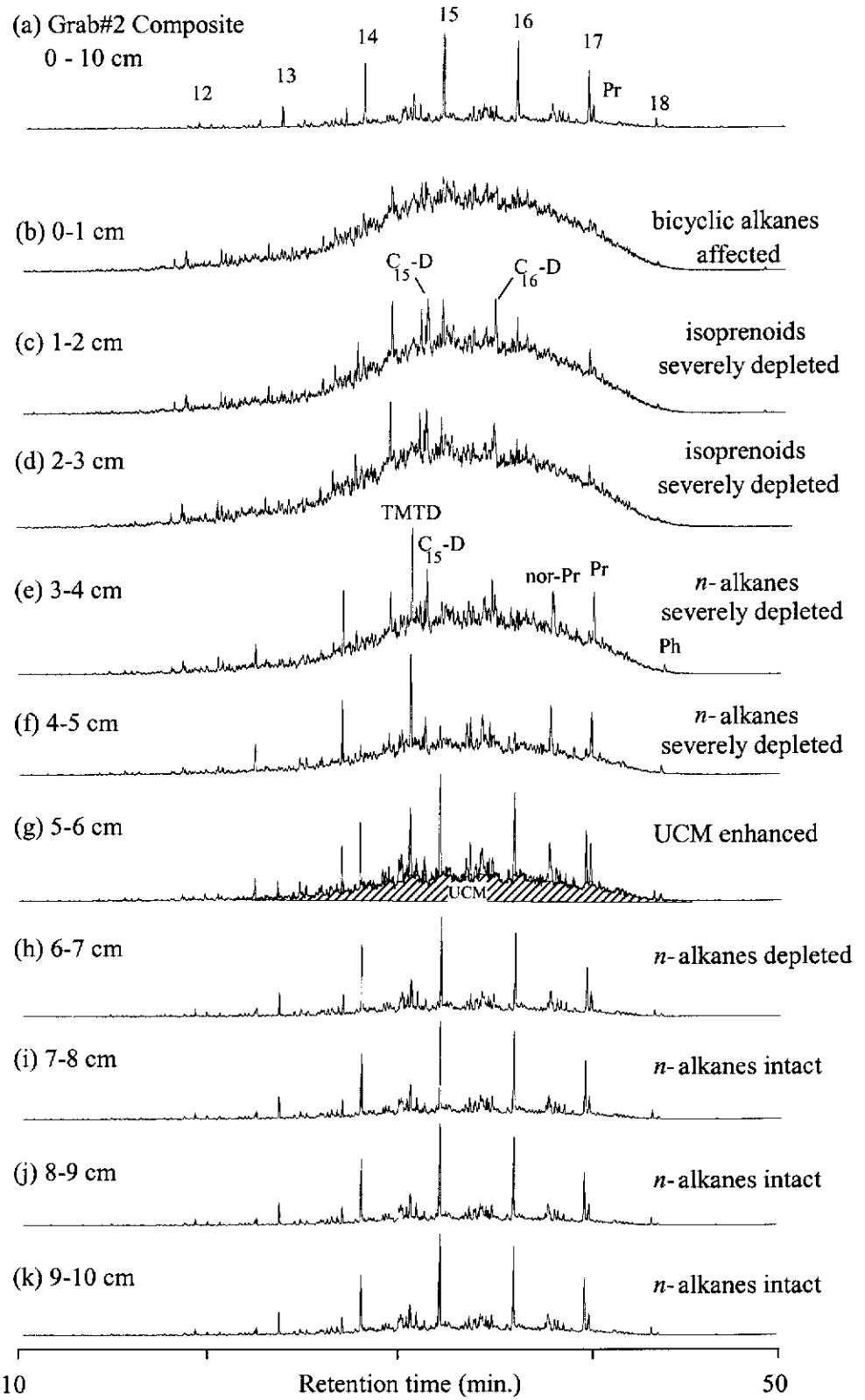

Figure 4-20: Total ion chromatograms of TPH fractions obtained from (a) an homogenised composite sediment sample collected from the sea-floor cuttings pile at NRA in 1994 and from the following depth intervals below the sea-floor: 0-1 cm, 1-2 cm, 2-3 cm, 3-4 cm, 4-5 cm, 5-6 cm, 6-7 cm, 7-8 cm, 8-9 cm, 9-10 cm [(b) – (k)].

In order to further study the biodegradation of individual compounds, the TPH fractions were separated into saturated and aromatic hydrocarbon fractions and each fraction was analysed using GC-MS.

Saturated hydrocarbons

The various ratios of saturated hydrocarbons measured in the core intervals are compared with those from the homogenised (0-10 cm) sample S1 (0 m) in 1991 in Table 4-6. This comparison reveals that although the hydrocarbons residing deeper in the sediment core are relatively well preserved, they still display a more biodegraded signature than those collected in the initial survey, indicating clearly that biodegradation has occurred in the interim.

Table 4-6: Relative abundances of the total of resolved peaks, the unresolved complex mixture (UCM), *n*-tetradecane (*n*-C_{14}), *n*-pentadecane (*n*-C_{15}), *n*-heptadecane (*n*-C_{17}), trimethyltridecane (TMTD), pristane (Pr) and 8β(H)-homodrimane (C_{16}-D). Peak areas were obtained from the total ion chromatogram from GC-MS analysis of saturated hydrocarbons extracted from the cuttings pile at site S1 (0 m) adjacent to NRA.

Depth Below Cuttings Pile Surface (cm)	Peak Area Ratio						
	Resolved / UCM	*n*-C_{14} / *n*-C_{17}	*n*-C_{15} / TMTD	*n*-C_{17} / Pr	*n*-C_{16} / C_{16}-D	TMTD / C_{16}-D	Pr / C_{16}-D
9-10	0.48	1.3	4.0	2.6	150	44	33
8-9	0.49	1.3	4.0	2.6	150	44	33
7-8	0.50	1.2	3.9	2.6	150	43	37
6-7	0.48	1.2	2.8	2.3	120	51	36
5-6	0.26	1.2	1.2	1.2	65	53	31
4-5	0.20	1.2	0.22	0.29	11	44	25
3-4	0.17	n.d.	0.21	0.26	5.2	16	14
2-3	0.11	n.d.	n.d.	1.1	3.4	0	2.7
1-2	0.10	n.d.	n.d.	1.2	3.3	0	2.7
0-1	0.13	n.d.	n.d.	n.d.	n.d.	0	n.d.
S1 (0-10 cm)	1.2	1.4	4.6	3.0	280	n.d.	50

Within the lower 3 cm of the core, all of the abundance ratios in Table 4-6 are similar, reflecting the similarity in petroleum composition. At 6 to 7 cm below the top of the cuttings pile, there is a perceptible decrease in the abundance of the *n*-alkanes relative to the isoprenoids TMTD and pristane and the bicyclic alkane C_{16}-D. The *n*-C_{15}/TMTD, *n*-C_{17}/Pr, and *n*-C_{17}/Pr ratios continue to decrease with decreasing depth below the surface until within 3 cm of the surface. In the upper 3 cm, the decrease in the *n*-C_{16}/C_{16}-D is a more useful indication of the depletion of the *n*-alkanes due to the severe depletion of TMTD and pristane.

The depletion of these isoprenoids precedes the depletion of the *n*-alkanes as indicated by the pronounced decrease in abundance relative to C_{16}-D at 3 to 4 cm below the surface. Within 2 to 3 cm of the surface, pristane is severely depleted, while TMTD is completely removed. None of the alkanes determined here were detected in the uppermost 1 cm of the core. From these observations, it emerges that although the *n*-alkanes are depleted in preference to the isoprenoids, they are not completely removed prior to the partial removal of the isoprenoids. Therefore, the progressive, quasi-stepwise removal of the saturated hydrocarbons according to their molecular structure proposed by Volkman et al. (1984) and Peters and Moldowan (1993), occurs in this environment, where there appears to be considerable overlap between at least the isoprenoids and the *n*-alkanes.

The value of the *n*-C_{14}/*n*-C_{17} ratio for the relatively well-preserved LTOBM between 7 and 10 cm below the cuttings pile surface (1.2 to 1.3) is similar to that measured in the intervals between 4 and 7 cm (1.2). This indicates that the more volatile alkanes are not depleted in preference to those less volatile. In the upper 4 cm, this value is not reported due to severe depletion of these *n*-alkanes. It is apparent from the chromatograms shown in Figure 4-20, however, that there is no discrimination against the lower molecular weight alkanes in these upper intervals where severe biodegradation of the LTOBM is evident.

Comparison of these chromatograms with those from the composite sea-floor collected in 1991 (see Figure 4-8) reveals that the extent of removal of the volatile alkanes from samples S5 (800 m NW) and S12 (400 m NE) is not commensurate

with the extent of biodegradation at these sites. This is also apparent from the relatively low value of the n-C_{14}/n-C_{17} ratio (Table 4-2) measured at S5 (0.39) and S12 (0.25). It is therefore likely that the volatile hydrocarbons have been removed by a different process at these sites.

Table 4-7: Relative abundances of 8β(H)-drimane (C_{15}-D) and its two rearranged analogues (R_1 and R_2), 8β(H)-homodrimane (C_{16}-D), and pristane (Pr) in a sediment core from the cuttings pile at NRA. Peak areas, obtained from m/z =123 mass chromatograms are not corrected for differences in detector response.

Depth Below Cuttings Pile Surface (cm)	Peak Area Ratio					
	$\frac{R_1}{C_{15}\text{-D}}$	$\frac{R_2}{C_{15}\text{-D}}$	$\frac{R_1+R_2}{C_{15}\text{-D}}$	$\frac{R_1}{R_2}$	$\frac{C_{15}\text{-D}}{C_{16}\text{-D}}$	$\frac{R_1+R_2}{C_{16}\text{-D}}$
9-10	0.55	0.35	0.90	1.57	0.70	0.63
8-9	0.55	0.35	0.90	1.57	0.70	0.63
7-8	0.78	0.46	1.24	1.70	0.66	0.82
6-7	0.83	0.58	1.41	1.44	0.67	0.94
5-6	0.87	0.55	1.42	1.58	0.61	0.88
4-5	0.80	0.54	1.34	1.49	0.60	0.80
3-4	0.83	0.43	1.27	1.93	0.62	0.78
2-3	0.79	0.43	1.21	1.84	0.71	0.86
1-2	0.70	0.34	1.04	2.06	0.76	0.79
0-1	0.65	0.40	1.04	1.64	0.60	0.62

This is further illustrated by considering the distribution of the bicyclic alkanes in the cuttings pile core, shown in Table 4-7. In contrast to the series of samples collected at various distances from the platform in 1991, there was little change in relative abundance among the bicyclic alkanes over the depth of the core. Although some variability was observed in all ratios, there was no correlation with proximity to the cuttings pile surface. It is therefore unlikely that in the sea-floor sediments collected in 1991, *in-situ* biodegradation is the sole process by which the preferential depletion of the bicyclic alkanes R_1 and R_2 occurred. Instead, their removal may indicate that the sediments remote from the platform in the so-called transition zone contain

migrant cuttings that have been eroded from the cuttings pile. During transport, the composition of the adhering hydrocarbon mixture may have been altered by dissolution in the sea-water, resulting in the loss of components according to their aqueous solubilities.

Aromatic hydrocarbons: polymethylnaphthalenes

The aromatic hydrocarbons isolated from the cuttings pile core sections were also analysed using GC-MS techniques from which the relative abundances of the polymethylnaphthalenes were determined. The results shown in Figure 4-21, reveal that in the sediments between 6 and 10 cm below the surface of the pile, the proportion of DMNs, TMNs and TeMNs remains constant. In sediments recovered from closer to the surface, the abundance of the TeMNs gradually increases relative to the DMNs and TMNs, indicating their greater resistance to biodegradation. In broad agreement with results of the 1991 survey shown in Figure 4-11, the depletion of the DMNs (5 to 6 cm) occurs deeper in the sediment core than the TMNs (3 to 4 cm). Furthermore, depletion of the TMNs occurs deeper in the core than does the complete removal of the DMNs (1 to 2 cm). In the uppermost 1 cm of the core, only the TeMNs remain.

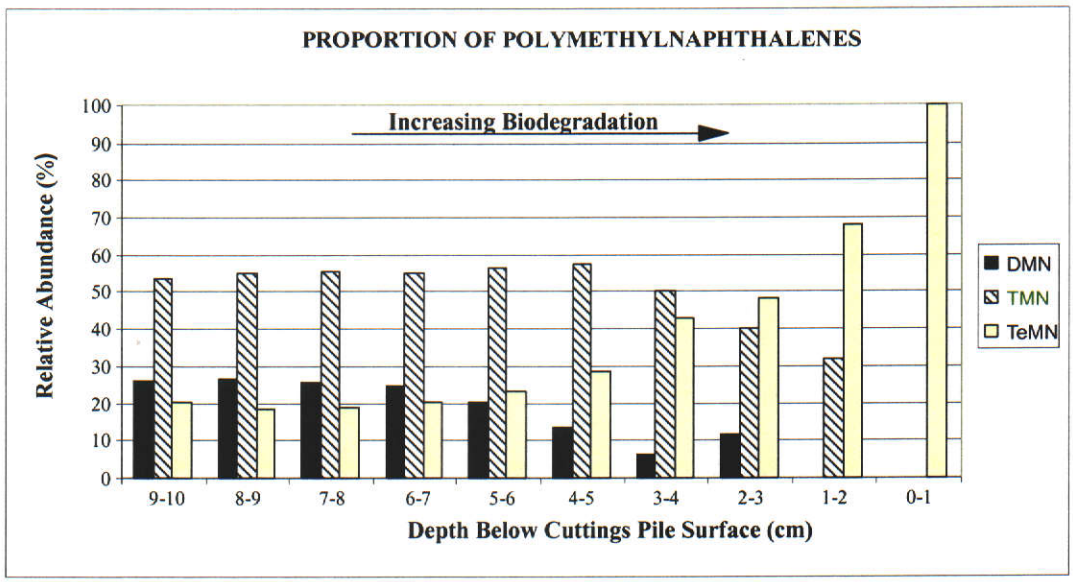

Figure 4-21: Relative abundances of dimethylnaphthalenes (DMNs), trimethylnaphthalenes (TMNs) and tetramethylnaphthalenes (TeMNs) in aromatic hydrocarbon fractions isolated from sediments collected in 1994 from various depths belowthe surface of the NRA sea-floor cuttings pile.

The depletion of individual isomers of each of the polymethylnaphthalenes was also investigated, however the investigation was somewhat superficial since GC-FTIR techniques were not used to discriminate between co-eluting isomers. The results are presented in Figure 4-22 in a similar manner to those obtained from the sediments collected in 1991, using 1,3,5,7-TeMN as conserved internal marker. Here, the hydrocarbons from the sediments 9 to 10 cm below the cuttings pile surface was used as a reference for each of the polymethylnaphthalenes, against which the abundances in sediments closer to the surface were normalised. Where possible, the results for each compound are presented in the same order as for the earlier sea-floor survey. Although the co-eluting isomers complicate the interpretation of these results, it is apparent that the order of depletion of these compounds is similar for both sample sets: in particular, the relative susceptibility to biodegradation of the 1,6-disubstituted polymethylnaphthalenes and which compounds are more resistant.

Comparison of these results with the relative abundances of the total DMNs, TMNs and TeMNs shown in Figure 4-21, reveals that depletion of the 1,6-disubstituted congeners (1,6-DMN, 1,3,6-TMN and 1,3,6,7-TeMN) provides a very sensitive indication of biodegradation in these sediments. For example, although the relative abundance of the total DMNs does not decrease significantly in the sediments deeper than 5 to 6 cm below the sea-floor, the depletion of 1,6-DMN occurs at least one centimetre deeper in the sediment profile.

Aromatic hydrocarbons: phenanthrene and alkylphenanthrenes

A mixture of phenathrene, methylphenanthrene (MP) isomers and dimethylphenanthrene (DMP) isomers was also discernible in the aromatic hydrocarbon fractions isolated from some of the extracts from the depth intervals. These compounds, present in these samples at very low concentrations, were detected only in the sediments from directly under the cuttings chute from the 1991 survey (S1, 0 m). At more remote locations, the lower concentrations of TPH precluded their measurement, thereby preventing the investigation of their susceptibility to biodegradation.

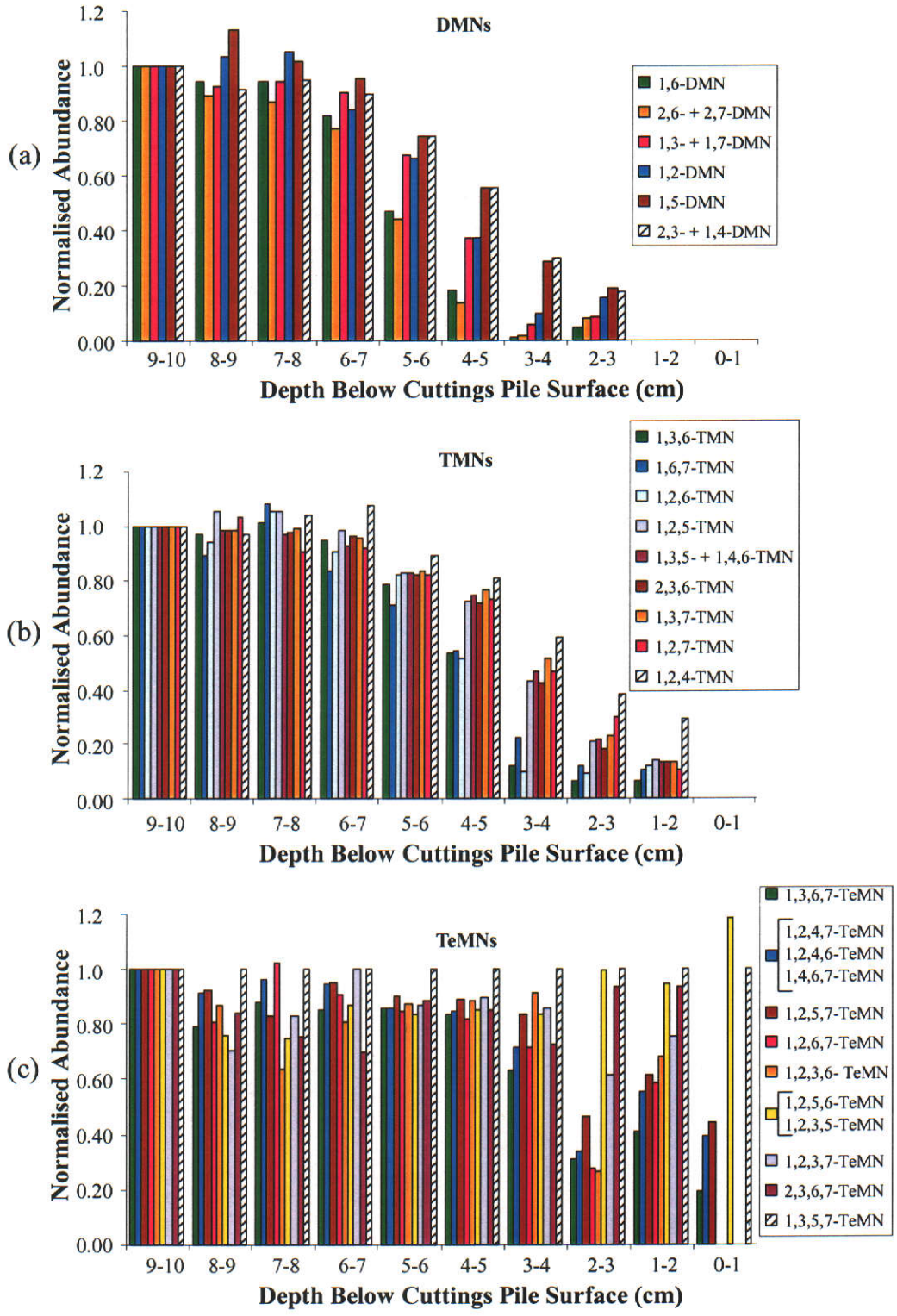

Figure 4-22: Bar charts showing changes in the relative abundances of individual (a) DMN, (b) TMN and (c) TeMN isomers present in a sediment core collected from the sea-floor cuttings pile directly under the NRA cuttings chute. Abundances are normalised against that of 1,3,5,7-TeMN and are expressed as a proportion of those measured at 9–10 cm below the cuttings pile surface.

The relative abundances of the DMPs isolated from the sediment core were broadly similar in all of the aromatic hydrocarbon fractions in which they were detected. Close inspection of the m/z 206 mass chromatograms shown in Figure 4-23, however, reveals that peaks corresponding to 1,7-DMP (Peak 52) and the co-eluting pair 2,6-DMP and 3,5-DMP (Peak 42+43) are significantly diminished relative to other DMP isomers. The low abundance of the DMPs in the hydrocarbon mixture prohibited the application of GC-FTIR techniques to confirm which of the co-eluting isomers was present, however, due to the energetically unfavourable configuration of 3,5-DMP, (Budzinski et al., 1993a) this compound is unlikely to be present in the petroleum from which the LTOBM was refined. One can therefore assign 2,6-DMP to Peak 42 + 43. It is therefore reasonable to assume that 2,6-DMP and 1,7-DMP are preferentially depleted from the DMP mixture.

The abundances of the MPs changed significantly with proximity of the sediment to the surface as illustrated by Figures 4-23 (a) and (b). An approach similar to that described for the alkylnaphthalenes was applied to measure this change in abundance of the MPs. Here, 1,8-DMP was chosen as the compound against which the MPs were normalised, since it is apparently resistant to biodegradation (Figure 4-23), has similar abundance and gas chromatographic retention behaviour to the MPs, and its identification is not confounded by co-elution with other isomers (Garrigues et al., 1987).

It is clear from the results shown in Figure 4-24 and from the chromatograms shown in Figure 4-23, that phenanthrene is more susceptible to biodegradation than any of its mono-methylated and di-methylated homologues. In the interval between 5 cm and 6 cm below the sea-floor surface, the abundance of phenanthrene relative to 1,8-DMP has been reduced to approximately half of that in the least biodegraded hydrocarbon mixture, that is to a similar extent of depletion as 1,6-DMN as shown in Figure 4-22.

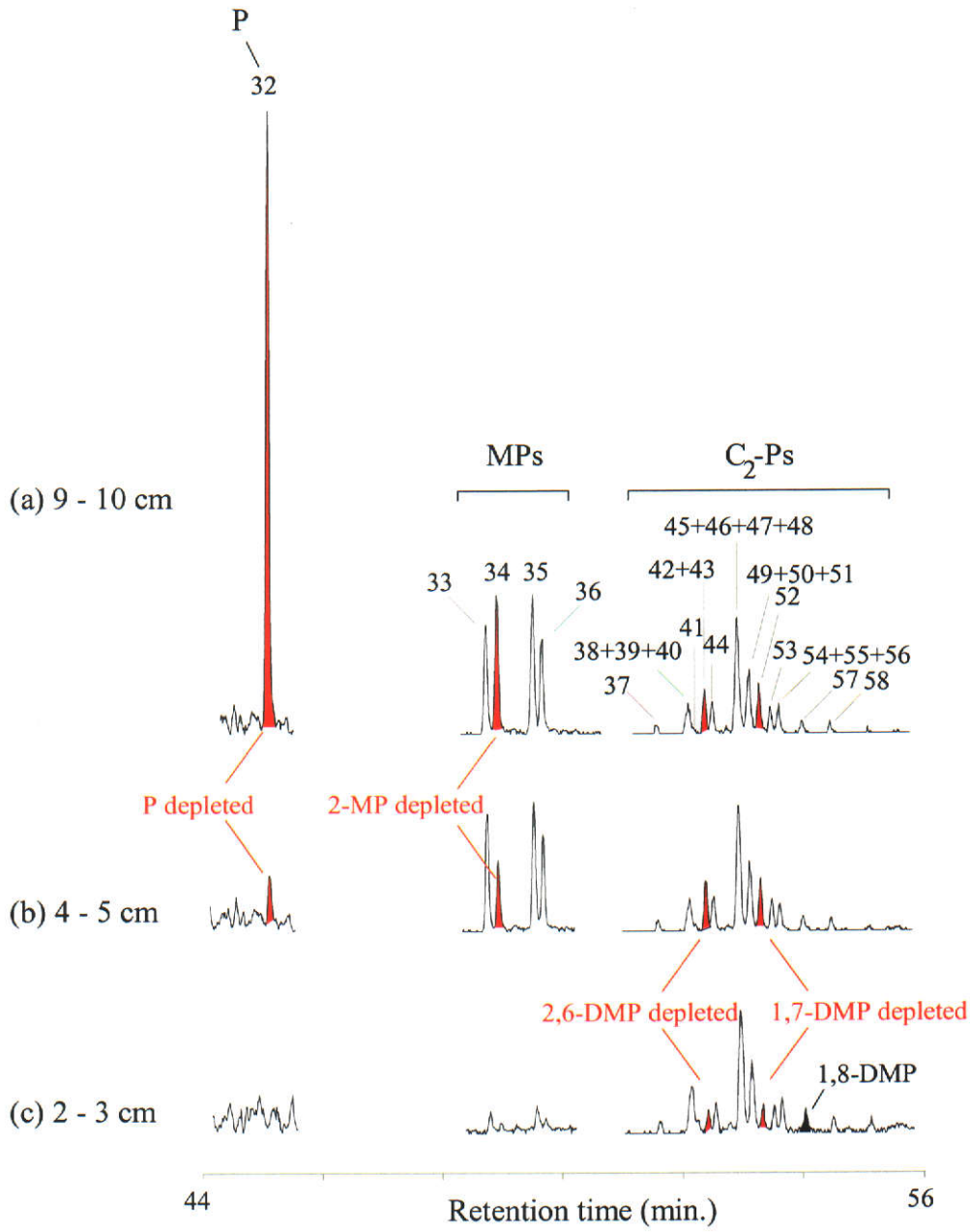

Figure 4-23: Partial mass chromatograms showing changes in the relative abundance of phenanthrene (m/z 178), methylphenanthrenes (m/z 192) and dimethylphenanthrenes (m/z 206) present in a sediment core collected from the sea-floor cuttings pile at the NRA platform. Chromatograms are shown for sediments (a) 9-10 cm, (b) 4-5 cm and (c) 2-3 cm below the surface of the cuttings pile. Peak identifications are as follows: (32) P, (33) 3-MP; (34) 2-MP; (35) 9-MP; (36) 1-MP; (37) 3-EP; (38) 3,6-DMP; (39) 9-EP; (40) 2-EP; (41) 1-EP; (42) 3,5-DMP; (43) 2,6-DMP; (44) 2,7-DMP; (45) 3,9-DMP; (46) 3,10-DMP; (47) 2,10-DMP; (48) 1,3-DMP; (49) 1,6-DMP; (50) 2,9-DMP; (51) 2,5-DMP; (52) 1,7-DMP; (53) 2,3-DMP; (54) 4,9DMP; (55) 1,9-DMP; (56) 4,10-DMP; (57) 1,8-DMP; (58) 1,2-DMP.

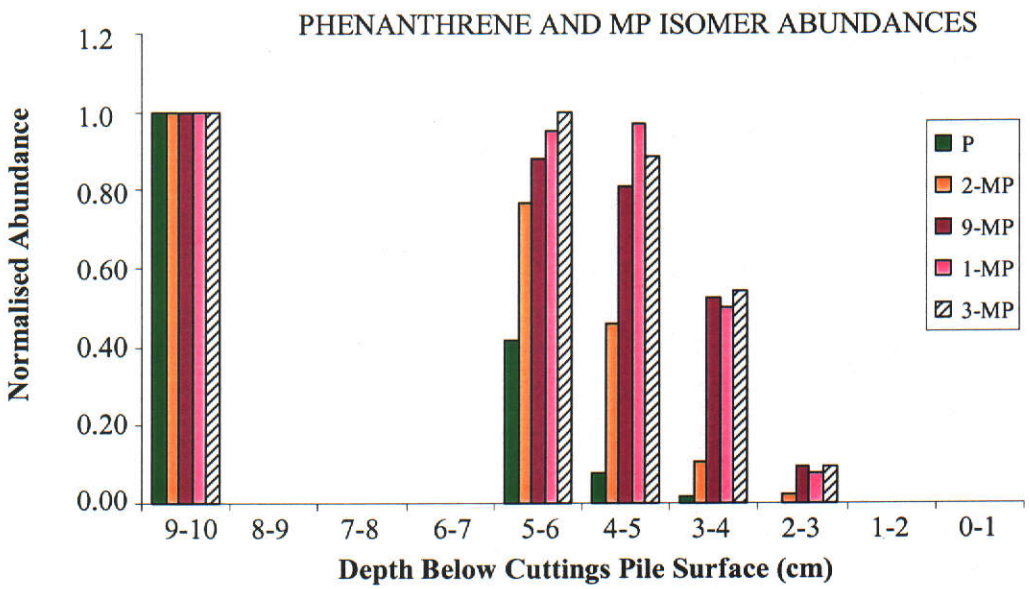

Figure 4-24: A bar chart showing changes in the relative abundances of phenanthrene and methylphenanthrene isomers present in a sediment core collected from the sea-floor cuttings pile directly under the NRA cuttings chute. Abundances are normalised against that of 1,8-DMP and are expressed as a proportion of those measured at 9–10 cm below the cuttings pile surface.

Among the methylphenanthrenes, 2-MP is depleted to a greater extent than the other isomers. Although the evidence is somewhat unconvincing, 9-MP appears to be the next most susceptible to biodegradation while differences in the extent of biodegradation of the 1-MP and 3-MP are indiscernible. Comparison with the results from the polymethylnaphthalenes reveals that the extent of biodegradation of 2-MP resembles that of 1,3,6-TMN at a given depth below the surface of the cuttings pile.

These observations are consistent with the results from in-vitro biodegradation of 2-MP using a marine bacterium isolated from coastal sediments (Gilewicz et al., 1997). In this work, the bacterium tentatively identified as a *Sphingomonas* sp. was shown to utilise 2-MP, 9-MP and phenanthrene separately as the sole source of carbon under aerobic conditions. Interestingly, this bacterium strain failed to exhibit growth or oxygen consumption using *n*-hexadecane as an energy source.

Although no attempt has been made in the present study to enumerate or identify micro-organisms in the sediments, it is reasonable to assume that a consortium rather than a single strain of bacteria was responsible for the biodegradation of the LTOBM components. Reviewing the results shown in Table 4-6, *n*-hexadecane (*n*-C_{16}) is depleted to approximately 40 to 50% of its abundance at 5 to 6 cm below the sea-floor: approximately to the same extent to which phenanthrene has been biodegraded. The inability of *Sphingomonas* sp. to metabolise *n*-hexadecane (albeit separately) under the same conditions under which both phenanthrene and 2-MP are metabolised supports the above.

4.11 Conclusions

A pile of discharged cuttings formed on the sea-floor during drilling operations at NRA. These cuttings contained a mixture of hydrocarbons consistent with the kerosene-like LTOBM used to facilitate drilling.

The TPH concentration of the sea-floor sediments decreased rapidly with increasing distance from the cuttings chute. Sediment collected from the cuttings pile contained 75000 mg kg^{-1} of a mixture consisting of biodegraded LTOBM residues, adsorbed onto near-surface sediments, and relatively well-preserved hydrocarbons adsorbed onto deeper sediments that dominate the mixture. In sediments 800 m from the platform, the hydrocarbons (37 mg kg^{-1}) were contained within 5 cm of the sediment surface. At locations intermediate between these two environments, the depth of the cuttings layer decreased, thereby exposing a greater proportion of hydrocarbons to near-surface sediment conditions amenable to aerobic biodegradation.

Changes in the saturated and aromatic hydrocarbon distributions with increasing severity of biodegradation were studied. The restricted molecular weight range of the hydrocarbons from which the LTOBM was formulated precluded the use of many of the conventional indicators based on changes in chemical composition of the saturated hydrocarbons to assess the extent of biodegradation. The successive depletion of the *n*-alkanes and pristane relative to the various isomers of bicyclic alkanes was observed, however.

The LTOBM residues also contained significant concentrations of DMNs, TMNs and TeMNs. Depletion occurred to different extents between groups of these compounds, with a direct relationship generally observed between the susceptibility to biodegradation and the extent of substitution of the aromatic nucleus (i.e. DMNs > TMNs > TeMNs), however, some overlap occurs between these groups. Detailed analysis of these compounds using the complementary techniques of GC-MS and GC-FTIR enabled the unambiguous determination of the abundance of each of the isomers present in the petroleum. From this, the individual compounds were arranged according to their susceptibility to biodegradation. It was evident from this that, without exception, polymethylnaphthalenes with a 1,6-dimethyl substitution pattern are more susceptible to biodegradation than other isomers that lack this feature. An expalantion for this effect will be provided later in this thesis (see Section 6.4).

The susceptibility to biodegradation of phenanthrene, the MPs and DMPs was also investigated, albeit less rigorously. Of these compounds, phenanthrene was the most susceptible, while 2-MP was the most susceptible amongst the MPs. Although a smaller change in relative abundances between the DMP isomers was observed, 1,7-DMP and 2,6-DMP are apparently the most susceptible to biodegradation.

The observed differences in susceptibility to biodegradation amongst the alkylnaphthalene and alkylphenanthrene isomers are potentially useful as indicators of biodegradation. This will be discussed further in detail in Chapter 6.

CHAPTER 5

5 Biodegradation of petroleum in sediments in a mangrove swamp following a discharge of oil.

5.1 Abstract

Following the release of petroleum from a buried pipe into a tropical mangrove swamp in North Western Australia, a monitoring program was implemented involving the determination of petroleum hydrocarbon concentrations in sediment samples. Chemical analysis revealed that at least two separate releases of light petroleum had occurred, affecting two different areas in the swamp. Since no bioremediation was attempted in either area, the natural attenuation of the two different petroleum materials was monitored by detailed chemical analysis of the sediment samples collected on nine occasions over a three-year period. Analysis of the saturated and aromatic hydrocarbon components of each petroleum revealed that both hydrocarbon fractions exhibited an increasingly biodegraded profile with increased residence time in the sediments. As a result, the depletion of the alkylnaphthalenes and alkylphenanthrenes by biodegradation under the conditions in the mangrove swamp could be related to that observed for the saturated hydrocarbons for which the susceptibility to biodegradation is better understood.

The relative susceptibilities of saturated and aromatic hydrocarbons were determined from this study, revealing that in broad terms, the more highly substituted polymethylnaphthalenes and alkylphenanthrenes in the samples are more resistant to biodegradation. The depletion of each of the individual alkylnaphthalenes and alkylphenanthrenes with increasing biodegradation was also determined, enabling an order of susceptibility to biodegradation to be established. From this order, it is apparent that polymethylnaphthalenes with a 1,6-dimethyl substitution pattern are more susceptible to micobial attack than are the other isomers in this environmental setting. Similarly, the rate of depletion of the MPs and DMPs appears to be

dependent on the position of the methyl substituent on the aromatic nucleus, however this relationship is not as striking as for the 1,6-dimethyl substituted naphthalenes.

5.2 Introduction

The Woodside Onshore Treatment Plant is situated on the Burrup Peninsula, within the Dampier Archipelago in North-Western Australia as shown in Figure 5-1. The tropical climate experienced in the Dampier Archipelago and the presence of several protected embayments and tidal creeks supports the existence of several species of mangroves, described in detail elsewhere (Woodside Offshore Petroleum Pty Ltd, 1990).

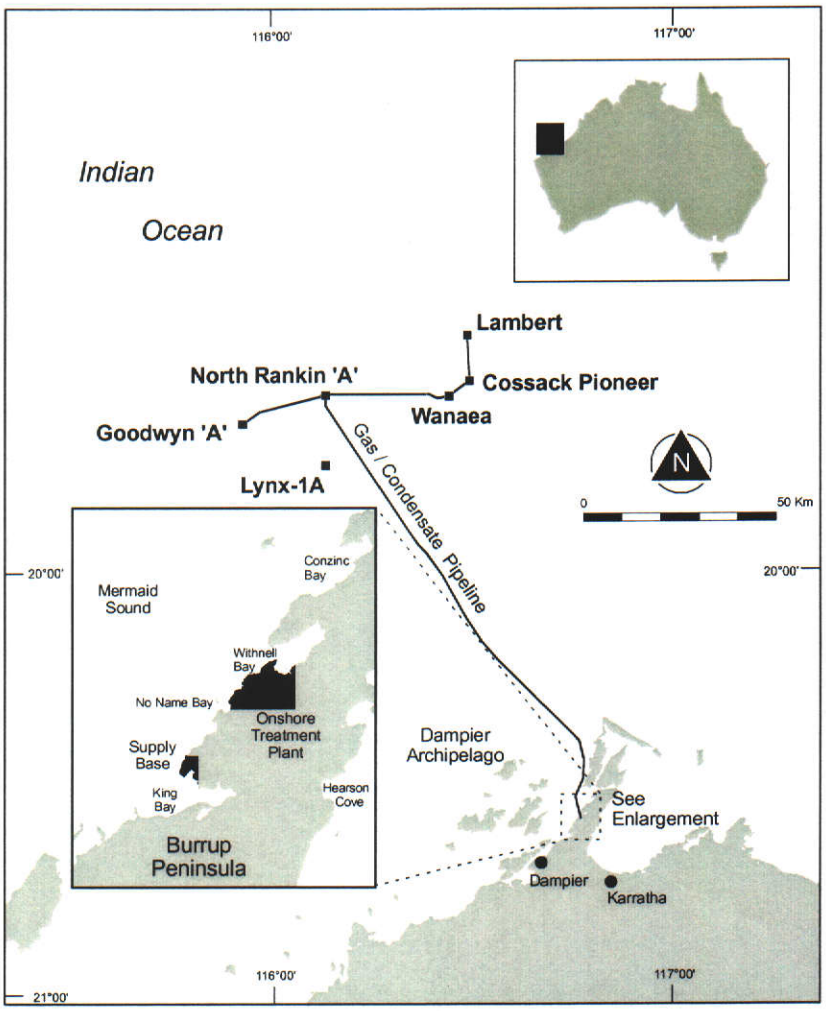

Figure 5-1: A map showing the location of the offshore and onshore production facilities on the North West Shelf and Burrup Peninsula in North-Western Australia.

In August 1987, the obvious deterioration of approximately 70 mangrove trees lead to the discovery of liquid hydrocarbon seeps into the North East Creek (NE Creek), a small tidal creek east of the Onshore Treatment Plant (shown in the map of the Withnell Bay study area presented in Figure 5-2). Subsequent thorough inspections of the northern and eastern boundaries of the Plant resulted in the discovery of similar seeps at the Slug Catcher Vent (SCV) Beach.

Both of these sites are typical of mangrove habitats (Duke, Ellison and Burns, 1998), where the sediments are anaerobic and highly reduced, evidenced by the presence of hydrogen sulphide and necessitating the development of above-ground air-breathing roots. Both are also greatly affected by the local tidal fluctuations of several metres, causing cyclical periods of inundation by sea-water and exposure. Immediately following the discovery of the leaked petroleum, the sediments appeared to be oil-wet with pools of oil evident at the surface.

Pressure testing of the oil-contaminated water (OCW) system revealed several leaking joints between the cement pipes that form this system, in the vicinity of the NE Creek hydrocarbon seeps. This system, consisting of cement pipes, holding basins, and other infrastructure, contains water associated with the production and subsequent treatment of the gas and condensate from the offshore production facilities shown in Figure 5-1. Associated petroleum from these facilities is also contained in this system as both a dissolved and a free floating phase, the latter of which is physically removed through a series of interceptor units and holding basins prior to legal discharge of the water into the ocean. Although the characteristics of the petroleum contained in the OCW system is therefore likely to change over time reflecting the various operations of the production facilities, condensate from the North Rankin 'A' platform is likely to be the major petroleum component of the OCW system.

Significant leaks in the OCW system were also discovered near the SCV Beach seeps at the junction of the cement pipes, a holding basin, and its associated corrugated plate interceptor unit. Inspection of the below-ground contour plans of these areas (Woodside Offshore Petroleum Pty Ltd, 1990) indicated that hydrocarbons from

these discharges from the OCW system would be expected to flow into the vicinity of the seeps and were therefore the probable sources of the hydrocarbon seeps. Despite immediate remedial action on discovery of the leaking OCW system, analysis of ground water samples in close proximity to the pollution sources at NE Creek indicated that hydrocarbons had permeated the ground water table to an extent such that the contamination episode was likely to persist for several years.

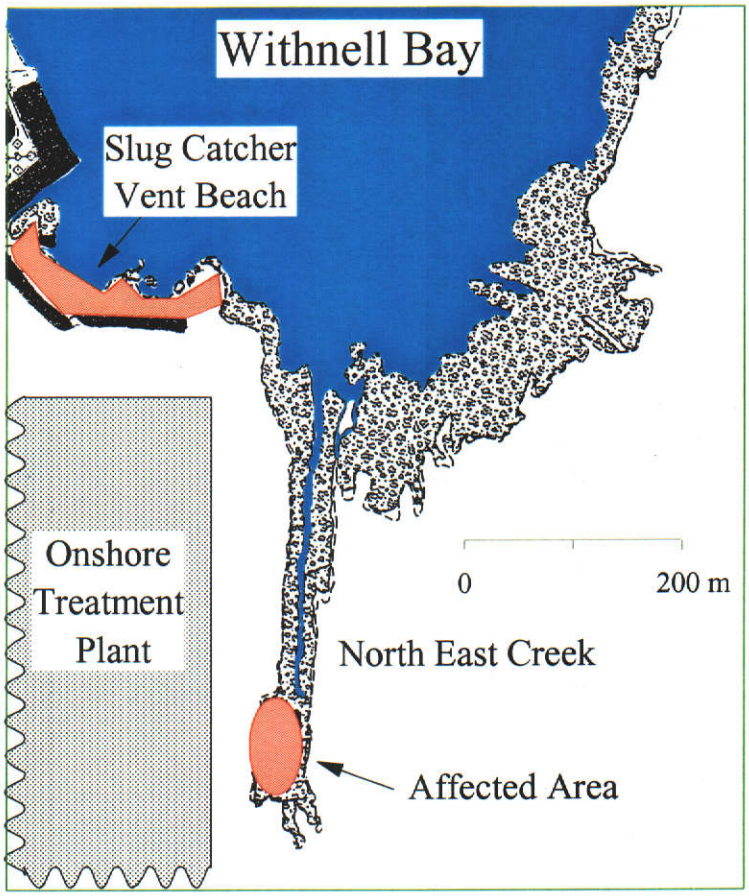

Figure 5-2: A detailed section of the map shown in Figure 5-1, showing the location of areas in the vicinity of the Onshore Treatment Plant at which hydrocarbon seeps were detected.

A program designed to monitor the extent of the hydrocarbon pollution of the NE Creek and SCV Beach was implemented in the Withnell Bay area in September 1987. This program comprised mangrove monitoring, where several physical characteristics of the mangrove trees were studied, and chemical analysis of sediment samples where the quantity and composition of the petroleum was established. From this, it was estimated that greater than 50 tonnes of condensate was released, affecting a total area of approximately 5 hectares (Duke, Ellison and Burns, 1998).

Here, the sediment samples collected from the mangrove swamp provided partially biodegraded petroleum samples with which to thoroughly investigate the relative susceptibilities to biodegradation of the hydrocarbons in this environment, and to compare the relative susceptibilities of the aromatic hydrocarbons with those determined earlier (Chapter 4) in the sea-floor sediments.

5.3 Sampling strategy and technique

Sediment samples were collected from several sites around Withnell Bay on 11 occasions during a three-year period from September 1987 to September 1990. The first five sampling events were conducted at approximately monthly intervals between September 1987 and March 1988. During this period, sediments were collected from 30 sites that encompassed the areas most likely to be contaminated by the hydrocarbons from the OCW system as well as some locations more distant from the pollution sources. Generally, samples comprised the upper two centimetres of sediment, although periodically the sub-surface was also sampled to a depth of approximately 10 to 15 cm.

Having established the extent of the area of hydrocarbon contamination during the first six months of the study, subsequent sampling trips were less frequent and targeted only the more heavily contaminated areas. These surveys were conducted at approximately quarterly intervals (sampling trips 6, 7 and 8) and then biannually (9,10 and 11).

5.3.1 Sample treatment

All sediment samples were subjected to chemical analysis involving a combination of solvent extraction followed by gravimetric and gas chromatographic analysis to determine the total petroleum hydrocarbon concentrations, and the composition of the hydrocarbon extracts in a similar manner to that described in the preceding chapter (Chapter 4) for the sea-floor sediments. This procedure entailed freezing the sediment samples in sealed glass jars until analysis to protect the hydrocarbons from further alteration due to evaporation and biodegradation after sampling. Samples were thawed, air-dried at ambient temperature, then the hydrocarbons and other

soluble organic matter were extracted with dichloromethane. A total petroleum hydrocarbon fraction was obtained from the soluble organic matter using liquid chromatography on alumina, eluting with a mixture of *n*-pentane and dichloromethane. The solvent was evaporated, and where practical, (i.e. > 1 mg of isolated hydrocarbons) the hydrocarbon residue was weighed. Hydrocarbon concentrations were obtained by expressing this weight as a proportion of the weight of dried, extracted sediment. The extracted hydrocarbons were diluted with *n*-hexane, then analysed using GC-MS from which the nature and abundance of the hydrocarbons in the extract could be evaluated. Where the extract was insufficient for weighing, or the chromatogram showed the presence of relatively high abundances of non-petroleum derived compounds in the hydrocarbon extracts, GC-MS was used to estimate the total petroleum hydrocarbon concentration of the sediment using an internal reference standard.

A sample of floating, non-aqueous phase liquid (NAPL), recovered from the leaks in the OCW system at the time that the discharge into the mangroves at the SCV Beach was discovered was similarly analysed by gas chromatography to establish its hydrocarbon composition. This material provided an insight into the initial composition of the petroleum released at the SCV Beach.

5.3.2 Selection of samples for further analysis

From the large number (157) of sediment extracts analysed in this manner, a subset of ten was selected for further, more specialised chemical analysis. Extracts were chosen primarily to represent various stages of the biodegradation scale, initially proposed by Volkman et al. (1984) and later refined by Peters and Moldowan (1993), based on the appearance of the gas chromatogram, however other criteria were applied including the location from which the sediment sample was collected.

Although some care was taken to ensure that the location of each of the sites was consistent between sampling events, a differential global positioning satellite system (DGPSS) was not used. Instead, the locations were mapped using distance and compass bearings from prominent landmarks. As a result, it is estimated that an error of approximately 10 to 20 m in locating the sample sites may apply to the first

five sampling excursions. This error was likely to be exacerbated in later visits by the relative lack of continuity in the sampling. Therefore, for the purposes of this study, several different sampling sites close to heavily contaminated areas were categorised as having been collected from one of two areas, namely North East Creek (NEC) and Slug Catcher Vent Beach (SCVB). It is estimated that samples from within NEC were collected within a maximum of approximately 50 m of each other, and within 100 m of each other within SVCB, as shown in Figure 5-2.

Only samples collected from the upper two centimetres of the sediment were selected for further analysis to minimise the possibility of mixing relatively well preserved petroleum in the underlying sediments, with the more weathered petroleum contained in the surface sediments. This is illustrated in Figure 5-3, where the gas chromatograms presented were obtained from the petroleum extracted from a sediment core collected in September 1990 from the NE Creek. It is evident from inspection of these that although an unresolved complex mixture is perceptible in all samples, the hydrocarbons are better preserved from aerobic biodegradation in sediments deeper than approximately 5 cm below the sediment surface, indicated by the prominence of the *n*-alkanes. The total petroleum hydrocarbon (TPH) concentration determined at each depth interval is also shown in this figure. From these, it is evident that there is substantial variation in the TPH concentration with depth, perhaps reflecting the inhomogeneous nature of the sediment structure.

The mass of the soluble organic material obtained from the sediment sample was also considered, where a minimum of 1 mg was required for meaningful results to be obtained from the subsequent fractionation and analysis of the extract. Finally, to check that losses of volatile hydrocarbons due to evaporation during storage were minimised, the extracts were re-analysed using GC-MS prior to final selection.

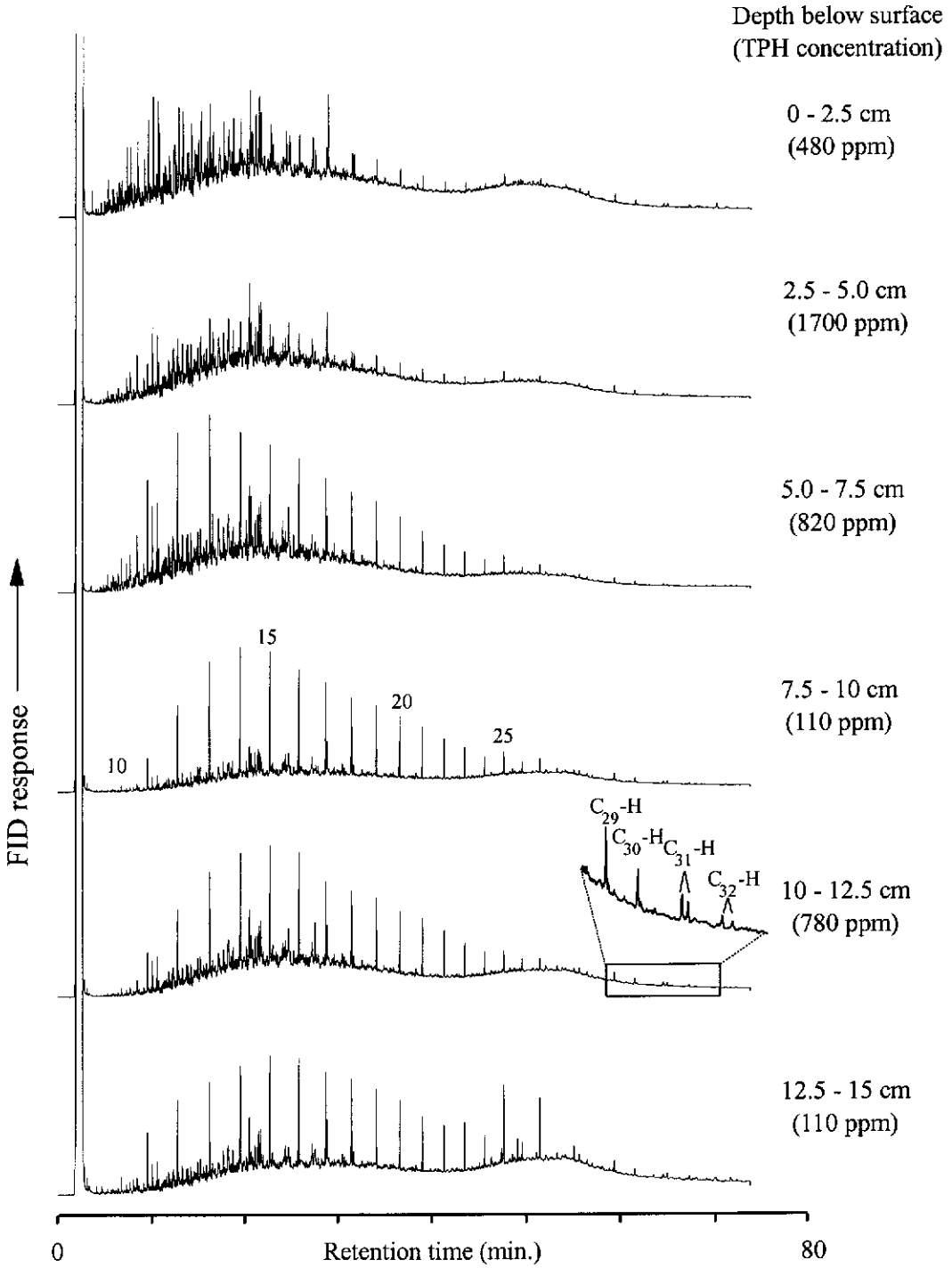

Figure 5-3: Gas chromatograms with flame ionisation detection (FID) obtained from combined saturated and aromatic hydrocarbon fractions isolated from various depths below the sediment surface from the NE Creek collected in Setember 1990. The identity of the labelled peaks are as follows: 10 through 25 = *n*-C_{10} to *n*-C_{25}; C_{29}-H = norhopane; C_{30}-H = hopane; C_{31}-H through C_{32}-H = homohopanes. TPH concentrations of the sediments (ppm, mg kg^{-1}, dry weight) are also shown.

In summary, extracts from five samples from each area were selected, each satisfying the above criteria. The date of sample collection and the TPH concentration of the sediments from which these extracts were obtained are summarised in Table 5-1. In addition, the NAPL recovered from the OCW system was selected for further analysis. Bearing in mind the variability in TPH concentration with depth in the core sediments from the NE Creek (Figure 5-3), these concentrations may not provide a reliable measure of hydrocarbon attenuation. Although the concentrations in Table 5-1 should therefore be interpreted with caution, the initial rapid decline in TPH concentration at SCVB might be attributed to losses from evaporation and water washing at this site. This will be discussed in detail later. Concentrations decrease more slowly at the NEC site, however this could be indicative of a greater release of petroleum into this site.

Table 5-1: Location and collection date of selected sediment samples removed from North East Creek (NEC) and the Slug Catcher Vent Beach (SCVB) between August 1987 and September 1990. The concentration of total petroleum hydrocarbons (TPH) determined in each of the samples. Similar information is shown for non-aqueous phase liquid (NAPL) obtained from the oil-contaminated water (OCW) system.

Sample Identity	Location	Collection Date	TPH concentration (mg kg^{-1}, dry weight)
NAPL	OCW system	Aug. 1987	n.a.
SCVB 1	SCVB	Dec. 1987	2000
SCVB 2	SCVB	Feb. 1988	120
SCVB 3	SCVB	July 1989	60
SCVB 4	SCVB	Jan. 1990	180
SCVB 5	SCVB	Sept. 1990	29
NEC 1	NEC	Sept. 1987	3400
NEC 2	NEC	Oct. 1987	5800
NEC 3	NEC	Sept. 1988	1500
NEC 4	NEC	Jan. 1989	1100
NEC 5	NEC	Jan. 1990	70

5.4 Chemical analysis

Hydrocarbon extracts from the selected samples shown in Table 5-1 were further examined by separating the saturated hydrocarbons from the aromatic hydrocarbons using liquid chromatography on silica gel. The saturated hydrocarbons were eluted with *n*-pentane, and the aromatic hydrocarbons with a mixture of dichloromethane and *n*-pentane. For each sample, the whole saturated hydrocarbon fraction was analysed using GC-MS techniques, prior to further fractionation using molecular sieves to enable the identification and semi-quantification of the branched and cyclic saturated hydrocarbons. To this end, the saturated hydrocarbon fractions from the NAPL, NEC 1 and NEC 2 were treated using ZSM-5 molecular sieves, to remove the *n*-alkanes. Due to the low abundances of the *n*-alkanes, the remaining fractions from both the NEC and SCVB sites did not require such treatment. The three fractions excluded from ZSM-5 and the eight saturated hydrocarbon fractions were subjected to GC-MS analysis operating in the selected ion monitoring (SIM) mode.

Each of the total aromatic hydrocarbon fractions was also analysed using GC-MS techniques before fractionation using thin layer liquid chromatography on alumina to obtain separate dinuclear and trinulcear aromatic hydrocarbon fractions upon which GC-FTIR and GC-MS analyses were performed to differentiate between the various isomers of the alkylnaphthalenes and alkylphenanthrenes.

5.4.1 Saturated hydrocarbons

The total ion gas chromatograms obtained from the saturated hydrocarbons isolated from the NEC and SCVB sediment extracts are shown in Figure 5-4 and 5-5 respectively. In each case, these are compared with the NAPL, the hydrocarbon distribution of which is consistent with that of a condensate from which the lower molecular weight hydrocarbons have been removed by evaporation (Kagi, Fisher and Alexander, 1988). From earlier discussion of evaporative losses from the petroleum samples due to treatment in the laboratory (Chapter 4), it is likely that only hydrocarbons more volatile than *n*-C_{11} are likely to be affected. For this study, alterations to hydrocarbons less volatile than this were attributed to the effect of in-situ weathering processes, including water washing, evaporation and biodegradation.

It is apparent that the composition of the saturated hydrocarbons isolated from the sediments at both sites changed over the duration of the sampling program. The most noticeable feature is a decrease in the abundance of the resolved compounds, in particular the *n*-alkanes, relative to the unresolved complex mixture of hydrocarbons, with increasing residence time in the sediments. This gross compositional change is consistent with those usually associated with the biodegradation of petroleum (Connan, 1984; Gough, Rhead and Rowland, 1992). Further, the successive removal of the *n*-alkanes and alkylcyclohexanes, resulting in the enhanced abundance of the more biodegradation-resistant bicyclic alkanes (Volkman et. al., 1984) is also apparent in chromatograms from both sample sets.

From comparison of the gas chromatograms obtained from the NEC samples, it is evident that NEC 3 contains a higher abundance of volatile saturated hydrocarbons (more volatile than *n*-C_{15}) than other samples. Their enhanced abundance in NEC 3 (collected Sept. '88) relative to NEC 1 (Sept. '87) and NEC 2 (Oct. '87), is anomalous, as one would expect these compounds to be removed by weathering in the interim between collection of the samples. Closer inspection, however, reveals that relative to fresher samples, the biodegradation is more advanced in NEC 3 (e.g. the *n*-alkanes have been reduced relative to pristane). This apparent inconsistency in hydrocarbon composition is attributed to protection of the NEC 3 hydrocarbons from other weathering processes, especially water washing and evaporation, evidence for which will be presented later.

Inspection of the gas chromatograms obtained from the NEC samples also reveals the presence of compounds identified by comparison with published mass spectra and retention time (Peters and Moldowan, 1993) as the homologous series norhopane (C_{29}), hopane (C_{30}) and the two C_{31} homohopane diastereomers. It is evident that these compounds increase in prominence in the chromatograms with increasing residence time in the sediments. Although the prominence of these compounds is surprising as polycyclic alkanes are usually present at very low abundance in condensates (Peters and Moldowan, 1993), their abundances have most likely been enhanced by removal of components of the condensate more susceptible to weathering. This will be discussed in detail later in this Section (p179).

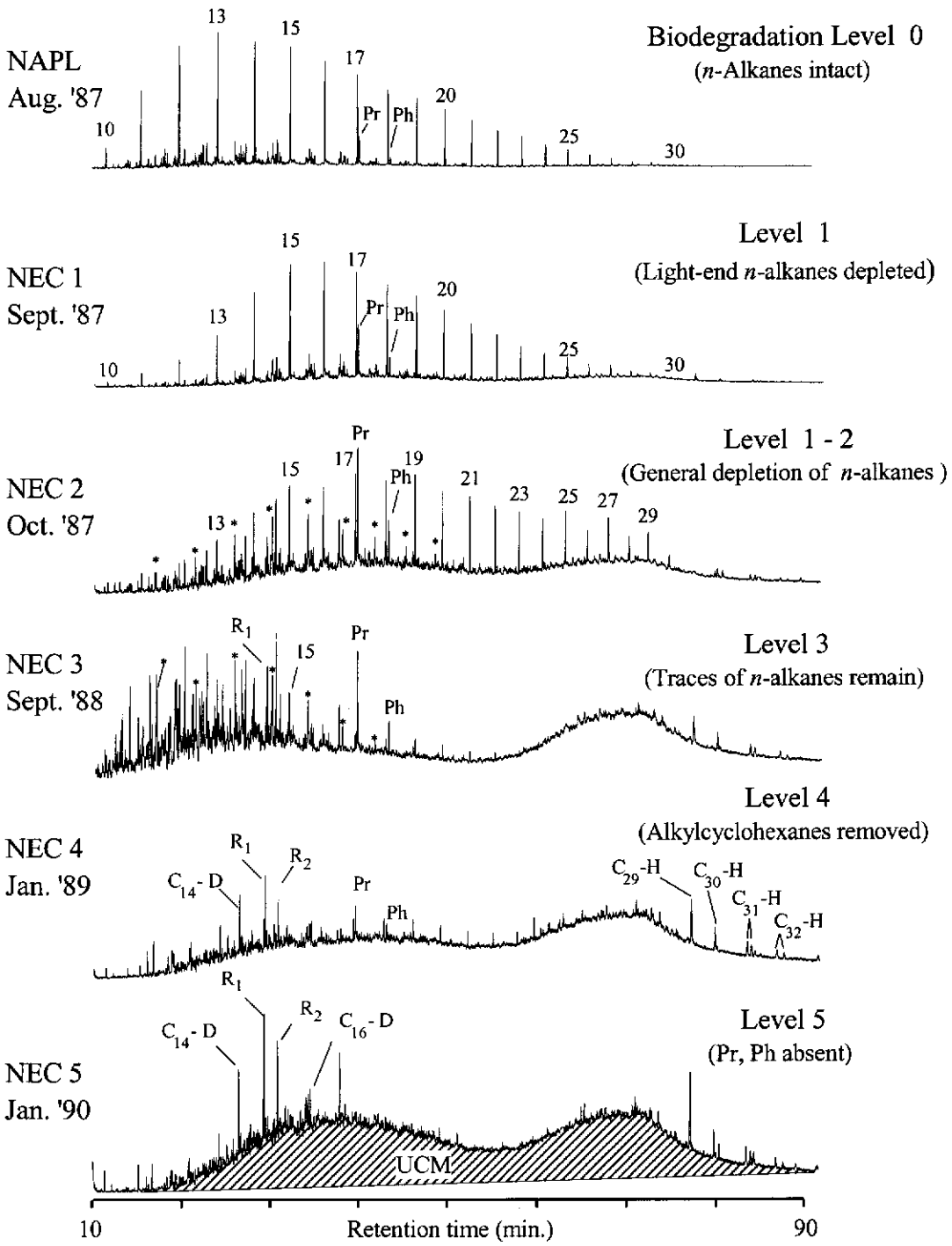

Figure 5-4: Total ion chromatograms from the saturated hydrocarbon fractions isolated from a sample of NAPL collected in August 1987, and sediments collected from the NEC contaminated site between September 1987 and January 1990. The identity of the labelled peaks are as follows: 10 through 30 = *n*-C_{10} to *n*-C_{30}; Pr = pristane; Ph = phytane; C_{14}-D = C_{14}-drimane; R_1 and R_2 = rearranged analogues of 8β(H)-drimane; C_{16}-D = 8β(H)-homodrimane; C_{29}-H = norhopane; C_{30}-H = hopane; C_{31}-H through C_{32}-H = homohopanes. A series of alkylcyclohexanes is denoted by asterisks.

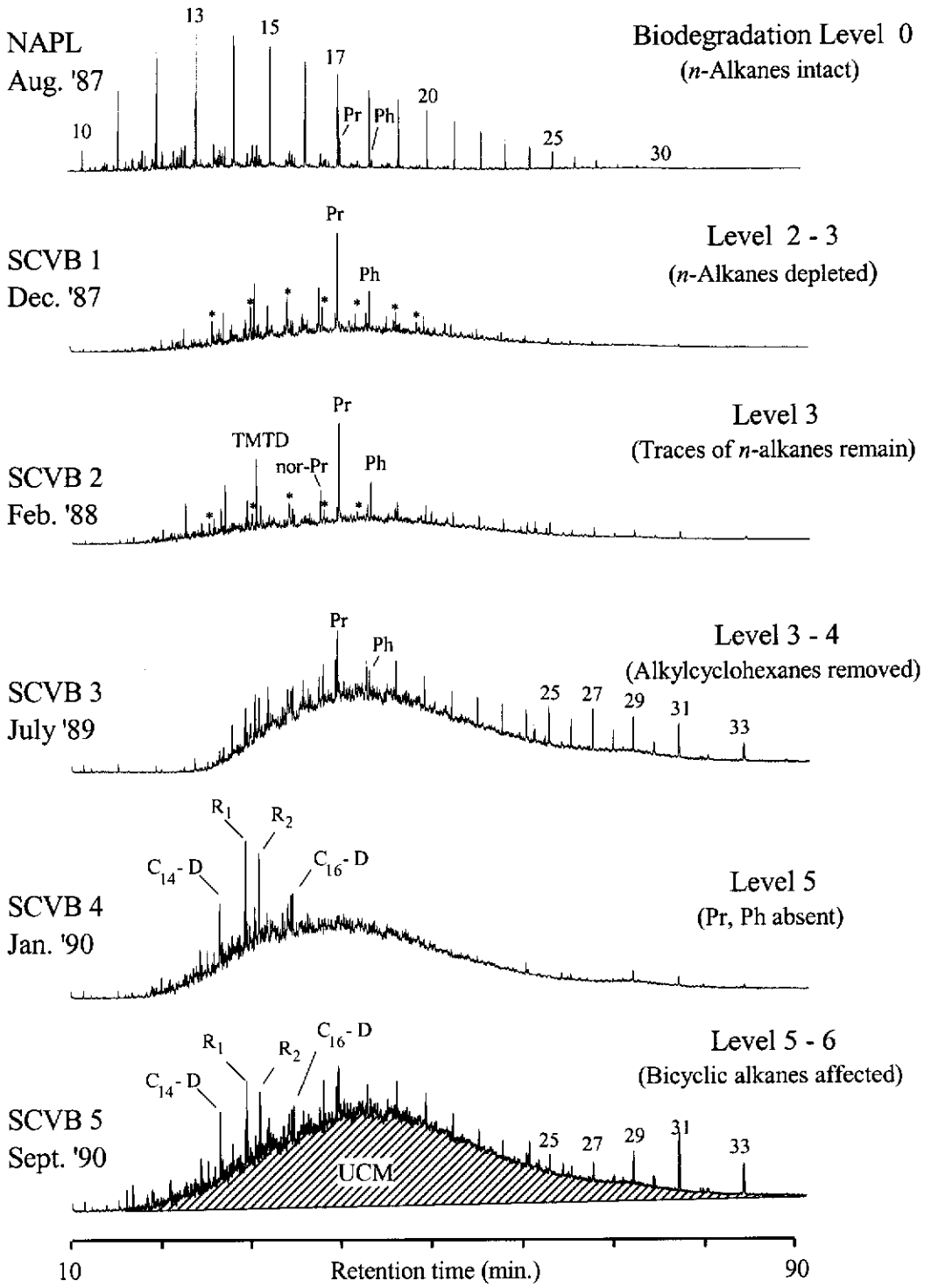

Figure 5-5: Total ion chromatograms from the saturated hydrocarbon fractions isolated from a sample of NAPL collected in August 1987, and sediments collected from the SCVB contaminated site between December 1987 and September 1990. The identity of the labelled peaks are as follows: 10 through 33 = *n*-C_{10} to *n*-C_{33}; Pr = pristane; Ph = phytane; C_{14}-D = C_{14}-drimane; R_1 and R_2 = rearranged analogues of 8β(H)-drimane; C_{16}-D = 8β(H)-homodrimane; TMTD = 2,6,10-trimethyltridecane; C_{29}-H = norhopane; C_{30}-H = hopane; C_{31}-H through C_{32}-H = homohopanes. A series of alkylcyclohexanes is denoted by asterisks.

A further feature of these gas chromatograms is a bimodal UCM. Both of these features are absent from the chromatogram obtained from the NAPL and the SCVB sediments, shown in Figure 5-5. Samples SCVB 3 and SCVB 5 both contain an anomalously high abundance of the *n*-alkanes, particularly pronounced for *n*-C_{27}, *n*-C_{29}, *n*-C_{31} and *n*-C_{33}. It is likely that these originate from a non-petrogenic source such as higher plant waxes (cf. Burns et al., 1999), their relative abundances enhanced due to the relatively low TPH concentrations of these samples (Table 5-1).

The branched and cyclic saturated hydrocarbons from the 11 samples were analysed to confirm the similarities in composition amongst samples from the same site, and to highlight differences between the two. The mass chromatograms showing response to the steranes (m/z 217) and hopanes (m/z 191) from each are shown in Figures 5-6 and 5-7. It is apparent that the distribution of abundances of the steranes is distinctly different between the two sites. The SCVB samples are distinguished by the very low abundance of the C_{27} steranes, especially those exhibiting the 14β(H),17β(H) configuration, relative to the C_{29} rearranged steranes (diasteranes). The similarity between the distributions of the steranes exhibited by the NAPL and the SCVB samples is also evident, indicating that the NAPL is the likely hydrocarbon fluid from which these compounds in the SCVB sediments were sourced. However, the mass chromatograms show the NEC samples are richer in steranes, especially those exhibiting the 14β(H),17β(H) configuration, so the relationship between the NAPL and the NEC samples is not at all obvious.

Previous workers (Seifert and Moldowan, 1979; Mackenzie et al., 1983 and Goodwin, Park and Rawlinson, 1983) have observed the preferential depletion of the (non-rearranged) steranes relative to the rearranged steranes in biodegraded crude oils. Alexander et al. (1983) also observed the reduction in abundance of 20R 5α(H)14α(H),17α(H)-ethylcholestane (i.e. C_{29} sterane) relative to the 20S isomer. At both sites, the distribution of these steranes was unaltered between the time of the initial sample collection and the final sampling, indicating that biodegradation has not proceeded to this extent (Biodegradation Level 7) at either site.

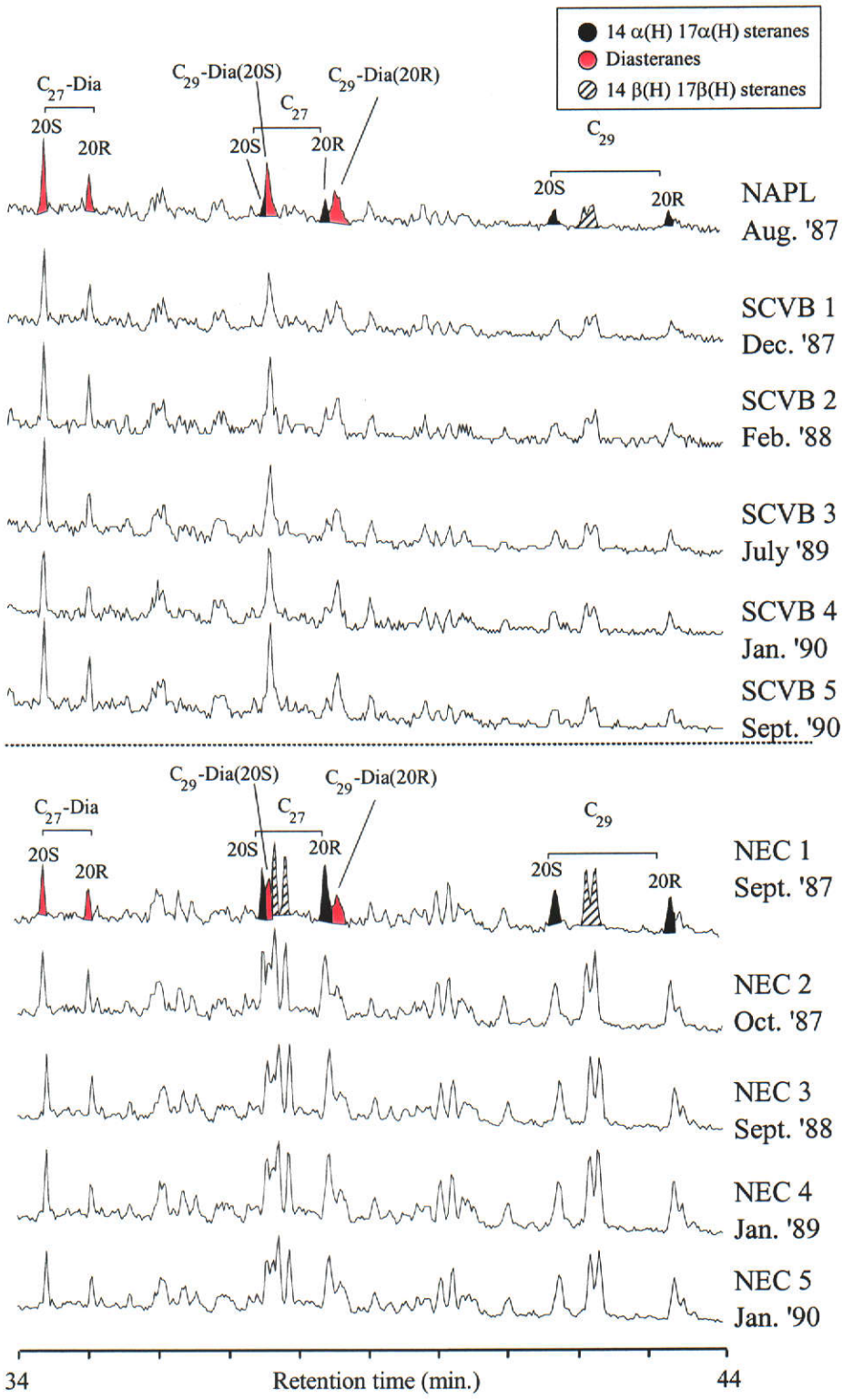

Figure 5-6: Mass chromatograms (m/z 217) showing the C_{27} to C_{29} steranes contained in branched and cyclic saturated hydrocarbon fractions isolated from a sample of NAPL collected in August 1987, and sediments collected from the NEC and SCVB contaminated sites between September 1987 and September 1990.

Inspection of the m/z 191 chromatograms shown in Figure 5-7 reveals that the hydrocarbons from each site may similarly be distinguished by the relative abundances of the series of hopanes. Here the abundance of 17α(H),21β(H)-norhopane (C_{29}-H) relative to that of 17α(H),21β(H)-hopane (C_{30}-H) is substantially higher in the NEC sediments than in the SCVB sediments and the NAPL. As well, members of the series of 22S and 22R diastereomers of the 17α(H),21β(H)-homohopanes (C_{31}-H to C_{35}-H) observed in the NEC samples are barely perceptible above the background signal in the SCVB and NAPL hydrocarbons.

Also consistent with observations from the steranes is the preservation of the distributions of the hopanes during the three-year period over which samples were collected. Furthermore, the absence of a series of demethylated hopanes (17α(H),21β(H)-25-norhopanes, i.e. 25-norhopanes) confirms that biodegradation has not proceeded to Biodegradation Level 7, where the abundance of the hopanes from which they are formed is diminished (Seifet and Moldowan, 1979; Volkman et al., 1983; Prince et al., 1994; Moldowan and McCaffrey, 1995; Peters et al., 1996).

The bicyclic alkanes were investigated using the m/z 123 mass chromatograms shown in Figure 5-8. Unlike for the steranes and hopanes, there are no significant differences in the distribution of these compounds in the NAPL or in the SCVB 1 and NEC 1 sediments. Furthermore, with the exception of the hydrocarbons extracted from SCVB 3, where the abundance of the C_{14}-bicyclic alkanes is low, there is no obvious change in the distribution of these compounds with increasing residence time in the mangrove sediments at either site.

It is evident from the analysis of these saturated biomarkers that the sediments from the two sites contain hydrocarbon mixtures that have different saturated hydrocarbon signatures, with SCVB correlating with the NAPL and the NEC not correlating. This observation is seemingly contradicted by the circumstance of the discharge of petroleum fluid into the mangrove, that is that the discharge points were identified as a common section of the OCW system.

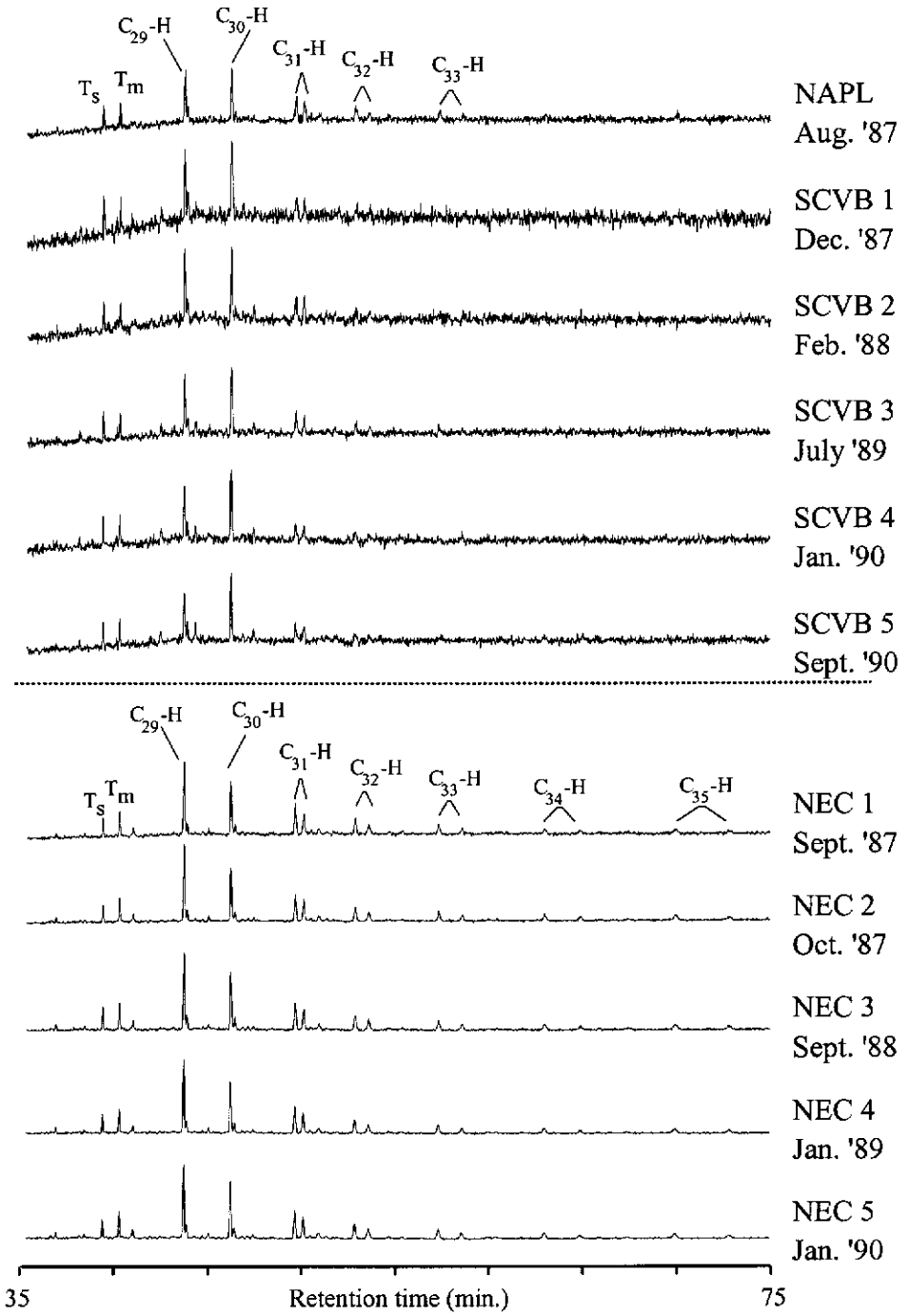

Figure 5-7: Mass chromatograms (m/z 191) showing the C_{27} (T_s and T_m) to C_{35} hopanes contained in branched and cyclic saturated hydrocarbon fractions isolated from a sample of NAPL collected in August 1987, and sediments collected from the NEC and SCVB contaminated sites between September 1987 and September 1990.

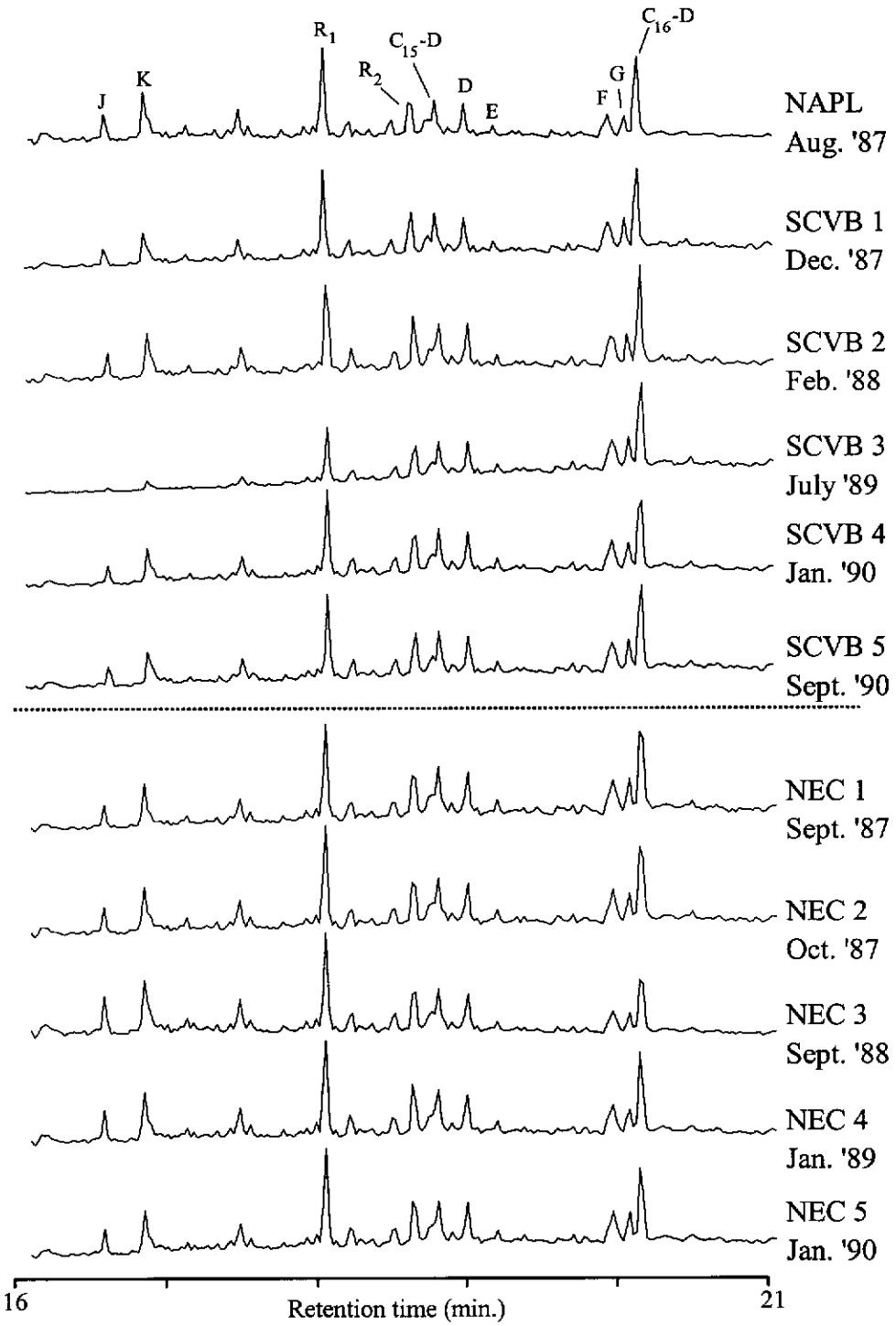

Figure 5-8: Mass chromatograms (m/z 123) showing drimane (C_{15}-D), the rearranged drimanes R_1 and R_2, and 8β(H)-homodrimane (C_{16}-D) contained in branched and cyclic saturated hydrocarbon fractions isolated from a sample of NAPL collected in August 1987, and sediments collected from the NEC and SCVB contaminated sites between September 1987 and September 1990. Peaks labelled J and K, D and E, and F and G refer to C_{14}- , C_{15}- and C_{16}- bicyclic alkanes respectively, identified by Noble (1986).

One explanation consistent with these observations is that the NEC site experienced chronic exposure to a NAPL leaking from the OCW system over a period of several years prior to the collection of the initial samples in August 1987. In the interim, the composition of the hydrocarbon mixture was altered by weathering processes, with the most resistant compounds, including the hopanes and the UCM, persisting. At the time of the initial sampling, the sediments contained a mixture of older, weathered residues and the recently discharged NAPL. Although feasible, this does not adequately explain the disparity in hydrocarbon composition. Hydrocarbons contained in the sample SCVB 5 were resident in the sediments for at least three years, yet the distribution of the hopanes, steranes and compounds comprising the UCM does not resemble that found in NEC 1. It is therefore unlikely that the composition of the hydrocarbon fluid contained in the NAPL from the OCW system, closely resembling that of the SCVB 1 sediments, could be altered sufficiently by the weathering processes occurring in the mangrove sediments to resemble that found in the sediments at NEC 1.

Insight into the source of the petroleum at the NEC site is provided by comparison of the chromatograms (e.g. 10 – 12.5 cm) from the NE Creek sediment core from September 1990, shown in Figure 5-3, and the NEC 1 sample (Figure 5-4) collected three years earlier. This reveals that the relatively well-preserved hydrocarbons residing in the sediments 10 cm to 12.5 cm below the surface at the NE Creek are broadly similar in composition to those in NEC 1, characterised by the bimodal appearance of the UCM and the series of hopanes. It is probable that the hydrocarbons deeper in the sediment profile have been somewhat protected from weathering and therefore are representative of those initially released into the NE Creek. If the petroleum in the NEC samples were indeed a mixture of materials of varying extent of weathering, mixing did not occur after the collection of the NEC 1 sample, but more likely before release into the NEC site. It is therefore more probable that the composition of the NAPL in the OCW system changed over time, and that accidental releases at different times may have resulted in the different hydrocarbon compositions at the two sites. At the SCVB site, the hydrocarbon composition was consistent with the NAPL collected from the OCW system at that time. Since no material was recovered from the OCW system at the time of the

accidental discharge into the NEC site, the sample from NEC 1 provides the closest authentic model for this material.

5.4.2 Biodegradation of individual saturated hydrocarbons

Inspection of the chromatograms shown in Figures 5-4 and 5-5 reveals that the progressive depletion of saturated hydrocarbons according to their structural type is occurring with increasing residence time in the environment. These changes in the composition between the 11 samples of petroleum are reflected in Table 5-2. Here, the abundances of *n*-alkanes, alkylcyclohexanes and acyclic isoprenoids containing 16, 17 and 19 carbon atoms per molecule have been normalised against that of the relatively biodegradation-resistant rearranged drimane R_1 (Volkman et al., 1984). This compound was selected as a conserved internal marker for estimating biodegradation in preference to other drimanes due to its higher relative abundance and chromatographic resolution from other compounds. Although Williams et al. (1986) reported that the rearranged bicyclic alkanes were degraded in preference to non-rearranged homologues, this is not evident from the m/z 123 mass chromatograms shown in Figure 5-8.

SCVB sediments

The initial rapid depletion of the *n*-alkanes, indicated by the decreasing peak area ratio between the NAPL and SCVB 1, is a striking feature of Table 5-2. In samples collected subsequent to these, the depletion of *n*-alkanes continued until they were barely detectible in SCVB 4. The ratio increases slightly for SCVB 5, due in part to the presence of a minor amount of *n*-alkanes and to the apparent depletion of R_1 relative to the UCM, as shown in Figure 5-5. As discussed earlier, it is likely that this sample contains higher molecular weight *n*-alkanes (*n*-C_{25}, *n*-C_{27}, *n*-C_{29}, *n*-C_{31} and *n*-C_{33}) from a non-petrogenic origin, perhaps common to the *n*-alkanes for which the ratios are presented. Of the other compounds measured in SCVB 5, only pristane is enhanced relative to R_1, and is also most likely from a non-petrogenic source (Gassmann, 1981).

Table 5-2: Relative abundances of *n*-alkanes, alkylcyclohexanes and acyclic isoprenoids containing 16, 17 and 20 carbon atoms per molecule measured in sediment samples removed from NEC and the SCVB contaminated sites between September 1987 and September 1990. Abundances were calculated from peak areas from the GC-MS total ion chromatograms shown in Figures 5-4 and 5-5, normalised against that of the rearranged drimane, R_1. Similar information is also shown for NAPL collected from the OCW system in August 1987.

Sample Identity	*n*-alkanes			Alkylcyclohexanes			Acyclic isoprenoids		
	n-C_{16}	*n*-C_{19}	*n*-C_{20}	C_{16}	C_{19}	C_{20}	TMTD	Pr	Ph
NAPL	21	12	11	1.2	0.60	0.50	3.3	6.3	2.6
SCVB 1	0.82	0.81	0.80	1.0	0.49	0.57	2.5	5.2	2.1
SCVB 2	0.36	0.69	0.66	0.48	0.20	0.41	2.7	4.7	1.7
SCVB 3	0.70	1.0	0.75	0.21	0.18	0.13	1.4	1.8	0.89
SCVB 4	0.09	0.08	0.07	0.02	0.02	<0.01	0.53	0.12	0.10
SCVB 5	0.26	0.38	0.36	<0.01	<0.01	<0.01	0.12	0.77	0.04
NEC 1	11	7.2	6.2	1.4	0.81	0.54	3.8	6.9	2.5
NEC 2	2.1	2.3	2.2	1.2	0.48	0.37	2.2	3.7	1.5
NEC 3	0.25	0.19	0.16	0.20	<0.01	0.01	1.4	1.3	0.50
NEC 4	0.15	0.27	0.23	0.05	0.04	0.06	0.34	0.52	0.29
NEC 5	0.01	0.07	0.01	<0.01	0.01	0.01	0.08	0.01	0.08

The decrease in the peak area ratios for the other compounds in all samples occurred in a similar, though less pronounced manner, with the initial significant depletion in the alkylcyclohexanes occurring between SCVB 1 and SCVB 2 and in the isoprenoids between SCVB 2 and SCVB 3. The decreasing abundances of all of the compounds shown in Table 5-2 relative to R_1 indicates that the bicyclic alkanes are the most resistant to biodegradation of these compounds. This observed order of depletion, namely *n*-alkanes > alkylcyclohexanes > acyclic isoprenoids > bicyclic alkanes is in general agreement with that observed during the early stages of biodegradation (Levels 0 to 6) by Volkman et al. (1984) and Peters and Moldowan (1993).

NEC Sediments

Although a similar order of biodegradation susceptibility is apparent in the NEC samples, there is more overlap between successive compound groups in contrast to the apparent stepwise removal observed in the SCVB samples. This is most noticeable in NEC 2, where a significant depletion of TMTD, pristane and phytane has occurred while the *n*-alkanes are still present in relatively high abundance.

As discussed earlier, the hydrocarbons extracted from the NEC sediments also contained a series of hopanes, clearly identified in the mass chromatograms shown in Figure 5-7. The most abundant of these, 17α(H), 21β(H)-norhopane (C_{29}-hopane), was used as a conserved marker against which the depletion of the selected alkanes, including the bicyclic alkanes could be compared. This approach followed that of Prince et al. (1994), who used this compound in a similar manner to evaluate the extent of biodegradation of crude oil during *in-vitro* biodegradation experiments, and others (Wang, Fingas and Sergy, 1995; Barakat et al., 2001) who used the concentration of the C_{29} and C_{30} 17α(H),21β(H)-hopanes to quantify the weathering of severely weathered crude oils.

To minimise interference by co-eluting compounds, the semi-quantitative determination of the bicyclic alkanes and C_{29}-hopane was performed using m/z 123 and m/z 191 mass chromatograms. From analysis of these results, shown in Table 5-3, it is apparent that although the bicyclic alkanes show a much greater resistance to biodegradation than other major petroleum alkane components, their abundances are also depleted relative to the C_{29}-hopane with increasing residence time in the sediments. In accordance with expectations based on previous observations by Volkman et al. (1984) in crude oil reservoirs, the decrease in relative abundances in these samples reflects the different biodegradation rates of the alkanes. These differences in rate are smaller than expected, however, and the quasi-stepwise removal of the compounds with biodegradation is not so apparent. Furthermore, from the similarity in the extent of depletion amongst the four bicyclic alkanes we can conclude that although these compounds are depleted, there is no perceptible discrimination amongst these compounds as a result of biodegradation. This is contrary to observations by Williams et al. (1986) who reported that the

rearranged bicyclic alkanes were degraded in preference to non-rearranged homologues, and to those observed in the drilling fluid discharged to the sea-floor discussed previously in this thesis (Chapter 4). As suggested earlier (Section 4.10.2), processes other than biodegradation may have caused the discrimination amongst the drimanes during redistribution of the sediments on the sea-floor.

Table 5-3: Relative abundances of *n*-hexadecane(*n*-C_{16}), *n*-decylcyclohexane (C_{16}-ACH), 2,6,10-trimethyltridecane (TMTD) and the bicyclic alkanes drimane (C_{15}-D), the rearranged drimanes R_1 and R_2, and 8β(H)-homodrimane (C_{16}-D) measured in sediment samples removed from the NEC contaminated site between September 1987 and January 1990. Abundances were calculated from GC-MS peak areas obtained from the specified chromatograms normalised against that of C_{29}-hopane from the m/z 191 mass chromatogram.

	Acyclic alkanes (TIC)			Bicyclic alkanes (m/z 123)			
	n-C_{16}	C_{16}-ACH	TMTD	C_{15}-D	R_1	R_2	C_{16}-D
Sample							
NEC 1	170	6.5	61	0.37	0.90	0.60	0.93
NEC 2	31	3.9	34	0.37	0.88	0.57	0.78
NEC 3	3.9	1.2	22	0.30	0.79	0.46	0.51
NEC 4	1.9	0.48	4.3	0.28	0.71	0.47	0.52
NEC 5	0.15	0.45	0.95	0.27	0.69	0.41	0.53

The observed changes in the composition of the saturated hydrocarbons for each of the eleven sites is summarised in Table 5-4. Here the classification system used by Peters and Moldowan (1993) to rank petroleum according to the extent of biodegradation was applied to describe each sample. This approach places crude oils into eleven classes according to the level of biodegradation of the saturated hydrocarbons, ranging from undegraded petroleum (Level 0) to severely degraded petroleum (Level 10). For example, at the SCVB site, the hydrocarbons from which the NAPL is composed were designated biodegradation Level 0, that is unbiodegraded. The sample SCVB 3, collected six months after the initial discovery of the release, was classified as moderately biodegraded (Level 3) since only traces of the *n*-alkanes remained. SCVB 5, containing the most biodegraded petroleum observed in sediments at this site, was assessed as extensively biodegraded (Level 5-6) due to the partial depletion of the C_{15}- and C_{16}-bicyclic alkanes.

In the absence of an authentic sample of spilled material, the NAPL from the SCVB site was used as a model for unbiodegraded petroleum broadly representative of the hydrocarbons released into the NEC sediments. As shown in Figure 5-4, NEC 1 contained a lesser abundance of *n*-alkanes in the C_{10} to C_{15} range than did the NAPL, and was therefore assigned Biodegradation Level 1. The depletion of the series of alkylcyclohexanes, observed in the saturated hydrocarbon chromatograms (Figure 5-4) and normalised abundances (Tables 5-2 and 5-3) of the samples NEC 2, NEC 3 and NEC 4 respectively, was the principal discriminator between the levels of biodegradation assigned to these samples (Volkman et al., 1984).

Table 5-4: The effect of biodegradation on the composition of saturated hydrocarbons contained in sediment samples removed from the NEC and SCVB contaminated sites. Similar information is shown for a sample of NAPL obtained from the OCW system.

Sample Identity	Assigned Level of Biodegradation	Rationale
NAPL	0	undegraded hydrocarbons
SCVB 1	2-3	greater than 90% of the *n*-alkanes removed
SCVB 2	3	*n*-alkanes absent alkylcyclohexanes affected
SCVB 3	3-4	acyclic isoprenoids affected
SCVB 4	5	acyclic isoprenoids absent
SCVB 5	5-6	bicyclic alkanes affected
NEC 1	1	light-end *n*-alkanes depleted
NEC 2	1-2	general depletion of *n*-alkanes
NEC 3	3	*n*-alkanes absent, alkylcyclohexanes affected, acyclic isoprenoids affected,
NEC 4	4	alkylcyclohexanes absent, acyclic isoprenoids affected
NEC 5	5	acyclic isoprenoids absent

5.5 The effect of biodegradation on naphthalene and alkylnaphthalene abundances

5.5.1 Gross changes in composition of the aromatic hydrocarbon mixture

Chromatograms obtained from the aromatic hydrocarbon fractions of the study sets are shown in Figures 5-9 and 5-10 respectively. Again, as the residence time increased, one observes an increasingly biodegraded signature, with the enhancement of the UCM relative to the resolved peaks, such as those for naphthalene, phenanthrene and the alkylated homologues of each. As with the saturate fractions, the aromatic hydrocarbon distributions are bimodal at the NEC site but not at the SCVB site, suggesting that the petroleum at each site originated from different sources.

From each chromatogram, the relative abundances of naphthalene (N), the methylnaphthalenes (MNs), ethylnaphthalenes (ENs), dimethylnaphthalenes (DMNs), trimethylnaphthalenes (TMNs) and tetramethylnaphthalenes (TeMNs) were calculated from the sum of the peak areas corresponding to each of the isomers, corrected for differences in the mass selective detector response. The investigation of the depletion of these compounds while resident in the mangrove sediments is facilitated by the use of a conserved (microbially resistant) internal marker compound, against the abundance of which the alkylnaphthalene abundances may be normalised. Based on its apparent resistance to biodegradation in drilling wastes discharged to the sea-floor discussed earlier (Section 4.10.2), 1,8-dimethyl-phenanthrene (1,8-DMP) was identified as a suitable internal marker. The normalised abundances of naphthalene and its alkylated homologues are presented in Table 5-5.

From these results for the NEC sediments, it is apparent that NEC 3 contains anomalously high abundances of the alkylnaphthalenes, especially the lower molecular weight compounds. Leaving aside this sample, in broad terms the alkylnapththalenes were depleted in the order N > MNs > DMNs ~ ENs > TMNs > TeMNs over the approximately three-year period during which samples were collected. The abundance of naphthalene is significantly depleted in the interim

between NEC 1 and NEC 2, while that of the MNs, ENs, DMNs and TMNs was depleted between NEC 2 and NEC 4. The abundance of the TeMNs in the first four samples remained relatively constant, but decreased significantly between NEC 4 and NEC 5.

Table 5-5: Relative abundances of naphthalene (N), methylnaphthalenes (MNs), dimethylnaphthalenes (DMNs), trimethylnaphthalenes (TMNs), tetramethylnaphthalenes (TeMNs) and the sum of naphthalene and these alkylnaphthalenes ($\sum$ANs) measured in selected sediment samples removed from the NEC and SCVB sites between August 1987 and September 1990. Abundances were calculated from the sum of GC-MS peak areas corrected for differences in detector response normalised against that of 1,8-DMP. Similar information is also shown for NAPL obtained from the OCW system.

Sample	N	MNs	ENs	DMNs	TMNs	TeMNs	$\sum$ANs
NAPL	72	410	28	540	300	91	1400
SCVB 1	0.010	0.47	1.2	28	97	66	190
SCVB 2	0.00	0.00	1.3	28	99	69	200
SCVB 3	0.00	0.00	1.1	13	64	58	140
SCVB 4	0.00	0.00	3.5	45	140	100	290
SCVB 5	0.00	0.00	0.00	0.00	2.1	12	14
NEC 1	0.70	7.3	4.5	48	120	84	260
NEC 2	0.38	7.6	7.0	62	100	71	250
NEC 3	0.00	15	15	200	240	96	570
NEC 4	0.00	0.00	0.78	16	73	87	180
NEC 5	0.00	0.00	1.5	13	45	55	110

The normalised abundances for SCVB samples and for the NAPL are also shown in Table 5-5. These reveal that the NAPL contains a greater abundance of naphthalene and the alkylnaphthalenes than does SCVB 1, however the difference decreases with increasing extent of alkylation of naphthalene. For example, the abundance of naphthalene in the NAPL is several orders of magnitude greater than that found in SCVB 1, yet the TeMNs present in the NAPL exceed those in SCVB 1 by a factor of only approximately 1.4.

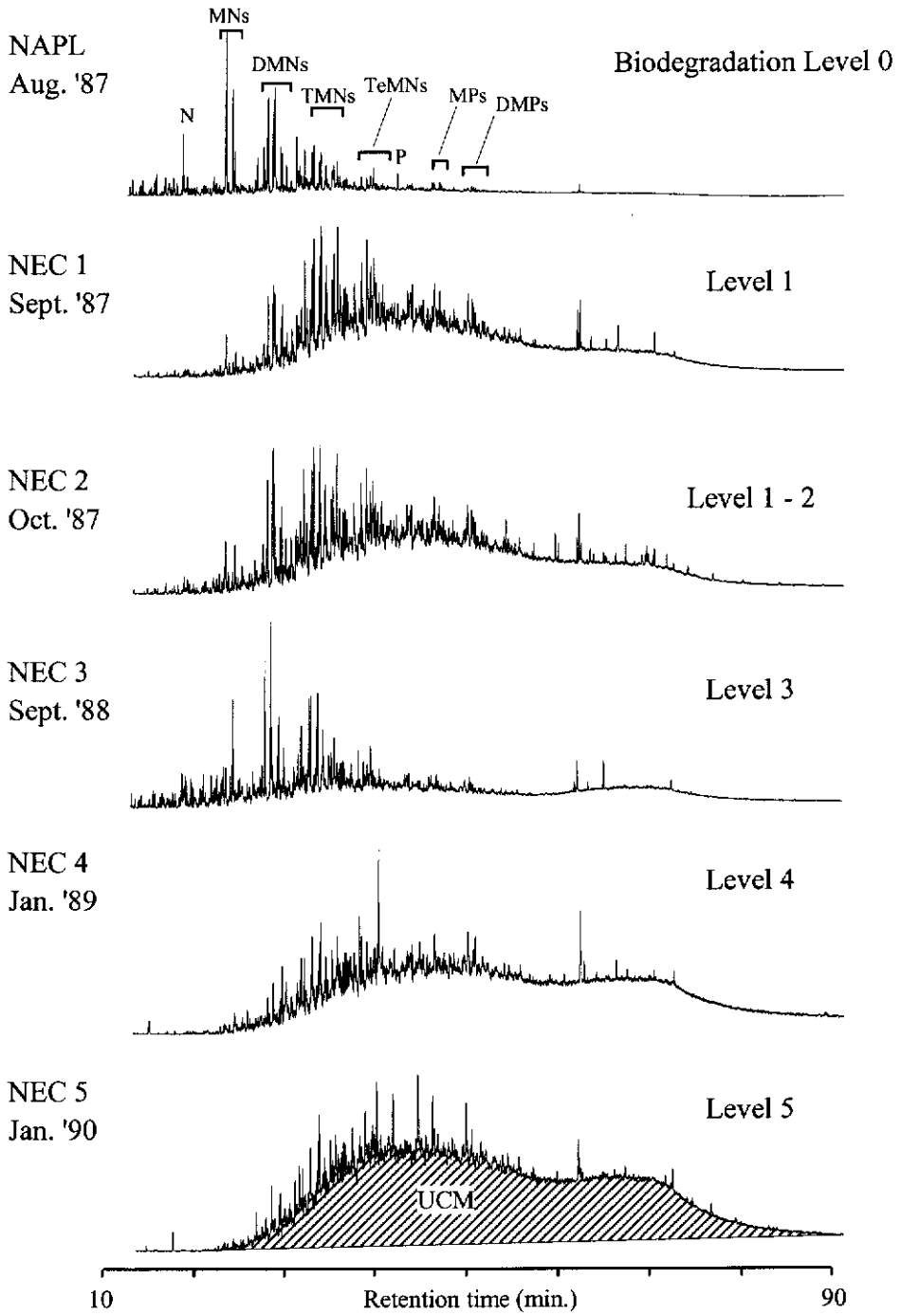

Figure 5-9: Total ion chromatograms from the aromatic hydrocarbon fractions isolated from a sample of NAPL collected in August 1987, and sediments collected from the NEC contaminated site between September 1987 and January 1990. The identity of the labelled groups of peaks are as follows: MNs = methylnaphthalenes; DMNs = dimethylnaphthalenes; TMNs = trimethylnaphthalenes; TeMNs = tetramethylnaphthalenes; P = phenanthrene; MPs = methylphenanthrenes; DMPs = dimethylphenanthrenes.

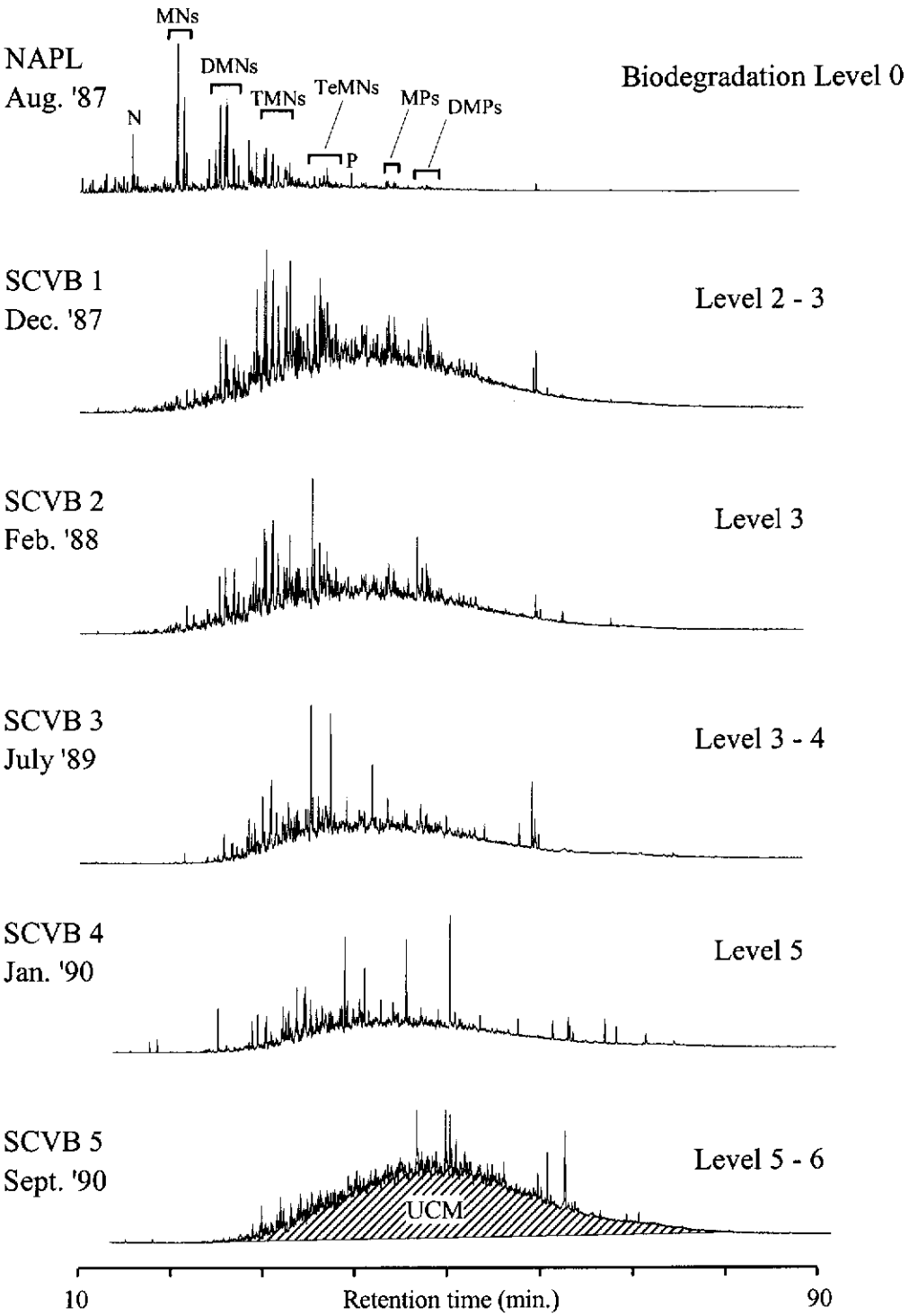

Figure 5-10: Total ion chromatograms from the aromatic hydrocarbon fractions isolated from a sample of NAPL collected in August 1987, and sediments collected from the SCVB contaminated site between September 1987 and September 1990. The identity of the labelled groups of peaks are as follows: MNs = methylnaphthalenes; DMNs = dimethylnaphthalenes; TMNs = trimethylnaphthalenes; TeMNs = tetramethylnaphthalenes; P = phenanthrene; MPs = methylphenanthrenes; DMPs = dimethylphenanthrenes.

Amongst the five SCVB sediment samples, the values are more comparable. The comparison is especially close between SCVB 1 and SCVB 2, where with the exception of naphthalene and the MNs that have been depleted to below detection limits in SCVB 2, the alkylnaphthalene abundances are almost identical. A similar trend in the order of depletion of the alkylnaphthalenes to that observed for the NEC sediments is also apparent, although somewhat compromised by the anomalously high values for SCVB 4.

A plausible interpretation of these results is that between release of the NAPL from the OCW system and the collection of the initial sediment samples SCVB 1, the composition of the NAPL was changed by the processes of evaporation and water washing. In laboratory studies examining the passive volatilisation of petroleum from soil, Arthurs, Stiver and Zytner (1995) observed that gasoline-range hydrocarbons were rapidly removed from soil at room temperature. Half-lives ranged from hours to several days decreasing with the vapour pressure of the hydrocarbon, the density of the soil type and the depth of the contaminant in the soil profile. By comparison, the volatilisation of *n*-hexadecane was negligible.

The vapour pressures of several hydrocarbons contained in the NAPL are shown in Table 5-6. Based solely on similarity in vapour pressure, the abundance of the TMNs (approx. 0.3 Pa) should be altered only to approximately the same extent as *n*-hexadecane (approx. 0.2 Pa) by evaporation. There is however a large disparity in the aqueous solubility of these compounds, also shown in Table 5-6, where those of the TMNs are approximately four orders of magnitude greater than the *n*-hexadecane solubility. Page et al. (2000) demonstrated that an inverse relationship exists between the aqueous saturation concentrations and the degree of alkyl-substitution of naphthalene in laboratory experiments investigating the partitioning of aromatic hydrocarbons into water from crude oil. The saturation concentration of naphthalene (0. 18 mg L^{-1}) exceeded that of the C_1-naphthalenes (0.16 mg L^{-1}), C_2-naphthalenes (0.044 mg L^{-1}), C_3-naphthalenes (0.0060 mg L^{-1}) and the C_4-naphthalenes (0.0020 mg L^{-1}). These closely reflect the trends in aqueous solubilities of the individual compounds, shown in Table 5-6, and the extent of depletion of these compounds from the NAPL shown in Table 5-5.

Table 5-6: Aqueous solubility and vapour pressure at 25°C of several hydrocarbons. Values are presented as the average ± the standard deviation based on n measurements reported by Mackay, Shiu and Ma (1992) unless stated otherwise.

Compound	Aqueous solubility (mg L^{-1})	*n*	Vapour Pressure (Pa)	*n*
Naphthalene	31 ± 4.2	49	10 ± 2.0	29
1-MN	28 ± 1.5	15	7.9 ± 0.89	11
2-MN	26 ± 3.1	10	8.4 ± 1.1	10
1-EN	11 ± 0.53	14	2.5 ± 0.01	3
2-EN	7.8 ± 0.23	5	3.9 ± 0.56	3
1,3-DMN	8.9 ± 1.7	7	7.0	1
1,4-DMN	12 ± 0.47	8	3.0 ± 1.3	3
1,5-DMN	3.1 ± 0.53	10	1.1 [1]	1
1,6-DMN	0.9 [2]	1	2.0 [3]	1
2,3-DMN	2.5 ± 0.43	10	1.1 ± 0.54	6
2,6-DMN	1.6 ± 0.42	12	1.3 ± 0.53	8
1,3,5-TMN	3.1 ± 1.5	8	0.68	1
1,2,6-TMN	2.1 [4]	1	0.34 [1]	1
1,6,7-TMN	4.8 [2]	1	0.34 [1]	1
2,3,6-TMN	1.7 [2]	1	0.34 [1]	1
Phenanthrene	1.2 ± 0.32	39	0.040 ±0.030	21
1-MP	0.26 ± 0.01	3	0.0067 [1]	1
2-MP	0.28 [5]	1	0.0067 [1]	1
3-MP	0.26 [2]	1	0.0067 [1]	1
3,6-DMP	0.071 [2]	1	0.0024 [1]	1
n-decane	0.016 [6], 0.052 [4]	2	260 [7], 190 [8], 120 [9]	3
n-tetradecane	0.0022 [10]	1	1.5 [8]	1
n-hexadecane	0.00090 [10]	1	0.17 [7], 0.19 [8]	2

References: 1: Neely and Blau (1985); 2: Meylan and Howard (1996); 3: Riddick, Bunger and Sakano. (1986); 4: Yalkowsky and Dannenfleiser (1992); 5: Isnard and Lambert (1989); 6: Sanemasa, Wu and Toda (1997); 7: Lee et al. (1992); 8: Daubert and Danner (1989); 9: Carruth and Kobyashi (1973); 10: Sutton and Calder (1974).

In summary, it is likely that the initial depletion of the alkylnaphthalenes was mainly due to dissolution in the inundating sea-water, and to evaporation. As discussed earlier, however, the saturated hydrocarbons exhibited a simultaneous general depletion of the *n*-alkanes that cannot be attributed purely to these processes. This is supported by the results from a field-scale experimental oil spill in mangrove sediments reported by Burns et al., (1999) where evaporation and water washing were identified as the predominant removal processes of the oil. Furthermore, a lag time of at least one month before the onset of microbial biodegradation of the *n*-alkanes was observed. In a similar study by Scherrer and Mille (1989), an induction period of one to three months was observed prior to the commencement of microbial biodegradation.

Depletion of the aromatic hydrocarbons by aqueous dissolution and evaporation may also account for the anomalously high abundances of the alkylnaphthalenes in the samples SCVB 4 and NEC 3. It is probable that at the time of any of the sample collection excursions, local heterogeneity occurred at each site, given the assumed spatial resolution of 50 to 100 m and the time elapsed between the sample collection events. It is therefore feasible that the hydrocarbons resident in the sediments at any given time have been exposed to varying extents of water-washing, evaporation and perhaps biodegradation depending on their varying immediate environments. Although one criterion for inclusion of collected sediment samples into the NEC and SCVB sample sets was that the sediment must have been collected from within 2 cm of the surface, physical displacement of the top 5 cm of the sediment by, for example, tidal activity prior to sampling would result in the collection of less weathered hydrocarbons as illustrated by Figure 5-3.

5.5.2 The effect of biodegradation on individual alkylnaphthalene isomers

To further examine the susceptibility of the alkylnaphthalenes to biodegradation, changes within the isomer groups were considered for samples from both sites.

SCVB sediments

Selected mass chromatograms revealing the presence of naphthalene, the MNs and the DMNs contained in the aromatic hydrocarbon fraction obtained from the SCVB samples in comparison with those contained in the NAPL are shown in Figure 5-11. For the NAPL and each sediment extract, the peak sizes for the three chromatograms have been preserved relative to each other to reflect the relative abundances, albeit uncorrected for differences in detector response.

Inspection of these chromatograms reveals that while naphthalene and both of the MN isomers are almost completely removed from the NAPL between the time of the initial release into the mangrove swamp and the collection of the SCVB 1 sediments, the relative abundance amongst the DMN isomers remains unchanged. Subsequent to this, that is beyond Biodegradation Level 2 to 3, changes in the distribution of the DMNs become apparent, with the depletion of 1,6-DMN and either or both of the co-eluting 2,6-DMN and 2,7-DMN relative to the other isomers the most obvious. Eventually, all of the DMN isomers are completely removed from the mixture as observed in the chromatogram from SCVB 5 (Level 5 to 6). The rapid decline in DMN abundance between release of the NAPL and collection of SCVB 1 (Table 5-5) attributed to water washing and evaporation is not accompanied by a change in the relative abundances amongst the DMNs. Conversely, the depletion of 1,6-DMN is coincident with a relatively small change in the abundance of the total DMNs.

Mass chromatograms showing the presence of the TMNs (m/z 156) and the TeMNs (m/z 184) contained in SCVB samples are shown in Figure 5-12. In each instance, the peak sizes of the TMNs relative to the TeMNs are indicative of the relative abundances of each. Inspection of these reveals that the distribution of TMN abundances remained relatively unaltered between the release of the NAPL and the collection of SCVB 1 (Level 2 to 3). In all samples collected after this, there is an obvious sequential depletion of 1,3,6-TMN relative to the other TMNs, while between SCVB3 (Level 3 to 4) and SCVB4 (Level 5), a decrease in abundance of 1,2,5-TMN (i.e. 1,5,6-TMN) is also apparent. The TMNs are almost completely removed from the mixture of alkylnaphthalenes in SCBV5 (Level 5 to 6).

As with the DMNs, the marked decrease in total TMN abundance (Table 5-5) between the NAPL (300) and SCVB 1 (97) attributed to water washing and evaporation is not concurrent with the selective depletion of the 1,3,6-TMN. Conversely, the TeMN distribution is relatively unaltered in all samples with the exception of SCVB 5 (Level 5 to 6), where there is an obvious depletion in the abundance of 1,3,6,7-TeMN, 1,2,6,7-TeMN and one or more of the co-eluting triplet of 1,4,6,7-TeMN, 1,2,4,6-TeMN and 1,2,4,7-TeMN. The transition between these two samples is also marked by the general decrease in abundance of the earlier eluting mixture of C_4-naphthalenes (i.e. not TeMNs) that will not be discussed in further detail here. Although the total TeMN abundance in the NAPL is somewhat greater than that measured in SCVB 1, the most significant decrease coincides with the perceptible change in isomer distribution between SCVB 4 and SCVB 5. To enable the quantification of the co-eluting alkylnaphthalenes, the aromatic fractions were also analysed using direct deposition GC-FTIR as described in Chapter 3. The results from these analyses are summarised in Table 5-7, where the abundance of each compound is expressed relative to the conserved internal marker 1,8-DMP.

To emphasise the susceptibility to biodegradation of individual compounds, the most resistant isomer within each group was chosen as a local, conserved internal marker against the abundance of which the other compounds were normalised. This approach was adopted to minimise the effects of variable water washing and evaporation on the basis that the isomers differ little in vapour pressure and aqueous solubility, as shown in Table 5-6. For example, amongst the two isomers of methylnaphthalene, 1-MN was identified as the most resistant isomer from the chromatograms shown in Figure 5-11, and the normalised abundances in Table 5-7. Based on similarities in vapour pressure and aqueous solubility, the abundance of naphthalene has also been calculated relative to the methylnaphthalene isomers.

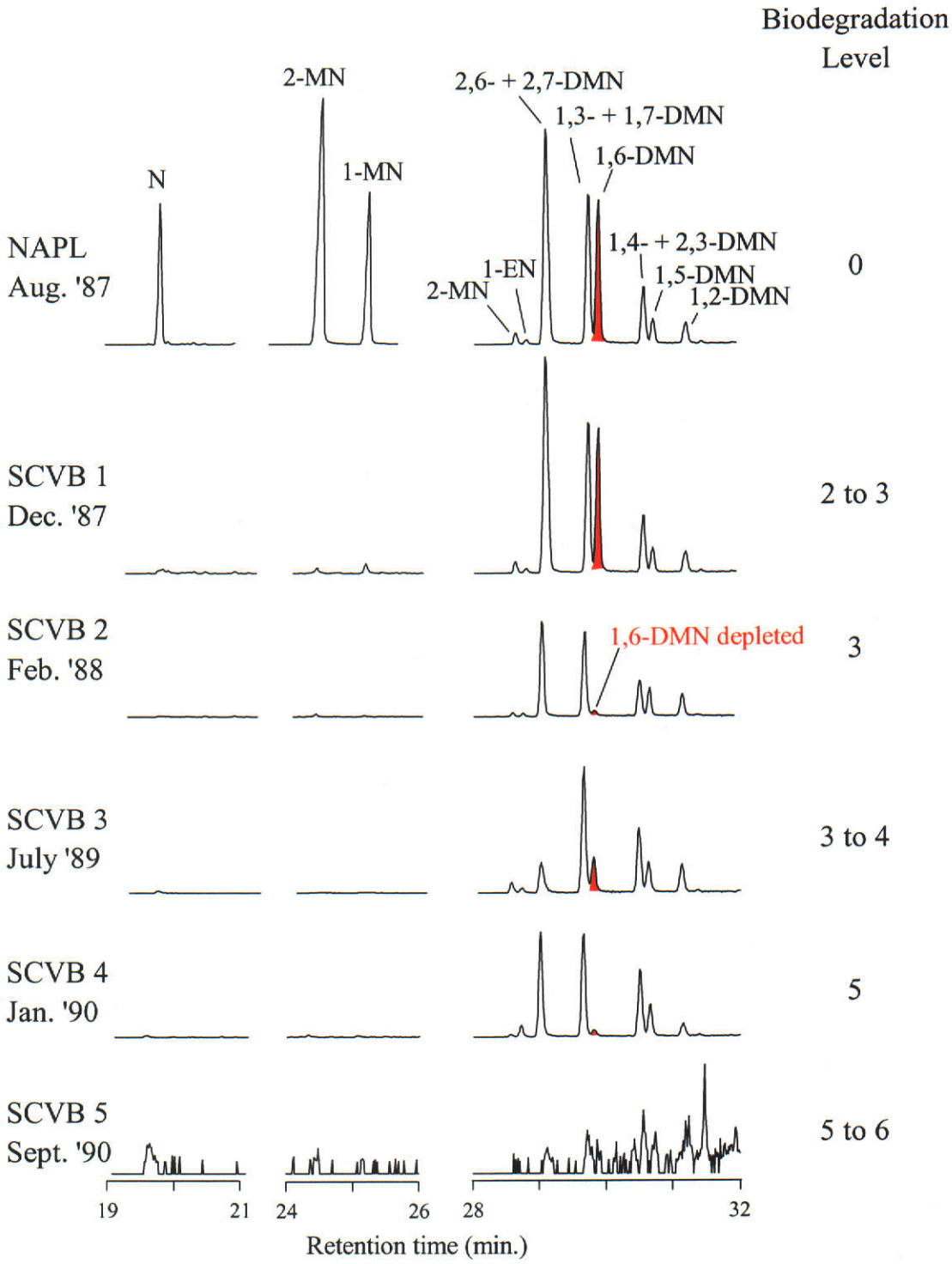

Figure 5-11: Mass chromatograms showing naphthalene (N, m/z 128), methylnaphthalenes (MNs, m/z 142) and dimethylnaphthalenes (DMNs, m/z 156) present in sediments collected from the SCVB contaminated site.

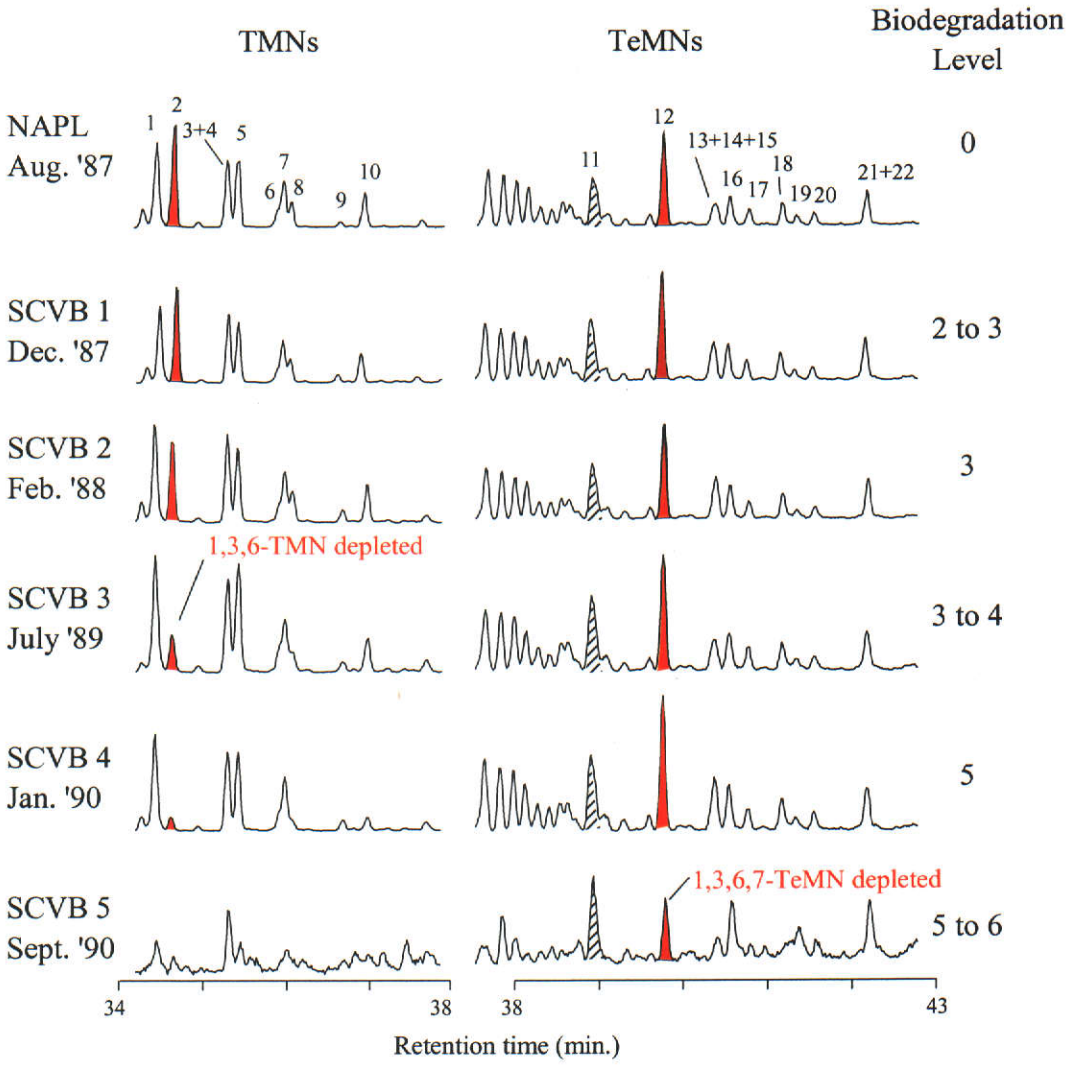

Figure 5-12: Mass chromatograms showing trimethylnaphthalenes (TMNs, m/z 170), and tetramethylnaphthalenes (TeMNs, m/z 184) present in sediments collected from the SCVB contaminated site. Peak identifications: (1) 1,3,7-TMN; (2) 1,3,6-TMN; (3) 1,4,6-TMN; (4) 1,3,5-TMN;(5) 2,3,6-TMN; (6) 1,2,7-DMN; (7) 1,6,7-TMN; (8) 1,2,6-TMN; (9) 1,2,4-TMN; (10) 1,2,5-TMN; (11) 1,3,5,7-TeMN; (12) 1,3,6,7-TeMN; (13) 1,2,4,6-TeMN; (14) 1,2,4,7-TeMN; (15) 1,4,6,7-TeMN; (16) 1,2,5,7-TeMN; (17) 2,3,6,7-TeMN; (18) 1,2,6,7-TeMN; (19) 1,2,3,7-TeMN; (20) 1,2,3,6-TeMN;(21) 1,2,3,5-TeMN and (22) 1,2,5,6-TeMN.

Table 5-7: Relative abundances of naphthalene (N), methylnaphthalenes (MNs), ethylnaphthalenes (ENs), dimethylnaphthalenes (DMNs), trimethylnaphthalenes (TMNs) and tetramethylnaphthalenes (TeMNs) measured in the SCVB sample set. Abundances were calculated from GC-MS and GC-FTIR peak areas corrected for differences in detector response normalised against that of 1,8-DMP. Similar information is also shown for NAPL obtained from the OCW system.

Sample Name	NAPL	SCVB 1	SCVB 2	SCVB 3	SCVB 4	SCVB 5
Level of Biodegradation	0	2-3	3	3-4	5	5-6
N	72	0.01	0.00	0.00	0.00	0.00
2-MN	280	0.18	0.00	0.00	0.00	0.00
1-MN	130	0.29	0.00	0.00	0.00	0.00
2-EN	21	0.89	0.71	0.76	0.59	0.00
1-EN	7.2	0.30	0.64	0.33	2.9	0.00
2,6-DMN	120	6.1	8.1	1.1	13	0.00
2,7-DMN	96	5.0	1.4	0.38	0.71	0.00
1,3-DMN	76	3.9	3.1	2.3	1.4	0.00
1,7-DMN	55	2.9	5.6	2.8	13	0.00
1,6-DMN	110	5.6	0.53	1.3	0.85	0.00
2,3-DMN	19	1.0	2.3	1.7	7.4	0.00
1,4-DMN	29	1.5	1.7	1.0	2.6	0.00
1,5-DMN	20	0.95	2.5	1.2	4.4	0.00
1,2-DMN	20	0.94	2.3	1.3	1.9	0.00
1,3,7-TMN	61	19	21	16	38	0.41
1,3,6-TMN	66	21	16	4.6	4.9	0.10
1,3,5-TMN	26	7.7	9.5	6.3	14	0.54
1,4,6-TMN	25	8.7	8.8	5.6	16	0.15
2,3,6-TMN	43	14	15	14	26	0.34
1,2,7-TMN	9.9	3.5	3.1	3.3	5.0	0.08
1,6,7-TMN	29	10	11	6.6	21	0.26
1,2,6-TMN	15	5.0	5.5	2.4	3.6	0.06
1,2,4-TMN	5.4	2.0	2.6	1.4	3.8	0.12
1,2,5-TMN	21	6.7	7.4	4.2	4.8	0.03
1,3,5,7-TeMN	20	14	15	14	23	4.7
1,3,6,7-TeMN	25	18	18	15	27	2.1
1,2,4,7-TeMn	2.8	2.1	3.2	1.4	4.1	1.1[1]
1,2,4,6-TeMn	2.8	2.1	3.2	1.4	4.1	n.d.
1,4,6,7-TeMn	4.8	3.9	3.7	2.9	5.7	n.d.
1,2,5,7-TeMn	8.9	6.2	6.7	5.3	10	2.3
2,3,6,7-TeMN	4.7	3.1	3.2	3.2	4.8	n.d.
1,2,6,7-TeMn	6.5	4.9	5.4	4.1	8.1	n.d.
1,2,3,7-TeMN	2.6	1.8	2.0	1.8	3.2	n.d.
1,2,3,6-TeMN	3.3	2.2	2.2	2.0	4.1	n.d.
1,2,5,6-TeMN	6.0	4.7	5.0	3.6	5.9	1.2
1,2,3,5-TeMN	4.0	3.1	3.0	3.1	3.9	1.0

NB (1): The sum of 1,2,4,7-TeMN, 1,2,4,6-TeMN and 1,4,6,7-TeMN is presented for SCVB 5.

The results from this treatment are represented graphically in Figure 5-13, where the level of biodegradation is based on the alteration of the saturated hydrocarbons summarised in Table 5-4. Although naphthalene and the MNs are present only in the NAPL and SCVB 1, it is evident that naphthalene is depleted to a greater extent than 2-MN, which in turn is far more susceptible to depletion than 1-MN.

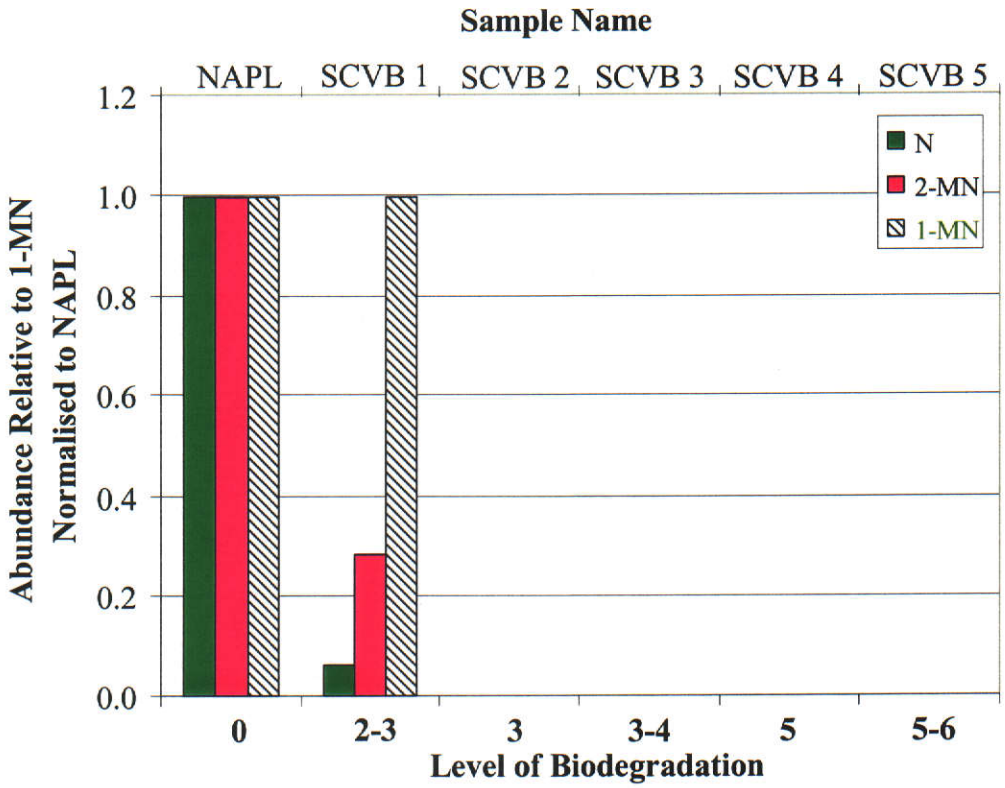

Figure 5-13: A bar chart showing changes in the abundances of naphthalene, 1-MN and 2-MN relative to the conserved internal marker 1-MN in sediments collected from the SCVB contaminated site. Abundances are expressed as a proportion of those measured in the sample of NAPL recovered from the OCW system.

Based on the results presented in Table 5-7, the selection of a suitable biodegradation-resistant internal marker compound from within the DMNs is less clear. To this end, the contribution (per cent relative abundance) of each DMN isomer to the sum of the isomers was calculated for each sample. The relative abundance for each was expressed as a proportion of that measured in the NAPL to investigate the depletion between samples, as shown in Figure 5-14(a). From this representation of the data, the extent to which a compound is depleted in the petroleum between collection of successive samples is inversely related to the

gradient of the line between the two. The relative abundance of 1,6-DMN exhibits a negative gradient between SCVB 1 and SCVB 2, illustrative of its severe and rapid depletion relative to that of 2,3-DMN, which shows a positive gradient between these and subsequent sampling events. On this basis 2,3-DMN was identified as the internal marker against which the abundances of the other isomers were compared, including that of the two ethylnaphthalenes. The results of this treatment are shown in Figure 5-14(b), from which the susceptibility to biodegradation emerges. It is evident that 1,7-DMN, 1,2-DMN, 1,5-DMN and 2,3-DMN display an apparent resistance to biodegradation, 1,6-DMN and 2,7-DMN exhibit a strong susceptibility to biodegradation, while 1,3-DMN, 1,4-DMN and 2.6-DMN are intermediate between these.

The apparent susceptibility of 2-EN relative to 1-EN is also evident, consistent with the order of the depletion amongst the MNs. Although the discrimination between the isomers commences at approximately the same extent of biodegradation as for the DMNs (Level 3), it is also clear that the susceptibility to biodegradation of 1-EN is somewhat greater than the more resistant DMN isomers.

The TMNs were examined in a similar manner and the results are presented in Figure 5-15. The most striking features here are the successive depletion of 1,3,6-TMN relative to the other isomers, initially between SCVB 1 (Level 2 to 3) and SCVB 2 (Level 3), and the relative resistance of 1,2,4-TMN. Normalisation against the abundance of 1,2,4-TMN revealed the susceptibility of other isomers including 1,2,6-TMN and 1,2,5-TMN (i.e. 1,5,6-TMN), and to a lesser extent 1,6,7-TMN. Four of the five isomers present in SCVB samples with a 1,6-substitution pattern are therefore amongst the most susceptible to biodegradation. Furthermore, the fifth of these, 1,4,6-TMN, is rapidly depleted relative to 1,3,5-TMN between biodegradation Level 5 (SCVB 4) and Level 5 to 6 (SCVB 5).

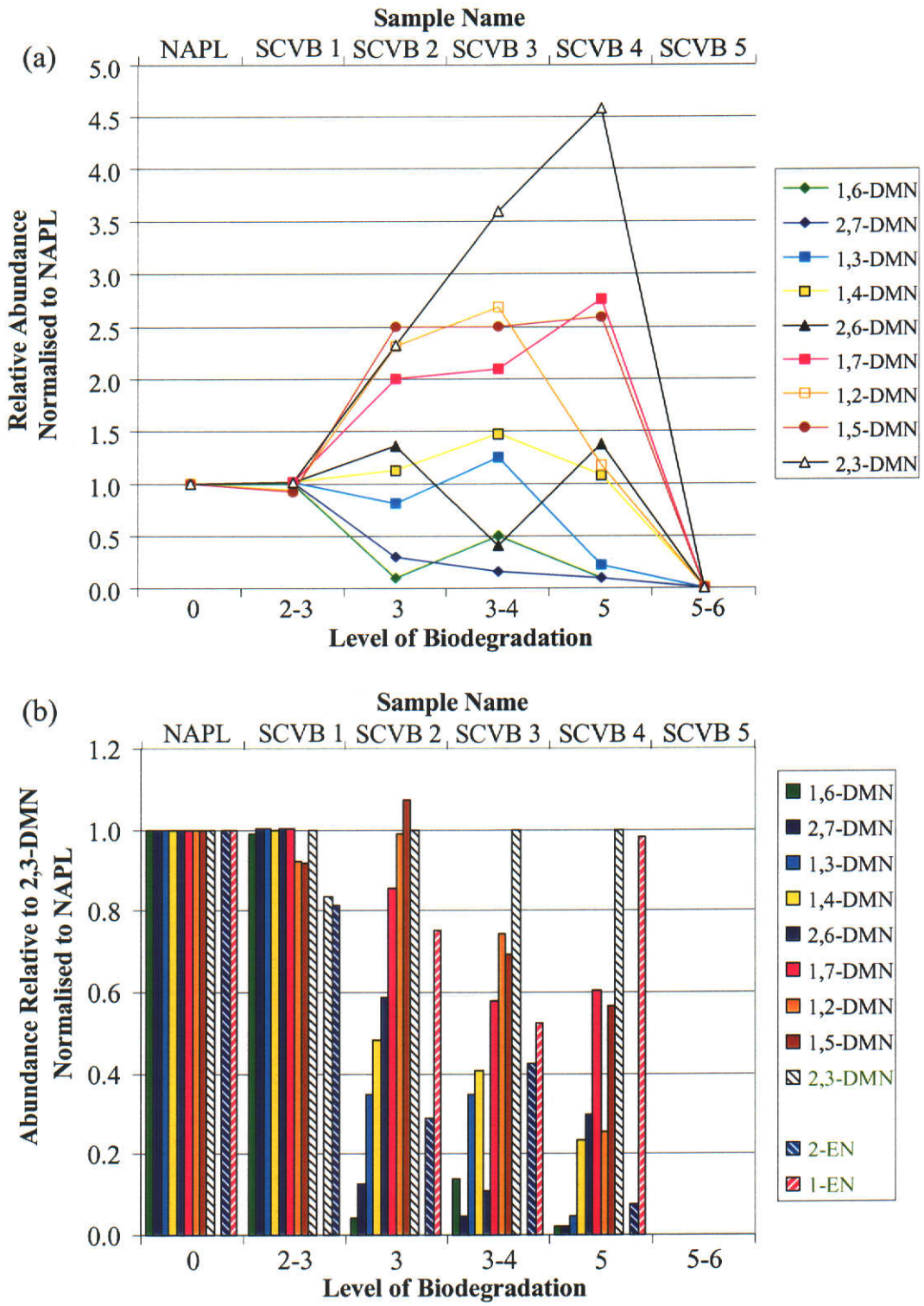

Figure 5-14: Graphs showing changes in the relative abundances of individual DMNs and ENs present in sediments collected from the SCVB contaminated site. Abundances are expressed as a proportion of those measured in the sample of NAPL collected from the OCW system.

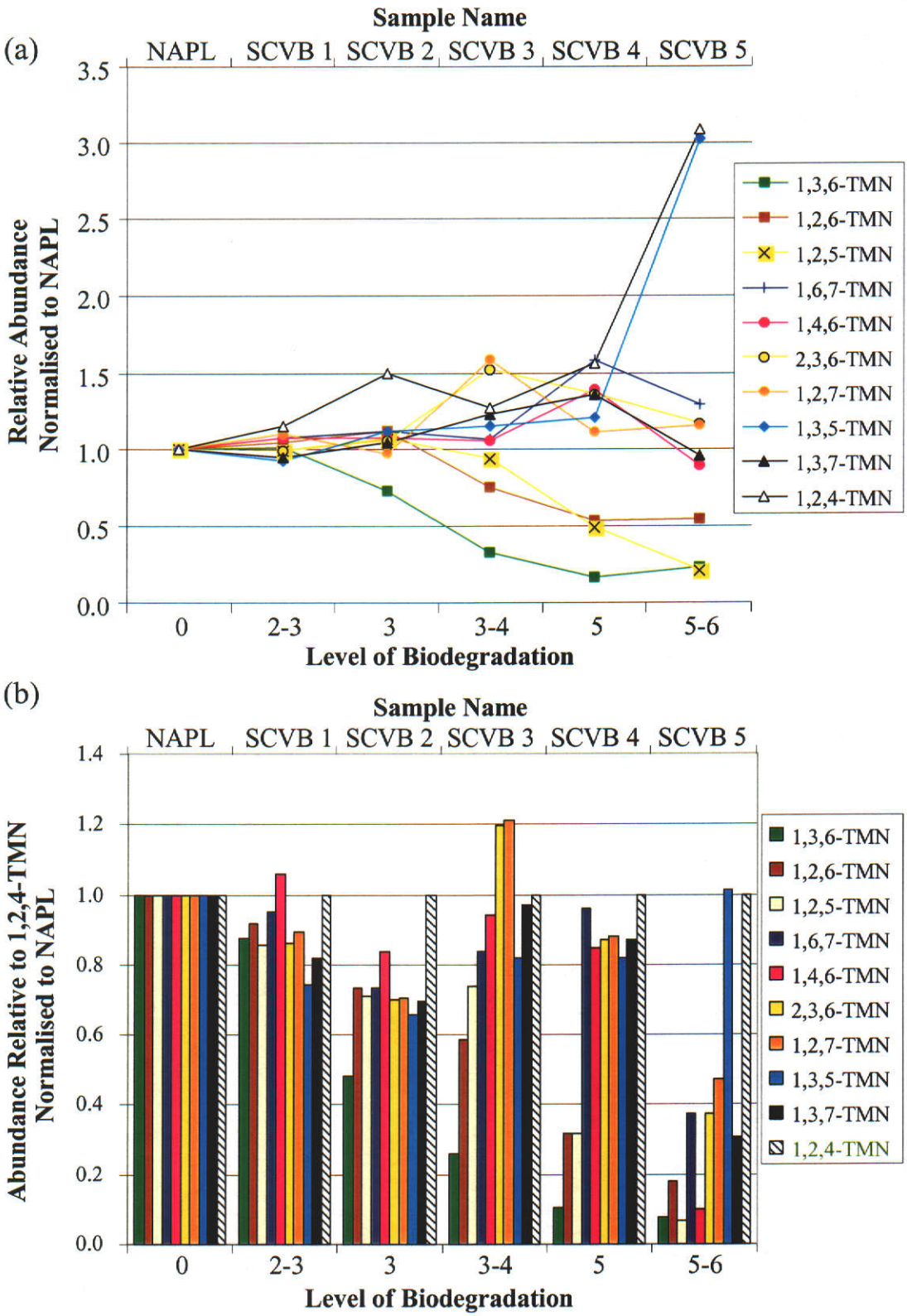

Figure 5-15: Graphs showing changes in the relative abundances of individual TMNs present in sediments collected from the SCVB contaminated site. Abundances are expressed as a proportion of those measured in the sample of NAPL collected from the OCW system.

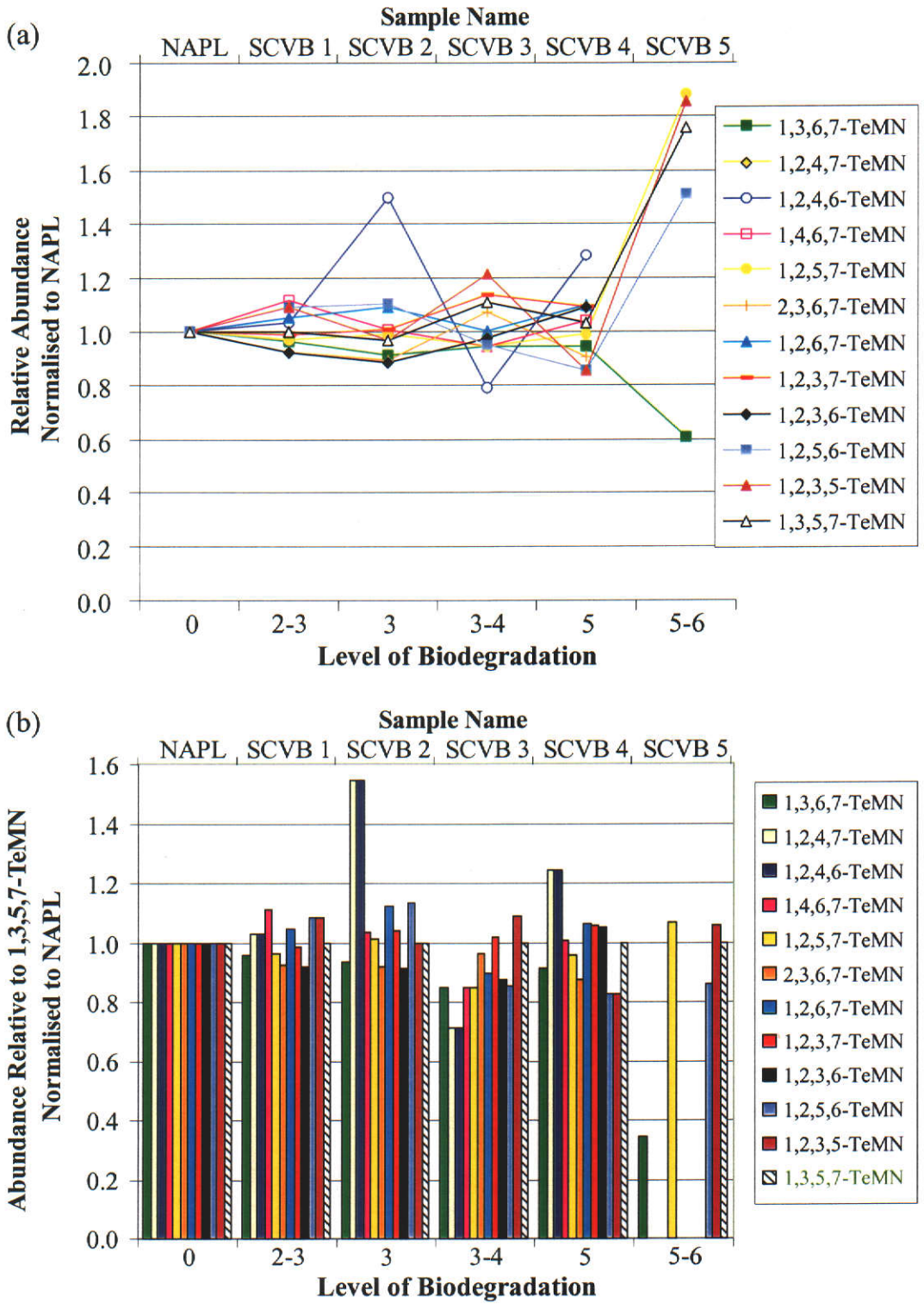

Figure 5-16: Graphs showing changes in the relative abundances of individual TeMNs present in sediments collected from the SCVB contaminated site. Abundances are expressed as a proportion of those measured in the sample of NAPL collected from the OCW system.

The results from the analysis of the TeMN are similarly presented in Figure 5-16. It is evident that until the extent of biodegradation reaches Level 5 (SCVB 4), the relative isomer abundances are comparatively unaltered. Beyond this level, only five TeMNs could be positively identified in the mixture due to severe interference from co-eluting compounds. Amongst these identified compounds, there is a significant decrease in the abundance of 1,3,6,7-TeMN, while that of the other four isomers remains relatively constant. Although other isomers not identified in the mixture may have also been depleted to a greater extent, for example one or more of the co-eluting 1,2,4,7-TeMN, 1,2,4,6-TeMN and 1,4,6,7-TeMN, these could not be quantified.

NEC Sediments

Mass chromatograms were obtained from the NEC samples to reveal the presence of naphthalene, the MNs and DMNs. These are presented in Figure 5-17. For comparison, similar chromatograms obtained from the NAPL are also shown in this figure. Although there is insufficient evidence to identify the NAPL as the source of the aromatic hydrocarbons in the NEC sediments, the distributions of DMNs in the NAPL and the petroleum extracted from NEC 1 are similar.

The MNs are detectable in the extracts from the first three members of this series and naphthalene in the first two, albeit in lower abundance. It is evident from examination of these chromatograms that naphthalene is depleted more rapidly than 2-MN which in-turn is depleted more rapidly than 1-MN. These observations are summarised in Figure 5-18, which shows the depletion of the other two compounds relative to 1-MN with increasing extent of biodegradation. In the absence of an authentic sample of the material released into this site, changes in abundance are expressed relative to NEC 1.

Coincident with these changes is the reduction of 2-EN relative to 1-EN, and the depletion of 1,6-DMN relative to the other DMN isomers, the diminution of which continues through the latter samples in this series. Less obvious is the narrowing of the peak arising from the co-elution of 2,6-DMN and 2,7-DMN, perhaps indicating the removal of one of these from the mixture. In fact this was shown to be the case

when the abundance of each of the individual isomers was determined by complementing these GC-MS analyses with GC-FTIR techniques, the results of which are shown in Table 5-8.

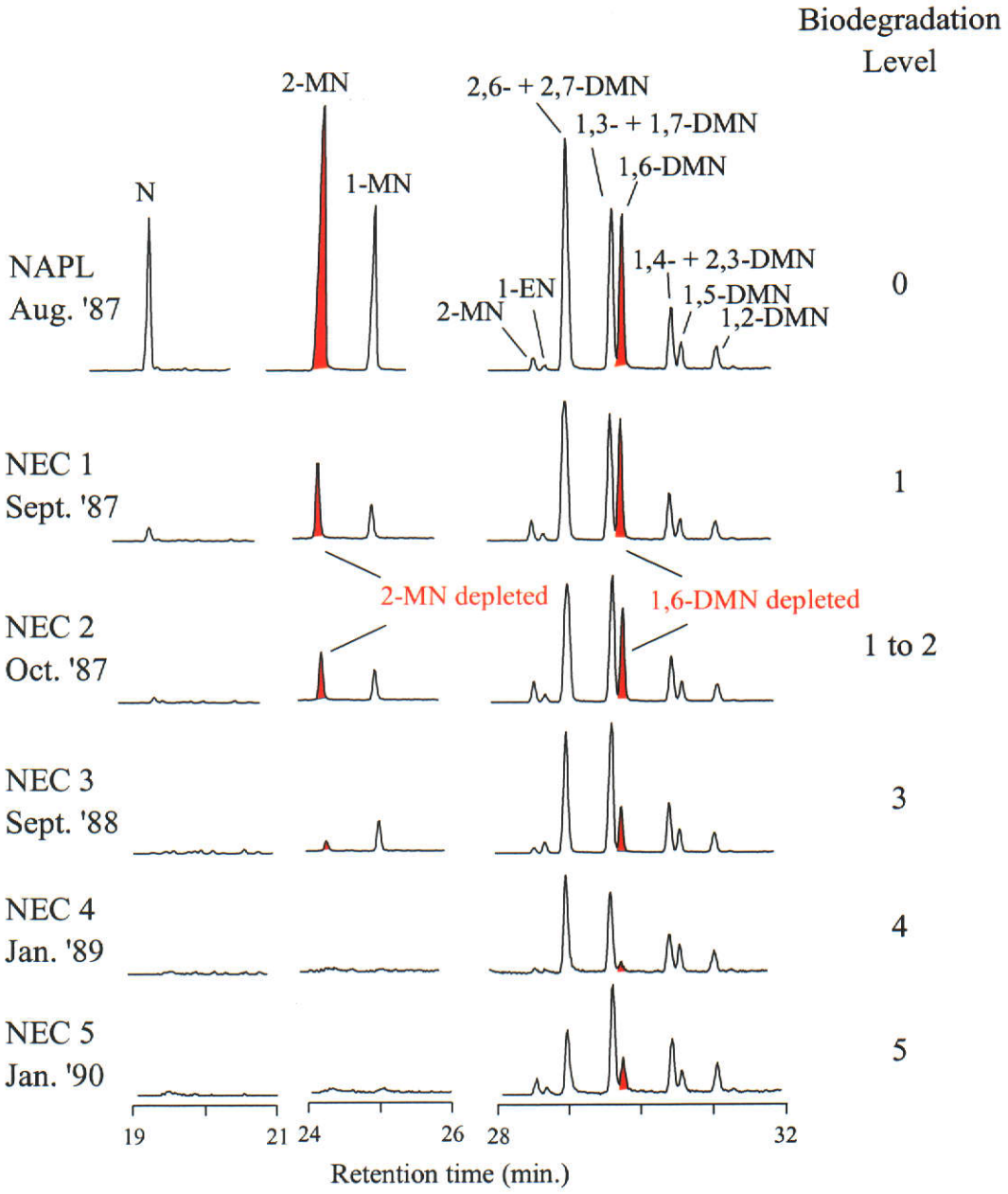

Figure 5-17: Mass chromatograms showing naphthalene (N, m/z 128), methylnaphthalenes (MNs, m/z 142) and ethylnaphthalenes and dimethylnaphthalenes (ENs and DMNs, m/z 156) present in a sample of NAPL and sediments collected from the NEC contaminated site.

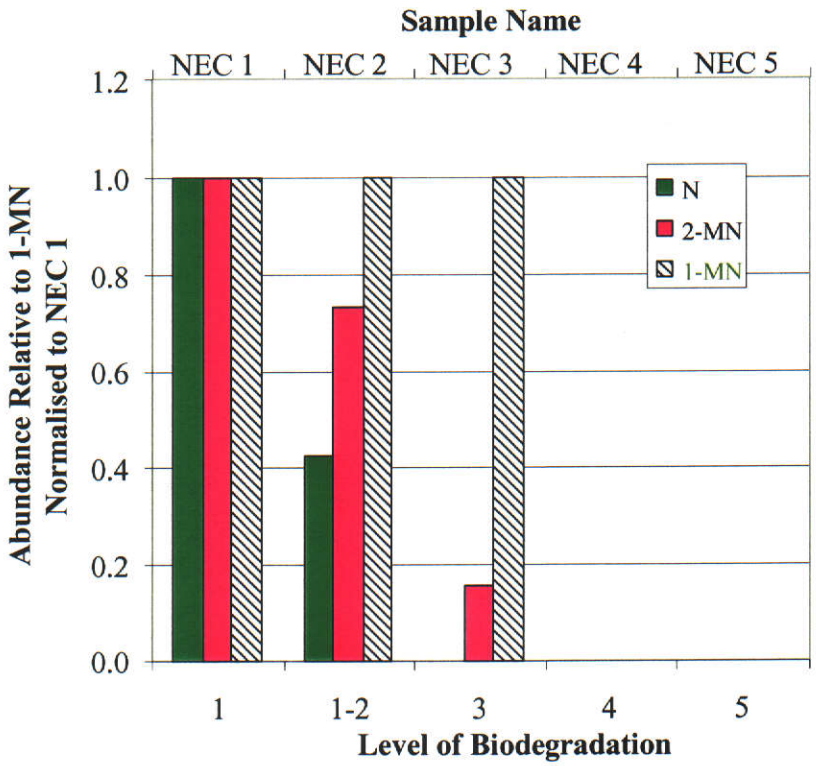

Figure 5-18: A bar chart showing changes in the abundances of naphthalene, 1-MN and 2-MN relative to the conserved internal marker 1-MN in sediments collected from the NEC contaminated site. Abundances are expressed as a proportion of those measured in the sample NEC 1, which contained the petroleum with the least-biodegraded hydrocarbon signature.

The alteration within the DMN and EN isomer distribution is illustrated by Figure 5-19. As for the SCVB sediments, 2,3-DMN was selected as the conserved internal marker amongst these compounds on the basis of its resistance to biodegradation. It is evident that 1,7-DMN, 1,2-DMN, 1,5-DMN and 2,3-DMN are resistant to biodegradation, 1,6-DMN and 2,7-DMN are susceptible to biodegradation, while 1,4-DMN, 1,3-DMN and 2,6-DMN are intermediate between these.

Notably, the most degraded petroleum sample (NEC 5, Biodegradation Level 5) exhibits a less biodegraded signature within the C_2-naphthalenes than NEC 4 (Level 4). This behaviour is evidently not related to anomalies in the overall abundance of the DMNs, as shown in Table 5-5. In spite of this non-conformance, the observations of biodegradation susceptibility for the MNs, ENs and DMNs are generally consistent with those from the SCVB site.

Table 5-8: Relative abundances of naphthalene (N), methylnaphthalenes (MNs), ethylnaphthalenes (ENs), dimethylnaphthalenes (DMNs), trimethylnaphthalenes (TMNs) and tetramethylnaphthalenes (TeMNs) measured in the NEC sample set. Abundances were calculated from GC-MS and GC-FTIR peak areas, corrected for differences in detector response, normalised against that of 1,8-DMP. Similar information is also shown for NAPL obtained from the OCW system.

Sample Name	NAPL	NEC 1	NEC 2	NEC 3	NEC 4	NEC 5
Level of Biodegradation	0	1	1-2	3	4	5
N	72	0.70	0.38	0.0	0.0	0.0
2-MN	280	5.0	4.6	3.7	0.0	0.0
1-MN	130	2.3	3.0	11	0.0	0.0
2-EN	21	3.3	5.1	4.7	0.46	0.96
1-EN	7.2	1.3	1.9	10	0.32	0.50
2,6-DMN	120	9.8	12	41	4.9	2.0
2,7-DMN	96	8.0	9.7	22	0.87	0.86
1,3-DMN	76	6.5	10	27	0.80	2.3
1,7-DMN	55	5.9	8.3	44	3. 8	2.2
1,6-DMN	110	10	11	21	0.46	1.3
2,3-DMN	19	2.3	3.9	18	1.5	1.5
1,4-DMN	29	2.1	2.3	6.4	0.83	0.70
1,5-DMN	20	1.8	2.5	10	1.4	0.98
1,2-DMN	20	1.8	2.5	10	1.2	1.2
1,3,7-TMN	61	20	19	49	20	11
1,3,6-TMN	66	23	21	45	4.9	1.7
1,3,5-TMN	26	11	8.7	17	7.8	5.6
1,4,6-TMN	25	9.6	9.2	21	6.9	5.2
2,3,6-TMN	43	16	15	37	14	7.8
1,2,7-TMN	9.9	3.5	3.1	8.8	1.8	1.4
1,6,7-TMN	29	16	10	25	8.0	4.8
1,2,6-TMN	15	5.8	4.9	12	2.8	2.1
1,2,4-TMN	5.4	2.6	2.6	4.4	2.4	1.4
1,2,5-TMN	21	8.8	7.4	16	4.1	3.9
1,3,5,7-TeMN	20	19	16	22	21	13
1,3,6,7-TeMN	25	21	17	26	19	12
1,2,4,7-TeMN	2.8	3.1	3.0	3.3	3.5	2.3
1,2,4,6-TeMN	2.8	3.1	3.0	3.3	3.5	2.3
1,4,6,7-TeMN	4.8	4.9	4.3	5.1	5.9	3.6
1,2,5,7-TeMN	8.9	8.4	6.6	8.9	7.5	5.7
2,3,6,7-TeMN	4.7	4.3	3.6	4.4	4.0	2.7
1,2,6,7-TeMN	6.5	6.6	5.5	7.0	6.1	3.7
1,2,3,7-TeMN	2.6	2.1	1.6	2.5	2.3	1.8
1,2,3,6-TeMN	3.3	2.5	2.5	3.5	2.9	1.7
1,2,5,6-TeMN	6.0	6.5	5.3	6.3	6.9	3.8
1,2,3,5-TeMN	4.0	3.6	2.6	3.7	3.9	2.6

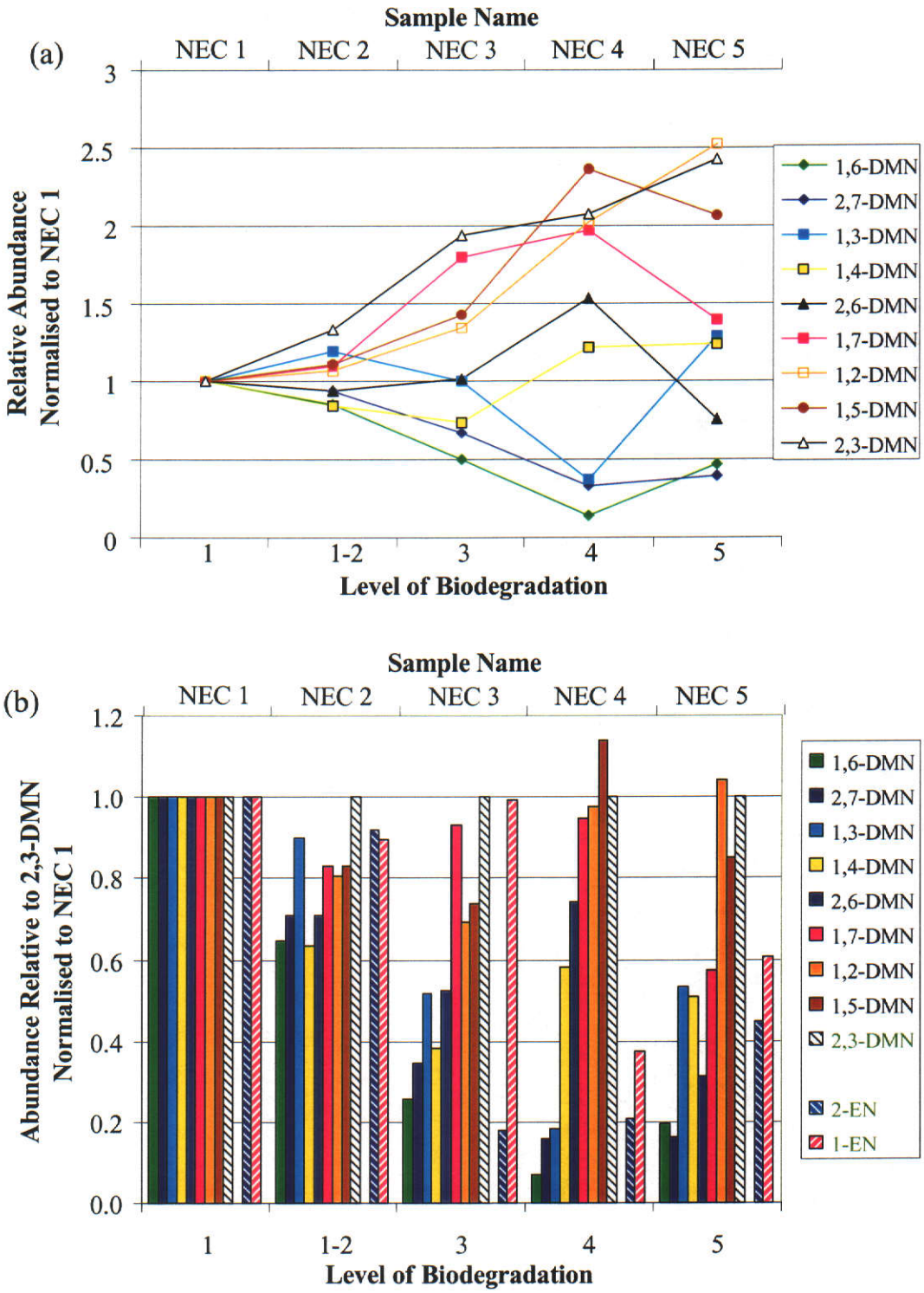

Figure 5-19: Graphs showing changes in the relative abundances of individual DMNs and ENs present in sediments collected from the NEC contaminated site. Abundances are expressed as a proportion of those measured in NEC 1, which contained the petroleum with the least biodegraded hydrocarbon signature.

Mass chromatograms showing the presence of the TMNs and the TeMNs in the NEC sample set are shown in Figure 5-20. From comparison with the corresponding chromatograms from the SCVB site, shown in Figure 5-12, it is clear that the distribution of both groups of compounds is less extensively altered in the NEC sediments. The extent of alteration is commensurate with the extent of biodegradation assigned to each sample, especially evident from comparison of the TMNs contained in samples NEC1 (Biodegradation Level 1), NEC 2 (Level 1.5) and NEC 3 (Level 3) with those in SCVB 1 (Level 2.5), SCVB 2 (Level 3) and SCVB 3 (Level 3.5).

The relative abundances of the TMNs also shown in Table 5-8 are graphed in Figure 5-21. The most obvious alteration within the NEC sample set is the sequential depletion of 1,3,6-TMN between the collection of NEC 3 (Level 3) and NEC 5 (Level 5). Although 1,2,4-TMN does not exhibit an outstanding resistance to biodegradation in these sediments, for consistency with the SCVB sediments it was chosen as the conserved internal marker for the TMNs in preference to 1,3,7-TMN.

Although biodegradation is less extensive in the NEC sediments, changes in the relative abundances of the TMN isomers are broadly consistent with those observed for the SCVB sediments. Here the preferential depletion of four of the five isomers with a 1,6-subtitution pattern, namely 1,3,6-TMN, 1,2,6-TMN, 1,2,5-TMN and 1,6,7-TMN is again evident. Consistent with observations for the C_2-naphthalenes, the TMNs contained in NEC 5 (Level 5) also display a less biodegraded signature than NEC 4 (Level 4), especially with 1,2,5-TMN, 1,2,6-TMN and 1,4,6-TMN.

From the chromatograms shown in Figure 5-20, the change in the distribution of the TeMN isomers is barely perceptible. This is illustrated in Figure 5-22, where 1,3,5,7-TeMN was selected as the conserved TeMN isomer. Although there is some evidence for the depletion of 1,3,6,7-TeMN, as shown in Figure 5-22 (b), this decrease in abundance is minor and perhaps no more significant than for several other isomers including 1,2,6,7-TeMN, 1,2,5,6-TeMN, 1,2,5,7-TeMN and 2,3,6,7-TeMN.

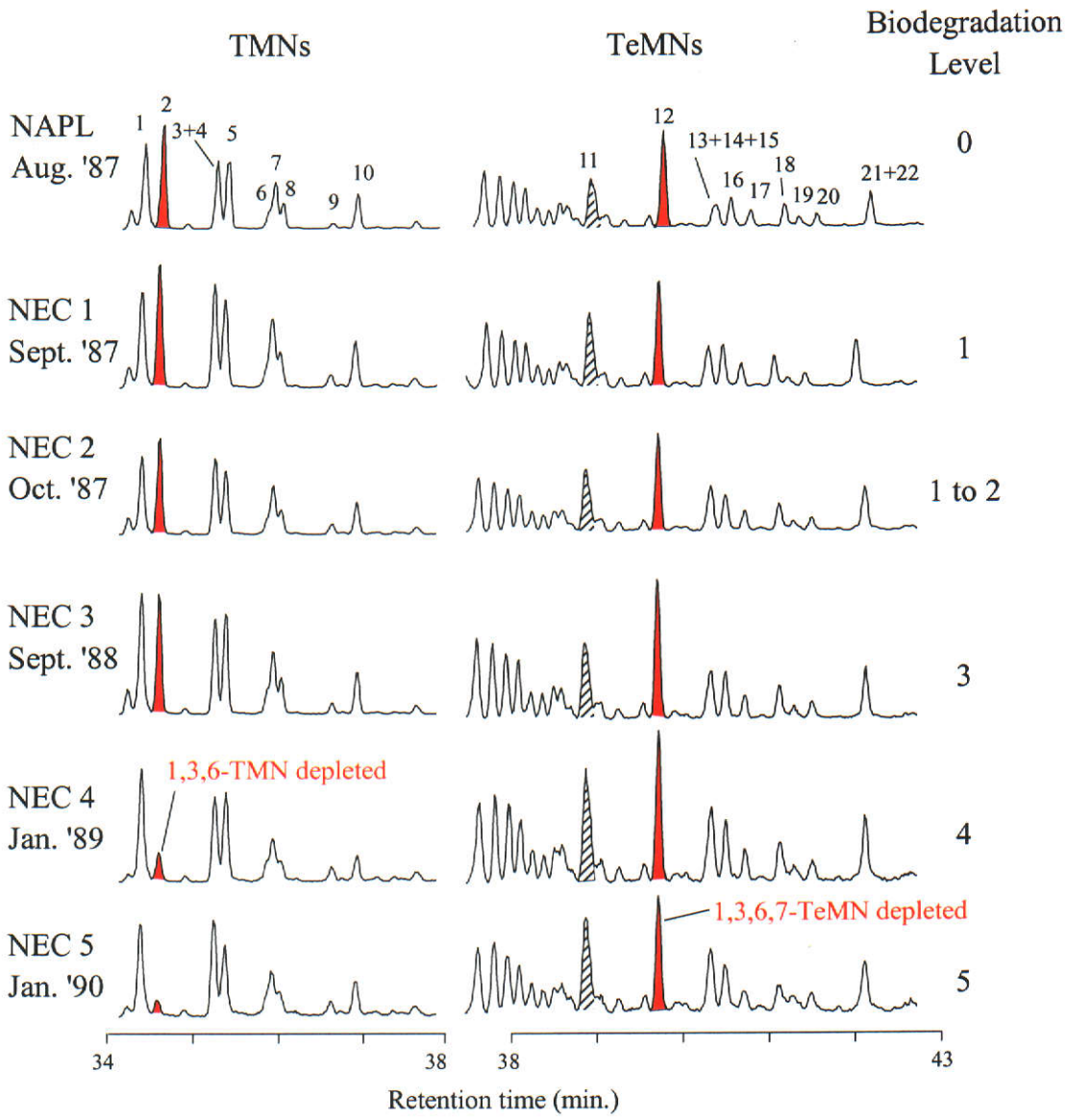

Figure 5-20: Mass chromatograms showing trimethylnaphthalenes (TMNs, m/z 170), and tetramethylnaphthalenes (TeMNs, m/z 184) present in a sample of NAPL, and sediments collected from the NEC contaminated site. Peak identifications: (1) 1,3,7-TMN; (2) 1,3,6-TMN; (3) 1,4,6-TMN; (4) 1,3,5-TMN;(5) 2,3,6-TMN; (6) 1,2,7-DMN; (7) 1,6,7-TMN; (8) 1,2,6-TMN; (9) 1,2,4-TMN; (10) 1,2,5-TMN; (11) 1,3,5,7-TeMN; (12) 1,3,6,7-TeMN; (13) 1,2,4,6-TeMN; (14) 1,2,4,7-TeMN; (15) 1,4,6,7-TeMN; (16) 1,2,5,7-TeMN; (17) 2,3,6,7-TeMN; (18) 1,2,6,7-TeMN; (19) 1,2,3,7- TeMN; (20) 1,2,3,6-TeMN;(21) 1,2,3,5-TeMN and (22) 1,2,5,6-TeMN.

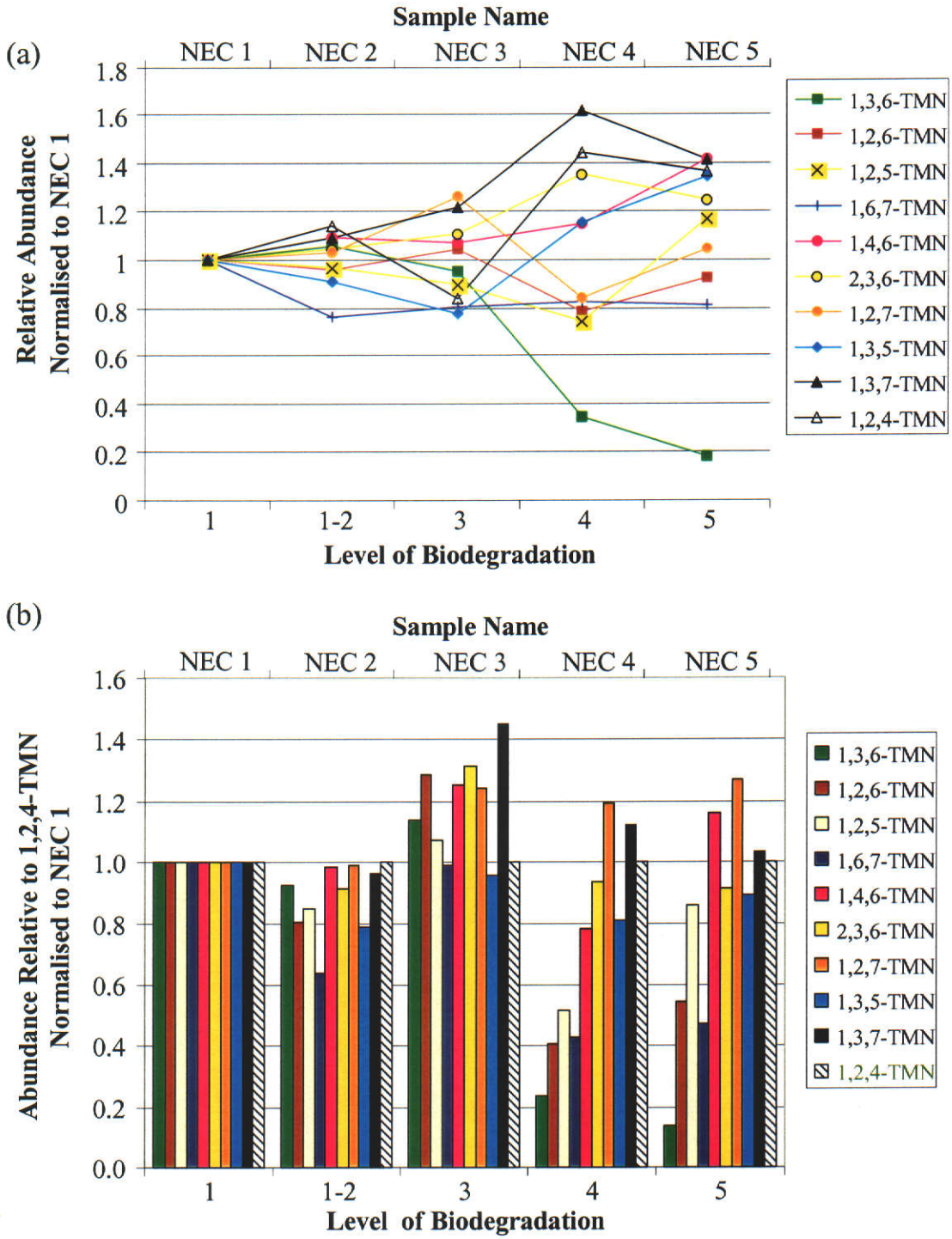

Figure 5-21: Graphs showing changes in the relative abundances of individual TMNs present in sediments collected from the NEC contaminated site. Abundances are expressed as a proportion of those measured in NEC 1, which contained the petroleum with the least-biodegraded hydrocarbon signature.

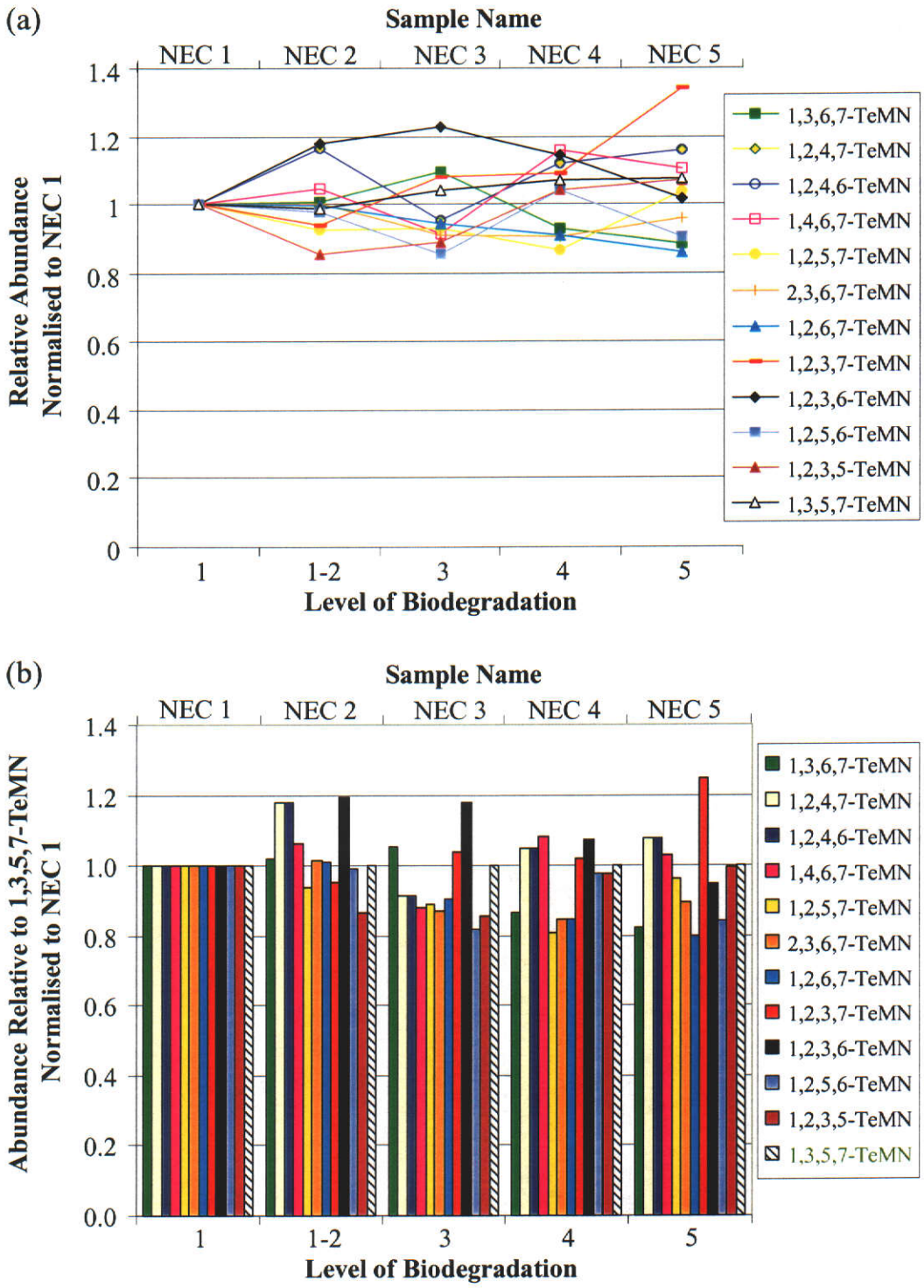

Figure 5-22: Graphs showing changes in the relative abundances of individual TeMNs present in sediments collected from the NEC contaminated site. Abundances are expressed as a proportion of those measured in measured in NEC 1, which contained the petroleum with the least-biodegraded hydrocarbon signature.

There is a striking similarity between the relative abundances of the individual TeMNs measured in the NAPL and in the NEC 1, shown in Table 5-8. This similarity extends to all samples within this series with the exception of NEC 5, where there is a general decrease in all isomers of the TeMNs. This similarity indicates that the NAPL may in fact be a good model of the bulk of the source material of the contaminant petroleum at the NEC site, in spite of the confounding evidence of the steranes and hopanes, and the bimodal UCM distribution. The similarity in the abundances of the TeMNs observed between NEC 1 and NEC 3 is particularly notable, since NEC 3 contains anomalously high abundances of the less alkylated homologues of naphthalene. Although somewhat tenuous, this evidence further supports the assertion that exposure to water washing and evaporation greatly influence the total abundance of naphthalene, the MNs, DMNs and TMNs, while the TeMNs are effected to a much lesser extent.

Summary of alkylnaphthalene attenuation with biodegradation

The results presented thus far emphasise that the hierarchy of susceptibility to biodegradation of the alkylated naphthalenes according to the extent of alkylation, that is N > MNs > ENs > DMNs > TMNs > TeMNs. Furthermore, there is a correspondence between the biodegradation levels established from the composition of the saturated hydrocarbons and the observed changes in the aromatic hydrocarbons. For example, 2-MN is depleted relative to 1-MN at approximately Biodegradation Level 1 to 2 (NEC 2) while the depletion of 1,6-DMN commences at Level 3 (NEC 3 and SCVB 2). The distribution of TMNs is similarly initially altered at Level 3 to 4 (NEC 3, SCVB 3) marked by the depletion of 1,3,6-TMN. The TeMNs are altered only in the most biodegraded samples, namely NEC 5 (Level 5) and SCVB 5 (Level 5 to 6).

Within each of these groups of alkylnaphthalenes, preferential depletion of isomers occurs upon biodegradation. The order of susceptibility to biodegradation is summarised below, where the numbers refer to the position of methyl substituents on the naphthalene nucleus. Here, compounds were considered susceptible if their relative abundance decreased at the onset of alteration of the isomer distribution, and resistant if they maintained their abundance relative to the conserved internal marker

compound. Remaining compounds were classified as intermediate between these extremes. Although not identical, there is a striking similarity in the order of susceptibility to biodegradation at the two contaminated sites.

Most susceptible	**Intermediate**	**Most resistant**

Naphthalene and MNs

N > 2-MN >>1-MN (SCVB)

N >> 2-MN >>1-MN (NEC)

ENs

2 >> 1 (SCVB)

2 >> 1 (NEC)

DMNs

1,6 ~ 2,7 >> 1,3 ~ 1,4 ~ 2,6 > 1,7 ~ 1,2 ~1,5 >> 2,3 (SCVB)

1,6 ~ 2,7 > 1,3 ~ 1,4 ~ 2,6 >> 1,7 ~ 1,2 ~1,5 ~ 2,3 (NEC)

TMNs

1,3,6 > **1,2,6** ~ **1,2,5** >> **1,6,7** ~ **1,4,6** ~ 2,3,6 ~ 1,2,7 ~ 1,3,5 ~ 1,3,7 > 1,2,4 (SCVB)

1,3,6 > **1,2,6** ~ **1,2,5** ~ **1,6,7** > **1,4,6** ~ 2,3,6 ~ 1,3,5 > 1,3,7 ~ 1,2,7 ~ 1,2,4 (NEC)

TeMNs

1,3,6,7 >> 1,3,5,7 (SCVB)

1,3,6,7 > 1,3,5,7 (NEC)

From these relationships, it is evident that polymethylnaphthalenes with a 1,6-dimethyl substitution pattern (shown in bold) are more susceptible to biodegradation than other isomers which lack this feature, mindful of the fact that 1,2,5-TMN (i.e. 1,5,6-TMN) also contains methyl substituents on carbon atoms 1 and 6 of the naphthalene nucleus. This trend was also observed in the petroleum extracted from the sea-floor sediments discussed earlier in Chapter 4.

There is also a clear trend within the mono-alkylated naphthalenes for the enhanced susceptibility to biodegradation of the 2-substituted compounds. This alteration of the MNs is consistent with that observed in moderately biodegraded crude oils by Volkman et al. (1984) and by Williams et al. (1986). More recently, Johnston, Fisher and Rayner (2001) also reported the enhanced depletion of 2-MN relative to both

1-MN and naphthalene associated with the aerobic biodegradation of refined petroleum. Contrary to the behaviour observed here, in both of the studies of crude oils, the ENs were more resistant to biodegradation than the DMNs. Moreover, Volkman et al. (1984) concluded that 1-EN is more susceptible to biodegradation than 2-EN.

Water washing and evaporation also affected the alkylnaphthalenes at both contaminated sites investigated here. This is particularly evident between the release of the NAPL and the collection of the SCVB 1 some three months later. During this time, apart from the depletion of naphthalene and 2-MN relative to 1-MN, the isomer abundances were relatively unchanged. Reviewing the aqueous solubilities shown in Table 5-6 reveals that there is no correlation between solubility and the susceptibility to biodegradation within groups of isomers.

5.6 The effect of biodegradation on the abundances of phenanthrene and individual alkylphenanthrenes.

5.6.1 Gross changes in composition of the aromatic hydrocarbon mixture

As discussed earlier, sediment extracts from both sites and the NAPL contain phenanthrene, MPs and C_2-Ps, identified in the chromatograms shown in Figures 5-9 and 5-10. Using a similar approach to that used for the quantification of the alkylnaphthalenes, the abundance of phenanthrene, the total abundance of the MPs and the total of the C_2-Ps were determined relative to 1,8-DMP for the NAPL and both sets of sediment extracts. These results are presented in Table 5-9.

For the NEC sediments, the abundances of these compounds remain relatively constant in samples NEC 1(biodegradation Level 1), NEC 2 (Level 1 to 2) and NEC 3 (Level 3). Although the abundances of the MPs and C_2-Ps measured in NEC 3 are slightly higher than those measured in both the preceding samples, this increase is much less pronounced than that observed for the alkylnaphthalenes. Following this approximately one year long period of stable abundances, the abundance of phenanthrene and of the MPs decreased sharply between collection of NEC 3 and NEC 4 (Level 4), before again stabilising between the samples NEC 4 and NEC 5

(Level 5), collected one year afterwards. This behaviour is also observed in the abundances of the C_2-Ps, although the changes are much less pronounced.

Comparison of the values in Table 5-9 for the NAPL and SCVB 1 reveals that the NAPL contained 8.1 times the abundance of phenanthrene and 1.9 times that of the MPs extracted from the sediment. The C_2-Ps, however, are of similar abundance in both hydrocarbon mixtures. This direct relationship between the extent of alkylation of phenanthrene and similarity in abundance between the NAPL and the initial SCVB sediment extract is consistent with that observed for the alkylnaphthalenes and may also be indicative of water washing processes. As shown in Table 5-6, there is a substantial difference in aqueous solubility of phenanthrene (1.2 mg L^{-1}), the MPs (0.26-0.28 mg L^{-1}) and 3,6-DMP (0.071 mg L^{-1}). Further comparison shows that the solubility of phenanthrene is similar to that of the TMNs (1.7-4.8 mg L^{-1}) and from earlier discussion of the observations by Page et al. (2000), it is probable that the TeMNs and MPs have comparable solubilities.

Table 5-9: Relative abundances of phenanthrene (P), methylphenanthrenes (MPs), and ethylphenanthrenes and dimethylphenanthrenes (C_2-Ps), and the sum of P and these alkylphenanthrenes (∑APs) measured in sediment samples collected from the NEC and SCVB sites between September 1987 and September 1990. Abundances were calculated from the sum of GC-MS peak areas corrected for differences in detector response normalised against that of 1,8-DMP. Similar information is also shown for a NAPL sample collected from the OCW system.

Sample	Level of Biodegradation	P	MPs	C_2-Ps	∑APs
NAPL	0	30	71	53	150
SCVB 1	2-3	3.7	37	52	93
SCVB 2	3	2.0	31	52	85
SCVB 3	3-4	1.7	13	39	54
SCVB 4	5	0.50	16	42	59
SCVB 5	5-6	0.00	0.00	22	22
NEC 1	1	4.9	34	48	87
NEC 2	1-2	5.9	31	44	81
NEC 3	3	4.6	39	49	92
NEC 4	4	0.0	6.2	33	39
NEC 5	5	0.0	7.0	29	36

The SCVB sample set shows a more gradual depletion of phenanthrene and the MPs over the approximately three-year period between collection of SCVB 1 (biodegradation Level 2 to 3) and SCVB 5 (Level 5 to 6). Similarly to observations for the NEC 3 sediments, the anomalously high sum of the abundances of alkylnaphthalenes measured in SVCB 4 are not reflected in that of the alkylphenanthrenes. The abundance of the C_2-Ps remains constant in the first two samples SCVB 1 (Level 2 to 3) and SCVB 2 (Level 3), before decreasing significantly in SCVB 3 (Level 3 to 4). The most pronounced change in abundance, however, occurs between SCVB 4 (Level 5) and SCVB 5 (Level 5 to 6).

5.6.2 Changes in the abundances of individual alkylphenanthrene isomers

NEC sediments

The selected mass chromatograms showing the presence of phenanthrene, the MPs and C_2-Ps in the NEC sample set and the NAPL are shown in Figure 5-23. In a similar vein to chromatograms showing the alkylnaphthalenes, the peak sizes within the three chromatograms have been preserved relative to each other to reflect the relative abundances, albeit uncorrected for differences in detector response.

The distribution within the MPs is maintained for both NEC 1 (Level 1) and NEC 2 (Level 1 to 2) after which 2-MP is preferentially depleted in NEC 3 (Level 3), then almost completely removed from NEC 4 (Level 4). This dramatic decrease in the abundance of 2-MP is accompanied by a general depletion of the remaining MP isomers from the mixture, although these have not been completely removed from the most biodegraded sample, NEC 5 (Level 5). The C_2-Ps remain intact within the isomer mixture in the petroleum less degraded than NEC 4 (Level 4), where the depletion of 2,6-DMP (Peak 33) and 1,7-DMP (Peak 41) become apparent. Simultaneously, one or more of the co-eluting isomers 3,9-DMP, 3,10-DMP, 2,10-DMP and 1,3-DMP (Peaks 35 to 38) is also depleted. This signature is maintained in the DMP abundances for NEC 5.

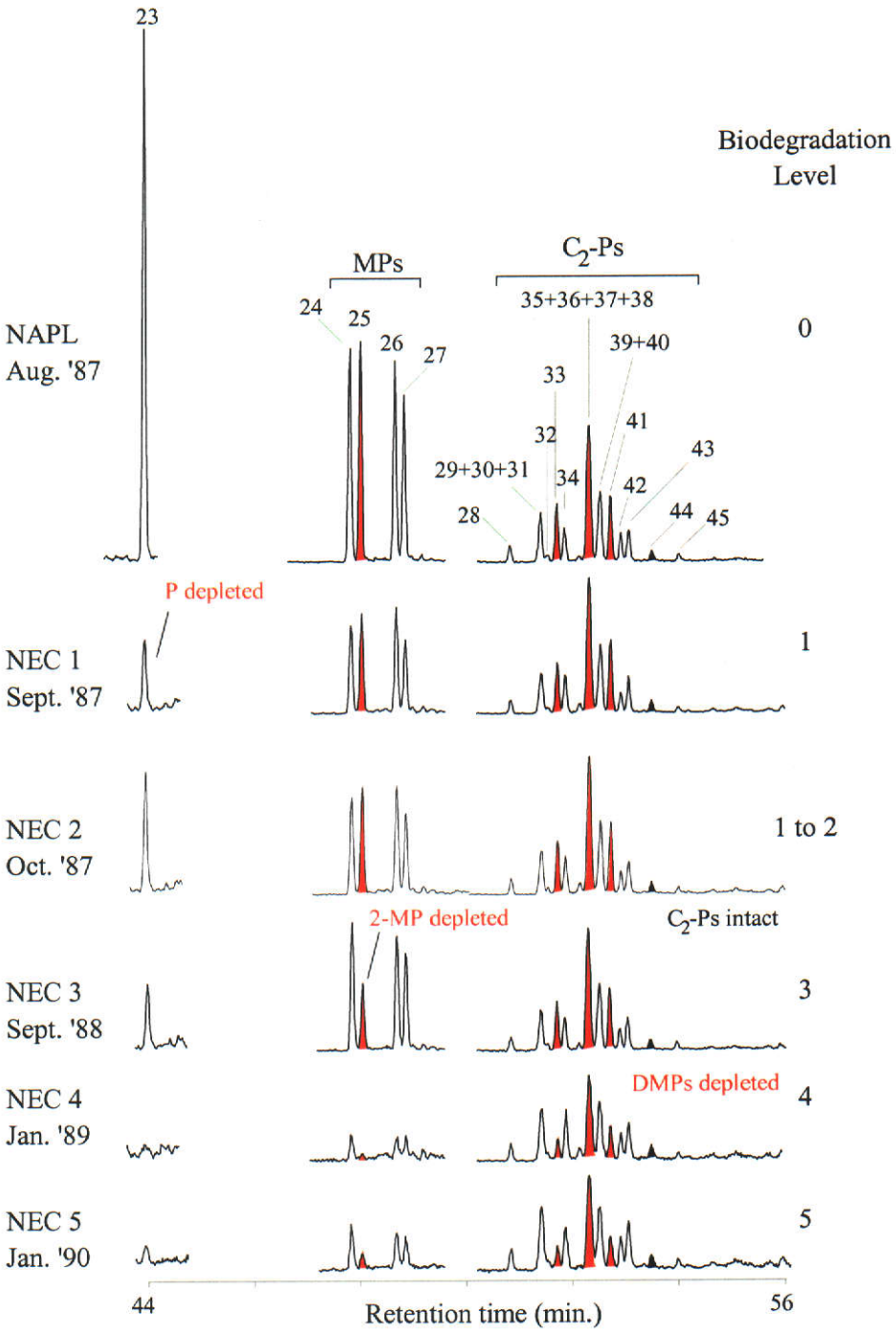

Figure 5-23: Partial mass chromatograms showing changes in the relative abundance of phenanthrene (P, m/z 178), methylphenanthrenes (MP, m/z 192) and C_2-phenanthrenes (C_2-Ps, m/z 206) in sediments collected from the NEC contaminated site. Similar chromatograms are shown for a sample of NAPL. Peak identifications are as follows: (23) P, (24) 3-MP; (25) 2-MP; (26) 9-MP; (27) 1-MP; (28) 3-EP; (29) 3,6-DMP; (30) 9-EP; (31) 2-EP; (32) 1-EP; (33) 2,6-DMP; (34) 2,7-DMP; (35) 3,9-DMP; (36) 3,10-DMP; (37) 2,10-DMP; (38) 1,3-DMP; (39) 1,6-DMP; (40) 2,9-DMP; (41) 1,7-DMP; (42) 2,3-DMP; (43) 1,9-DMP; (44) 1,8-DMP; (45) 1,2-DMP.

As discussed earlier (Section 5.6.1,Table 5-9), the abundance of phenanthrene and the sum of abundances of each of the MPs and C_2-Ps relative to 1,8-DMP decreases with increasing biodegradation in a less erratic manner than that observed for the alkylnaphthalenes, presumably due to the diminished effects of water washing and evaporation. The abundance of each individual compound was therefore also normalised against that of 1,8-DMP, the results of which are presented in Table 5-10.

Changes in abundance previously masked by co-elution of several compounds were observed from interpretation of the (GC-FTIR) infrared spectra. Closer inspection reveals the change in relative abundance of each the components of the co-eluting 1,3-DMP, 2,10-DMP, 3.10-DMP and 3,9-DMP isomer mixture, where 1,3-DMP is evidently more resistant to depletion by biodegradation processes. The relative constancy in the abundances of the components of each of the other two co-eluting mixtures, that is 3,6-DMP, 9-EP and 2-EP, and 1,6-DMP and 2,9-DMP throughout the duration of the study is also noticeable.

These and other changes are further illustrated by Figure 5-24, where the abundances of phenanthrene, the MPs and the DMPs in the NEC sample set are expressed as a proportion of that measured in NEC 1. Here, the results for compounds most susceptible to biodegradation have been grouped to the left of the graph and those with the greatest resistance to the right. It is apparent from these that phenanthrene was the most affected, having been completely removed from NEC 4 (Level 4). 2-MP is significantly depleted in NEC 3 (Level 3), while the remaining MPs were depleted concurrently with the most susceptible of the DMP isomers, namely 1,7-DMP, 2,6-DMP, 3,10-DMP and 2,10-DMP, when the extent of biodegradation reached Level 4 (NEC 4). There was little change in these distributions between the two most degraded samples, NEC 4 and NEC 5 (Level 5 to 6).

Table 5-10: Relative abundances of phenanthrene (P), methylphenanthrenes (MPs), ethylphenanthrenes (EPs) and dimethylphenanthrenes (DMPs) measured in the NEC sample set. Abundances were calculated from GC-MS and GC-FTIR peak areas corrected for differences in detector response normalised against that of 1,8-DMP. Similar information is also shown for NAPL obtained from the OCW system.

Sample Name	NAPL	NEC 1	NEC 2	NEC 3	NEC 4	NEC 5
Biodegradation Level	0	1	1-2	3	4	5
P	30	4.9	5.9	4.6	0.0	0.0
3-MP	20	8.4	8.1	13	2.2	2.2
2-MP	20	9.2	8.5	6.3	0.31	1.1
9-MP	17	9.6	8.6	11	2.0	2.0
1-MP	14	6.9	6.0	9.0	1.7	1.6
3-EP	1.6	1.2	1.1	1.5	1.3	1.2
9-EP	0.88	0.73	0.52	0.91	0.67	0.57
2-EP	1.6	1.2	1.1	1.5	1.3	1.2
1-EP	0.73	0.56	0.40	0.70	0.51	0.44
3,6-DMP	2.7	2.5	2.6	2.2	2.9	2.3
2,6-DMP	5.2	4.6	4.1	4.6	1.3	1.2
2,7-DMP	3.3	3.4	2.7	3.1	3.3	2.4
1,3-DMP	4.0	3.6	3.2	3.5	3.2	3.2
3,9-DMP	3.8	3.4	3.0	3.4	1.7	1.5
2,10-DMP	3.6	3.3	2.9	3.2	1.3	1.1
3,10-DMP	4.4	4.0	3.5	3.9	1.6	1.0
1,6-DMP	4.1	3.7	3.6	4.2	2.6	2.4
2,9-DMP	4.1	3.7	3.3	3.7	2.6	1.9
1,7-DMP	6.2	6.3	5.5	5.9	2.3	2.0
2,3-DMP	2.1	1.7	1.6	1.9	1.9	1.7
1,9-DMP	3.0	2.8	2.8	3.1	2.7	3.0
1,8-DMP	1.0	1.0	1.0	1.0	1.0	1.0
1,2-DMP	0.66	0.55	0.56	0.60	0.49	0.56

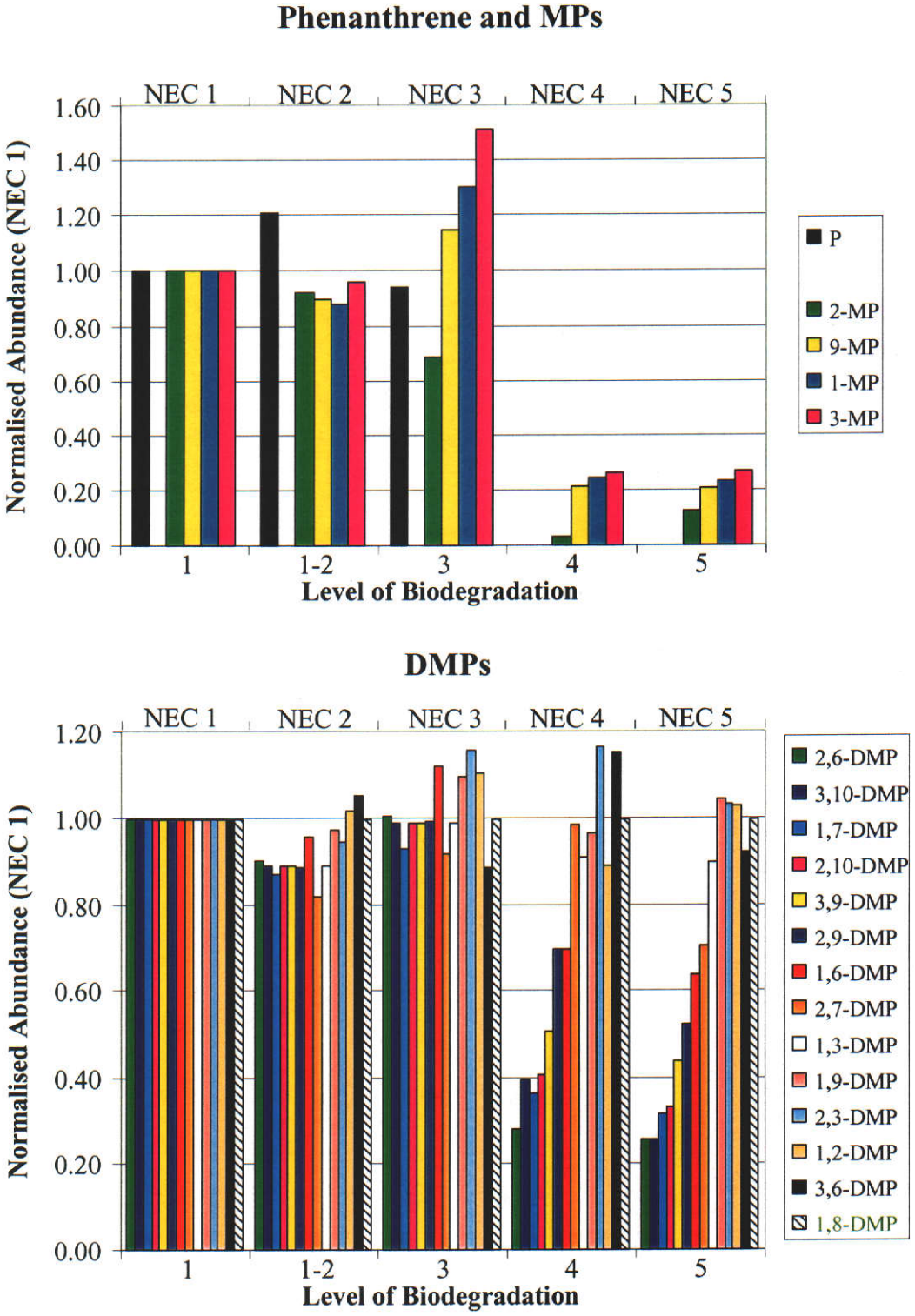

Figure 5-24: Bar charts showing changes in the abundances of phenanthrene and individual MPs and DMPs, relative to the conserved internal marker 1,8-DMP, in sediments collected from the NEC contaminated site. Abundances are expressed as a proportion of those measured in NEC 1, which contained the petroleum with the least-biodegraded hydrocarbon signature.

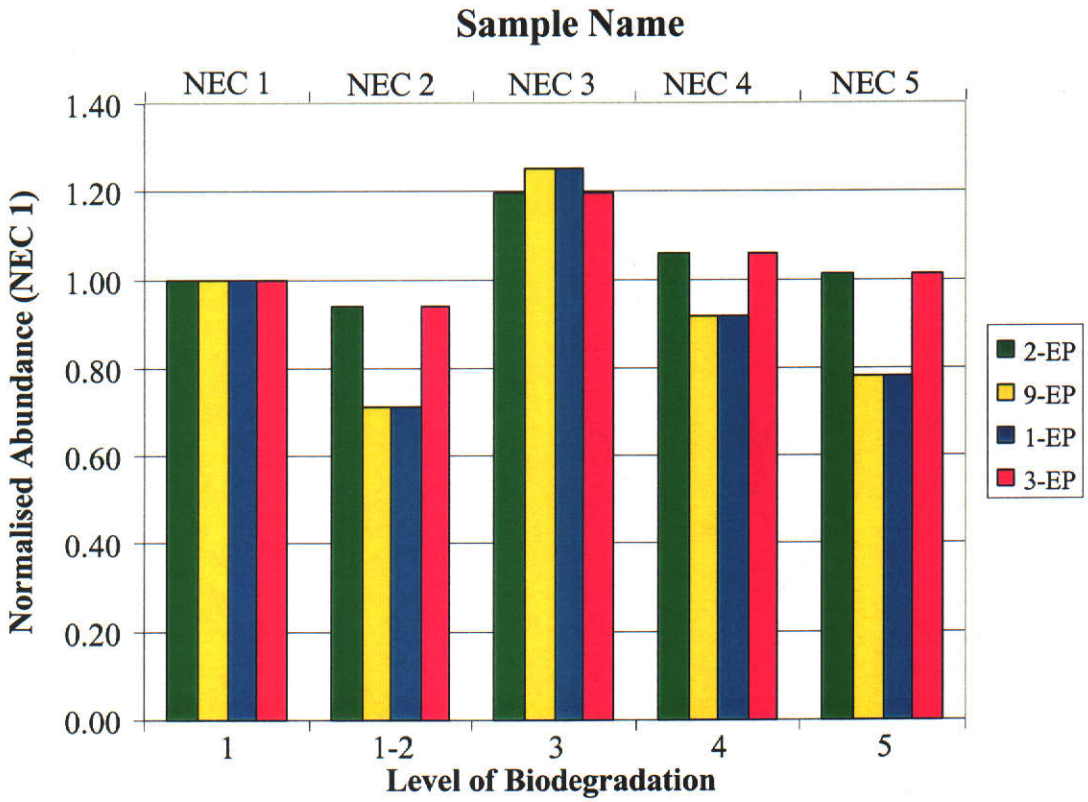

Figure 5-25: A bar chart showing changes in the abundances of EPs, relative to the conserved internal marker 1,8-DMP, in sediments collected from the NEC contaminated site. Abundances are expressed as a proportion of those measured in NEC 1, which contained the petroleum with the least-biodegraded hydrocarbon signature.

The changes in relative abundances of the EPs with increasing extent of biodegradation are similarly represented in Figure 5-25. These data should be interpreted with caution since both 9-EP and 2-EP are minor constituents of the co-eluting mixture with 3,6-DMP. Their low abundances are difficult to determine using GC-FTIR techniques, particularly in the residues of the more degraded petroleum where interference from the UCM is heightened. In addition to this, 1-EP is only partially resolved from the mixture in these samples as shown in Figure 5-23, further confounding the determination of all of the isomers with the exception of 3-EP. With this in mind, the small variations in the relative abundances, and the lack of a clear trend in depletion of the isomers indicates that there is no clear difference in susceptibility to biodegradation amongst these compounds.

SCVB sediments

Chromatograms for samples from the SCVB site are presented in Figure 5-26. While all of the MP isomers show depletion as biodegradation progresses, 2-MP decreases more rapidly than the other isomers beyond biodegradation Level 2 to 3 (SCVB 1). This discrimination between the isomers was particularly marked between SCVB 3 (biodegradation Level 3 to 4) and SCVB 4 (Level 5), before the complete removal of the MPs from the mixture in SCVB 5 (Level 5 to 6).

The distribution of C_2-P abundances across the isomer mixture also remains relatively constant between the NAPL (Level 0) and SCVB 1 (Level 2 to 3). This similarity also extends to SCVB 2 (Level 3), however some changes in abundance become apparent in the residues of the more severely biodegraded petroleum. The most obvious of these occurs between SCVB 4 (Level 5) and SCVB 5 (Level 5 to 6), marked by the depletion of one or more of the constituents of the co-eluting mixture of 1,3-DMP, 2,10-DMP, 3,9-DMP and 3,10-DMP (Peaks 35 to 38), and by the severe depletion of 2,6-DMP (Peak 33) and 1,7-DMP (Peak 41). The decrease in abundance of 2,6-DMP in particular and to a lesser extent 1,7-DMP is also perceptible between SCVB 2 and SCVB 3.

The susceptibility to biodegradation of the individual alkylphenanthrenes in the SCVB samples was investigated in the same way as the NEC sediments. Abundances relative to that of 1,8-DMP are presented in Table 5-11, and these are expressed as a proportion of that measured in the NAPL in Figure 5-27. It is apparent from these that phenanthrene was the most rapidly depleted compound, with depletion occurring between biodegradation Levels 0 and 2-3. This is followed by 2-MP, which is significantly depleted relative to the other isomers between Biodegradation Levels 3 and 3-4. The depletion of the remaining MPs coincided with that of the most susceptible of the DMP isomers, namely 1,7-DMP, 2,6-DMP, 3,10-DMP and 2,10-DMP, when the extent of biodegradation reached Level 3-4. The residues from the most severely degraded sample (SCVB 5, Level 5-6) were devoid of MPs, while the above-mentioned susceptible DMP isomers were barely perceptible.

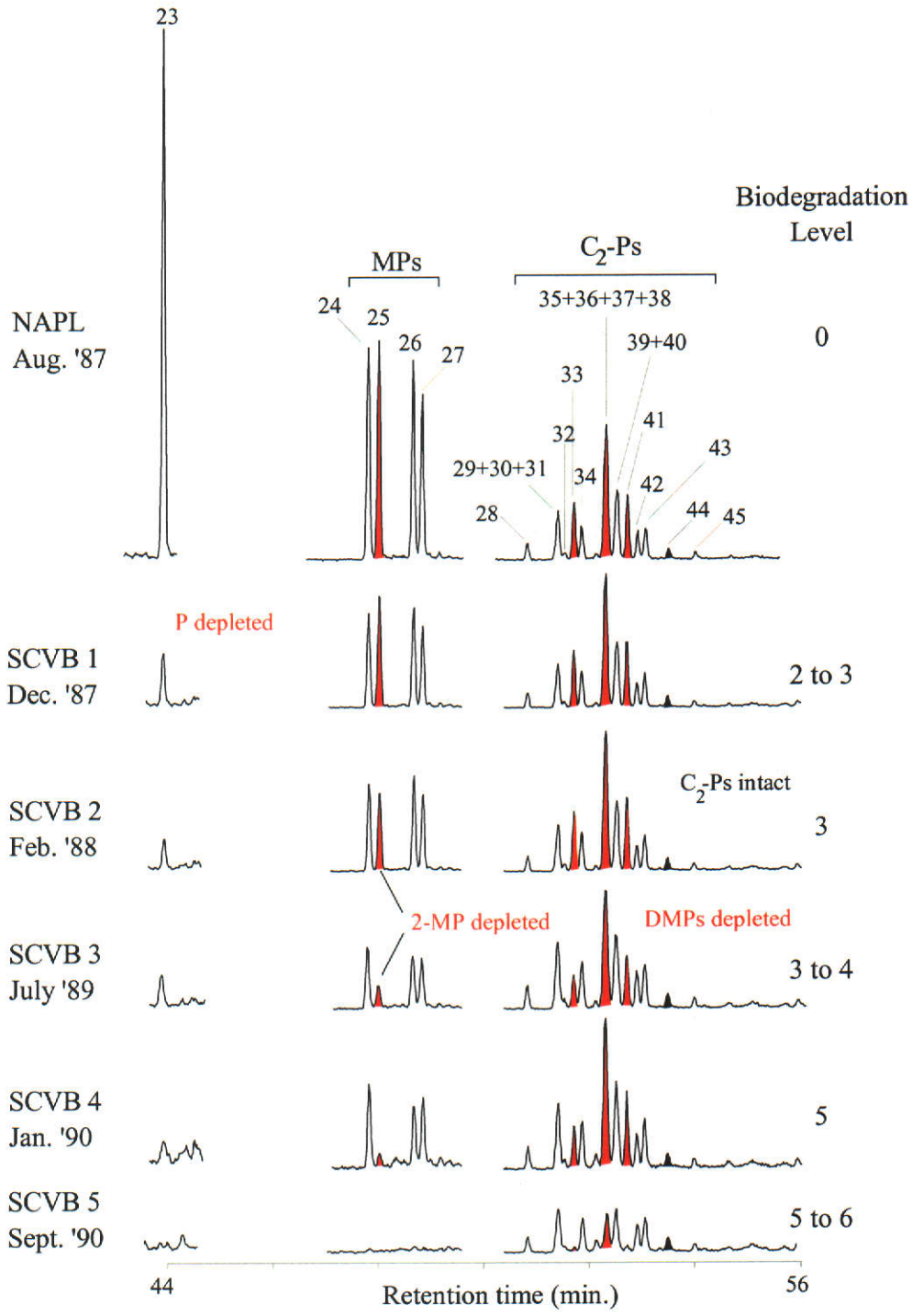

Figure 5-26: Partial mass chromatograms showing changes in the relative abundance of phenanthrene (m/z 178), methylphenanthrenes (m/z 192) and dimethylphenanthrenes (m/z 206) present in in sediments collected from the SCVB contaminated site. Similar chromatograms are shown for a sample of NAPL. Peak identifications are as follows: (23) P, (24) 3-MP; (25) 2-MP; (26) 9-MP; (27) 1-MP; (28) 3-EP; (29) 3,6-DMP; (30) 9-EP; (31) 2-EP; (32) 1-EP; (33) 2,6-DMP; (34) 2,7-DMP; (35) 3,9-DMP; (36) 3,10-DMP; (37) 2,10-DMP; (38) 1,3-DMP; (39) 1,6-DMP; (40) 2,9-DMP; (41) 1,7-DMP; (42) 2,3-DMP; (43) 1,9-DMP; (44) 1,8-DMP; (45) 1,2-DMP.

Table 5-11: Relative abundances of phenanthrene (P), methylphenanthrenes (MPs), ethylphenanthrenes (EPs) and dimethylphenanthrenes (DMPs) measured in the SCVB sample set. Abundances were calculated from GC-MS and GC-FTIR peak areas corrected for differences in detector response normalised against that of 1,8-DMP. Similar information is also shown for NAPL obtained from the OCW system.

Sample name	NAPL	SCVB 1	SCVB 2	SCVB 3	SCVB 4	SCVB 5
Biodegradation Level	0	2-3	3	3-4	5	5-6
P	30	3.7	2.0	1.7	0.50	0.00
3-MP	20	9.2	8.3	4.4	5.7	0.00
2-MP	20	11	7.3	1.8	0.93	0.00
9-MP	17	9.9	8.9	3.8	4.4	0.00
1-MP	14	7.4	6.8	3.4	5.1	0.00
3-EP	1.6	1.4	1.3	1.5	1.4	1.2
9-EP	0.88	0.55	0.72	0.62	0.58	0.29
2-EP	1.6	1.4	1.3	1.5	1.4	1.2
1-EP	0.73	0.46	0.60	0.51	0.49	0.24
3,6-DMP	2.7	3.1	3.0	3.1	2.9	2.6
2,6-DMP	5.2	5.4	5.1	2.2	2.8	0.26
2,7-DMP	3.3	3.3	3.5	3.2	3.1	2.6
1,3-DMP	4.0	3.8	3.8	3.5	4.1	2.9
3,9-DMP	3.8	3.6	3.7	2.9	3.4	0.17
2,10-DMP	3.6	3.5	3.5	1.8	2.1	0.14
3,10-DMP	4.4	4.2	4.3	1.8	2.1	0.14
1,6-DMP	4.1	4.1	4.5	3.0	3.7	1.8
2,9-DMP	4.1	3.8	3.6	3.2	3.1	1.8
1,7-DMP	6.2	6.2	6.4	3.3	4.3	0.28
2,3-DMP	2.1	2.2	2.0	2.4	2.1	2.0
1,9-DMP	3.0	3.0	3.2	2.9	3.2	2.5
1,8-DMP	1.0	1.0	1.0	1.0	1.0	1.0
1,2-DMP	0.66	0.61	0.67	0.67	0.59	0.62

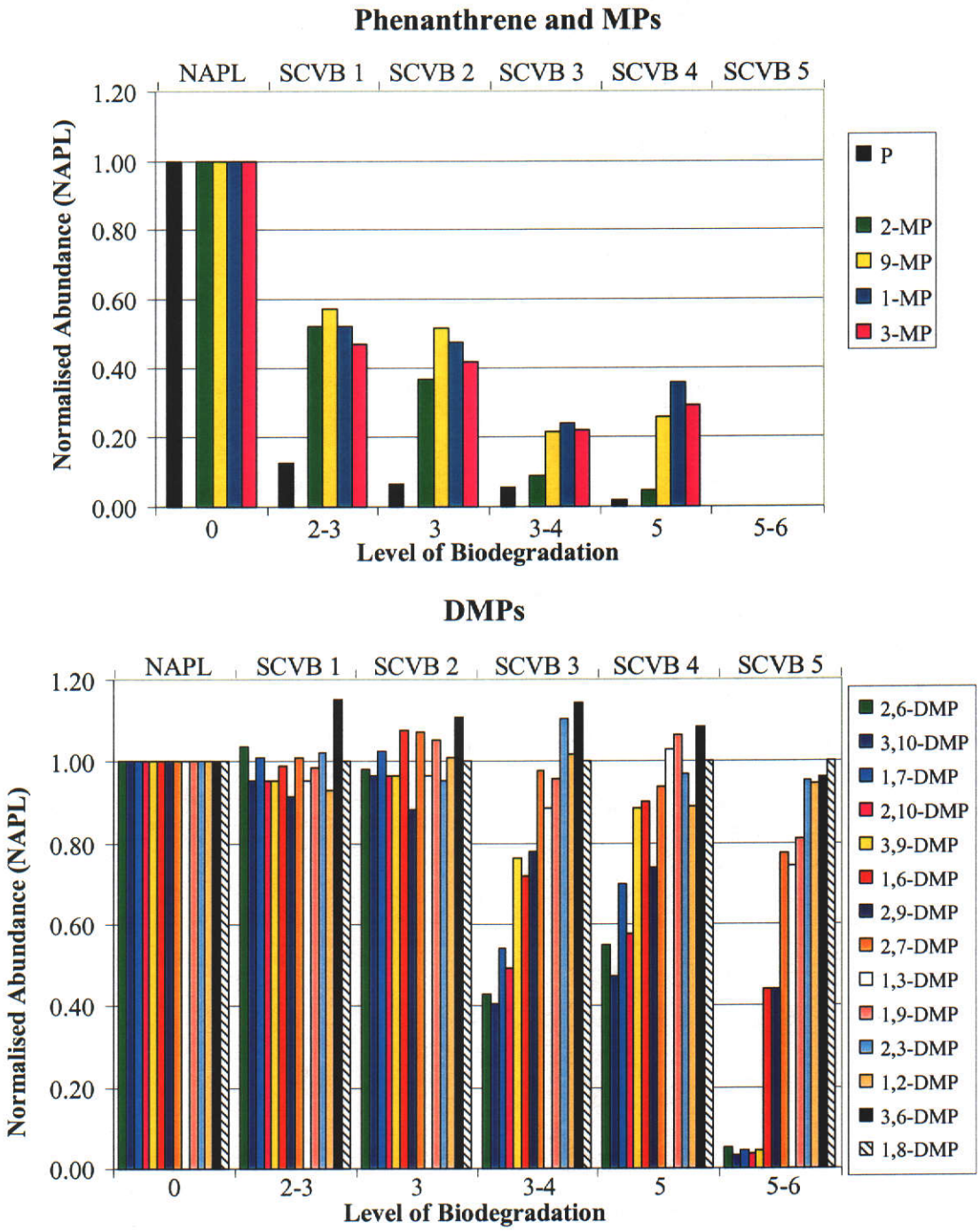

Figure 5-27: Bar charts showing changes in the abundances of phenanthrene and individual MPs and DMPs, relative to the conserved internal marker 1,8-DMP, in sediments collected from the SCVB contaminated site. Abundances are expressed as a proportion of those measured in the sample of NAPL recovered from the OCW system.

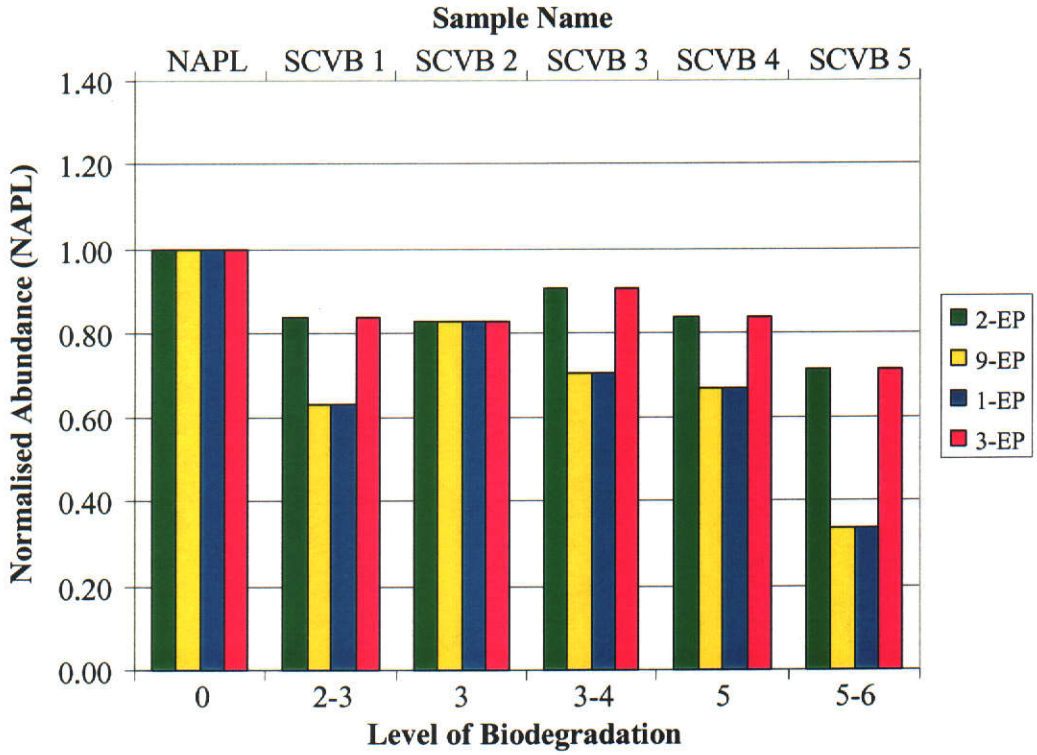

Figure 5-28: A bar chart showing changes in the abundances of EPs, relative to the conserved internal marker 1,8-DMP, in sediments collected from the SCVB contaminated sites. Abundances are expressed as a proportion of those measured in the sample of NAPL recovered from the OCW system.

The changes in relative abundances of the EPs with increasing extent of biodegradation are represented in Figure 5-28. As for the NEC samples, although variations in the relative abundances amongst these isomers is greater for the SCVB sediments in the more biodegraded petroleum samples (SCVB 4, Level 5 and SCVB 5, Level 5-6), this variation is erratic. There is therefore insufficient evidence to indicate that there is a difference in susceptibility to biodegradation amongst these compounds. More encouragingly, the abundance of 3-EP, the only isomer unaffected by co-elution, decreases somewhat between biodegradation Level 5 (SCVB 4) and Level 5 to 6 (SCVB 5), indicating that the EPs may indeed be undergoing biodegradation processes. Examination of petroleum samples containing residues biodegraded to a more severe extent than Level 5-6 would be necessary to confirm this observation. The expected increase in abundance of the EPs relative to the DMPs in such a petroleum sample may also assist in the determination of the co-eluting EP isomers.

Comparison of biodegradation susceptibilities at the NEC and SCVB sites

Comparison of Figure 5-23 and 5-26 reveals that the mass chromatograms of the samples from NEC 1 (collected Sept. '87) and SCVB 1 (Dec. '87) are almost identical. From the results shown in Tables 5-10 and 5-11, it is apparent that the relative abundances of phenanthrene and each of the MPs and the C_2-Ps are in fact almost identical in both samples collected within approximately three months of each other. This similarity suggests that the distribution of the alkylphenanthrenes in the sample of NAPL is representative of that in the original, unbiodegraded petroleum at the source of the contamination for both sites. This allowed consolidation of the two data sets into one, comprising 11 samples representing nine different extents of biodegradation.

Results for the individual MPs and DMPs are represented in Figures 5-29 and 5-30 respectively, where the isomer abundances determined in each sediment extract are compared with that in the NAPL. With the exception of the SCVB 4 sample (Biodegradation Level 5), and the NEC 3 sample (Level 3), the relationship between the depletion of phenanthrene and the MPs from the NAPL and the extent of biodegradation is continuous. Further, the relative abundance amongst these compounds in all ten sediment extracts is also altered in a monotonic manner, with 2-MP showing the greatest propensity for depletion from the petroleum.

The similarity in biodegradation susceptibility between the sites is also borne out in the alteration of the DMPs, with only those from the SCVB 4 showing a significant discontinuity from the overall trend for the preferential depletion of 2,6-DMP, 1,7-DMP, 3,10-DMP and 2,10-DMP. The non-conformance of the SCVB 4 sample to the trends exhibited by phenanthrene and the MPs and the DMPs is noteworthy. For both groups of compounds, although SCVB 4 contains a higher than expected abundance of the MPs, the distribution amongst the isomers is consistent with the designated biodegradation level. This is clearly illustrated by comparing the relative abundances in SCVB 4 with NEC 5, each assigned a biodegradation level of 5, in Figures 5-29 and 5-30.

Referring to Tables 5-5 and 5-9, we recall that SCVB 4 contained anomalously high concentrations of alkylnaphthalenes and to a lesser extent, alkylphenanthrenes, presumably due to the diminished effect of water washing. The other sediment sample for which exposure to less severe weathering conditions was proposed, NEC 3, also displays some anomalous behaviour in its MP signature due to their greater than expected abundance. From comparison of the distribution amongst the MP isomers contained in NEC 3 with SCVB 2 and SCVB 3, it is evident that the extent of depletion is consistent with the designated biodegradation level of 3. The DMPs are relatively unaltered, also consistent with biodegradation Level 3. These observations indicate that while the effects of water washing and evaporation may have been diminished in this sediment sample, the effect of biodegradation was not.

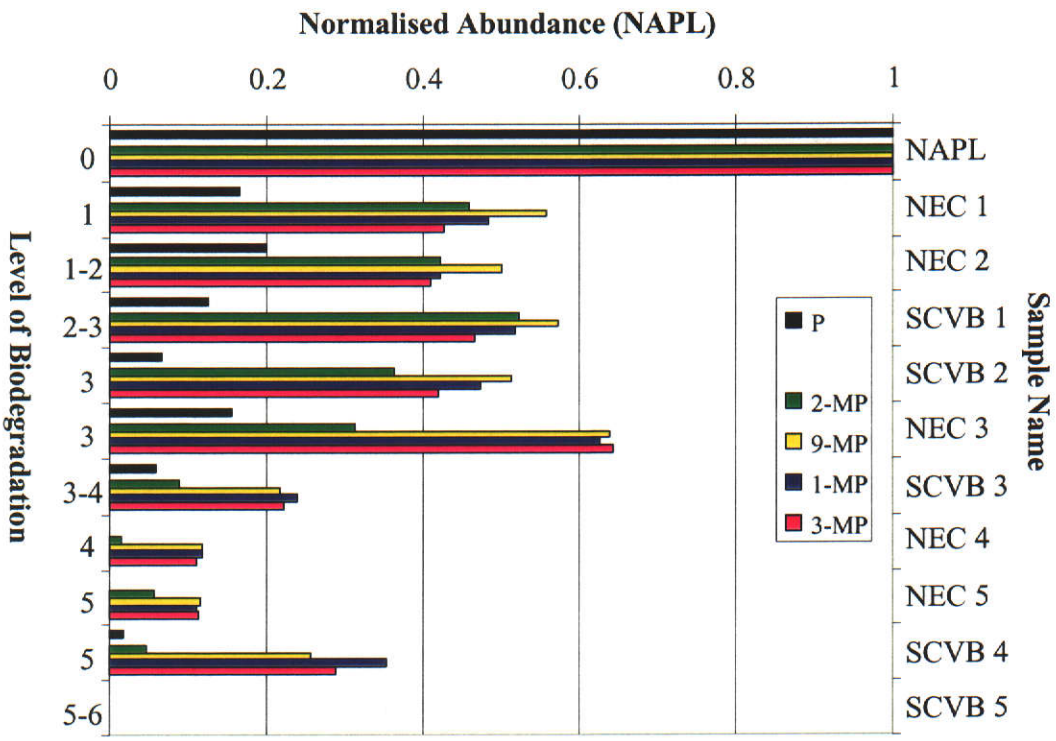

Figure 5-29: A bar chart showing changes in the abundances of phenanthrene and MPs, relative to the conserved internal marker 1,8-DMP, in sediments collected from the SCVB and NEC contaminated sites. Abundances are expressed as a proportion of those measured in the sample of NAPL recovered from the OCW system.

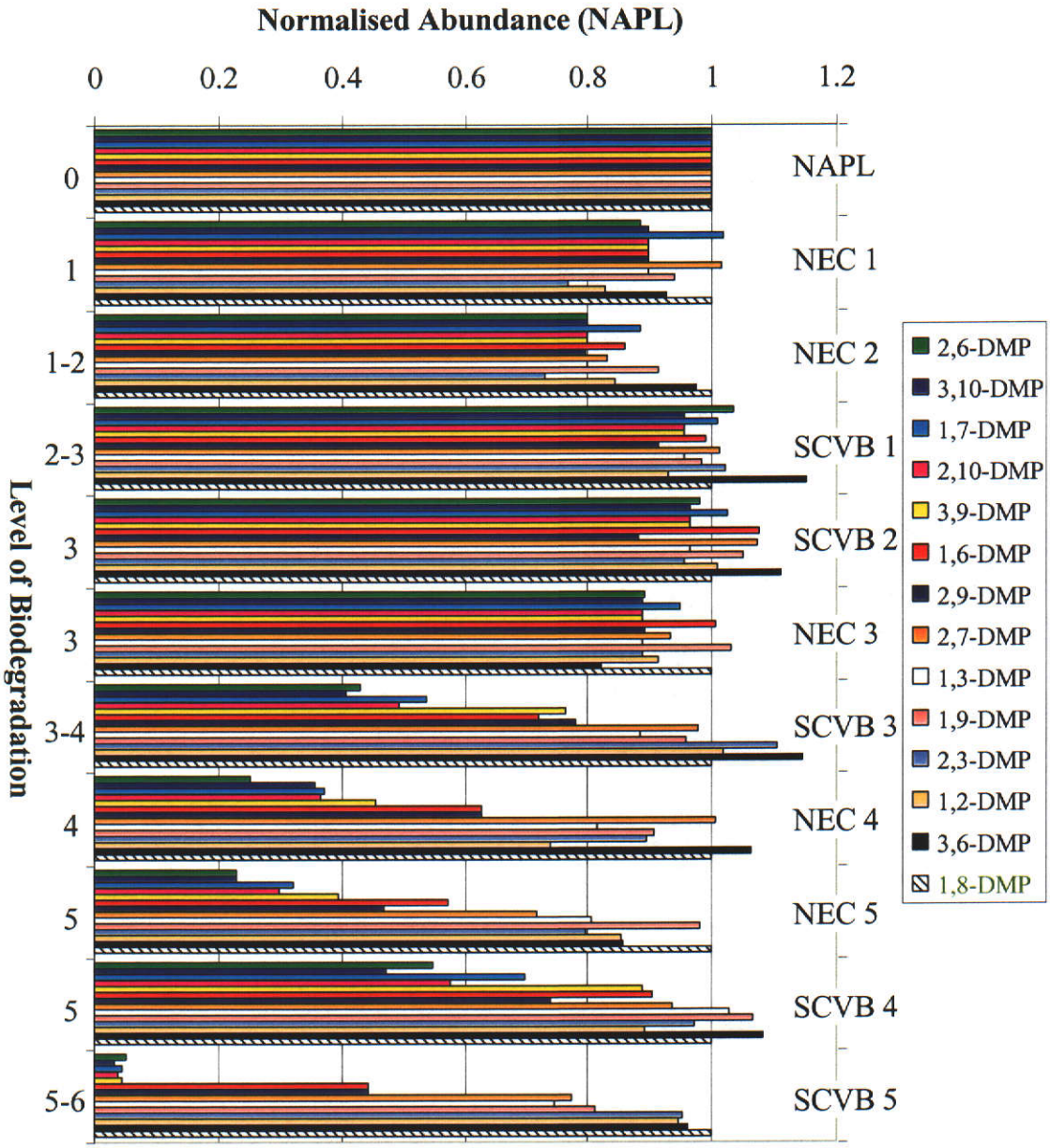

Figure 5-30: A bar chart showing changes in the abundances of DMPs, relative to the conserved internal marker 1,8-DMP, in sediments collected from the SCVB and NEC contaminated sites. Abundances are expressed as a proportion of those measured in the sample of NAPL recovered from the OCW system.

Summary of alkylphenanthrene depletion

From the consolidated sample set, it is possible to establish the following order of decreasing susceptibility to biodegradation amongst the isomers of the MPs and of the DMPs, where the numbers refer to the position of methyl substituents on the phenanthrene nucleus.

Most susceptible Least susceptible

MPs

$$2 >> 9 \sim 1 \sim 3$$

DMPs

$$1,7 \sim 2,6 \sim 3,10 \sim 2,10 > 1,6 \sim 2,9 \sim 3,9 > 2,3 \sim 1,9 \sim 1,8 \sim 1,2 \sim 2,7 \sim 3,6 \sim 1,3$$

5.7 Conclusions

The extent of biodegradation of petroleum extracted from sediments from two contaminated areas was assessed on the basis of changes in the composition of the saturated hydrocarbons. These changes were accompanied by the alteration of the aromatic hydrocarbons contained in the petroleum, in particular the alkylnaphthalenes and alkylphenanthrenes. These observations are summarised and presented in Table 5-12.

Depletion occurred to different extents between groups of these compounds, with a direct relationship generally observed between the susceptibility to biodegradation and the extent of substitution of the aromatic nucleus, but some overlap occurs between these groups. Detailed analysis of these compounds using the complementary techniques of GC-MS and GC-FTIR enabled the unambiguous determination of the abundance of each of the isomers present in the petroleum. From this, the individual compounds were arranged according to their susceptibility to biodegradation.

Table 5-12: The effect of biodegradation on the composition of aromatic hydrocarbons in petroleum-contaminated sediment samples collected from NEC and SCVB between August 1987 and September 1990. The level of biodegradation is based on observed changes in the saturated hydrocarbons (after Peters and Moldowan, 1993).

Biodegradation Level	Sample	Change in Aromatic Hydrocarbon Composition									
		N	MNs	DMNs	ENs	TMNs	TeMNs	P	MPs	DMPs	EPs
0	NAPL	Undeg.	Undeg.	Undeg.	Undeg.	Undeg.	Undeg.	Undeg.	Undeg.	Undeg.	Undeg.
1	NEC 1	Dep.	Undeg.	Undeg.	Undeg.	Undeg.	Undeg.	Dep.	Undeg.	Undeg.	Undeg.
1-2	NEC 2	Dep.	Undeg.	Alt.	Undeg.	Undeg.	Undeg.	Dep.	Undeg.	Undeg.	Undeg.
2-3	SCVB 1	Sev. dep.	Sev. dep.	Undeg.	Alt.	Undeg.	Undeg.	Dep.	Undeg.	Undeg.	Undeg.
3	NEC 3	Abs.	Sev. dep.	Alt.	Alt.	Undeg.	Undeg.	Dep.	Alt.	Undeg.	Undeg.
3	SCVB 2	Abs.	Abs.	Alt.	Alt.	Alt.	Undeg.	Dep.	Undeg.	Undeg.	Undeg.
3-4	SCVB 3	Abs.	Abs.	Alt.	Alt.	Alt.	Undeg.	Dep.	Alt.	Alt.	Undeg.
4	NEC 4	Abs.	Abs.	Alt.	Alt.	Alt.	Undeg.	Abs.	Alt.	Alt.	Undeg.
5	SCVB 4	Abs.	Abs.	Alt.	Alt.	Alt.	Undeg.	Sev. dep.	Alt.	Alt.	Undeg.
5	NEC 5	Abs.	Abs.	Sev. dep.	Sev. dep.	Sev. dep.	Alt.	Abs.	Alt.	Alt.	Undeg.
5-6	SCVB 5	Abs.	Abs.	Abs.	Abs.	Abs.	Alt.	Abs.	Abs.	Alt.	Alt.

Key to Table 5-12: Undeg. = undegraded; Alt. = altered; Dep. = depleted; Sev. dep. = severely depleted; Abs. = absent

From these relationships, it is evident that polymethylnaphthalenes with a 1,6-dimethyl substitution pattern are more susceptible to biodegradation than other isomers that lack this feature. This trend was consistent with that observed in the petroleum extracted from the sea-floor sediments (Chapter 4). There is also a clear trend within the mono-alkylated naphthalenes, where 2-MN and 2-EN are more susceptible to biodegradation than 1-MN and 1-EN respectively

Although no relationship between structure and susceptibility to biodegradation is obvious amongst the mixture of alkylphenanthrenes, 2-MP was the most susceptible of the methylphenanthrenes while 1,7-DMP, 2,6-DMP, 3,10-DMP and 2,10-DMP were all significantly more susceptible to biodegradation than the other isomers.

It is likely that the initial depletion of the alkylnaphthalenes and alkylphenanthrenes was due to a great extent to dissolution in the water and evaporation. Observations consistent with the variable extents of water washing and evaporation at both sites throughout the study period have also been reported here. Although these processes discriminate between these compounds on the basis of extent of alkylation, reflected in the loss of the less alkylated homologues, there is evidently no discrimination between the isomers within each of these groups of compounds. The depletion amongst isomers therefore enables differentiation between microbial biodegradation and other abiotic weathering processes.

As a result of the above observations, criteria for determining the extent of biodegradation of petroleum in coastal oil spills on the basis of alteration to the aromatic hydrocarbons have been established to complement those based on the saturated hydrocarbons.

CHAPTER 6

6 Aromatic hydrocarbons as indicators of petroleum biodegradation

6.1 Abstract

The biodegradation of petroleum-derived aromatic hydrocarbons in three environments are compared: two sets of samples derived from oil-based drilling mud in sea-floor sediments discharged during the drilling of offshore oil and gas wells, two sets of samples arising from petroleum accidentally discharged into sediments in a coastal intertidal (mangrove) swamp, and the in-reservoir biodegradation of a suite of crude oils. The relative susceptibilities to biodegradation of the individual isomers of the alkylnaphthalenes and alkylphenanthrenes in petroleum from the sea-floor and the mangrove sediments compared very closely. The changes in the distribution of the aromatic hydrocarbons were related to the alteration of the saturated hydrocarbons, in particular those alkanes conventionally used to indicate the extent of petroleum biodegradation, and compound ratios reflecting the extent of biodegradation were calculated from the relative abundances of selected alkylnaphthalenes for these two systems. The changes in the values of these ratios with increasing extent of biodegradation were similar in both environments and in this chapter are used as molecular biodegradation indicators to differentiate between several crude oils that have been biodegraded to varying extents. These parameters also offer promise as indicators of multiple accumulation events in oil reservoirs where successive charges of petroleum fluids biodegraded to differing extents are mixed.

6.2 Introduction

The alteration of crude oils in reservoirs by microbial biodegradation has been well documented in the literature (Connan, 1984; Peters and Moldowan, 1993). Much of this work, for example Seifert and Moldowan (1979), Blanc and Connan (1992), Prince et al. (1994), Moldowan and McCaffrey (1995), Peters et al. (1996) and Ahsan, Karlsen and Patience (1997), has focussed on the compositional changes that

the saturated hydrocarbons undergo, in particular the terpenoid biomarkers such as steranes and hopanes. Laboratory experiments, aimed at assessing the biodegradation of these compounds in reservoirs have also been performed by Chosson et al. (1991) and by Grimalt et al. (1991) who also observed changes in the abundance of aromatic sulphur compounds and alkylbenzenes.

The biodegradation of the aromatic compounds, particularly the alkylnaphthalenes and alkylphenanthrenes, has not been as widely studied, although Volkman et al. (1984), Williams et al. (1986), Rowland et al. (1986), Cassani and Eglinton (1991) and Budzinski et al. (1995b) have investigated the alteration of the individual isomers of these compounds in biodegraded crude oils. More recently Ahmed, Smith and George (1999) studied the effects of biodegradation on the components of various mixtures of these compounds as well as alkylated fluorenes and dibenzothiophenes in Permian coals. The biodegradation of the alkylnaphthalenes and alkylphenanthrenes has also been examined in the laboratory (Jones et al., 1983; Solanas et al., 1984; Bayona et al., 1986; Kennicutt, 1988; Budzinski et al., 1995b; 1998), but the relative susceptibilities of these compounds to microbial attack is not as well defined as for the saturated hydrocarbons.

In this study, the biodegradation of petroleum was investigated in two instances where petroleum had been released into the marine environment. In the first of these, two sets of samples from intertidal coastal sediments which had been contaminated with condensate from the North West Shelf of Australia were sampled on several occasions over a period of approximately three years. The second case involved sampling sea-floor sediments adjacent to the NRA offshore exploration and production platform. These sediments contained discharged drill cuttings contaminated with entrained petroleum hydrocarbons from the low toxicity oil-based mud (LTOBM) used in the drilling program. Two sets of samples were collected: one set comprised sediments from seven locations at various distances from the platform, while the other set consisted of sediments from various depths below the surface of the cuttings pile directly under the cuttings discharge chute at NRA. The samples of sediment collected from these two environments provided four sets of partially biodegraded petroleum samples with which to thoroughly investigate and

compare the relative susceptibilities of the alkylnaphthalenes and alkylphenanthrenes to microbial attack in the marine environment. The relative susceptibilities of the alkylnaphthalenes in each system are also compared with that observed in several crude oils reservoired in two Australian sedimentary basins, namely the Gippsland Basin and the Carnarvon Basin.

6.3 Assignment of the extent of biodegradation to petroleum samples

6.3.1 Intertidal coastal sediments

The assignment of the extent of biodegradation to the petroleum in the intertidal coastal sediments is discussed in detail in Chapter 5. Progressive changes in petroleum composition are used widely to assess the extent of microbial biodegradation of petroleum. These changes have been summarised into a table (Peters and Moldowan, 1993), which is nowadays used as a level of biodegradation ready reckoner by geoscientists working with petroleum reservoirs and on environmental issues. In Table 6-1, this ready reckoner has been extended to include alterations to aromatic hydrocarbons observed in the intertidal sediments over the first six levels of biodegradation. Changes in the isomeric abundances of alkylbiphenyls and alkyldiphenymethanes in this sample set have also been investigated by Trolio et al. (1999), which allows the ready reckoner to be further extended to include these compounds.

6.3.2 Sea-floor sediments

The alteration of the hydrocarbons in sea-floor sediments adjacent to the NRA platform upon biodegradation has also been discussed in detail in Chapter 4. Two separate sets of sediments contaminated with LTOBM were examined. The first set consisted of 10 sub-samples removed from a single core. This core was retrieved from the uppermost 10 cm of the pile of cuttings formed on the sea-floor close to the point of discharge.

Table 6-1: The effects of biodegradation on the composition of petroleum spilled in coastal sediments in north Western Australia. NB: 1: After Peters and Moldowan (1993); 2: From Volkman et al. (1984).

Level[1] of biodegradation	Sample Identity	Change in Chemical Composition	
		Saturated Hydrocarbons	Aromatic Hydrocarbons
0	NAPL	Unchanged	Unchanged
1	NEC 1	Light end *n*-alkanes depleted	N depleted; P depleted MNs unaltered
1-2	NEC 2	General depletion of *n*-alkanes	N, P depleted MNs, DMNs, ENs, TMNs unaltered
2-3	SCVB 1	> 90% of *n*-alkanes removed	N, MN severely depleted P depleted; ENs altered DMNs, TMNs, TeMNs unaltered MPs, DMPs unaltered
3	NEC 3 and SCVB 2	*n*-Alkanes absent Alkylcyclohexanes affected[2] Acyclic isoprenoids affected	N absent; MNs severely depleted DMNs, ENs, TMNs altered P depleted, MPs altered TeMNs, DMPs unaltered
3-4	SCVB 3	Acyclic isoprenoids affected	N, MNs absent P depleted DMNs, ENs, TMNs altered MPs, DMPs altered TeMNs unaltered
4	NEC 4	Acyclic isoprenoids affected Alkylcyclohexanes absent[2]	N, MNs, P absent DMNs, ENs, TMNs, MPs, DMPs altered TeMNs, unaltered
5	SCVB 4	Acyclic isoprenoids absent Bicyclic alkanes affected[2]	P severely depleted DMNs, TMNs, MPs, DMPs altered TeMNs unaltered
5	NEC 5	Acyclic isoprenoids absent Bicyclic alkanes affected[2]	DMNs, ENs, TMNs severely depleted MPs, DMPs, TeMNs altered
5-6	SCVB 5	Bicyclic alkanes affected[2]	DMNs, ENs, TMNs, P, MPs absent DMPs, TeMNs altered EPs altered

The extent of hydrocarbon biodegradation in the cuttings pile core decreased with increasing depth below the sea-floor surface. The level of biodegradation could be assigned for all but the single most biodegraded (uppermost) of these samples based on changes in the saturated hydrocarbon composition illustrated in Figure 4-20 and Table 4-6 (see Section 4.10.2). Due to the restricted molecular weight range (between approximately n-C_{12} to n-C_{18}) of the hydrocarbons comprising the LTOBM, it was difficult to ascertain the extent of biodegradation beyond Level 6 in this sample on the basis of the alteration of the saturated hydrocarbons. Here, the enhanced abundance of the UCM relative to the resolved compounds (Table 4-5) in conjunction with the absence of the DMPs and EPs was used to assign the extent of biodegradation at Level 7. These results are summarised in Table 6-2.

Table 6-2: Assignment of the level of biodegradation based on the saturated hydrocarbon composition of LTOBM extracted from various depths below the surface of the NRA sea-floor cuttings pile and composite sea-floor sediments collected from various distances from the NRA cuttings chute. NB 1: Biodegradation Level determined from the aromatic hydrocarbon composition.

Sea-floor Cuttings Pile		Composite Sea-floor sediments	
Depth (cm) Below Surface	Level of Biodegradation	Distance from Cuttings Chute	Level of Biodegradation
9-10	0	0 m (S1)	mixed
8-9	0	100 m (S2)	mixed
7-8	0	200 m (S3)	mixed
6-7	1-2	400 m (S4)	mixed
5-6	2	800 m (S5)	mixed
4-5	3	100 m NE (S16)	mixed
3-4	4	200 m NE (S16)	mixed
2-3	5		
1-2	5		
0-1	7[1]		

The second set of sea-floor sediments comprised seven samples collected from various distances (0 m to 800 m) from the cuttings discharge chute. Although these samples display an increasingly biodegraded signature with increasing distance from the cuttings chute, (refer to Figure 4-8) it is probable that each contains mixtures of varying proportions of biodegraded LTOBM (near to the surface of the sea-floor) and better-preserved LTOBM buried deeper below the surface. These samples, henceforth described as composite samples, have therefore been assigned a mixed level of biodegradation in Table 6-2.

6.3.3 Biodegraded crude oils

In the three cases described above, the relative susceptibilities of the individual hydrocarbons could be established since the composition of the hydrocarbons constituting both the discharged condensate and LTOBM could be determined. A similar approach could not be taken to investigate the effects of biodegradation on crude oils, however, since a suite of oils of known identical source but varying extents of biodegradation was not available for analysis. Instead, several crude oils were selected from the Gippsland and Carnarvon Basins, the petroleum geology of which are detailed by Burns, Bostwick and Emmett (1987) and Volkman et al. (1984) respectively. Where possible, each of these oils was classified according to extent of biodegradation on the basis of the saturated hydrocarbon composition from previously published results (Burns, Bostwick and Emmett, 1987; Alexander et al., 1983; Volkman et al., 1984; Trolio et al., 1999). The classification of these oils is summarised in Table 6-3. Two oils, namely Eaglehawk and Windalia, were classified as mixed since the level of biodegradation could not be ascertained because of inconsistencies in the relative depletion of the saturated hydrocarbons. Alexander et al. (1983) concluded that at least two major phases of oil accumulation occurred at each of Eaglehawk and Windalia. They noted that the latter contained a series of demethylated hopanes, which suggested that at least one of the accumulations at Windalia had been subjected to conditions in the reservoir conducive to severe biodegradation (that is Level 7 and beyond).

Table 6-3: Assignment of petroleum biodegradation based on the saturated hydrocarbon composition of crude oils reservoired in the Gippsland and Carnarvon Basins, Australia. References - 1: Volkman et al. (1984); 2: Burns, Bostwick and Emmett (1987); 3:Trolio et al. (1999); 4: Alexander et al. (1983).

Crude Oil	Depth (m)	Basin	Level of Biodegradation	Reference
Barrow	1890	Carnarvon	0	1
Wirrah-1	2195.3	Gippsland	0	2,3
Snapper-4	1410	Gippsland	1	2,3
West Seahorse-1	1410	Gippsland	2	4
Dolphin-1	1219.2	Gippsland	3	2,3
Tuna-4	1400.5	Gippsland	3-4	2,3
Leatherjacket-1	765	Gippsland	4-5	2,3
Flinders Shoal	700	Carnarvon	5	1,4
Tubridgi-7	n.d.	Carnarvon	6-7	
Lakes Entrance	365	Gippsland	7	4
Windalia		Carnarvon	mixed	4
Eaglehawk	2750	Carnarvon	mixed	4

6.4 Comparison of the effect of biodegradation on aromatic hydrocarbon abundances in the different environments

The susceptibility to biodegradation of the individual alkylnaphthalenes and alkylphenathrenes within groups of isomers in the LTOBM discharged to the sea-floor has been discussed in detail in Chapter 4. Similar observations for these compounds contained in the petroleum discharged into the intertidal sediments were described in Chapter 5. These are summarised in Figure 6-1, from which it is apparent that although not identical, there is a strong similarity between the observed order of susceptibility in the two environments.

A common striking feature is the relatively strong susceptibility to biodegradation of polymethylnaphthalenes with a 1,6 substitution pattern. One possible explanation for this behaviour may be that there are examples of compounds with this substitution pattern which have naturally occurring precursors, so presumably microbes exist

with enzyme systems adapted to the 1,6 substitution pattern. This concept has some precedent in the greater susceptibility of the biologically-produced (20R) 5α(H),14α(H),17α (H)-steranes relative to the geologically produced (20S) isomer (Alexander et al., 1983).

Polymeric cadinene in the dammar resin of *Dipterocarpacae* angiosperms have been identified as a probable source of 1,6-DMN (van Aarssen et al., 1990; 1992). Williams et al. (1986) also noted the susceptibility of cadalene (1,6-dimethyl-4-isopropylnaphthalene) to biodegradation. Similarly 1,2,5-TMN (1,5,6-TMN, agathalene) is a characteristic geochemical marker for the input of conifer resins into sedimentary material formed from the natural precursors agathic and communic acids (Alexander et al., 1988). There is also commonality of the more resistant compounds, namely 1,5-DMN and 2,3-DMN, 1,2,4-TMN and 1,3,5,7-TeMN, between the different environments.

The susceptibilities to biodegradation of the MPs in the two systems are also similar, with 2-MP having a much greater susceptibility than the other isomers. This is consistent with the observations of Nadalig et al. (1996) and Gilewicz et al. (1997), who noted the enhanced degradation of 2-MP relative to 9-MP by a bacterial community isolated from sea-floor sediments. From other studies of petroleum biodegradation (Bayona et al., 1986; Rowland et al., 1986; Kennicutt, 1988; Hostettler and Kvenvolden, 1994; Budzinski et al., 1995b; 1998; Colombo, Cabello and Arambarri, 1996; Ahmed, Smith and George, 1999) there is no consensus as to the most susceptible MP isomer, but rather that 9-MP and 1-MP are more resistant than 2-MP and 3-MP.

For the DMPs, the relationship between the substitution pattern and the susceptibility to biodegradation is less clear. 2,6-DMP, 1,7-DMP (i.e. 2,8-DMP) and 2,10-DMP, three of the most susceptible of the DMPs each have a methyl substituent at the 2 position. However, this strong susceptibility is not reflected in the other 2- substituted isomers, particularly 2,7-DMP, 1,2-DMP and 2,3-DMP, which are amongst the least susceptible isomers. The enhanced susceptibility of 3,10-DMP relative to these isomers is also confounding.

Figure 6-1: A summary of the order of susceptibility to microbial attack of polymethylnaphthalenes, methylphenanthrenes and dimethylphenanthrenes in petroleum contained in two series of coastal sediments (SCVB, NEC coastal), sea-floor sediments (Sea-floor) and a sea-floor cuttings pile (Cuttings Pile). The numbers refer to positions of methyl substituents on the naphthalene or phenanthrene nucleus. Polymethylnaphthalenes with a 1,6-disubstitution pattern are shown in bold text.

The susceptibility of 1,7-DMP (pimanthrene) might also be explained by its structural similarity to the biosynthesised diterpane pimarane (Alexander et al., 1988), however, similar precursors for the other susceptible isomers are not apparent. As a final consideration, there is also no correlation between the thermodynamic stability of these isomers (Budzinski et al., 1993a) and their susceptibility to biodegradation.

Although a study by Hostettler and Kvenvolden (1994) of the biodegradation of DMPs in crude oil spilled into the marine environment was hampered by co-elution, the susceptibility of 2,6-DMP and one or more of the co-eluting mixture of 1,3-DMP, 3,10-DMP, 3,9-DMP and 2,10-DMP to biodegradation was observed. 1,7-DMP was not, however, depleted relative to the other isomers. The susceptibility of 2,6-DMP and one or more of the above-mentioned quartet of co-eluting DMPs was also evident from the *in-vitro* biodegradation of crude oil reported in Budzinski et al. (1998).

Changes in isomer abundances within the DMPs are useful for assessing the extent of biodegradation in more severely biodegraded petroleum, that is beyond Level 6. Such an application is illustrated in Figure 6-2, where the partial gas chromatograms showing the distribution of C_2-Ps obtained from the Flinders Shoal and Tubridgi-7 crude oils are shown. To simplify interpretation of these, the thermodynamically unstable DMPs substituted at the 4- or 5- positions (Budzinski et al., 1993a) have been disregarded. It is apparent from comparison of these chromatograms that the susceptible 2,6-DMP (Peak 33) and 1,7-DMP (Peak 41) isomers are absent from Tubridgi-7 crude oil. Furthermore, 2,7-DMP, 2,3-DMP, 1,2-DMP and 1,8-DMP (Peaks 34, 42, 44 and 45) are absent as well as 3-EP and 1-EP (Peaks 28 and 32). Based on this evidence, it is probable that Tubridgi-7 crude oil has been subjected to more severe biodegradation than Flinders Shoal crude oil (Level 5), and the most degraded of the petroleum samples from the intertidal coastal sediments (Level 5 to 6). Tubridgi-7 crude oil was therefore designated an extent of biodegradation of Level 6 to 7. It is also evident that most, if not all, of the DMPs with a substituent in the 2-position are absent from Tubridgi-7 crude oil, indicating that perhaps this substitution pattern is common to the most susceptible isomers.

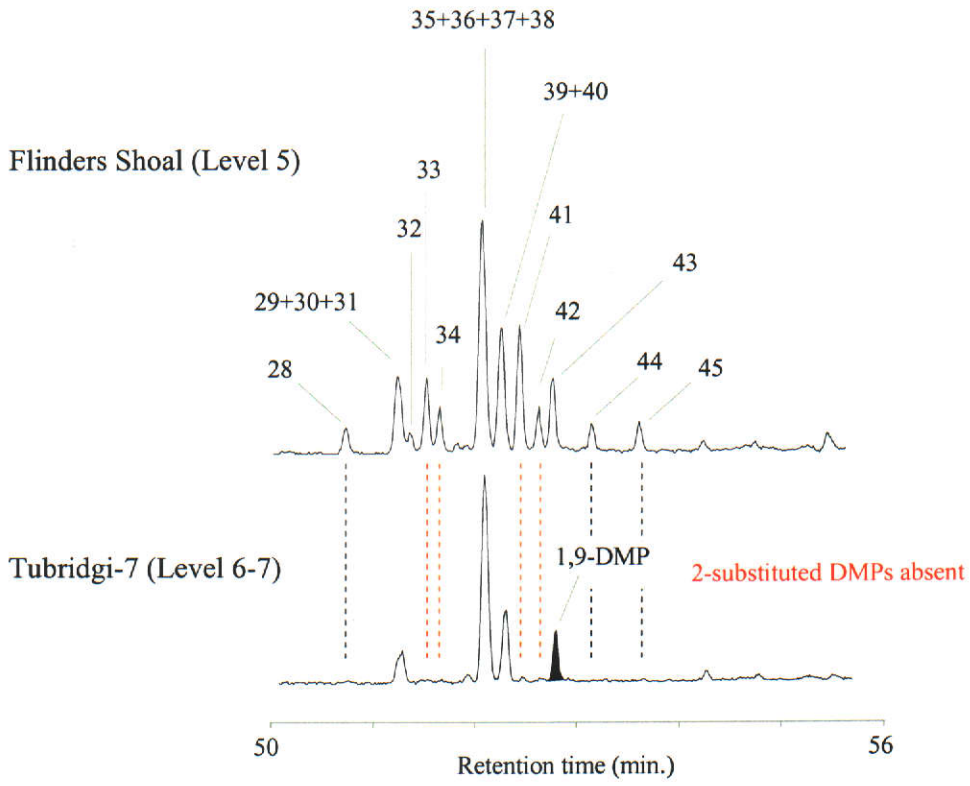

Figure 6-2: Partial mass chromatograms (m/z 206) obtained from the aromatic fraction isolated from Flinders Shoal and Tubridgi-7 crude oils showing the distribution of C_2-Ps contained in each. Peak identifications are as follows: (28) 3-EP; (29) 3,6-DMP; (30) 9-EP; (31) 2-EP; (32) 1-EP; (33) 2,6-DMP; (34) 2,7-DMP; (35) 3,9-DMP; (36) 3,10-DMP; (37) 2,10-DMP; (38) 1,3-DMP; (39) 1,6-DMP; (40) 2,9-DMP; (41) 1,7-DMP; (42) 2,3-DMP; (43) 1,9-DMP; (44) 1,8-DMP; (45) 1,2-DMP.

Due to co-elution of the isomers present in Tubridgi-7 crude oil, only 1,9-DMP can be identified, albeit tentatively assuming both 4,10-DMP and 4,9-DMP are absent from the mixture (refer to the retention indices shown in Table 3-5). The presence of 1,9-DMP is consistent with its relative resistance to biodegradation shown in Figure 6-1. Further analysis of this oil using GC-FTIR to elucidate the composition of the isomer mix might provide further insights into the relationship between structure and susceptibility to biodegradation of the DMPs, however this was not pursued here.

6.4.1 Development of biodegradation-indicating molecular ratios

To investigate whether the susceptibilities amongst the polymethylnaphthalene isomers also are observed upon biodegradation of the reservoired crude oils, three ratios of isomer abundances reflecting the extent of biodegradation within the DMNs, TMNs and TeMNs were developed. For each ratio, the abundance of the isomer with the greater resistance to biodegradation was assigned as the denominator, against which that of the more susceptible isomer was compared. Thus, a decreasing ratio indicates increasing severity of biodegradation (cf. Section 5.5.2, Figures 5-19, 5-21 and 5-22). 1,5-DMN was chosen as the resistant isomer for the dimethylnaphthalene biodegradation ratio (DBR) in preference to 2,3-DMN, since it does not co-elute with any other isomer under the chromatographic conditions used here and is therefore identifiable using routine GC-MS. Similarly, the trimethylnaphthalene biodegradation ratio (TBR) was calculated from the abundance of 1,3,6-TMN relative to 1,2,4-TMN and the tetramethylnaphthalene biodegradation ratio (TeBR) from the abundances of 1,3,6,7-TeMN and 1,3,5,7-TeMN. Values of these ratios for all of the samples of partially biodegraded petroleum are shown in Table 6-4.

The effect on each of the three isomer ratios with increasing severity of biodegradation are illustrated in Figure 6-3, where results from petroleum samples for which the extent of biodegradation could be established are presented (i.e. samples not designated as being of mixed level of biodegradation in Table 6-4). Key features of the relationship between the severity of biodegradation and its effect on the isomer ratios are summarised below.

Table 6-4: Polymethylnaphthalene ratios reflecting the extent of biodegradation of a condensate in coastal intertidal sediments, LTOBM in sea-floor sediments and crude oils reservoired within the Gippsland and Carnarvon Basins.

Sample	Level of Biodegradation	**DBR** 1,6-DMN / 1,5-DMN	**TBR** 1,3,6-TMN / 1,2,4-TMN	**TeBR** 1,3,6,7-TeMN / 1,3,5,7-TeMN
Intertidal Sediments				
NAPL (Aug. '87)	0	5.45	12.3	1.28
SCVB 1 (Dec. '87)	2-3	5.89	10.8	1.23
SCVB 2 (Feb. '88)	3	0.21	5.92	1.20
SCVB 3 (July '89)	3-4	1.10	3.18	1.09
SCVB 4 (Jan. '90)	5	0.20	1.29	1.17
SCVB 5 (Sept. '90)	5-6	n.d.	0.90	0.44
NEC 1 (Sept. '87)	1	5.71	8.95	1.09
NEC 2 (Oct. '87)	1-2	4.43	8.27	1.11
NEC 3 (Sept. '88)	3	1.99	10.17	1.15
NEC 4 (Jan. '89)	4	0.34	2.10	0.94
NEC 5 (Jan. '90)	5	1.31	1.21	0.89
Cuttings Pile Core				
Depth below surface (cm)				
9-10	0	2.52	10.8	1.32
8-9	0	2.11	10.8	1.05
7-8	0	2.34	10.6	1.16
6-7	1-2	2.15	9.57	1.12
5-6	2	1.58	9.57	1.13
4-5	3	0.84	7.19	1.10
3-4	4	0.11	2.19	0.83
2-3	5	0.63	1.87	0.41
1-2	5	n.d.	2.38	0.54
0-1	7	n.d.	n.d.	0.26

Table 6-4 (cont.): Polymethylnaphthalene ratios reflecting the extent of biodegradation of a condensate in coastal intertidal sediments, LTOBM in sea-floor sediments and crude oils reservoired within the Gippsland and Carnarvon Basins.

Sample	Level of Biodegradation	**DBR** 1,6-DMN / 1,5-DMN	**TBR** 1,3,6-TMN / 1,2,4-TMN	**TeBR** 1,3,6,7-TeMN / 1,3,5,7-TeMN
Sea-floor Sediments				
S1 (0 m)	mixed	2.42	13.9	1.13
S2 (100 m)	mixed	0.43	5.45	0.53
S3 (200 m)	mixed	0.18	5.17	0.50
S4 (400 m)	mixed	1.31	4.31	0.39
S5 (800 m)	mixed	n.d.	5.30	0.85
S16 (100 m)	mixed	0.52	3.04	0.31
S12 (200 m)	mixed	n.d.	5.14	0.56
Crude Oils				
Barrow	0	4.90	12.2	1.44
Wirrah 1	0	5.33	13.8	1.63
Snapper 4	1	5.19	13.1	1.44
West Seahorse 1	2	5.15	9.05	1.20
Dolphin 1	3	4.68	10.2	1.42
Tuna 4	3-4	3.10	9.50	1.30
Leatherjacket 1	4-5	n.d.	1.03	0.90
Flinders Shoal	5	1.26	1.28	1.13
Tubridgi 7	6-7	n.d.	n.d.	0.09
Lakes Entrance	7	n.d.	n.d.	n.d.
Windalia	mixed	4.65	10.3	1.35
Eaglehawk	mixed	3.28	3.76	0.25

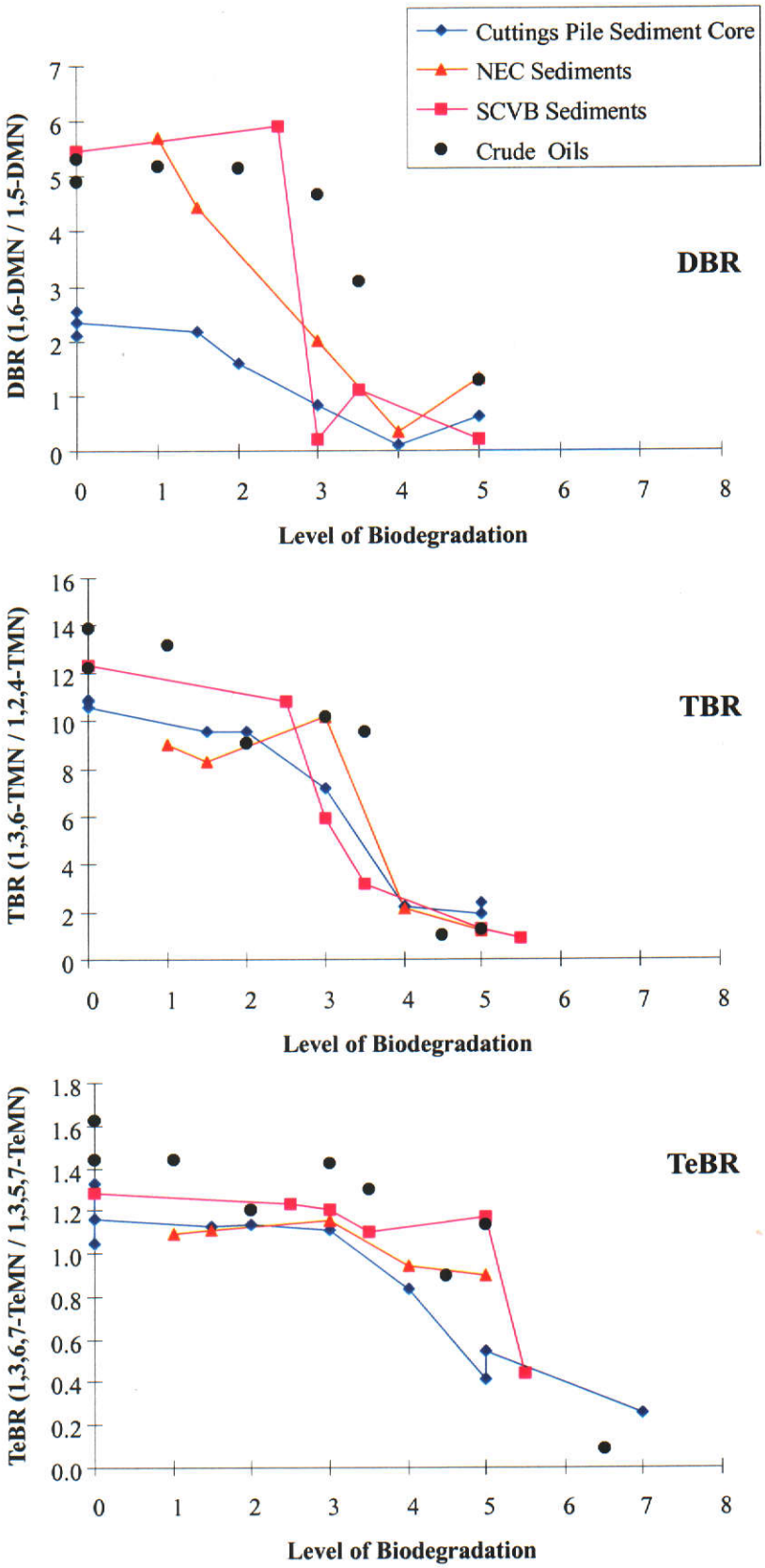

Figure 6-3: Polymethylnaphthalene ratios DBR, TBR and TeBR reflecting the extent of biodegradation in petroleum contained in coastal sediments, the NRA sea floor cuttings pile and reservoired crude oils.

DMN Biodegradation Ratio (DBR)

Although the value of the DBR is markedly lower in the undegraded sample of LTOBM, the ratio behaves in a similar manner with increasing biodegradation in each of the four systems. In the NEC series and the cuttings pile core, the decrease in the DBR commences where the petroleum has been subjected to minor biodegradation (Level 1 to 1.5) and continues to decrease sharply until Level 4, after which it approaches zero as the DMN isomers are depleted from the mixture. For the SCVB sediments, the onset of the decrease is delayed until the extent of biodegradation reaches Level 3, after which a sharp decline is observed at Level 3 to Level 4. The crude oils, particularly those that have undergone only mild biodegradation (approximately Level 0 to 2), display similar values to the SCVB intertidal coastal sediments with a discontinuity in the value of the DBR at biodegradation Level 2 to 3. Values of the ratio approach zero in crude oils subjected to moderate biodegradation (Level 4 to 5).

TMN Biodegradation Ratio (TBR)

The TBR decreases in each system with increasing extent of biodegradation in a strikingly similar manner. Furthermore, the value of the TBR in the least degraded petroleum of each series, including the LTOBM, is similar, facilitating a direct comparison. Between biodegradation Levels 3 and 4, petroleum in both sets of intertidal sediments (NEC and SCVB) show a sharp decrease in the value of the TBR from approximately 10 to 2.5. TMNs contained in the sea-floor cuttings pile display broadly similar behaviour; however, the TBR initially indicates that biodegradation commences between Levels 2 and 3. This range also coincides with a marked discontinuity in values of TBR for the various reservoired oils.

TeMN Biodegradation Ratio (TeBR)

The variation in the TeBR for the coastal sediments and the cuttings pile petroleum correlates very well with that observed in the crude oils. In all of these environments, petroleum biodegraded to a less severe extent than Level 4 to 5 displays a value of greater than one. In petroleum that has been biodegraded to a greater extent, the value of the TeBR is lower. The lack of more severely

biodegraded petroleum from the intertidal coastal sediments hinders further comparison, but it is evident from the most biodegraded sample of LTOBM from the cuttings pile (0–1 cm, Level 7) and the Tubridgi-7 crude oil (Level 6-7) that the TeBR might usefully reflect the extent of biodegradation beyond Level 6. Inspection of Table 6-4 reveals that the TeMNs were completely absent from Lakes Entrance crude oil indicating that the upper limit of the TeBR is less than Level 7.

Summary

The distribution of polymethylnaphthalenes in the reservoired oils, the sea-floor cuttings pile and the coastal sediments are apparently altered by biodegradation processes in a similar way. The value of DBR is significantly altered at Biodegradation Level 2-3, the TBR between Levels 3 and 5; and the TeBR at Level 5-6, indicating the depletion of the isomer more susceptible to microbial attack in each case.

6.5 The use of polymethylnaphthalenes to assess multiple accumulations of petroleum

We observed from Figure 6-3 that for all of the systems, the TBR decreases with increasing biodegradation (Level 3-5) to a value of approximately 2.5 while the TeBR remains relatively constant at a value greater than 1. Where the extent of biodegradation exceeds Level 5, the TeBR decreases. None of the samples therefore exhibit TeBR values of less than 1 when the TBR value is greater than 2.5. This is illustrated in Figure 6-4, where the values of TBR and TeBR for all of the samples analysed here are compared. It is apparent from this figure that six of the composite sea-floor samples and the Eaglehawk crude oil are grouped apart from the other samples due to a disproportionately low value for the TeBR relative to the TBR. This internal inconsistency between the two ratios reflects the mixing of petroleum with differing extents of alteration in these samples.

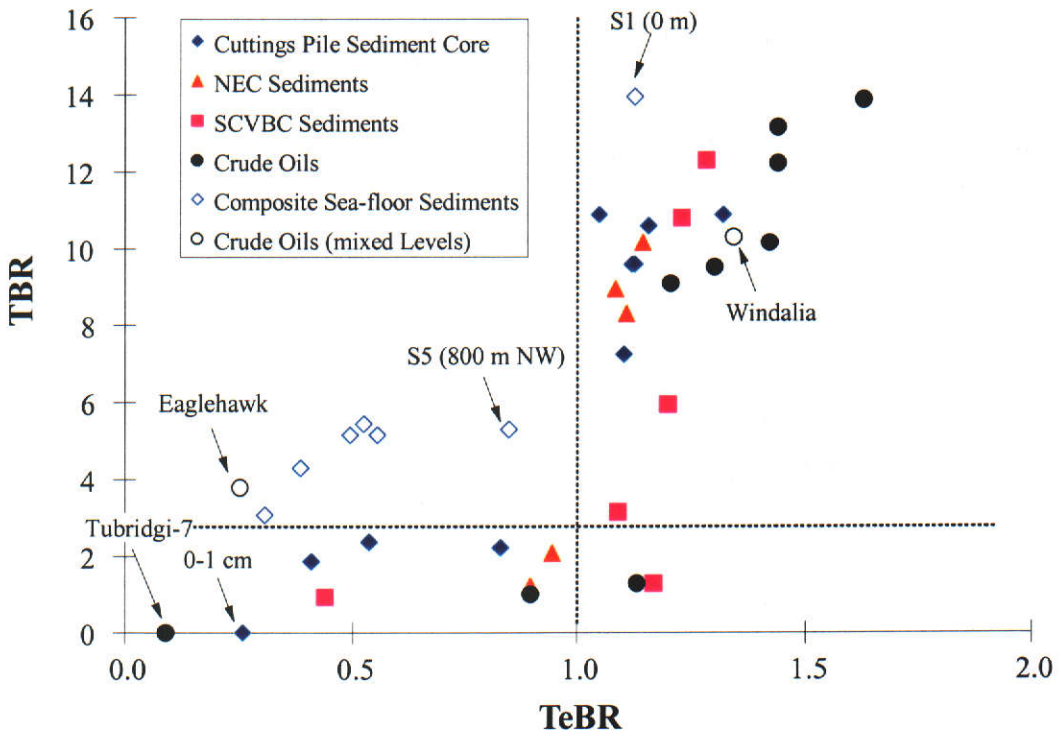

Figure 6-4: A comparison of the polymethylnaphthalene ratios TBR and TeBR reflecting the extent of biodegradation in condensate contained in coastal sediments, LTOBM in the NRA sea-floor cuttings pile and (composite) sediments remote from NRA, and reservoired crude oils.

Consider the isomer ratios obtained from the sea-floor sediments shown in Table 6-4. For S1 (0 m), the values of the DBR (2.42), TBR (13.9) and TeBR (1.13) are similar to those measured in the least degraded samples extracted from the cuttings pile core, namely 2.52, 10.8 and 1.32 respectively. At S2, however, while the value of the DBR (0.43) and TBR (5.45) indicates a Biodegradation Level of 3 to 4 (from Figure 6-2), the TeBR (0.53) value is indicative of more severe biodegradation to Level 5.

Interpretation of the biodegradation ratios measured in all of the composite sea-floor samples is summarised in Table 6-5. For all samples, this interpretation is consistent with the mixing of varying proportions of undegraded and biodegraded residues of the LTOBM as discussed previously (see Section 4.10). Here the mixture in S1 is so dominated by the unbiodegraded LTOBM, that it does not appear as a mixed petroleum in Figure 6-4. Conversely, although S5 contains predominantly moderately degraded LTOBM, the enhanced value of the TBR suggests input of less degraded petroleum, causing a slight deviation from the trend for unmixed petroleum.

Table 6-5: Polymethylnaphthalene ratios DBR, TBR and TeBR, reflecting the extent of biodegradation of LTOBM contained in sea floor sediments collected at various sampling sites on the sea-floor adjacent to the NRA platform. Values are also shown for two crude oils where in-reservoir multiple accumulations have occurred.

Sample Name	Extent of Biodegradation		
Sea-floor Sediments	**DBR** 1,6-DMN / 1,5-DMN	**TBR** 1,3,6-TMN / 1,2,4-TMN	**TeBR** 1,3,6,7-TeMN / 1,3,5,7-TeMN
S1 (0 m)	0	0	0
S2 (100 m NW)	3-4	3-4	5
S3 (200 m NW)	>4	3-4	5
S4 (400 m NW)	2-3	3-4	>6
S5 (800 m NW)	>4	3-4	4-5
S16 (100 m NE)	3-4	4	>6
S12 (200 m NE)	>4	3-4	5
Crude Oils			
Eaglehawk	3-4	4-5	6
Windalia	3	<3	<5

A similar approach was applied to the two crude oils assigned mixed levels of biodegradation, results of which are also shown in Table 6-5. For Windalia crude oil, the value of the DBR (4.65) and TBR (10.3) in comparison with those from other crude oils (e.g. Dolphin-1) indicates that an assignment of Level 3 appropriately describes the extent of biodegradation. This is consistent with the composition of the saturated hydrocarbons reported by Alexander et al. (1983), where *n*-alkanes are present and the acyclic isoprenoids appear unaffected. According to the value for the TeBR (1.35), the severity of biodegradation has not exceeded Level 5. Although this is consistent with the interpretation of the DBR and TBR, it is not consistent with the occurrence of the series of demethylated hopanes (biodegraded to greater than Level 7), also reported by Alexander et al. (1983). A probable explanation for this discrepancy is that an original accumulation of oil was subjected to very extensive biodegradation, resulting in the formation of the series of demethylated hopanes and the complete removal of the polymethylnaphthalenes. Subsequent accumulations of oil in this reservoir have been biodegraded to a maximum extent of Level 4. The

value of the TeBR (0.25) calculated from Eaglehawk crude oil indicates that an initial oil accumulation was subjected to Biodegradation Level 6, retaining the resistant TeMNs. On the basis of the TBR value (3.76), subsequent accumulations were biodegraded to approximately Level 4-5, while the value of the DBR (3.28) also provides evidence for a further accumulation of oil, degraded to a maximum of Level 3.

These latter two phases of oil accumulation for Eaglehawk crude oil are consistent with the accumulation history proposed by Alexander et al. (1983), who concluded that two phases of oil accumulation occurred. The first, larger accumulation was biodegraded to less than Level 5, based on the enhanced abundance of the bicyclic alkanes, followed by a smaller charge of *n*-alkane rich petroleum (biodegraded to less than Level 2). There was no evidence, however, to suggest that an accumulation prior to these had been biodegraded to beyond Level 5.

A likely explanation for the difference in interpretation is that the input of saturated hydrocarbons from the undegraded oil masked the biodegradation signature in the biodegraded accumulation. As shown in Table 6-1, the depletion of the acyclic isoprenoids and bicyclic alkanes are the principal criteria for assigning Biodegradation Levels 4 to 6. It is difficult to detect the depletion of these, however, with the input of less degraded petroleum. The alteration of the sterane distributions, where the depletion of the series of (20R) 5α(H),14α(H),17α(H)-steranes provides a characteristic signature in the biodegraded residues, may be less prone to interference, but does not occur until biodegradation has reached Level 6-7 (Volkman et al., 1984). The TeBR on the other hand, was apparently less affected by the fresh accumulation and provided a less ambiguous measure of the extent of biodegradation of the degraded accumulation. This example illustrates how changes in the TeBR may be used to complement the saturated hydrocarbon biodegradation indicators from the onset of the depletion of the acyclic isoprenoids (Level 4) to the depletion of the 20R steranes (Level 6-7).

6.6 Conclusions

The relative susceptibilities to biodegradation of the polymethylnaphthalenes are very similar in the coastal sediments and the sea-floor sediments. In general, polymethylnaphthalenes with a 1,6-dimethyl substitution pattern are more susceptible to biodegradation than those isomers that lack this feature.

The biodegradation susceptibilities for the MPs and DMPs are also similar in these two systems. Amongst the MP isomers, 2-MP is the most susceptible to biodegradation. DMPs with a 2-methyl substitution pattern are among the most susceptible isomers.

Although it is not possible to determine such an order of susceptibility for these aromatic hydrocarbons in the crude oils, there is evidence that the composition of the polymethylnaphthalenes contained in the reservoired crude oils is altered by biodegradation in a similar manner to the other environments.

Parameters calculated from the abundance of selected polymethylnaphthalenes isomers in petroleum are useful in the assessment of the extent of biodegradation of petroleum. The DBR, TBR and TeBR provide an accurate assessment in instances where the extent of biodegradation does not exceed Level 6. The alkylphenanthrenes might similarly be useful in more biodegraded petroleum.

These parameters also show potential as indicators of multiple accumulations of oil in reservoirs where the extent of biodegradation is different in each of the components of the mixture, and does not exceed Level 6 in either.

References

Ahmed, M., Smith, J.W. and George, S.C., 1999. Effects of biodegradation on Australian Permian coals. *Organic Geochemistry*, **30**, 1311-1322.

Ahsan, A., Karlsen, D.A. and Patience, R.L., 1997. Petroleum biodegradation in the Tertiary reservoirs of the North Sea. *Marine and Petroleum Geology*, **14**, 55-64.

Alexander, R., Kagi, R.I. and Sheppard, P.N., 1983. Relative abundance of dimethylnaphthalene isomers in crude oil. *Journal of Chromatography*, **267**, 367-372.

Alexander, R., Kagi, R.I., Woodhouse, G.W. and Volkman, J.K., 1983. The geochemistry of some biodegraded Australian oils. *The APEA Journal*, **23**, 53-63.

Alexander, R., Kagi, R.I., Noble, R.A. and Volkman, J.K., 1984. Identification of some bicyclic alkanes in petroleum. *Organic Geochemistry*, **6**, 63-70.

Alexander, R., Kagi, R.I., Rowland, S.J., Sheppard, P.N. and Chirila, T.V., 1985. The effects of thermal maturity on distributions of dimethylnaphthalenes and trimethylnaphthalenes in some Ancient sediments and petroleums. *Geochimica et Cosmochimica Acta*, **49**, 385-395.

Alexander, R., Larcher, A.V., Kagi, R.I. and Price, P.L., 1988. The use of plant-derived biomarkers for correlation of oils with source rocks in the Cooper / Eromanga Basin system, Australia. *The APEA Journal*, **28**, 310-324.

Alexander, R., Bastow, T.P., Kagi, R.I. and Singh, R.K. 1992. Identification of 1,2,2,5-teramethyltetralin and 1,2,2,5,6-pentamethyltetralin as racemates in petroleum. *Journal of the Chemical Society, Chemical Communications*, **23**, 1712-1714.

Alexander, R., Bastow, T.P., Fisher, S.J. and Kagi R.I., 1993. Tetramethylnaphthalenes in crude oils. *Polycyclic Aromatic Compounds*, **3**, 629-633.

Alexander, R., Bastow, T.P., Fisher, S.J. and Kagi, R.I., 1995. Geosynthesis of organic compounds: II. Methylation of phenanthrene and alkylphenanthrenes. *Geochimica et Cosmochimica Acta*, **59**, 4259–4266.

Allan, J., Bjorøy, M. and Douglas, A.G., 1980. A geochemical study of the exinite group maceral alginite, selected from three Permo-Carboniferous Torbanites. In A.G. Douglas and J.R. Maxwell (Eds.), *Advances in Organic Geochemistry, 1979*. Pergamon Press, Oxford, pp. 599-618.

Arthurs, P., Stiver, W.H. and Zytner, R.G. 1995. Passive volatilization of gasoline from soil. *Journal of Soil Contamination*, **4**, 123-135.

Barakat, A.O., Qian, Y., Kim, M. and Kennicutt, M.C., 2001. Chemical characterization of naturally weathered oil residues in arid terrestrial environment in Al-Alamein, Egypt. *Environment International*, **27**, 291-310.

Barnett, H.A. and Bartoli, A., 1960. Least-squares treatment of spectrometric data. *Analytical Chemistry*, **32**, 1153-1156.

Bastow, T.P., 1998. Sedimentary processes involving aromatic hydrocarbons. Ph.D. Thesis, Curtin University of Technology.

Bastow, T.P., Alexander, R., Fisher, S.J., Singh, R.K., van Aarssen, B.G.K. and Kagi, R.I., 2000. Geosynthesis of organic compounds. Part V–methylation of alkylnaphthalenes. *Organic Geochemistry*, **31**, 523-534.

Bayona, J.M., Albaigés, J., Solanas, A.M., Parés, R., Garrigues, P. and Ewald, M., 1986. Selective aerobic degradation of methyl-substituted polycyclic aromatic hydrocarbons in petroleum by pure microbial cultures. *International Journal of Environmental Analytical Chemistry*, **23**, 289-303.

Blanc, P. and Connan, J., 1992. Origin and occurrence of 25-norhopanes: a statistical study. *Organic Geochemistry*, **18**, 813-828.

Blumer, M., Ehrhardt, M. and Jones, J.H., 1973. The environmental fate of stranded crude oil. *Deep-Sea Research*, **20**, 239-259.

Bourne, S., Hill, S.L., Powell, J.R., Prasad, D.R. and Krishnan, K., 1990a. High sensitivity Fourier transform infrared spectra of gas chromatographic fractions using a liquid-nitrogen cold-trapping technique. *Digilab FTS/IR Notes No. 75.*

Bourne, S., Haefner, A.M., Norton, K.L. and Griffiths, P.R., 1990b. Performance characteristics of a real-time direct deposition gas chromatography / Fourier transform infrared spectrometry system. *Analytical Chemistry*, **62**, 2448-2452.

Brooks, J.M., Kennicutt, M.C., Wade, T.L., Hart, A.D., Denoux, G.J. and McDonald, T.J., 1990. Hydrocarbon distributions around a shallow water multiwell platform. *Environmental Science and Technology*, **24**, 1079-1085.

Brown, C.W., Lynch, P.F., Ombremski, R.J. and Lavery, D.S., 1982. Matrix representations and criteria for selecting analytical wavelengths for multi-component spectroscopic analysis. *Analytical Chemistry*, **54**, 1472-1479.

Brown, C.W., 1984. Multicomponent infrared analysis using P-matrix methods. *Journal of Testing and Evaluation*, **12**, 86-90.

Budzinski, H., Radke, M., Garrigues, P., Wise, S.A., Bellocq, J. and Willsch, H., 1992. Gas chromatographic retention behaviour of alkylated phenanthrenes on a smectic liquid crystalline phase: application to organic geochemistry. *Journal of Chromatography*, **627**, 227-239.

Budzinski, H., Garrigues, P., Radke, M., Connan, J. and Oudin, J.-L., 1993a. Thermodynamic calculations on alkylated phenanthrenes: geochemical applications to maturity and origin of hydrocarbons. *Organic Geochemistry*, **20**, 917-926.

Budzinski, H., Pierard, C., Garrigues, P. and Bellocq, J., 1993b. Analysis of compounds by capillary gas chromatography / Fourier transform infrared spectroscopy. *Polycyclic Aromatic Compounds*, **3**, 329-335.

Budzinski, H., Garrigues, P., Connan, J., Devillers, J., Domine, D., Radke, M. and Oudin, J.L., 1995a. Alkylated phenanthrene distributions as maturity and origin indicators in crude oils and rock extracts. *Geochimica et Cosmochimica Acta*, **59**, 2043-2056.

Budzinski, H., Baumard, P., Rivet, L., Lacotte, D., Mille, G., Acquaviva, M., Bertrand, J.C. and Garrigues, P., 1995b. Aerobic biodegradation of alkylated aromatic hydrocarbons. In. J.O. Grimalt, and C. Dorronsoro (Eds.), *Organic Geochemistry: Developments and Applications to Energy, Climate, Environment and Human History*. A.I.G.O.A., San Sebastian, Spain, pp. 588-590.

Budzinski, H., Raymond, N., Nadalig, T., Gilewicz, M., Garrigues, P., Bertrand, J.C. and Caumette, P., 1998. Aerobic biodegradation of alkylated aromatic hydrocarbons by a bacterial community. *Organic Geochemistry*, **28**, 337-348.

Burns, B.J., Bostwick, T.R. and Emmett, J.K., 1987. Gippsland terrestrial oils – recognition of compositional variations due to maturity and biodegradation effects. *The APEA Journal*, **27**, 73-84.

Burns, K.A., Codi, S., Pratt, C. and Duke, N.C., 1999. Weathering of hydrocarbons in mangrove sediments: testing the effects of using dispersants to treat oil spills. *Organic Geochemistry*, **30**, 1273-1286.

Carruth, G.F. and Kobyashi, R., 1973. Vapor pressure of normal paraffins ethane through *n*-decane from their triple points to about 10 mm Hg. *Journal of Chemical Engineering Data*, **18**, 115-126.

Cassani, F. and Eglinton, G., 1991. Organic geochemistry of Venezuelan extra-heavy crude oils 2. Molecular assessment of biodegradation. *Chemical Geology*, **91**, 315-333.

Chegwidden, A., Fisher, S.J., Alexander, R. and Kagi, R.I., 1993. The fate of hydrocarbons associated with drilling from the North Rankin 'A' gas and condensate platform, Western Australia. *The APEA Journal,* **33**, 386-394.

Chosson, P., Lanau, C., Connan, J. and Dessort, D., 1991. Biodegradation of refractory hydrocarbon biomarkers from petroleum under laboratory conditions. *Nature*, **351**, 640-642.

Colombo, J.C., Cabello, M. and Arambarri, A.M., 1996. Biodegradation of aliphatic and aromatic hydrocarbons by natural soil microflora and pure cultures of imperfect and lignolitic fungi. *Environmental Pollution*, **94**, 355-362.

Connan, J., 1984. Biodegradation of crude oils in reservoirs. In J. Brooks and D.H. Welte (Eds.), *Advances in Petroleum Geochemistry Vol. 1.* Academic Press, New York, pp. 299-335.

Culler, S.R., Gillette, P.C., Ishida, H., and Koenig, J.L., 1984. Factor analysis applied to a silane coupling agent on E-glass fiber system. *Applied Spectroscopy*, **38**, 495-500.

Daubert, T.E. and Danner, R.P, 1989. *Physical and Thermodynamic Properties of Pure Chemicals Data Compilation*. Taylor and Francis, Washington, D.C.

Davies, J.M., Addy, J.M., Blackman, R.A., Blanchards, J.R., Ferbrache, J.E., Moore, D.C., Sommerville, H.J., Whitehead, A. and Wilkinson, T., 1984. Environmental effects of the use of oil-based drilling muds in the North Sea. *Marine Pollution Bulletin,* **15,** 363-370.

Davies, J.M., Bedborough, D.R., Blackman, R.A.A., Addy, J.M., Appelbee, J.F., Grogan, W.C., Parker, J.G. and Whitehead, A., 1989. The environmental effect of oil-based mud drilling in the North Sea. In F.R. Englehardt, J.P. Ray and A.H. Gillam (Eds), *Drilling Wastes.* Elsevier Applied Science, London, pp. 59-89.

Degouy, D., Argillier, J.-F., Demoulin, A. and Velghe, F., 1993. Biodegradable muds: an attractive answer to environmental legislations around offshore drilling. *Proceedings of the Offshore European Conference, Aberdeen, Scotland, 7-10 September, 1993.* Society of Petroleum Engineers (SPE), Richardson, Texas, USA, pp. 507-514.

Derenne, S., Largeau, C., Casadevall, E., Sinninghe Damsté, J.S., Tegelaar, E.W. and de Leeuw, J.W., 1990. Characterization of Estonian Kukersite by spectroscopy and pyrolysis: evidence for abundant alkyl phenolic moieties in an Ordovician, marine, type II/I kerogen. In B. Durand and F. Behar (Eds.), *Advances in Organic Geochemistry, 1989.* Pergamon Press, Oxford. *Organic Geochemistry,* **16,** 873-888.

Douglas, A.G., Sinninghe Damsté, J.S., Fowler, M.G., Eglinton, T.I. and de Leeuw, J.W., 1991. Unique distributions of hydrocarbons and sulphur compounds released by flash pyrolysis from the fossilized alga *Gloeocapsomorpha prisca*, a major constituent in one of four Ordovician kerogens. *Geochimica et Cosmochimica Acta*, **55**, 275-291.

Dubreuil, C., Derenne, S., Largeau, C., Berkaloff, C. and Rousseau, B., 1989. Mechanism of formation and chemical structure of Coorongite-I. Role of the resistant biopolymer and of the hydrocarbons of *Botryococcus braunii*. Ultrastructure of Coorongite and its relationship with Torbanite. *Organic Geochem*istry, **14**, 543-553.

Duke, N.C., Ellison, J.C. and Burns, K.A., 1998. Surveys of oil spill incidents affecting mangrove habitat in Australia: a preliminary assessment of incidents, impacts on mangroves and recovery of deforested areas. *The APPEA Journal*, **38**, 646-654.

Ellis, L., Kagi, R.I. and Alexander, R., 1992. Separation of petroleum hydrocarbons using dealuminated mordenite molecular sieve—I. Monoaromatic hydrocarbons. *Organic Geochemistry*, **18**, 587-593.

Ellis, L., Alexander, R. and Kagi, R.I., 1994. Separation of petroleum hydrocarbons using dealuminated mordenite molecular sieve—II. Alkylnaphthalenes and alkylphenanthrenes. *Organic Geochemistry*, **21**, 849-855.

Ellis, L., Fisher, S.J., Singh, R.K., Alexander, R. and Kagi, R.I., 1999. Identification of alkenylbenzenes in pyrolyzates using GC-MS and GC-FTIR techniques: evidence for kerogen aromatic moieties with various binding sites. *Organic Geochemistry*, **30**, 651-665.

Englehardt, F.R., Ray, J.P. and Gillam, A.H., 1989. *Drilling Wastes*. Elsevier Appied Science, London.

Fisher, S.J., Alexander, R., Ellis, L. and Kagi, R.I., 1996. The analysis of dimethylphenanthrenes by direct deposition gas chromatography-Fourier transform infrared spectroscopy (GC-FTIR). *Polycyclic Aromatic Compounds*, **9**, 257-264.

Fisher, S.J., Alexander, R., Kagi, R. I. and Oliver, G.A., 1998. Aromatic hydrocarbons as indicators of petroleum biodegradation and multiple accumulation events in North Western Australian Oil Reservoirs. In P.G. and R.R. Purcell (Eds.) *The Sedimentary Basins of Western Australia 2:* Proceedings of the Petroleum Exploration Society of Australia Symposium, Perth, WA, 1998, pp. 185-194.

Forster, P.G., Alexander, R. and Kagi, R.I., 1989. Identification and analysis of tetramethylnaphthalenes in petroleum. *Journal of Chromatography*, **483**, 384-389.

Friedheim, J.E. and Pantermuehl, R.M., 1993. Superior performance with minimal environmental impact: a novel nonaqueous drilling fluid. In *Proceedings of the 1993 SPE / IADC Drilling Conference, Amsterdam, Netherlands*, Society of Petroleum Engineers of AIME, Richardson, Texas, USA, pp. 713-726.

Frolov, E.B. and Smirnov, M.B., 1994. Unsaturated hydrocarbons in crude oils. *Organic Geochemistry*, **21**, 189-208.

Garrigues, P., de Vazelhes-de Sury, R., Angelin, M.L., Ewald, M., Oudin, J.L. and Connan, J., 1984. Analysis of series of aromatic isomers by high resolution spectrofluorimetry and capillary gas chromatography in HPLC fractions of crude petroleums and sedimentary rock extracts. *Organic Geochemistry*, **6**, 829-837.

Garrigues, P., Parlanti, E., Radke, M., Bellocq, J., Willsch, H. and Ewald, M., 1987. Identification of alkylphenanthrenes in shale oil and coal by liquid and capillary gas chromatography and high-resolution spectrofluorimetry (Shpol'skii effect). *Journal of Chromatography*, **395**,217-228.

Gassmann, G., 1981. Chromatographic separation of diastereomeric isoprenoids for the identification of fossil oil contamination. *Marine Pollution Bulletin*, **12**, 78-84.

Gelin, F., de Leeuw, J.W., Sinninghe Damsté, J.S., Derenne, S., Largeau, C. and Metzger, P., 1994. The similarity of chemical structures of soluble aliphatic polyaldehyde and insoluble algaenan in the green microalga *Botryococcus braunii* race A as revealed by analytical pyrolysis. *Organic Chemistry,* **21**, 423-435.

George, S.C., 1992. Effect of igneous intrusion on the organic geochemistry of a siltstone and an oil shale horizon in the Midland Valley of Scotland. *Organic Geochemistry*, **18**, 705-723.

Gilewicz, M., Ni'matuzahroh, Nadalig, T., Budzinski, H., Doumenq, P., Michotey, V. and Bertrand, J.C., 1997. Isolation and characterization of a marine bacterium capable of utilizing 2-methylphenanthrene. *Applied Microbiology and Biotechnology*, **48**, 528-533.

Gillette, P.C., Lando, J.B. and Koenig, J.L., 1983. Factor analysis for separation of pure component spectra from mixture spectra. *Analytical Chemistry*, **55**, 630-633.

Goodwin, N.S., Park, P.J.D. and Rawlinson, A.P., 1983. Crude oil biodegradation under simulated and natural conditions. In M. Bjorøy et al. (Eds.), *Advances in Organic Geochemistry, 1981*. Wiley, Chichester, pp. 650-658.

Gough, M.A., Rhead, M.M. and Rowland, S.J., 1992. Biodegradation studies of unresolved complex mixtures of hydrocarbons: model UCM hydrocarbons and the aliphatic UCM. *Organic Geochemistry*, **18**, 17-22.

Grahl-Nielsen, O., Sporstøl, S., Sjøgren, C.E. and Oreld, F., 1989. The five-year fate of sea-floor petroleum hydrocarbons from discharged drill cuttings. In F.R. Englehardt, J.P. Ray and A.H. Gillam (Eds.), *Drilling Wastes.* Elsevier Applied Science, London, pp. 667-682.

Grimalt, J.O., Grifoll, M., Solanas, A.M. and Albaigés, J., 1991. Microbial degradation of marine evaporitic crude oils. *Geochimica et Cosmochimica Acta*, **55**, 1903-1913.

Hostettler, F.D. and Kvenvolden, K.A., 1994. Geochemical changes in crude oil spilled from the *Exxon Valdez* supertanker into Prince William Sound, Alaska. *Organic Geochemistry*, **21**, 927-936.

Isnard, P. and Lambert, S., 1989. Aqueous solubility and n-octanol / water partition coefficient correlations. *Chemosphere*, **18**, 1837-1853.

Johnston, C.D., Fisher, S.J. and Rayner, J.L., 2001. Removal of petroleum from the vadose zone during multiphase extraction at a contaminated industrial site. In *Preprints of Papers, Third International Conference on Groundwater Quality, Groundwater Quality 2001*. Sheffield, United Kingdom, 18-21 June 2001, pp. 334-346.

Jones, D.M., Douglas, A.G., Parkes, R.J., Taylor, J., Giger, W. and Schaffner, C., 1983. The recognition of biodegraded petroleum-derived aromatic hydrocarbons in Recent marine sediments. *Marine Pollution Bulletin*, **14**, 103-108.

Kagi, R.I., Fisher, S.J. and Alexander, R., 1988. Behaviour of petroleum in northern Australian waters. In P.G. and R.R. Purcell (Eds.), *Proceedings of the North West Shelf Symposium*. Petroleum Exploration Society of Australia, pp. 633-642.

Keim, W., Kohnes, A. and Meltzow, W., 1991. Enantiomer separation by gas chromatography on cyclodextrin chiral stationary phases. *Journal of High Resolution Chromatography*, **14**, 507-529.

Kennicutt, M.C., 1988. Effect of biodegradation on crude oil bulk and molecular composition. *Oil and Chemical Pollution*, **4**, 89-112.

Kennicutt, M.C., Green, R.H., Montagna, P. and Roscigno, P.F., 1996. Gulf of Mexico Offshore Operations Monitoring Experiment (GOOMEX), phase 1: sublethal responses to contaminant exposure- introduction and overview. *Canadian Journal of Fisheries and Aquatic Sciences*, **53**, 2540-2553.

Largeau, C., Derenne, S., Casadevall, E., Kadouri A. and Sellier, N., 1986. Pyrolysis of immature Torbanite and of the resistant biopolmer (PRB A) isolated from extant alga *Botryococcus braunii*. Mechanism of formation and structure of Torbanite. In D. Leythaeuser. and J. Rullkötter (Eds.), *Advances in Organic Geochemistry 1985*. Pergamon Press, Oxford. *Organic Geochem*istry, **10**, 1023-1032.

Larter, S. R. and Horsfield, B., 1993. Determination of structural components of kerogens by the use of analytical pyrolysis methods. In M.H. Engel and S.A. Macko (Eds.), *Organic Geochemistry: Principles and Applications*. Plenum Press, New York, pp. 271-284.

Lee, M.L., Vassilaros, D.L., White, C.M. and Novotny, M., 1979. Retention indicies for programmed-temperature capillary-column gas chromatography of polycyclic aromatic hydrocarbons. *Analytical Chemistry*, **51**, 768-774.

Lee, C.H, Dempsey, D.M., Mohamed, R.S. and Holder, G.D., 1992. Vapor-liquid equilibrium in systems of *n*-decane / tetralin, *n*-hexadecane / tetralin, *n*-decane / 1-methylnaphthalene, and 1-methylnaphthalene / tetralin. *Journal of Chemical Engineering Data*, **37**, 183-186.

Li, M., Osadetz, G., Yao, H., Obermajer, M., Fowler, M.G., Snowdon, L.R. and Christensen, R., 1998. Unusual crude oils in the Canadian Williston Basin, southeastern Saskatchewan. *Organic Geochemistry*, **28**, 477-488.

Mackay, D., Shiu, W.Y. and Ma, K.C., 1992. *Illustrated Handbook of Physical-Chemical Properties and Environmental Fate for Organic Chemicals. Volume II. Polynuclear Aromatic Hydrocarbons, Polychlorinated Dioxins and Dibenzofurans*. Lewis, Michigan.

Mackenzie, A.S., Wolff, G.A. and Maxwell, J.R., 1983. Fatty acids in some biodegraded petroleums: possible origins and significance. In M. Bjorøy et al. (Eds.), *Advances in Organic Geochemistry, 1981*. Wiley, Chichester, pp 637-649.

Maris, M.A., Brown, C.W. and Lavery, D.S., 1983. Non-linear multicomponent analysis by infrared spectrophotometry. *Analytical Chemistry*, **55**, 1694-1703.

Massie, L.C., Ward, A.P. and Davies, J.M., 1985. The effects of oil exploration and production in the northern North Sea: Part 2—Microbial biodegradation of hydrocarbons in water and sediments, 1978-1981. *Marine Environmental Research*, **15**, 235-262.

Mayer, T.J. and Duswalt, J.M., 1973. Preparation and spectra of trimethyl-naphthalene isomers. *Journal of Chemical and Engineering Data*, **18**, 337-344.

Meylan, W.M. and Howard, P.H., 1996. Improved method for estimating water solubility from octanol/water partition coefficients. *Environmental Toxicology and Chemistry,* **15**,100-106.

Mitchell, W.J., Topsom, R.D. and Vaughan, J., 1962. 1,8-Dimethylnaphthoic acids. *Journal of the Chemical Society*, **1962**, 2526-2528.

Moldowan, J.M. and McCaffrey, M.A., 1995. A novel microbial hydrocarbon degradation pathway revealed by hopane demethylation in a petroleum reservoir. *Geochimica et Cosmochimica Acta*, **59**, 1891-1894.

Nadalig, T., Budzinski, H., Raymond, N., Garrigues, P. and Caumette, P., 1996. Aerobic degradation of methylphenanthrenes by an enrichment bacterial community. *Polycyclic Aromatic Compounds*, **11**, 107-114.

Nakanishi, K. and Solomon, P., 1977. *Infrared Absorption Spectroscopy*, Holden - Day, Oakland, pp. 14-18.

Neely, W.B. and Blau, G.E., 1985. *Environmental Exposure from Chemicals*. CRC Press, Boca Raton, Florida.

Noble, R.A., 1986. A geochemical study of bicyclic alkanes and diterpenoid hydrocarbons in crude oils, sediments and coals. Ph.D. Thesis, Department of Chemistry, University of Western Australia, Perth.

Oliver, G.A. and Fisher, S.J., 1999. The persistence and effects of non-water based drilling fluids on Australia's North West Shelf: progress findings from three seabed surveys. *The APPEA Journal,* **39**, 647-662.

Page, C.A., Bonner, J.S., Sumner, P.L. and Autenrieth, R.L., 2000. Solubility of petroleum hydrocarbons in oil / water systems. *Marine Chemistry*, **70**, 79-87.

Papp, R. and Fisher, S.J., 1999. Drilling fluids and their environmental management: characterisation of base fluids and the introduction of quality control procedures. *The APPEA Journal,* **39**, 628-639.

Perrin, D.D. and Armarego, W.L.F., 1988. *Purification of Laboratory Chemicals, 3rd edition*. Pergamon Press, Oxford.

Peters, K.E. and Moldowan, J.M., 1993. *The Biomarker Guide: Interpreting Molecular Fossils in Petroleum and Ancient Sediments*, Prentice Hall, Englewood Cliffs, New Jersey.

Peters, K.E., Moldowan, J.M., McCaffrey, M.A. and Fago, F.J., 1996. Selective biodegradation of extended hopanes to 25-norhopanes in petroleum reservoirs. Insights from molecular mechanics. *Organic Geochemistry*, **24**, 765-783.

Petersen, S.P., Kruse, B. and Jensen, K., 1991. Degradation of low toxicity drilling mud base oil in sediment cores. *Marine Pollution Bulletin*, **22**, 452-455.

Press, W.H., Teukolsky, S.A., Vetterling, W.T. and Flannery, B.P., 1992. *Numerical Recipes in C: The Art of Scientific Computing, Second Edition*. Cambridge University Press, New York.

Prince, R.C., Elmendorf, D.L., Lute, J.R., Hsu, C.S., Haith, C.E., Senius, J.D., Dechert, G.J., Douglas, G.S. and Butler, E.L., 1994. 17α(H),21β(H)-Hopane as a conserved internal marker for estimating the biodegradation of crude oil. *Environmental Science and Technology*, **28**, 142-145.

Radke, M., Willsch, H., Garrigues, P., de Sury, R. and Ewald, M., 1984. Identification of dimethyl- and ethylphenanthrenes in HPLC fractions of rock and coal extracts by capillary gas chromatography and high resolution spectrofluorometry. *Chromatographia*, **19**, 355-361.

Radke, M., Willsch, H. and Welte, D.H., 1984. Class separation of aromatic compounds in rock extracts and fossil fuels by liquid chromatography. *Analytical Chemistry*, **56**, 2538-2546

Radke, M., 1987. Organic geochemistry of aromatic hydrocarbons. In J. Brooks and D.H. Welte (Eds.), *Advances in Petroleum Geochemistry Vol. 2.* Academic Press, New York, pp 141-207.

Radke, M., Garrigues, P. and Willsch, H., 1990. Methylated dicyclic and tricyclic aromatic hydrocarbons in crude oils from the Handil field, Indonesia. *Organic Geochemistry*, **15**, 17-34.

Radke, M., Budzinski, H., Pierard, C., Willsch, H. and Garrigues, P., 1993. Chromatographic retention behaviour of trimethylphenanthrenes and their identification by GC-FTIR in geological samples. *Polycyclic Aromatic Compounds*, **3**, 467-474.

Radke, M., Rullkötter, J. and Vriend, S.P., 1994. Distribution of naphthalenes in crude oils from the Java Sea: source and maturation effects. *Geochimica et Cosmochimica Acta*, **58**, 3675-3689.

Reiersen, L. -O., Gray, J.S., Palmork, K.H. and Lange, R., 1989. Monitoring in the vicinity of oil and gas platforms; results from the Norwegian Sector of theNorth Sea and recommended methods for forthcoming surveillance. In F.R. Englehardt, J.P. Ray and A.H. Gillam (Eds.), *Drilling Wastes*. Elsevier Applied Science, London, pp. 91-117.

Riddick, J.A., Bunger, W.B. and Sakano T.K., 1986. *Techniques of Chemistry, 4th Edition, Volume II. Organic Solvents*. John Wiley and Sons, New York.

Roeges, N.P.G., 1994. *A Guide to the Complete Interpretation of Infrared Spectra of Organic Structures*. John Wiley and Sons Ltd., Chichester.

Roscigno, P.F. and Kennicutt, M.C., 1995. Marine ecosystems: assessing the impacts of chronic contamination from offshore platforms. *MTS Journal*, **27**, 66-71.

Rowland, S.J., Alexander, R. and Kagi, R.I., 1984. Analysis of trimethyl-naphthalenes in petroleum by capillary gas chromatography. *Journal of Chromatography*, **294**, 407-412.

Rowland, S.J., Alexander, R., Kagi, R.I., Jones, D.M. and Douglas, A.G., 1986. Microbial degradation of aromatic components of crude oils: a comparison of laboratory and field observations. *Organic Geochemistry*, **9**, 153-161.

Sanemasa, I., Wu, J.-S. and Toda, K., 1997. Solubility product and solubility of cyclodextrin inclusion complex precipitates in an aqueous medium. *Bulletin of the Chemical Society of Japan*, **70**, 365-369.

Scherrer, P. and Mille, G., 1989. Biodegradation of crude oil in an experimentally polluted peaty mangrove soil. *Marine Pollution Bulletin*, **9**, 430-432.

Seifert, W.K. and Moldowan, J.M., 1979. The effect of biodegradation on steranes and terpanes in crude oils. *Geochimica et Cosmochimica Acta*, **43**, 111-126.

Smith, J.W., George, S.C. and Batts, B.D., 1995. The geosynthesis of alkylaromatics. *Organic Geochemistry*, **23**, 71-80.

Smyrl, N.R., Hembree Jr., D.M., Davis, W.E., Williams D.M. and Vance, J.C., 1992. Simultaneous GC-FT-IR/GC-MS analysis for isomer-specific identification and quantitation of complex mixture components. *Applied Spectroscopy*, **46**, 277-282.

Solanas, A.M., Parés, R., Bayona, J.M. and Albaigés, J., 1984. Degradation of aromatic petroleum hydrocarbons by pure microbial cultures. *Chemosphere*, **13**, 593-601.

Steedman Science and Engineering, 1993. Review of oceanography of North West Shelf and Timor Sea regions pertaining to the environmental impact of the offshore oil and gas industry, 1. *Report to Woodside Offshore Petroleum Pty Ltd.*, unpublished.

Sternberg, J.C., Stillo, H.S. and Schwendeman, R.H., 1960. Spectrophotometric analysis of multicomponent systems using the least squares method in matrix form. The ergosterol irradiation system. *Analytical Chemistry*, **32**, 84-90.

Sutton, C. and Calder, J.A., 1974. Solubility of higher molecular weight *n*-paraffins in distilled water and seawater. *Environmental Science and Technology*, **8**, 654-657.

Terrens, G.W., Gwyther, D. and Keough, M.J., 1998. Environmental assessment of synthetic-based drilling mud discharges to Bass Strait, Australia. *The APPEA Journal*, **38**, 610-625.

Tibbetts, P.J.C. and Large, R., 1986. Degradation of low-toxicity oil-based drilling mud in benthic sediments around the Beatrice Oilfield. *Proceedings of the Royal Society of Edinburgh*, **91B**, 349-356.

Trolio, R., Grice, K., Fisher, S.J., Alexander, R. and Kagi, R.I., 1999. Alkylbiphenyls and alkyldiphenylmethanes as indicators of petroleum biodegradation. *Organic Geochemistry*, **30**, 1241-1253.

van Aarssen, B.G.K., Cox, H.C., Hoogendoorn, P. and de Leeuw, J.W., 1990. A cadinene biopolymer present in fossil and extant dammar resins as a source for cadinanes and bicadinanes in crude oils from South East Asia. *Geochimica et Cosmochimica Acta*, **54**, 3021-3031.

van Aarssen, B.G.K., Hessels, J.K.C., Abbink, O.A. and de Leeuw, J.W., 1992. The occurrence of polycyclic sesqui-, tri-, and oligoterpenoids derived from a resinous polymeric cadinene in crude oils from South East Asia. *Geochimica et Cosmochimica Acta*, **56**, 1231-1246.

Visser, T. and Vredenbregt, M.J., 1990. Cryotrapping gas chromatography-Fourier transform infrared spectrometry in environmental analysis: a pilot study. *Vibrational Spectroscopy*, 1, 205-210.

Volkman, J.K., Alexander, R., Kagi, R.I and Woodhouse, G.W., 1983. Demethylated hopanes in crude oils and their applications in petroleum geochemistry. *Geochimica et Cosmochimica Acta*, **47**, 785-794.

Volkman, J.K., Alexander, R., Kagi, R.I., Rowland, S.J. and Sheppard, P.N., 1984. Biodegradation of aromatic hydrocarbons in crude oils from the Barrow Sub-basin of Western Australia. In P.A. Schenk, J.W. de Leeuw and G.W.M. Lijmbach (Eds.), *Advances in Organic Geochemistry 1983*. Pergamon Press, Oxford. *Organic Geochemistry*, **6**, 619-632.

Wang, Z., Fingas, M. and Sergy, G., 1995. Chemical characterization of crude oil residues from an Arctic beach by GC/MS and GC/FID. *Environmental Science and Technology*, **29**, 2622-2631.

Williams, J.A., Bjorøy, M., Dolcater, D.L. and Winters, J.C., 1986. Biodegradation in South Texas Eocene oils - effects on aromatics and biomarkers. In D. Leythaeuser and J. Rullkötter (Eds.), *Advances in Organic Geochemistry 1985, Organic Geochemistry*, **10**, 451-461.

Woodside Offshore Petroleum Pty. Ltd., 1990. Investigation into the effects of condensate on the sediments and mangroves of Withnell Bay: a monitoring program associated with the oil contaminated water system oil leaks. *Document ENV-150*, unpublished.

Worrall, R.D., 1996. *Oil Spill Identification*. Australian Government Publishing Service, Canberra

Xiao, L. and Piatti, C., 1995. Biodegradable invert oil emulsion drilling fluids for offshore operations: A comprehensive laboratory evaluation and comparison. *Proceedings of the International Meeting on Petroleum Engineering Volume 1, 1995*. Society of Petroleum Engineers (SPE), Richardson, Texas, USA. pp. 553-567.

Yalkowsky, S.H. and Dannenfelser, R.M., 1992. AQUASOL database of aqueous solubility, 5th edition. College of Pharmacy, University of Arizona.